

REGGE THEORY AND PARTICLE PHYSICS

P.D.B. COLLINS

Physics Department, University of Durham, Durham City, England



NORTH-HOLLAND PUBLISHING COMPANY – AMSTERDAM

REGGE THEORY AND PARTICLE PHYSICS

P. D. B. COLLINS

Physics Department, University of Durham, Durham City, England

Received 6 November 1970

Contents:

1. Introduction	105
2. Outline of Regge theory	108
3. Regge trajectories and resonances	132
4. Properties of Regge poles	133
5. Regge cuts	158
6. Duality	181
7. High energy phenomenology	201
8. Some conclusions	223
Acknowledgements	226
References	226

Abstract:

An introductory review of the application of complex J -plane theory, or Regge theory, to the analysis of elementary particle processes is given. We describe how a helicity amplitude may be represented in terms of its J -plane singularities, and the restrictions which can be placed on those singularities. The properties of Regge poles and cuts, and the evaluation of cut contributions, are discussed, and the concept of duality, and the formulation of dual models is considered. The way in which information about the Regge singularities can be deduced from the experimental data, both from the resonance spectrum and from the high-energy behaviour of scattering amplitudes is described, and an attempt is made to assess the current state of Regge phenomenology and its place in particle physics.

Single orders for this issue

PHYSICS REPORTS (Section C of PHYSICS LETTERS) 1, no. 4 (1971) 103-234.

Copies of this issue may be obtained at the price given below. All orders should be sent directly to the Publisher. Orders must be accompanied by check.

Single issue price Dfl. 36.-, \$10.50, postage included.



CHAPTER 1

INTRODUCTION

Most current attempts to understand the strong interactions of elementary particles are characterized by a concern with the complex angular momentum plane (or J -plane), and much of the literature makes at least some reference to it. But we have travelled a long way since Regge's pioneering work of 1959 [1-3], and there is now not much use of the framework of potential scattering on which the original discussions were based. In fact almost from the beginning most of the interest has centred on the phenomenological implications of Regge theory rather than on its relation to the fundamental dynamical principles (whatever these may be).

The basic idea of Regge theory, to be explained in more detail later, is that scattering amplitudes are analytic functions of the angular momentum, J , and that a particle of mass m and spin σ will lie on a Regge trajectory $\alpha(t)$ (where t is the square of the centre of mass energy) such that the partial wave amplitude has a pole of the form $[J - \alpha(t)]^{-1}$, and such that $\alpha(m^2) = \sigma$. Such particles are said to be 'composite' because they behave in the angular momentum plane like the bound states of potential scattering rather than the fixed spin 'elementary' particles of a Lagrangian field theory, which do not correspond to J -plane poles. Since $\alpha(t)$ may pass through several integer values (or half-odd-integers for fermions) several particles, of increasing spin, may lie on the same trajectory.

It is generally believed that the strong interactions forces are due to the exchange of such composite particles, or Regge poles, and, as we shall see, such an exchange (see fig. 1) gives a definite prediction for the high energy behaviour of the scattering amplitude $A(s, t)$ (where now s is the square of the centre of mass energy, and $-t$ is the momentum transfer) viz.

$$A(s, t) \sim s^{\alpha(t)} \quad (1.1)$$

where $\alpha(t)$ is the highest trajectory.

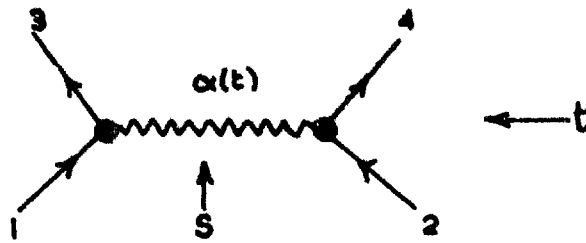


Fig. 1. The exchange of a t -channel Regge pole $\alpha(t)$ in the s -channel scattering process $1+2 \rightarrow 3+4$.

Similarly Regge cuts in the J plane correspond, in a rather complicated way, to the exchange of two or more particles, and their asymptotic behaviour may include logarithmic terms, such as

$$A(s, t) \sim s^{\alpha_c(t)} (\log s)^{-1} \quad (1.2)$$

where $\alpha_c(t)$ is the position of the highest branch point. In general there will be many poles and cuts exchanged in a given amplitude, so the asymptotic behaviour may be a sum of terms like (1.1) and (1.2).

Though Regge pole phenomenology excited much interest in the early years (1961-1963) [4, 5] this enthusiasm was short-lived, mainly it would seem because of the failure of one important prediction - that if a single pole dominated the forward peak of the πN elastic scattering differential cross section it would shrink with increasing energy. It remained fairly easy to fit all the available data with Regge poles, but the number of parameters needed seemed disproportionate to the amount of data fitted. However, as better data, particularly on inelastic processes, became available, starting about 1965, interest revived, and Regge phenomenology has become a thriving industry.

This certainly does not mean that Regge theory is without its problems, or that all the available data can be fitted by a few J -plane singularities without ambiguity. But it does mean that there is now widespread agreement that the complex J -plane is a good place to try and analyse what is going on.

In this sense Regge analysis is in a rather similar position to partial wave analysis. It is well recognised that where sufficient low energy data is available an essential preliminary to a thorough understanding of the scattering process is to resolve the amplitude into partial waves. One does not, of course, expect that such an analysis will always be free from ambiguity, or that it will be possible to interpret the amplitude by a simple model, such as a sum of Breit-Wigner resonances. It is rather that by making use of such a basic notion as angular-momentum conservation one expects to get nearer to the heart of the problem.

Similarly with Regge analysis, whenever there is sufficient high energy data it must now be regarded as an essential preliminary to analyse the amplitudes in terms of crossed channel J -plane singularities. Again there will be ambiguities, and there is certainly no reason why a few Regge poles should suffice, but once one has some idea of the J -plane structure of an amplitude one can start trying to deduce the basic dynamics on which that structure is based.

In fact our understanding of the fundamental dynamics lying behind the successes of Regge phenomenology has made very little if any real progress since the introduction of Regge's ideas into S -matrix theory in 1961 [6-9]. Indeed we shall argue in the concluding chapter that the foundations of Regge theory now seem if anything less comprehensible than they did a few years ago, though there have been some promising developments, such as the multiperipheral bootstrap, and the introduction of dual models. But there has been a tremendous increase in our understanding of how to apply the basic ideas of Regge theory to scattering amplitudes involving particles with spin, and unequal masses, and a great improvement in the availability of experimental data with which to try and locate the dominant poles and cuts.

In this report we shall attempt to review the progress which has been made in recent years in sharpening the tools of Regge analysis, particularly as regards the kinematics of Regge poles and the evaluation of Regge cuts. Our emphasis throughout is on those aspects of Regge theory which are of interest to the phenomenologist. We assume that the reader is already acquainted with the basic ideas of S -matrix theory [10-13], and begin, in the next chapter, with the representation of an helicity amplitude in terms of its J -plane singularities. Chapter 3 contains a brief review of the information about Regge trajectories which can be obtained from an examination of the resonance spectrum. In chapter 4 we summarise the various kinematical and dynamical requirements which must be satisfied by Regge poles - their analyticity properties, the conspiracy relations, etc. Chapter 5 is devoted to a discussion of the theoretical aspects of Regge cuts, and recent attempts to estimate their magnitude.

In chapter 6 we give a rather brief survey of the idea of duality, which has played such an important, but as yet controversial role in particle physics, and then in chapter 7 we review the application of the preceding theory to the experimental data. Some conclusions are drawn in the final chapter.

We have restricted ourselves almost entirely to the two particle \rightarrow two particle amplitudes, partly because the evidence here is so much more complete than it is for multiple production processes, and partly through lack of space. The literature on Regge fits is so vast that one can not hope to be comprehensive, nor in a rapidly changing field can one be completely up to date, but we have tried to give a reasonably balanced survey of the successes and difficulties. We have omitted almost all applications of Regge theory outside phenomenology. In particular we do not discuss the several different types of bootstrap equations using Regge poles, some of which seem to offer exciting prospects for putting Regge theory on a deeper theoretical foundation.

We hope that the treatment given is sufficiently detailed to serve as an introduction, but the going may be rather heavy for the reader who is meeting these things for the first time, and he is advised to skip the more complicated parts at first reading. He may also wish to consult some of the earlier introductory works on Regge poles in potential scattering [4, 5, 14], and in S -matrix theory [10-14]. The author has already collaborated in a review of the subject [15], but that was three years ago, a long time in particle physics, and in any case the viewpoint here is rather different. However, reference is frequently made to that book for points we do not have space to discuss fully here, and where possible the same notation is used. This does not of course mean that this is the only, or the best, place where the required material can be found.

Because of the fairly comprehensive references to early work which can be

found in refs. [4, 5, 15] it has not been thought necessary to give full credit for the older established parts of the subject. More care has been taken with references to work since 1967, but of course no claim to comprehensiveness can be made. The reader is also recommended to other recent reviews such as refs. [16-18].

CHAPTER 2 OUTLINE OF REGGE THEORY

2.1. Introduction

In this chapter we shall outline the basic ideas involved in complex angular momentum theory - or Regge theory for short.

We begin by defining our kinematics, and introduce helicity amplitudes, $A_H(s, t)$ (for both the s and t channels) which we shall use to describe scattering processes involving particles with spin. We then define t -channel partial-wave amplitudes $A_{HJ}(t)$ using the conventional projection in terms of rotation functions $d_{\lambda\lambda'}^J(z)$. Defined in this way the partial wave series diverges outside the t -channel physical region at the point where we reach the nearest singularity in s , but we can circumvent this difficulty by writing a dispersion relation for the amplitude in s at fixed t . We then obtain the so-called Froissart-Gribov partial-wave projection.

These partial-wave amplitudes are shown to have a unique continuation in J , at least as long as the Froissart-Gribov projection is defined. Certain problems concerning signature and parity have to be discussed, however, and these considerably complicate the basic simplicity of the arguments which one would use for spinless particles. The partial wave series is then rewritten as a contour integral in the J -plane - the Sommerfeld-Watson transform - and the integration contour is opened up to expose the pole and branch point singularities in J of $A_{HJ}(t)$.

It is then found that the presence of a singularity at $J = \alpha(t)$ leads to the prediction of the power behaviour for the total amplitude given in (1.1), viz. $A_H(s, t) \sim s^{\alpha(t)}$ (with possible $\log s$ factors if the singularity is a cut). This profound connection between the t -channel J -plane singularities and the s -channel asymptotic behaviour is at the heart of Regge analysis. The well known physical interpretation of a J plane pole as the exchange of a t -channel particle, and of a cut as the exchange of several particles simultaneously, is left to subsequent chapters, but we conclude with a brief discussion of the restrictions which unitarity places on Regge singularities, including the Froissart bound, the absence of fixed poles unless there are also cuts, and the factorization of pole residues; and we show that cuts are needed to make the Gribov-Pomeranchuk fixed poles compatible with unitarity.

2.2. Kinematics

We consider the strong interaction process shown in fig. 2 in which the direct or s -channel consists of particles 1 and 2 entering the scattering region, and 3 and 4 emerging. It does not concern us here whether the particles are stable, or are resonances which subsequently decay. In either case it is found that the scattering is predominantly in the forward and/or backward directions at high energies, and controlled by the exchange forces from the t and u crossed channels respectively. We shall concentrate on describing how the t -channel forces govern the forward direction - the corresponding u channel description is then obvious.

Each particle (mass m_i ; $i = 1, \dots, 4$) carries a four momentum p_i (as shown in fig. 2) and from these we construct the usual Mandelstam invariants [19]

$$s = (p_1 + p_2)^2, \quad t = (p_1 + p_3)^2, \quad u = (p_1 + p_4)^2. \quad (2.1)$$

of which only 2 are independent since we have the constraint

$$s + t + u = \sum m_i^2 \equiv \Sigma. \quad (2.2)$$

Then \sqrt{s} is the centre of mass energy in the s -channel and, $-t$ the momentum transfer squared. The centre of mass 3-momentum of particles 1 or 2 is given by [20]

$$q_{s12}^2 = \frac{1}{4s} [s - (m_1 + m_2)^2][s - (m_1 - m_2)^2] \quad (2.3)$$

and the centre of mass scattering angle is

$$\cos \theta_s \equiv z_s = \frac{s^2 + s(2t - \Sigma) + (m_1^2 - m_2^2)(m_3^2 - m_4^2)}{4s q_{s12} q_{s34}} \quad (2.4)$$

Similarly if we consider scattering in the t -channel corresponding relations may be written down for q_{t13} , q_{t24} and $\cos \theta_t \equiv z_t$ by permuting the variables. The physical regions are bounded by $-1 \leq z_s \leq 1$, etc. and these boundaries are given by

$$\begin{aligned} \phi(s, t) \equiv & s t u - s(m_1^2 - m_3^2)(m_2^2 - m_4^2) - t(m_1^2 - m_2^2)(m_3^2 - m_4^2) \\ & - (m_1^2 m_4^2 - m_2^2 m_3^2)(m_1^2 + m_4^2 - m_2^2 - m_3^2) = 0, \end{aligned} \quad (2.5)$$

see fig. 3.

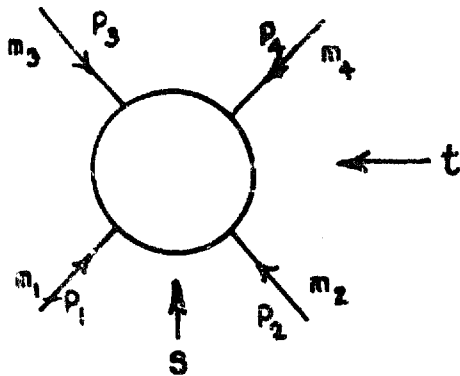


Fig. 2. The scattering amplitude for a general four-body process. The s -channel reaction is $1 + 2 \rightarrow \bar{3} + \bar{4}$, the t -channel is $2 + 4 \rightarrow \bar{1} + \bar{3}$, and the u -channel is $1 + 4 \rightarrow \bar{3} + \bar{2}$ where the bar indicates the anti-particle. These three processes are related by crossing.

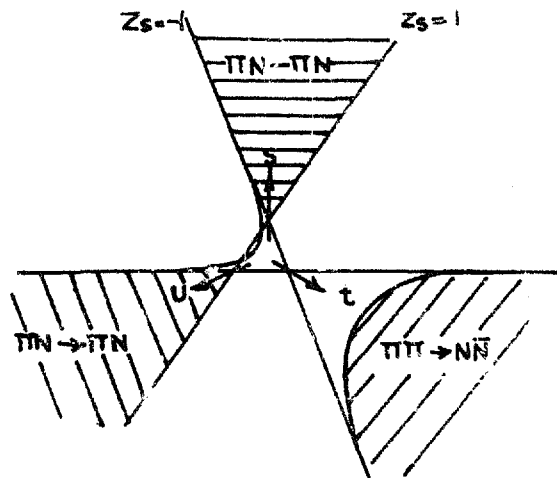


Fig. 3. The Mandelstam plot for $\pi N \rightarrow \pi N$ and its related processes. The physical regions of the three channels are shaded.

The helicity of a particle, μ , is defined as the projection of its spin, σ , in its direction of motion [21] i.e.

$$\mu = \frac{\mathbf{p} \cdot \boldsymbol{\sigma}}{|\mathbf{p}|} \quad (2.6)$$

where \mathbf{p} is the 3-vector momentum. μ spans the $2\sigma + 1$ values $\mu = \sigma, \sigma - 1, \dots, -\sigma$.

We denote a centre of mass helicity scattering amplitude [21] for our s -channel process by

$$\langle \mu_3 \mu_4 | A(s, t) | \mu_1 \mu_2 \rangle \equiv A_{H_S}(s, t) \quad (2.7)$$

since we know from Lorentz invariance that the amplitude is a function only of the Mandelstam invariants, s and t , and the four helicities μ_i . We represent these collectively by H_S , the suffix being used to indicate that the helicities are measured in the s -channel centre of mass system.

The amplitudes are chosen to be normalized as in ref. [15], so that the optical theorem reads

$$\sigma_{\text{tot}}(s) = \frac{1}{2q_s 12 \sqrt{s}} \text{Im} \langle \mu_1 \mu_2 | A(s, 0) | \mu_1 \mu_2 \rangle, \quad (2.8)$$

and the amplitudes are related to the unpolarized differential cross section by

$$\frac{d\sigma}{dt} = \frac{1}{64\pi s q_s^2 12} \frac{1}{(2\sigma_1 + 1)(2\sigma_2 + 1)} \sum_{H_S} |A_{H_S}(s, t)|^2, \quad (2.9)$$

where we sum over all the possible combinations of the μ_i .

We also need to use helicity amplitudes defined in the t -channel centre of mass system

$$\langle \lambda_2 \lambda_4 | A(s, t) | \lambda_1 \lambda_3 \rangle \equiv A_{H_t}(s, t) \quad (2.10)$$

where the λ_i are the t -channel helicities. The crossing postulate [10-13, 15] requires that (2.7) and (2.10) should be the same analytic function, apart from the need to rotate the helicities from the direction of motion of the particles in one centre of mass system to the other [22]. So we have

$$A_{H_S}(s, t) = \sum_{H_t} M(H_S, H_t) A_{H_t}(s, t) \quad (2.11)$$

where $M(H_S, H_t)$ is the helicity crossing matrix [22-24], which is simply the product of the rotation matrices needed to rotate the helicities of the particles

$$M(H_S, H_t) = d_{\lambda_1 \mu_1}^{\sigma_1}(\chi_1) d_{\lambda_2 \mu_2}^{\sigma_2}(\chi_2) d_{\lambda_3 \mu_3}^{\sigma_3}(\chi_3) d_{\lambda_4 \mu_4}^{\sigma_4}(\chi_4) \quad (2.12)$$

where the angles of rotation are

$$\cos \chi_1 = \frac{(s + m_1^2 - m_2^2)(t + m_1^2 - m_2^2) - 2m_1^2(m_1^2 - m_2^2 - m_3^2 + m_4^2)}{[[s - (m_1 + m_2)^2][s - (m_1 - m_2)^2][t - (m_1 + m_3)^2][t - (m_1 - m_3)^2]]^{\frac{1}{2}}} \quad (2.13)$$

etc. Because of the orthogonality of this matrix we can also write

$$\frac{d\sigma}{dt} = \frac{1}{64\pi s q_s^2} \frac{1}{(2\sigma_1 + 1)(2\sigma_2 + 1)} \sum_{H_t} |A_{H_t}(s, t)|^2. \quad (2.14)$$

Eqs. (2.9) and (2.14) are equivalent, but care is needed in interpreting this equality outside the physical regions of the s or t channels where the crossing matrix has singularities (see e.g. ref. [25]).

2.3. Partial wave amplitudes

We have already indicated that the basic idea of Regge theory is to relate the s -channel differential cross section, etc. to the angular momentum structure of the corresponding t -channel process.

The scattering amplitude may be expressed as a partial wave series by [21]

$$A_{H_t}(s, t) = 16\pi \sum_{J=M}^{\infty} (2J+1) A_{HJ}(t) d_{\lambda\lambda'}^J(z_t) \quad (2.15)$$

where J is the total angular momentum and is an integer or half-odd-integer depending on whether the t -channel has even or odd fermion number. The partial wave amplitudes $A_{HJ}(t)$ represent the scattering in the particular angular momentum state. (The suffix t is dropped from H for simplicity.) The $d_{\lambda\lambda'}^J(z_t)$ are the rotation functions [26] with

$$\lambda \equiv \lambda_1 - \lambda_3, \quad \lambda' \equiv \lambda_2 - \lambda_4 \quad \text{and} \quad M \equiv \max\{|\lambda|, |\lambda'|\}. \quad (2.16)$$

The sum starts at $J = M$ since the projection of the orbital angular momentum in the direction of motion is zero, so J can not be less than the sum of the spin projections in that direction.

The inverse to (2.15) is

$$A_{HJ}(t) = \frac{1}{32\pi} \int_{-1}^1 A_{H_t}(s, t) d_{\lambda\lambda'}^J(z_t) dz_t \quad (2.17)$$

where we have used the orthogonality relation

$$\int_{-1}^{+1} d_{\lambda\lambda'}^J(\theta) d_{\lambda\lambda'}^{J'}(\theta) d \cos \theta = \delta_{JJ'} \frac{2}{2J+1}. \quad (2.18)$$

The factor 16π in (2.15) is quite arbitrary, but is inserted for convenience (see ref. [15]).

The series (2.15) is only valid for the t -channel physical region and a small region beyond, until we reach the nearest dynamical s -singularity (i.e. inside the small Lehman ellipse [27]). It certainly can not be used in the s -channel physical region. To reach this we need to make an analytic continuation. (This point is discussed in greater detail in e.g. refs. [4, 10, 15].)

There are also kinematical s -singularities of (2.15) at $z_t = \pm 1$ which arise because of the rotation function [26]

$$d_{\lambda\lambda'}^J(z) = (-1)^{(\lambda-\lambda'-|\lambda-\lambda'|)/2} \left[\frac{(J+M)!(J-M)!}{(J+N)!(J-N)!} \right]^{\frac{1}{2}} \left(\frac{1-z}{2} \right)^{|\lambda-\lambda'|/2} \\ \times \left(\frac{1+z}{2} \right)^{|\lambda+\lambda'|/2} P_{J-M}^{|\lambda-\lambda'|, |\lambda+\lambda'|}(z), \quad (2.19)$$

where $P_C^{ab}(z)$ is a Jacobi polynomial and

$$N \equiv \min\{|\lambda|, |\lambda'|\}.$$

The polynomial is of course analytic in z so the only singularities stem from the 'half angle factor'

$$\xi_{\lambda\lambda'}(z) = \left(\frac{1-z}{2} \right)^{|\lambda-\lambda'|/2} \left(\frac{1+z}{2} \right)^{|\lambda+\lambda'|/2}. \quad (2.20)$$

Note that here we are using the phase convention of Edmonds [26]. The Rose [28] convention is also commonly used and differs from (2.19) by a factor $(-1)^{\lambda-\lambda'}$. The factor at the front of (2.19) is used to reflect the symmetry relations

$$d_{\lambda\lambda'}^J(z) = (-1)^{\lambda-\lambda'} d_{-\lambda-\lambda'}^J(z) = (-1)^{\lambda-\lambda'} d_{\lambda'\lambda}^J(z). \quad (2.21)$$

Later we shall wish to make an analytic continuation of $d_{\lambda\lambda'}^J(z)$ in J , and for this purpose it is convenient to re-express (2.19) in a form which exhibits its J -plane structure more explicitly,

$$d_{\lambda\lambda'}^J(z) = (-1)^{(\lambda-\lambda'-|\lambda-\lambda'|)/2} \left[\frac{(J+M)!(J-M+|\lambda-\lambda'|)!}{(J-M)!(J+M-|\lambda-\lambda'|)!} \right]^{\frac{1}{2}} \frac{1}{|\lambda-\lambda'|!} \xi_{\lambda\lambda'}(z) \\ \times F(-J+M; J+M+1, |\lambda-\lambda'|+1; \frac{1-z}{2}). \quad (2.22)$$

Since the hypergeometric function F is an entire function of J the only singularities stem from the square bracket. We shall also later need to make use of the fact that

$$d_{\lambda\lambda'}^J(z) \underset{z \rightarrow \infty}{\sim} (-1)^{(\lambda-\lambda'-|\lambda-\lambda'|)/2} \frac{2^J}{[(J+M)!(J-M+|\lambda-\lambda'|)!(J-M)!(J+M-|\lambda-\lambda'|)!]^{\frac{1}{2}}} \\ \times \xi_{\lambda\lambda'}(z) \left(\frac{z}{2} \right)^{J-M} + O(z^{J-M-2}) \dots + O(z^{-J-1}) + \dots \quad (2.23)$$

so

$$d_{\lambda\lambda'}^J(z) \sim \left(\frac{z}{2} \right)^J J > -\frac{1}{2} \quad \text{and} \quad (J-v) \neq \text{integer} < M, \quad (2.24)$$

where v is defined in (2.38).

2.4. Dispersion relations and the Froissart-Gribov projection

We have noted that the only singularities of (2.15) in z_t , and hence in s , stem from the half angle factor $\xi_{\lambda\lambda'}(z_t)$. This singularity has a simple physical interpretation in that for forward scattering, for which $z_t = 1$, λ and λ' are the projections of the total angular momentum of the initial and final states, respectively, and so the amplitude must vanish unless $\lambda = \lambda'$ by angular momentum conservation.

So if we define

$$\hat{A}_{H_t}(s, t) \equiv A_{H_t}(s, t) / \xi_{\lambda\lambda'}(z_t). \quad (2.25)$$

\hat{A}_{H_t} will be free of kinematical singularities in s (and u). It will, however, contain dynamical s -singularities corresponding to the s (and u) channel bound states, threshold branch points, etc., which result in the breakdown of (2.15). Thus, if we want to make an analytic continuation including these singularities, \hat{A}_{H_t} is a suitable amplitude in which to write dispersion relations in s (at fixed t), viz.

$$\hat{A}_{H_t}(s, t) = \frac{1}{\pi} \int_{s_0}^{\infty} \frac{D_{sH}(s', t)}{s' - s} ds' + \frac{1}{\pi} \int_{u_0}^{\infty} \frac{D_{uH}(u', t)}{u' - u} du', \quad (2.26)$$

where D_s is the discontinuity of \hat{A} across the s -channel dynamical cuts (above the s -channel threshold s_0); and similarly for D_u . Bound state poles may be added to this expression if necessary.

As far as the t channel is concerned D_{sH} contains the 'direct' forces, and D_{uH} the 'exchange' or Majorana forces. If the integrals in (2.26) converge the scattering amplitude is completely determined by its dynamical singularities. In general, however, the asymptotic s' or u' behaviour of D_s and D_u will be divergent for some t values, in which case the representation (2.26) is only defined up to the arbitrary subtractions needed to produce convergence. We shall see below how Regge theory serves to fix these subtractions, and hence completes the determination of A_H by its dynamical singularities.

Using the fact that (from the equivalent of (2.4) for z_t)

$$s' - s = 2q_t \sqrt{q_t^2 - z_t^2} (z' - z_t) \quad \text{and} \quad u' - u = -2q_t \sqrt{q_t^2 - z_t^2} (z' - z_t) \quad (2.27)$$

the substitution of (2.26) into (2.17) gives

$$A_{HJ}(t) = \frac{1}{32\pi} \int_{-1}^1 dz_t d_{\lambda\lambda'}^J(z_t) \xi_{\lambda\lambda'}(z_t) \left\{ \frac{1}{\pi} \int_{z_0}^{\infty} \frac{D_{sH}(s', t)}{z' - z} dz' + \frac{1}{\pi} \int_{-z_0}^{-\infty} \frac{D_{uH}(u', t)}{z' - z} dz' \right\}. \quad (2.28)$$

We now introduce the 'second type' functions corresponding to the $d_{\lambda\lambda'}^J$, with the definition [29, 30]

$$e_{\lambda\lambda'}^J(z) = (-1)^{(\lambda-\lambda' - |\lambda-\lambda'|)/2} (-1)^{\lambda-\lambda'} \left[\frac{(J+M)!(J-M)!}{(J+N)!(J-N)!} \right]^{\frac{1}{2}} \xi_{\lambda\lambda'}(z) \times Q_{J-M}^{|\lambda-\lambda'|, |\lambda+\lambda'|}(z), \quad (2.29)$$

where the Q_C^{ab} are the second type Jacobi functions. (These take the place of the second type Legendre functions $Q_l(z)$ in spinless particle scattering.). The d 's and e 's are related for integer $(J-M)$ by the 'generalized Neumann relation' [29]

$$\xi_{\lambda\lambda'}(z) e_{\lambda\lambda'}^J(z) = \frac{1}{2} \int_{-1}^1 \frac{dz'}{z-z'} d_{\lambda\lambda'}^J(z') \xi_{\lambda\lambda'}(z'). \quad (2.30)$$

When this is substituted in (2.28) we end up with the Froissart-Gribov projection

$$A_{HJ}(z) = \frac{1}{16\pi^2} \int_{-\infty}^{\infty} dz_t \{ D_{sH}(s, t) e_{\lambda\lambda'}^J(z_t) \xi_{\lambda\lambda'}(z_t) + (-1)^{J-\lambda} D_{uH}(s, t) e_{\lambda-\lambda'}^J(z_t) \xi_{\lambda-\lambda'}(z_t) \}, \quad (2.31)$$

where we have used [29]

$$e_{\lambda\lambda'}^J(-z) = (-1)^{J-\lambda+1} e_{\lambda-\lambda'}^J(z), \quad (2.32)$$

to obtain the second term. Since we can rewrite (2.29) in terms of the hypergeometric function as

$$e_{\lambda\lambda'}^J(z) = (-1)^{(\lambda-\lambda' - |\lambda-\lambda'|)/2} \frac{1}{(2J+1)!} [(J+M)!(J-M)!(J+N)!(J-N)!]^{\frac{1}{2}} \times \xi_{\lambda\lambda'}^{-1}(z) \frac{1}{2} \left(\frac{z-1}{2}\right)^{-J-1+M} F\left(J-M+1, J-M+|\lambda-\lambda'|+1, 2J+2, \frac{2}{1-z}\right) \quad (2.33)$$

and since the asymptotic behaviour of the hypergeometric function as $z \rightarrow \infty$ is 1, we get

$$e_{\lambda\lambda'}^J(z) \underset{z \rightarrow \infty}{\sim} (-1)^{(\lambda-\lambda')/2} \frac{1}{(2J+1)!} [(J+M)!(J-M)!(J+N)!(J-N)!]^{\frac{1}{2}} \frac{1}{2} \left(\frac{z}{2}\right)^{-J-1}, \quad (2.34)$$

so if $A_H(s, t) \sim z_t^{\delta(t)}$ for some value of t , then $D_H \sim z_t^{\delta(t)-M}$ and so the integral in (2.31) converges provided

$$\operatorname{Re} J > \delta(t).$$

We shall discuss the continuation to $\operatorname{Re} J < \delta(t)$ below. It is the presence of these divergences which requires the subtractions referred to above.

The symmetry relation

$$e_{\lambda\lambda'}^J(z) = (-1)^{\lambda-\lambda'} e_{\lambda\lambda'}^{-J-1}(z), \quad J-v = \text{half odd integer} \quad (2.35)$$

will be needed later.

2.5. Signature

Unfortunately (2.31) is not a suitable expression for continuation in J because of the $(-1)^{J-\lambda}$ factor in the second term. For large J the asymptotic behaviour of e is [29-31]

$$e_{\lambda\lambda'}^J(z) \underset{J \rightarrow \infty}{\sim} \left(\frac{\pi}{2}\right)^{\frac{1}{2}} \frac{e^{\pm \frac{1}{2} i \pi (\lambda-\lambda')}}{J^{\frac{1}{2}}} \frac{1}{(z^2-1)^{\frac{1}{2}}} e^{-(J+\frac{1}{2})\xi(z)} \quad (2.36)$$

$|\arg J| < \pi$

where $\xi(z) \equiv \log[z+(z^2-1)^{\frac{1}{2}}]$ and we take \pm for $\operatorname{Im} z \geq 0$. So, as long as the integral converges, the first term in (2.31) behaves like

$$\underset{J \rightarrow \infty}{\sim} \frac{e^{-(J+\frac{1}{2})i\xi(z_c)}}{J^{\frac{1}{2}}} \rightarrow 0, \quad (2.37)$$

but the second behaves like $e^{i\pi(J-\lambda)} \times (2.37)$, and so oscillates as $v \rightarrow \infty$.

Carlson's theorem [32] tells us that if $f(J)$ is a regular function of J and of the form $O(e^{k|J|})$, where $k < \pi$ for $\text{Re}(J) \geq 0$, then $f(J)$ is uniquely determined for all J by its values at positive integer J . This condition is satisfied by (2.37), but not by the second term of (2.31). To circumvent this difficulty, which is not present in potential scattering with only direct forces, we construct from $A_{HJ}(s, t)$ amplitudes of definite signature, $\sigma = \pm$, in the t channel, by replacing $(-1)^{J-v}$ with ± 1 , where

$$v = 0, \frac{1}{2} \text{ for physical } J = \text{integer, or half odd integer} \quad (2.38)$$

so

$$A_{HJ}^\sigma(t) = \frac{1}{16\pi^2} \int_{z_0}^{\infty} dz_t \{ D_{sH}(s, t) e_{\lambda\lambda}^J(z_t) \xi_{\lambda\lambda}(z_t) + \sigma (-1)^{\lambda-v} \times D_{uH}(s, t) e_{\lambda-\lambda}^J(z_t) \xi_{\lambda-\lambda}(z_t) \}. \quad (2.39)$$

The $A_{HJ}^\sigma(t)$ coincide with the physical $A_{HJ}(t)$ values for $J-v$ even/odd. So we can write

$$A_{HJ}(s, t) = 16\pi \sum_{J=M}^{\infty} (2J+1) [A_{HJ}^+(t) d_{\lambda\lambda}^+(J, z) + A_{HJ}^-(t) d_{\lambda\lambda}^-(J, z)], \quad (2.40)$$

where we have defined

$$d_{\lambda\lambda}^\sigma(J, z) \equiv \frac{1}{2} [d_{\lambda\lambda}^J(z) + \sigma (-1)^{\lambda-v} d_{\lambda-\lambda}^J(-z)], \quad (2.41)$$

$d_{\lambda\lambda}^\pm(J, z)$ vanishes for $J-v$ even/odd since [26]

$$d_{\lambda-\lambda}^J(-z) = d_{\lambda\lambda}^J(z) (-1)^{J-\lambda} \quad \text{for } J \geq M. \quad (2.42)$$

Thus A^+ contains the even part of A in z , and A^- the odd part, though neither need be purely even or odd. The physical J values of $A_{HJ}^\pm(t)$, i.e. $J-v = \text{even/odd integer}$, are known as 'right-signature' values of J , while the odd/even values are called 'wrong signature'.

As a result of Carlson's theorem, (2.39) gives us a unique definition of A_{HJ} for all J values for which the Froissart-Gribov projection is defined, i.e. all $\text{Re } J > \delta(t)$, which may now include $\text{Re } J < M$.

We have noted in section 2 that physical amplitudes must have $J \geq M$ since for the incoming channel only $J \geq |\lambda|$ is allowed, and for the outgoing only $J \geq |\lambda'|$. Amplitudes with integer $J-v$ and $J \geq M$ are known as 'sense-sense' (ss) amplitudes. When we make the analytic continuation we may also become involved with amplitudes having integer $J-v$, but with $N \leq J < M$. These are known as 'sense-nonsense' (sn) amplitudes, since for one of the two channels the J value does not make physical sense. Similarly integer $J-v$ with $J < N$ are known as 'nonsense-nonsense' (nn) amplitudes. We shall frequently use this notation below, sometimes referring to all integer $J-v$, $J < M$ as nonsense values.

2.6. Parity

An unfortunate complication of our formalism stems from the fact that two par-

helicity states of definite J and m_J are not parity eigenstates. Rather under the parity operator P we find [21]

$$P|J m_J \lambda_1 \lambda_3\rangle = \eta_1 \eta_3 (-1)^{J-\sigma_1-\sigma_3} |J M-\lambda_1-\lambda_3\rangle, \quad (2.43)$$

where η_1 and η_3 are the intrinsic parities of particles 1 and 3. So definite parity states are provided by the combinations

$$|J m_J \lambda_1 \lambda_3\rangle_{\pm} \equiv 2^{-\frac{1}{2}} \{ |J m_J \lambda_1 \lambda_3\rangle \pm \eta_1 \eta_3 (-1)^{\sigma_1+\sigma_3-v} |J m_J -\lambda_1 -\lambda_3\rangle \}. \quad (2.44)$$

So, assuming that parity is conserved in strong interactions, the scattering amplitude between such states is,

$$\begin{aligned} \langle \lambda_2 \lambda_4 | A_J^{\sigma \eta}(t) | \lambda_1 \lambda_3 \rangle &\equiv \langle \lambda_2 \lambda_4 | A_J^{\sigma}(t) | \lambda_1 \lambda_3 \rangle + \eta \eta_1 \eta_3 (-1)^{\sigma_1+\sigma_3-v} \\ &\quad \times \langle \lambda_2 \lambda_4 | A_J^{\sigma}(t) | -\lambda_1 -\lambda_3 \rangle, \end{aligned} \quad (2.45)$$

where $\eta = \pm$ for natural/unnatural parity. (A state has natural parity if $P = (-1)^{J-\sigma}$). These states are physical for $J-v$ even/odd, depending on the signature, so

$$P = \eta \sigma. \quad (2.46)$$

We then define the so called 'parity conserving' helicity amplitude [33] free of kinematical s singularities by the rule

$$\begin{aligned} \langle \lambda_2 \lambda_4 | \hat{A}_H^{\sigma \eta}(s, t) | \lambda_1 \lambda_3 \rangle &= \langle \lambda_2 \lambda_4 | A^{\sigma}(s, t) | \lambda_1 \lambda_3 \rangle \xi_{\lambda \lambda'}^{-1}(z_t) \\ &\quad + \eta (-1)^{\lambda'+M} \eta_1 \eta_3 (-1)^{\sigma_1+\sigma_3-v} \langle \lambda_2 \lambda_4 | A^{\sigma}(s, t) | -\lambda_1 -\lambda_3 \rangle \xi_{-\lambda \lambda'}^{-1}(z). \end{aligned} \quad (2.47)$$

In terms of partial-wave amplitudes this is

$$\begin{aligned} \hat{A}_H^{\sigma \eta}(s, t) &= 16\pi \sum_{J=M}^{\infty} (2J+1) A_{HJ}^{\sigma}(t) \frac{d_{\lambda \lambda'}^{\sigma}(J, z)}{\xi_{\lambda \lambda'}(z_t)} + \eta (-1)^{\lambda'+M} \\ &\quad \times \eta_1 \eta_3 (-1)^{\sigma_1+\sigma_3-v} A_{\bar{H}J}^{\sigma}(t) \frac{d_{-\lambda \lambda'}^{\sigma}(J, z)}{\xi_{-\lambda \lambda'}(z_t)}, \end{aligned} \quad (2.48)$$

where $\bar{H} \equiv \{-\lambda_1 -\lambda_3, \lambda_2, \lambda_4\}$; or, using (2.45),

$$\hat{A}_H^{\sigma \eta}(s, t) = 16\pi \sum_{J=M}^{\infty} (2J+1) \{ A_{HJ}^{\sigma \eta}(t) \hat{d}_{\lambda \lambda'}^{\sigma+}(J, z) + A_{HJ}^{\sigma-\eta}(t) \hat{d}_{\lambda \lambda'}^{\sigma-}(J, z) \}, \quad (2.49)$$

where we have defined

$$\hat{d}_{\lambda \lambda'}^{\sigma \eta}(J, z) \equiv \frac{1}{2} \left[\frac{d_{\lambda \lambda'}^{\sigma}(J, z)}{\xi_{\lambda \lambda'}(z)} + \eta (-1)^{\lambda'+M} \frac{d_{-\lambda \lambda'}^{\sigma}(J, z)}{\xi_{-\lambda \lambda'}(z)} \right]. \quad (2.50)$$

So partial waves of both parities contribute to the 'parity conserving' amplitudes in (2.49). But in the limit $z \rightarrow \infty$ we find, from (2.23)

$$\hat{d}_{\lambda\lambda'}^{\sigma\eta}(J, z) = (-1)^{(\lambda-\lambda' - |\lambda-\lambda'|)/2} \left[\frac{1 + \sigma(-1)^{J-\nu}}{2} \right] \frac{(2J)!}{[(J+M)!(J-M)!(J+N)!(J-N)!]^{\frac{1}{2}}} \\ \times \left(\frac{z}{2}\right)^{J-M} \left[\frac{1+\eta}{2} \right] + O(z^{J-M-1}), \quad \text{Re } J > -\frac{1}{2} \quad (2.51)$$

so to leading order in z the $d^{\sigma+}$ dominates over the $d^{\sigma-}$ in (2.49), and so asymptotically only $A_{HJ}^{\sigma\eta}(t)$ contributes to $A_{HJ}^{\sigma\eta}(s, t)$. It is only in this asymptotic sense that our amplitudes are parity conserving

2.7. The Sommerfeld-Watson transform

Having established the uniqueness of the analytic continuation of our signatured, parity conserving, partial-wave amplitudes, we can rewrite the partial wave series (2.49) as a Cauchy integral

$$\hat{A}_H^{\sigma\eta}(s, t) = -\frac{16\pi}{2i} \int_{c_1} \frac{2J+1}{\sin\pi(J+\lambda')} \{A_{HJ}^{\sigma\eta}(t) \hat{d}_{-\lambda\lambda'}^{\sigma+}(J, -z) + A_{HJ}^{\sigma-\eta}(t) \hat{d}_{-\lambda\lambda'}^{\sigma-}(J, -z)\} dJ, \quad (2.52)$$

where the contour c_1 encloses the real axis for $J \geq M$, but avoids any singularities of A_{HJ} , as shown in fig. 4. We have used $-z$ so that, because of (2.42), the $(-1)^{J+\lambda'}$ coming from the residue of the poles of $[\sin\pi(J+\lambda')]^{-1}$ is cancelled.

If we open up the contour to c_2 as in fig. 4 we know that because of (2.37) the contribution of the semi-circle at ∞ will vanish, but we pick up contributions from the singularities of A_J , and from the singularities of $[\sin\pi(J+\lambda')]^{-1}$ for $J < M$. The amplitude is expected to have pole and branch point singularities, and if we assume for simplicity that there is just one pole of the form

$$A_{HJ}^{\sigma\eta}(t) = \frac{\beta(t)}{J - \alpha(t)}, \quad (2.53)$$

and one branch point at $J = \alpha_c(t)$ with the cut drawn as in fig. 4, with discontinuity $\Delta(J, t)$, we get

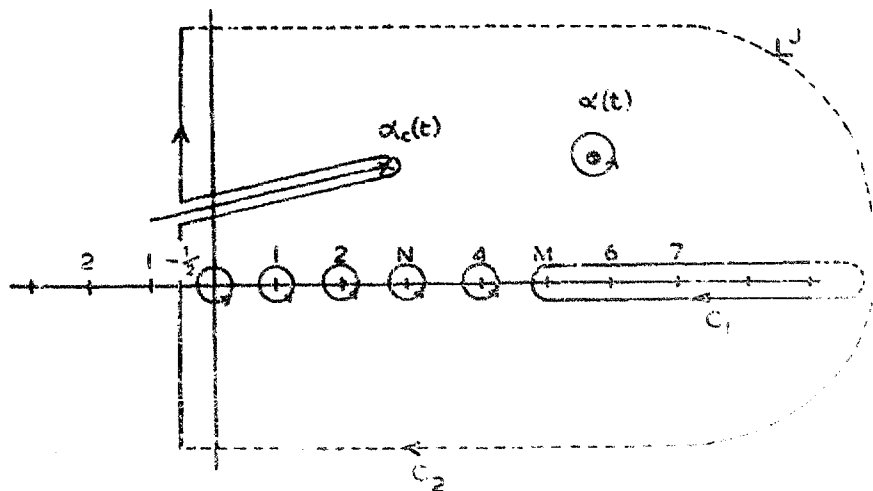


Fig. 4. The Sommerfeld-Watson transform for a helicity amplitude with $M = 5$ and $N = 3$. In the complex J plane the contour c_1 encloses the integer J values $\geq M$. When this contour is opened up to c_2 we also collect distributions from the Regge pole at $\alpha(t)$, from the branch cut starting at the branch-point $\alpha_c(t)$, and from the integer J values $-\frac{1}{2} < J < M$.

$$\begin{aligned}
\hat{A}_H^{\sigma\eta}(s, t) = & \frac{-16\pi}{2i} \int_{c_2} \frac{2J+1}{\sin\pi(J+\lambda')} \{ (2.52) \} - 16\pi^2 \frac{\beta\alpha(t)+1}{\sin\pi(\alpha+\lambda')} \beta_H^\eta(t) d_{-\lambda\lambda}^{\sigma+}(\alpha, -z_t) \\
& - \frac{16\pi}{2i} \int_{\alpha_c(t)}^{\alpha_c(t)} \frac{2J+1}{\sin\pi(J+\lambda')} \Delta(J, t) d_{-\lambda\lambda}^{\sigma+}(J, -z) dJ \\
& - \sum_{J=N}^{M-1} - \sum_{J=v}^{N-1} [16\pi(2J+1) \{ A_{HJ}^\eta(t) \hat{d}_{\lambda\lambda}^{\sigma+}(J, z) + A_{HJ}^{\sigma-\eta}(t) \hat{d}_{\lambda\lambda}^{\sigma-}(J, z) \}] . \quad (2.54)
\end{aligned}$$

Using the asymptotic form of $\hat{d}_{\lambda\lambda}^{\sigma\eta}(J, z)$ given in (2.51) we see that the first term in (2.54), the so called 'background integral', goes like $\sim (z_t)^{-\frac{1}{2}-M}$, and the pole term like $\sim (z_t)^{\alpha(t)-M}$. The behaviour of the cut term depends on the behaviour of the discontinuity $\Delta(J, t)$ at the branch point $J = \alpha_c(t)$. If it is finite we get $\sim (z_t)^{\alpha_c(t)-M} (\log z_t)^{-1}$, while if Δ vanishes like $(J-\alpha)^\delta$, $\delta < 0$, we have $\sim (z_t)^{\alpha_c(t)-M} (\log z_t)^{-(1+\delta)}$. At the sn. points in the fourth term, ($J = J_0$, where $J-v = \text{integer}$ with $N \leq J \leq M$) $d_{-\lambda\lambda}^{\sigma+}(J, z)$ vanishes like $(J-J_0)^{\frac{1}{2}}$ so this term will vanish unless $A_{HJ} \sim (J-J_0)^{-\frac{1}{2}}$. We shall discuss this possibility further in section 9 but for the moment we assume that this term vanishes. Similarly in the final term (at nn. points $v \leq J_0 < N$) the leading power vanishes, and in fact (see 2.23) $d_{\lambda\lambda}^{\sigma-}(z) \sim (z)^{-J-1}$ so the asymptotic behaviour is $(z_t)^{-v-1-M}$.

So we see that only the presence of the cut and pole singularities of A_{HJ} prevents the convergence of (2.39) for $-\frac{1}{2} < J \leq \delta(t)$. It is the principal hypothesis of Regge theory - often called maximal analyticity of the second kind [10, 15] - that in continuing the partial-wave amplitudes the only singularities met are isolated poles (called Regge poles) and branch points (Regge cuts). Thus $\delta(t) = \alpha_M(t)$ where $\alpha_M(t)$ is the rightmost J -plane singularity. And the 'undetermined subtractions' in dispersion relations like (2.26) are now identified as Regge poles and cuts. We have already mentioned that these singularities have a physical interpretation as the exchange of composite particles. Hence if all the particles in strong interaction physics are composite, i.e. they all correspond to Regge poles, there should be no arbitrary parameters left in the S -matrix. It is on this hypothesis that the bootstrap philosophy is based. (See e.g. refs. [10, 11, 15].)

There is no special significance about the line $\text{Re } J = -\frac{1}{2}$ in (2.54); it was chosen simply because, as we see from (2.23), it coincides with the most convergent behaviour of $d_{\lambda\lambda}^{\sigma\eta}(z)$. Mandelstam [34] has shown how one can continue (2.54) below this line by making the replacement [30]

$$\frac{\pi d_{\lambda\lambda}^{\sigma\eta}(z)}{\sin\pi(J+\lambda')} = \frac{e_{\lambda\lambda}^{\sigma\eta}(z)}{\cos\pi(J+\lambda')} - \frac{e_{-\lambda-\lambda}^{\sigma\eta}(z)}{\cos\pi(J+\lambda')} \quad (2.55)$$

in (2.49). We define, in analogy with (2.41) and (2.50),

$$\hat{e}_{\lambda\lambda}^{\sigma\eta}(J, z) = \frac{1}{2} [1 + \sigma e^{\pm i\pi(J-v)}] \left[\frac{e_{\lambda\lambda}^{\sigma\eta}(z)}{\xi_{\lambda\lambda}(z)} + \eta(-1)^{\lambda'+M} \frac{e_{-\lambda-\lambda}^{\sigma\eta}(J, z)}{\xi_{\lambda\lambda}(z)} \right] \quad (2.56)$$

where we use \pm for $\text{Im } z \geq 0$. From (2.34) we see that $e_{-\lambda-\lambda}^{\sigma\eta}(z)$ has the asymptotic z behaviour of $d_{\lambda\lambda}^{\sigma\eta}(z)$, and that $e_{\lambda\lambda}^{\sigma\eta}(z) \sim z^{-J-1}$. So we perform the Sommerfeld-Watson transform for each term in (2.56) separately, and displace the contour to $\text{Re } J < -k$. Then we replace J by $-J-1$ in the second term, and note that the symmetry (2.35) implies that, from the projection (2.39),

$$A_{HJ}^{\sigma\eta}(t) = (-1)^{\lambda-\lambda'} A_{H-J-1}^{\sigma'\eta}(t) \text{ for half odd integer } (J-v), \quad (2.57)$$

where $\sigma' = \sigma$ for $v = 0$ and $\sigma' = -\sigma$ for $v = \frac{1}{2}$. Hence we find that the contributions from the poles of $[\cos \pi(J+\lambda')]^{-1}$ at all integers $-k \leq J < M$ cancel pairwise between the two terms in (2.56). A similar cancellation occurs from the un. contributions in (2.54), and we are left with

$$\begin{aligned} \hat{A}_H^{\sigma\eta}(v, t) = & 16\pi(2\alpha(t) + 1) \beta_H(t) \frac{\hat{e}_{\lambda-\lambda'}^{\sigma'+}(-\alpha-1, -z)}{\cos \pi(\alpha + \lambda')} \\ & + \frac{16}{2i} \int^{\alpha_c(t)} \frac{(2J+1)}{\cos \pi(J+\lambda')} \Delta(J, t) e_{\lambda-\lambda'}^{\sigma'+}(-J-1, -z) dJ \\ & + \text{fixed poles + background integral}, \end{aligned} \quad (2.58)$$

where the background integral $< O(z^{-k})$.

The background can thus be pushed back as far as we like, exposing Regge poles and cuts, plus possible fixed poles which we shall discuss below.

2.8. Restrictions on Regge singularities from unitarity

Though there is a great deal of freedom in the types of singularities which can appear in the complex J -plane, there are some very important restrictions which stem from unitarity, namely the Froissart bound, the absence of fixed poles except in association with cuts, and the factorization of the pole residues. We discuss each of these briefly.

Froissart [35] has shown that if the strong-interaction forces are of finite range then s -channel partial-wave unitarity imposes the restriction [15]

$$|A_H(s, t)| \underset{s \rightarrow \infty}{\leq} \text{constant} \times s \log^2 s \text{ for } t = 0 \quad (2.59)$$

In view of the fact that poles and cuts give $A_H(s, t) \underset{s \rightarrow \infty}{\sim} s^{\alpha_M(t)}$ (neglecting $\log s$ factors) we see that, for all $t \leq 0$, $\alpha_M(t) \leq 1$. This means that if there are any Regge poles or cuts with $\alpha(t) > 1$ for $t < 0$ they must move with t to get under this bound for $t < 0$. An elementary particle of spin σ would give rise to a contribution

$$A_{HJ}(t) = \frac{g^2}{t - m^2} \delta_{J\sigma} \quad (2.60)$$

in a Lagrangian field theory, and so its asymptotic behaviour $A_H(s, t) \sim s^\sigma$ would violate the bound for $\sigma \geq 1$. This implies the compositeness of all particles with $\sigma \geq 1$.

The t -channel partial-wave unitarity condition for elastic scattering [13 -- 13] reads (see e.g. ref. [15])

$$B_{HJ}^\sigma(t_+) - B_{HJ}^\sigma(t_-) = 2i(q_t 13)^{2L} \rho(t) B_{HJ}^\sigma(t_+) B_{HJ}^\sigma(t_-) \quad t_0 < t < t_1 \quad (2.61)$$

where $\rho(t) \equiv 2q_t 13 i^{-\frac{1}{2}}$ is the kinematical factor, and we have defined

$$B_{HJ}^\sigma(t) \equiv A_{HJ}^\sigma(t) (q_t 13)^{-2L}, \quad (2.62)$$

where L is the orbital angular momentum at threshold t_0 (see (4.2)), t_+ and t_- are

evaluated above and below the unitary cuts, and t_1 is the inelastic threshold. Using the real analyticity of $B_{HJ}^{\sigma}(t)$, i.e. $[B_{HJ^*}^{\sigma}(t_+)]^* = B_{HJ}^{\sigma}(t_-)$ (where $*$ = complex conjugate) we may rewrite (2.61) as

$$B_{HJ}^{\sigma}(t) - B_{HJ^*}^{\sigma}(t)^* = 2i(q_{t13})^{2L} \rho(t) B_{HJ^*}^{\sigma}(t)^* B_{HJ}^{\sigma}(t). \quad (2.63)$$

Since the B_{HJ}^{σ} satisfy the conditions for Carlson's theorem so do both sides of this equation, which may thus be continued in J .

It is immediately apparent from (2.61) that there can not be a fixed J -plane pole of B_{HJ}^{σ} , i.e. one whose position is independent of t , since if we put $B_{HJ}^{\sigma}(t) = \beta(J, t)(J - J_0)^{-1}$ we have only a single pole at J_0 on the left, but a double one on the right. The only way in which this could be avoided would be if we have a J -plane cut passing through $J = J_0$ for all t for which the unitarity equation holds. Then we would approach this cut on different sides in B and B^* , and the pole could be present on one side and not the other. On the other hand a moving pole at $J = \alpha(t)$ can perfectly well satisfy (2.63). So we conclude that in the absence of cuts all poles must be moving poles. It is also evident that we cannot satisfy (2.63) for real t with $\text{Im } \alpha(t) = 0$, so a Regge pole can not cross the real J axis for real t .

Above the inelastic threshold, or in the presence of spin, the unitarity equation becomes a matrix equation [15] (the rows and columns representing the various open channels)

$$B_J^{\sigma}(t) - B_{J^*}^{\sigma}(t)^+ = 2i B_{J^*}^{\sigma}(t)^+ \rho_J(t) B_J^{\sigma}(t), \quad (2.64)$$

where $+$ = Hermitian conjugate, or ρ_J is a diagonal matrix of kinematical factors for the various channels. A fixed pole at J_0 on the real axis of the form $B_J^{\sigma}(t) = \beta(J, t)(J - J_0)^{-1}$ implies $\beta(J_0, t)\beta^+(J_0, t) = 0$ so $\beta = 0$, i.e. there is no pole. But if J_0 is off the real axis we simply have $\beta(J_0, t_+)\beta(J_0, t_-) = 0$ which does not imply $\beta = 0$. So fixed poles are allowed but not on the real axis.

Finally, we can write the unitarity equation for the many-channel partial-wave S -matrix as

$$S(J, t)S^+(J^*, t) = I \quad \text{or} \quad S(J, t) = \frac{\text{cof}(S^+)}{\det(S^+)}. \quad (2.65)$$

So if we consider a two-channel process this becomes

$$\begin{pmatrix} S_{11} & S_{12} \\ S_{21} & S_{22} \end{pmatrix} = \frac{\begin{pmatrix} S_{22}^* & -S_{21}^* \\ -S_{12}^* & S_{11}^* \end{pmatrix}}{(S_{11}^* S_{22}^* - S_{12}^* S_{21}^*)}. \quad (2.66)$$

Then if S has a pole of the form $S = \beta(J - \alpha)^{-1}$, the vanishing of the denominator of (2.66) implies that this residue must satisfy

$$\beta_{22}\beta_{11} = \beta_{12}\beta_{21},$$

from which it follows that we can write

$$\beta_{ij} = \gamma_i \gamma_j, \quad (2.67)$$

so the residue factorizes. A generalization of this result to an arbitrary number of channels was given by Charap and Squires [36] (see also ref. [37]).

The meaning of (2.67) is intuitively fairly obvious. If we consider a single-particle exchange diagram such as fig. 1 the pole is simply a product of two factors, one

associated with each vertex. Note that this result serves both to relate the residues of the various helicity amplitudes for a given process, and those of different processes.

2.9. Fixed J -plane singularities and SCR

The second type rotation function $e_{\lambda\lambda}^J$, which we used to define the partial-wave amplitudes in (2.39) has the J -plane singularities exhibited in (2.33). Since $x!$ has a pole for $x = -1, -2, \dots$, and F is an entire function of J , we find that for integer $J_0 - v$

$$e_{\lambda\lambda}^J(z) \sim (J - J_0)^{-\frac{1}{2}} \quad N \leq J_0 < M \quad \text{and} \quad -M \leq J_0 < -N$$

$$\sim (J - J_0)^{-1} \quad -N \leq J_0 < N \quad \text{and} \quad J_0 < -M, \quad (2.68)$$

and for $J < -M$ for example the residue of the pole is just $d_{\lambda\lambda}^J(z)$ (see e.g. refs. [30, 31]). So we obtain

$$A_{HJ}^{\sigma}(t) \approx \frac{1}{J - J_0} \frac{1}{16\pi^2} \int_{-1}^{\infty} dz_t \{ D_{SH}(s, t) \xi_{\lambda, \lambda}(z_t) d_{\lambda\lambda}^{J_0}(z_t) + \sigma(-1)^{\lambda-v}$$

$$\times D_{uH}(s, t) \xi_{\lambda-\lambda}(z_t) d_{\lambda-\lambda}^{J_0}(z_t) \}, \quad (2.69)$$

for $J \approx J_0 < -M$. These fixed, real axis J -plane singularities, which appear at all the nonsense points of the amplitude (in the nomenclature of section 5) are in conflict with our discussion in the previous section, so we conclude that in the absence of cuts the integral (2.69) must vanish like $(J - J_0)$. This integral relationship is known as a superconvergence relation (SCR). The satisfaction of such SCR allows us to conclude that $A_{HJ}^{\sigma}(t) \sim (J - J_0)^{\frac{1}{2}}$ for sn points so the fourth term of (2.54) can be neglected. However $A_{HJ}^{\sigma}(t)$ still has square-root branch point at all $N \leq J_0 < M$ and $-M \leq J_0 < -N$, and it is often convenient to take these branch points to be joined pairwise by cuts running from $J = M - 1 - k$ to $-M + k$; $k = 0, 1, \dots, M - 1$. In fact because of the unitarity equation each helicity amplitude will inherit the singularities of the others, so these cuts run from $J = \sigma_T - 1$ to $J = -\sigma_T$ where $\sigma_T \equiv \max \{ \sigma_1 + \sigma_3, \sigma_2 + \sigma_4 \}$.

However, it was shown by Gribov and Pomeranchuk [38] that $A_{HJ}^{\sigma}(t)$ must in fact have a pole at each wrong-signature nonsense point. This is because if one calculates the discontinuity of the partial-wave amplitude across the left-hand cut one obtains (see e.g. ref. [15])

$$\text{Im} A_{HJ}^{\sigma}(t) = \frac{1}{32\pi} \int_{-1}^{z_t(s, t_0)} dz_t \{ D_{SH}(s, t) \xi_{\lambda, \lambda}(z_t) d_{\lambda\lambda}^J(z_t) + \sigma(-1)^{\lambda-v}$$

$$\times D_{uH}(s, t) \xi_{\lambda-\lambda}(z_t) d_{\lambda-\lambda}^J(-z_t) \} + \frac{1}{16\pi^2} \int dz_t' \rho_H^{su}(s', u') e_{\lambda\lambda}^J(z_t') \left[\frac{1 - \sigma e^{-i\pi(J-v)}}{2} \right]. \quad (2.70)$$

This last term involving the 'third double spectral function', $\rho_H^{su}(s, u)$, vanishes for physical J values, i.e. at right signature points, but is finite at wrong signature points. The $e_{\lambda\lambda}^J$, thus gives rise to singularities in $\text{Im} A_{HJ}$ at these points, as described above. Unlike the previous type of singularities, however, these Gribov-

Pomeranchuk singularities can not be made to disappear by an SCR, because it can be shown that at least for some t values the integral is to be evaluated only over the elastic double spectral function, which is always positive. So there is no change of sign of the integrand in (2.70), and the integral can not vanish. Because of unitarity these singularities, of the form $(J - J_0)^{-\frac{1}{2}}$ or $(J - J_0)^{-1}$, occur for all wrong signature $J = \sigma_T - k$, $k = 2, 4, 6 \dots$ or $1, 3, 5 \dots$.

In chapter 5 we shall see how these fixed singularities are shielded by moving cuts - indeed their presence is one of the principal arguments for the existence of cuts - and shows why the cuts depend on the presence of a third double spectral function. The second term of (2.70) is absent from potential scattering, or indeed any scattering process which lacks an exchange force.

CHAPTER 3 REGGE TRAJECTORIES AND RESONANCES

3.1. Introduction

In the previous chapter we showed how a scattering amplitude can be expressed in terms of its J -plane poles and cuts. The poles interpolate between resonant states of increasing spin, and so in principle quite a lot can be learned about the behaviour of trajectories from an examination of the particle spectrum. In fact one can determine both $\text{Re } \alpha(t)$ and $\text{Im } \alpha(t)$ at the physical points for $t > 0$. The evidence is rather incomplete, but suggests that all the particles lie on roughly straight trajectories of the form

$$\alpha(t) = \alpha_0 + \alpha' t \quad (3.1)$$

and that the slopes α' are more or less the same for all trajectories. We shall see later that this behaviour is rather hard to understand from a theoretical point of view, however.

We begin by discussing the way in which a Regge trajectory gives rise to resonances, and some of the general properties of trajectory functions.

3.2. Regge poles and resonances

From (2.54) and (2.41) we can write the contribution of a Regge pole to a helicity amplitude as

$$A_{H_t}(s, t) = -16\pi^2 [2\alpha(t) + 1] \beta_H(t) \left[\frac{1 + \sigma e^{i\pi(\alpha-v)}}{2 \sin \pi(\alpha(t) + \lambda')} \right] d_{-\lambda\lambda'}^{\alpha(t)}(-z_t) \quad (3.2)$$

$$= -16\pi^2 [2\alpha(t) + 1] \beta_H(t) \left[\frac{e^{-i\pi(\alpha-v)} + \sigma}{2 \sin \pi(\alpha(t) - v)} \right] d_{\lambda\lambda'}^{\alpha(t)}(z_t), \quad (3.3)$$

where we have used (2.42). Evidently this expression has a pole in t whenever $\alpha(t) - v = \text{even/odd integer}$, depending on $\sigma = \pm$. The factor $[e^{-i\pi(\alpha-v)} + \sigma]$ is known as the 'signature factor'. In the analytically continued partial-wave amplitude this pole takes the form (2.53)

$$A_{HJ}^{\sigma}(t) \underset{J \rightarrow \alpha}{\approx} \frac{\beta(t)}{J - \alpha(t)}. \quad (3.4)$$

Above the t -channel threshold we expect $\alpha(t)$ to be complex, and so if, for some $t = t_{\mathbf{r}}$ (say), $\text{Re } \alpha(t_{\mathbf{r}}) - v = J_0$ where $J_0 = \text{even/odd integer}$, we get

$$A_{HJ_0}^{\sigma\eta}(t) \underset{t \rightarrow t_{\mathbf{r}}}{\approx} \frac{\beta(t_{\mathbf{r}})}{(t_{\mathbf{r}} - t)(\alpha'_{\mathbf{R}} + i\alpha'_{\mathbf{I}}) - i\alpha_{\mathbf{I}}(t_{\mathbf{r}})} \approx \frac{\beta(t_{\mathbf{r}})/\alpha'_{\mathbf{R}}}{(t_{\mathbf{r}} - t) - i\alpha_{\mathbf{I}}/\alpha'_{\mathbf{R}}} \quad \text{if } \alpha'_{\mathbf{I}} \ll \alpha'_{\mathbf{R}}, \quad (3.5)$$

where we have used the expansion

$$\alpha(t) - v \approx J_0 + \alpha'_{\mathbf{R}}(t - t_{\mathbf{r}}) + \dots + i\alpha_{\mathbf{I}}(t_{\mathbf{r}}) + i\alpha'_{\mathbf{I}}(t - t_{\mathbf{r}}) + \dots \quad (3.6)$$

the suffices R and I referring to the real and imaginary parts of α (for real t) respectively. If we put $\sqrt{t_{\mathbf{r}}} = M$, the resonance mass, and $\sqrt{t} = E$, the centre of mass energy, (3.5) becomes

$$A_{HJ_0}^{\sigma\eta}(t) \approx \frac{\beta(M^2)}{(M - E) - i\alpha_{\mathbf{I}}(M^2)/\alpha'_{\mathbf{R}} 2M}. \quad (3.7)$$

This corresponds to a Breit-Wigner resonance of mass M and total width

$$\Gamma = \alpha_{\mathbf{I}}(M^2)/\alpha'_{\mathbf{R}} M. \quad (3.8)$$

Thus if we find a resonance of spin J_0 , mass M , and width Γ , we know that $\text{Re } \alpha(M^2) = J_0$ and that $\text{Im } \alpha(M^2)$ can be found from (3.8). In section 4 we shall use this information to plot the trajectories corresponding to the known resonances. Evidently the signature factor will cause the resonances on any given trajectory to be spaced by two units of angular momentum.

If $\alpha(t) - v$ passes through an integer below threshold, $\text{Im } \alpha = 0$, and so there is a bound-state pole on the real t axis.

3.3. Properties of the trajectory function

The known analyticity properties of the scattering amplitudes imply that certain restrictions must be satisfied by the trajectory functions.

If $A_{HJ}^{\sigma}(t)$ has a pole at $J = \alpha(t)$ we have

$$[A_{HJ}^{\sigma}(t)]^{-1} \rightarrow 0 \quad \text{as } J \rightarrow \alpha(t). \quad (3.9)$$

The implicit function theorem tells us that if $[A_{HJ}^{\sigma}(t)]^{-1}$ is regular in t at some $t = t_{\mathbf{r}}$ (say) and

$$\frac{\partial}{\partial J} [A_{HJ}^{\sigma}(t)]^{-1} \neq 0 \quad \text{at } J = \alpha(t_{\mathbf{r}}), \quad (3.10)$$

then $\alpha(t)$ is also regular at $t_{\mathbf{r}}$. So we expect that $\alpha(t)$ will have cuts only where $A_{HJ}^{\sigma}(t)$ does. We shall see in the next chapter that $A_{HJ}^{\sigma}(t)$ has various kinematical singularities, but these are specific to a given helicity amplitude and so must be present in the residue of the pole. The same trajectory occurs in all those helicity amplitudes which are connected by unitarity. Hence $\alpha(t)$ inherits only the dynamical cuts of $A_{HJ}^{\sigma}(t)$. These are of course a right-hand cut above the t -channel threshold t_0 , and a left-hand cut stemming from the s - and u -channel singularities. We have seen in section 2.2 that the poles of $A_{HJ}^{\sigma}(t)$ come from the divergent behaviour of the integrand in (2.39) as $z_i \rightarrow \infty$ i.e. $s \rightarrow \infty$, and so the left-hand cut is

irrelevant in generating the singularity [15]. Hence the only dynamical singularity of $\alpha(t)$ is the right cut above t_0 .

The significance of the condition (3.10), however, is that this theorem breaks down if two trajectories cross. Expanding [39] $[A_{H\alpha}^{\sigma}(t)]^{-1}$ about $t = t_r$ we have

$$[A_{H\alpha}^{\sigma}(t)]^{-1} = a_1[\alpha(t) - \alpha(t_r)] + a_2[\alpha(t) - \alpha(t_r)]^2 + \dots + b_1(t - t_r) + b_2(t - t_r)^2 + \dots \quad (3.11)$$

if t_r is a regular point of $A_{HJ}^{\sigma}(t)$. So the condition for a pole (3.9) reads

$$\alpha(t) = \alpha(t_r) - \frac{b_1}{a_1}(t - t_r) + \dots \quad (3.12)$$

so $\alpha(t)$ is analytic at t_r as expected. But if $a_1 = 0$, i.e. (3.10) does not hold, then

$$\alpha(t) = \alpha(t_r) \pm (-b_1/a_2)^{\frac{1}{2}}(t - t_r)^{\frac{1}{2}} + \dots \quad (3.13)$$

and two trajectories cross at $\alpha(t_r)$. But if $b_1 = 0$ there need not be a branch-point, so the fact that two trajectories cross may, but need not, result in a branch-point occurring in each of the trajectory functions. The imaginary parts of the two trajectory contributions to the amplitude must be equal and opposite so that the amplitude itself is real for $t < t_0$. Otherwise there would be a violation of the Mandelstam representation.

So we can conclude that provided two trajectories do not cross the only singularities of $\alpha(t)$ will be a right-hand cut for $t > t_0$. We can thus write a dispersion integral of the form

$$\alpha(t) = \frac{1}{\pi} \int_0^{\infty} \frac{\text{Im } \alpha(t')}{t' - t} dt' \quad (3.14)$$

But of course (3.14) has only symbolic significance until we know the number of subtractions which are needed. We shall see that the experimental evidence seems to support a behaviour like $\text{Re } \alpha(t) \approx \alpha_0 + \alpha' t$ so (3.14) becomes

$$\alpha(t) = \alpha_0 + \alpha' t + \frac{1}{\pi} \int_0^{\infty} \frac{\text{Im } \alpha(t')}{t' - t} dt' \quad (3.15)$$

But the integral may also diverge, in which case it should also be subtracted, and we obtain instead

$$\alpha(t) = \alpha_0 + \alpha' t + \frac{t^2}{\pi} \int_0^{\infty} \frac{\text{Im } \alpha(t')}{t'^2(t' - t)} dt' \quad (3.16)$$

Note that for either (3.15) or (3.16)

$$\frac{d^n \alpha}{dt^n} = \frac{n!}{\pi} \int_0^{\infty} \frac{\text{Im } \alpha(t')}{(t' - t)^{n+1}} dt' \quad , \quad n > 1 \quad (3.17)$$

Since we have seen in chapter 2 that $\text{Im } \alpha$ can not change sign, but must remain positive, it is clear that for all $t < t_0$ all the derivatives of $\alpha(t)$ will be positive. Thus $\alpha(t)$ is a Herglotz function for $t < t_0$. Of course this will not be true for colliding trajectories with left-hand cuts.

There are also two points about the threshold behaviour of the trajectories which deserve a brief mention. Above the threshold for the elastic process $1+3 \rightarrow 1+3$ we have the unitarity relation (from (2.61))

$$\text{Im} \{ [B_{HJ}^\sigma(t)]^{-1} \} = -i \frac{2q_{t13}}{\sqrt{t}} (q_{t13})^{2L} . \quad (3.18)$$

Since the position of the trajectory is given by $[B_{HJ}^\sigma(t)]^{-1} = 0$ for $J = \alpha(t)$, the threshold behaviour of (3.18) is reflected in $\alpha(t)$ [40, 41]. In section 4.2 we shall show that the orbital angular momentum at threshold is $L = J - Y_{13}$, where Y_{13} represents the mis-match between J and L , and is given in (4.3). It is found (see refs. [40, 41], or e.g. ref. [15]) that the resulting threshold behaviour of the trajectory is

$$\alpha(t) = \alpha(t_0) + a(-q_{t13}^2)^{(\alpha(t_0) - Y_{13} + \frac{1}{2})} \quad \text{for} \quad \alpha(t_0) - Y_{13} > -\frac{1}{2} . \quad (3.19)$$

Thus both the real and imaginary parts of the trajectory functions have the threshold behaviour $(q_{t13}^2)^{\alpha(t_0) - Y_{13} + \frac{1}{2}}$. The generalization of this for any two-body threshold is obvious. However, it is found in potential scattering that such a threshold behaviour is not important, and it is not evident in particle physics either.

The second point [42-44] is that as $\alpha(t_0) - Y_{13} \rightarrow -\frac{1}{2}$ the equation

$$(-q_{t13}^2)^{J - Y_{13} + \frac{1}{2}} = \text{constant} \quad (3.20)$$

is satisfied by $J = \alpha_n$ for any α_n such that

$$[\log_2(q_{t13}^2) - i\pi][\alpha_n - Y_{13} + \frac{1}{2}] = \pm 2\pi n \quad (3.21)$$

or

$$\alpha_n = \frac{\pm 2\pi n}{\pi + i \log(q_{t13}^2)} + Y_{13} - \frac{1}{2} . \quad (3.22)$$

Hence we expect that an infinite number of trajectories will accumulate at $J = Y_{13} - \frac{1}{2}$ coming in from the complex plane as $q_{t13}^2 \rightarrow 0$. These low-lying trajectories do not seem to have much physical significance, but they serve as a warning against models which have only a small number of trajectories in the left-half J -plane.

Fermion trajectories suffer a further complication. As we shall discuss in the next chapter, definite parity amplitudes corresponding to channels with odd fermion number are subject to a constraint at $t = 0$. It is found that when the kinematical singularities have been removed such amplitudes are analytic in s and \sqrt{t} , and there is the relation (4.47)

$$\hat{A}_H^{\sigma\eta}(s, \sqrt{t}) = (-1)^{\lambda - \lambda' + 1} \hat{A}_H^{\sigma-\eta}(s, -\sqrt{t}) , \quad (3.23)$$

where, as before, $\eta = \pm$ refers to natural/unnatural parity. This result is a generalization of the well known MacDowell symmetry [45] of πN scattering. We shall see in chapter 4 that (3.23) is an example of a conspiracy relation.

In order to satisfy the relation we need two trajectories of opposite parity, $\alpha^+(\sqrt{t})$ and $\alpha^-(\sqrt{t})$ say, which meet at $\sqrt{t} = 0$ and are related by

$$\alpha^+(\sqrt{t}) = \alpha^-(-\sqrt{t}) \quad \text{for } t > 0, \quad (3.24)$$

the first containing particles of spin J and parity $(-1)^{J-\frac{1}{2}}$, and the second particles of parity $(-1)^{J+\frac{1}{2}}$. Of course if the trajectory takes the form

$$\alpha^+(\sqrt{t}) = \alpha_0 + \alpha' \sqrt{t} \quad \text{with } \alpha' > 0, \quad (3.25)$$

there will be physical particles only on α^+ and not on α^- . But if the trajectory is even in \sqrt{t} , such as

$$\alpha^+(\sqrt{t}) = \alpha_0 + \alpha' t, \quad (3.26)$$

then α^\pm coincide, and we expect the fermions to appear as parity doublets, coincident in mass. A more general form such as

$$\alpha^+(\sqrt{t}) = \alpha_0 + \alpha' \sqrt{t} + \alpha'' t + \dots \quad (3.27)$$

splits the degeneracy, but gives a curved trajectory.

The relation (3.13) also means that the dispersion relation for the trajectory function should be written in terms of \sqrt{t} rather than t , and in unsubtracted form it reads

$$\alpha(\sqrt{t}) = \frac{1}{\pi} \int_{\sqrt{t_0}}^{\infty} \frac{\text{Im } \alpha(\sqrt{t'})}{\sqrt{t'} - \sqrt{t}} d(\sqrt{t'}) + \frac{1}{\pi} \int_{-\infty}^{-\sqrt{t_0}} \frac{\text{Im } \alpha(\sqrt{t'})}{\sqrt{t'} - \sqrt{t}} d\sqrt{t'}, \quad (3.28)$$

so we need to know the imaginary parts in both physical regions of the trajectory. Subtractions may of course be needed as in (3.16).

3.4. The trajectories

a) Bosons

The principal means that we have for classifying resonances is the SU(3) scheme [46, 47]. All the well established meson resonances can be grouped into nonets consisting of an SU(3) singlet and an octet. The best established nonets have J^{PC} values 0^{-+} , 1^{-} , and 2^{++} though there are also 0^{++} , 1^{++} and 1^{+-} states of less certain status. Regge trajectories carry a given isospin I , hypercharge Y , baryon number B and $\eta = \pm$ (natural or unnatural parity), and produce physical particles spaced by two units of angular momentum. So taken alone the above states give us just one particle on each trajectory, and do not give much idea of how to draw the trajectories.

There are however several additional features which enable us to make a 'Chew-Frautschi plot' of $\text{Re } \alpha(t)$ versus t , such as fig. 5, with a certain amount of confidence.

These are: a) For some trajectories such as those corresponding to the f , ρ and A_2 we have a good idea from fits to high energy s -channel data what the values of $\alpha(t)$ are for $t < 0$. b) There exists a certain number of higher mass states which fall naturally onto straight lines projected through the lower mass resonances even though their spins are not known. c) The evidence from those meson trajectories that we do know (and from the baryon trajectories) is that all trajectories are roughly straight and parallel. d) There is evidence for exchange degeneracy i.e. for pairs of trajectories of opposite signature which lie essentially one on top of the other and so appear to be a single trajectory with a particle at every integer value of J . This means for example the 1^{-} trajectories are approximately degenerate with the 2^{++} ones. This degeneracy will occur if the exchange force (the u

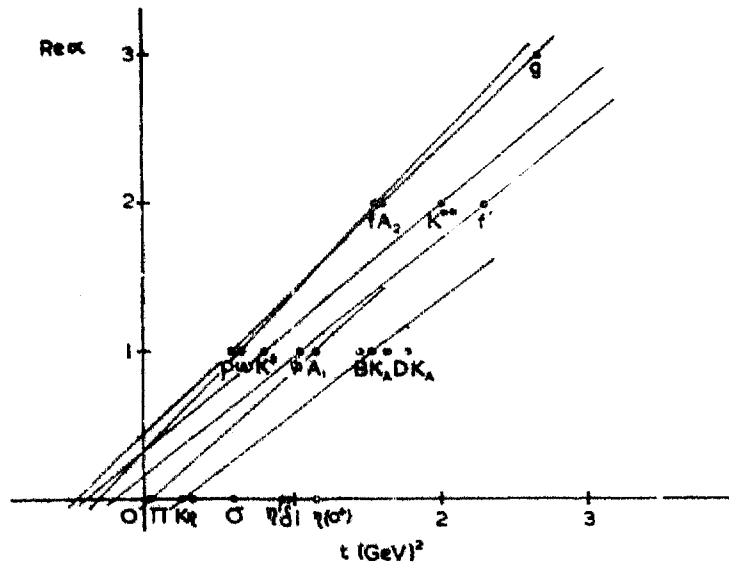


Fig. 5. A Chow-Frautschi plot of $\text{Re } \alpha(t)$ against t for the well established meson resonances.

discontinuity in (2.39)) is very small so that there is at least an approximate equality between $A_{HJ}^{\sigma}(t)$ and $A_{HJ}^{-\sigma}(t)$. There is no a priori reason why the effect of the u discontinuity should be small, but exchange degeneracy does seem to be in accordance with the facts as presented in fig. 5.

This figure contains all the boson resonances of ref. [48] whose existence and quantum numbers are well established (though we have ignored the fact that the A_2 seems to be split). There are however quite a lot of states whose existence is suspected, or which certainly exist but whose quantum numbers are undetermined, and if one wishes to try and include these a speculative picture such as fig. 6 may result. (See also ref. [49].)

Part of the motivation for this figure is that, as we shall discuss in later chapters, there are theoretical arguments in favour of the existence of daughter tra-

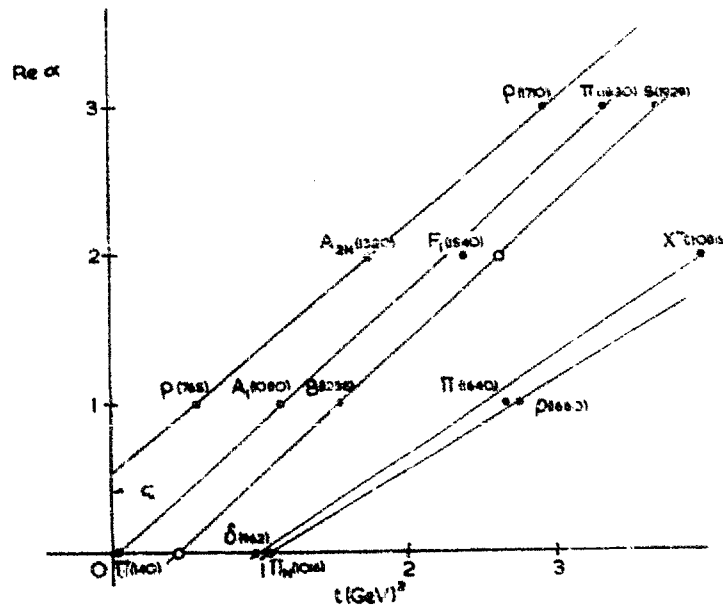


Fig. 6. A speculative Chow-Frautschi plot for the $I = 1$ resonances. An empty circle indicates that no appropriate state has been seen.

jectories which are spaced at integer units below the leading (parent) trajectory at $t = 0$ i.e. for the n th daughter we have

$$\alpha_n(0) = \alpha(0) - n \quad n = 1, 2, \dots \quad (3.29)$$

Since all trajectories have $\alpha(0) < 1$ (because of the Froissart bound) the daughters are always in the left-half J -plane at $t = 0$. However, if they rise parallel to the parents we should expect each partial wave to have a sequence of resonances separated by about $n(\alpha')^{-1}$ in t from the parent. Note that this equal spacing in t means that they get closer and closer together in mass ($=\sqrt{t}$). There is very little concrete evidence for such a complex structure. This is not necessarily damning because we can not observe purely bosonic scattering processes and so all the resonances have to be looked for in production experiments rather than in formation ones. If one remembers the large number of new baryon resonances claimed by the partial-wave analysts in πN scattering, one may expect that there are many boson states, even of quite low mass, remaining undetected.

There are some notable absentees however. The most striking perhaps is the lack of a ρ' resonance lying on the daughter of the ρ . This should have the rho quantum numbers and a mass of about 1250 MeV. Several experiments have searched for such a state without success [50-52]. We shall see in the next chapter that there is no good reason why the daughters should remain parallel to the parents, however.

The only trajectory for which there is a large number of candidates is the ρ - A_2 exchange degenerate trajectory. 'Missing mass' experiments [53], in which the recoil proton momentum is measured in reactions of the form $\pi^- p \rightarrow X^- p$ have identified a large number of narrow $I = 1$ states for X . Unfortunately bubble chamber experiments have not been able to confirm much of the structure [48], but if we

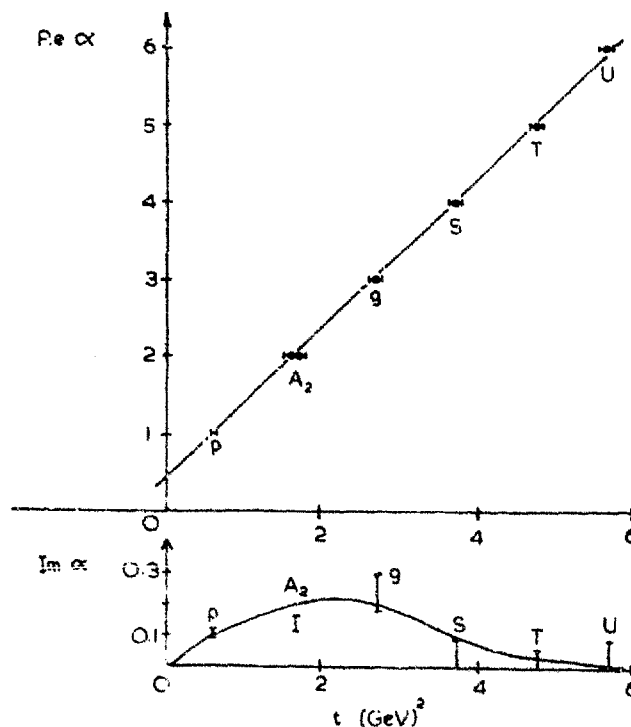


Fig. 7. A plot of $\text{Re } \alpha$ and $\text{Im } \alpha$ for the ρ - A_2 exchange degenerate trajectory as deduced from the missing-mass data of ref. [53].

take the states at their face we can draw an $I = \frac{1}{2}$ trajectory as in fig. 7. Since the widths of the states are also roughly known one can deduce the corresponding $\text{Im } \alpha$ from (3.8). $\text{Im } \alpha$ seems to fall for large t so we can expect the unsubtracted integral (3.15) to converge. In fact the whole contribution of the integral is very small [54], which may explain why the trajectory seems so straight.

In fig. 5 there are no trajectories with $\alpha(0)$ much above $J = \frac{1}{2}$, certainly none with $\alpha(0) \approx 1$. However it is well known that elastic scattering cross sections are roughly constant at high energies, and we shall see in the next chapter that if this is to be explained by Regge-pole exchange we need a Regge trajectory with 'vacuum' quantum numbers ($I = Y = B = 0$, $\eta = +$ and even signature) and $\alpha(0) = 1$, i.e. saturating the Froissart bound. The first particle on such a trajectory would obviously have spin 2, and so the f would seem to be a good candidate. On the other hand exchange degeneracy seems to demand that the f trajectory be degenerate with that of the ω . This is consistent with fig. 5, and we shall find that there are other theoretical grounds for such a degeneracy in chapter 6.

In fact the need for a vacuum trajectory with $\alpha(0) = 1$ was realized before any 2^{++} mesons were known, and so such a trajectory, called the Pomeron (for reasons which will be explained in chapter 7) was simply 'invented' [55]. If such a trajectory exists and is parallel to the others we expect a vacuum 2^{++} particle with a mass about 1 GeV and there have been indications that such a particle may exist [56], but this is not certain. There is also evidence from fits to elastic scattering data (see chapter 7) that the slope of the Pomeron (P) may be smaller than other trajectories, in which case identification with the f is still possible. It could be so flat, or turn over so quickly, that it does not reach $J = 2$, in which case no particle will be seen; or it may even be that there is no such trajectory and elastic scattering requires something other than Regge poles for its explanation. We shall see in chapter 6 that Regge cuts are likely to be important in elastic scattering, but it is hard to see how there could be cuts at $J = 1$ if there were no poles from which to generate them.

At present the nature of this Pomeron pole remains something of a mystery.

b) Fermions

Baryons come in SU(3) singlets, octets and decuplets, and, partly through partial-wave analysis, a large number of low mass states are known [48]. At higher energies many non-strange states have been identified by observing peaks and dips in the forward and backward cross sections [57, 58]. Thus the Chew-Frautschi plots shown in figs. 8-10 are a good deal more impressive than those for the bosons. In particular the evidence for almost straight Regge trajectories of slope $\approx 1 \text{ GeV}^{-2}$ is very good. There is also some evidence for exchange degeneracy though there seems to be a systematic displacement between the even and odd signature octets.

In figs. 11 and 12 we have plotted the natural and unnatural parity trajectories against t . There is a paucity of unnatural parity states which is in total conflict with the MacDowell symmetry requirement (3.24). Since the trajectories are linear in t rather than \sqrt{t} we would expect to find degenerate parity doublets. One way out of this difficulty is to suppose that for some reason the residues of the odd parity trajectories vanish when α passes through a physical integer. In fact we shall see in chapter 7 that there is some evidence for such a behaviour from fits to backward meson baryon scattering. However, it seems implausible that this should happen at every integer, so higher mass states are still expected. An alternative way out of this dilemma is discussed in chapter 5.

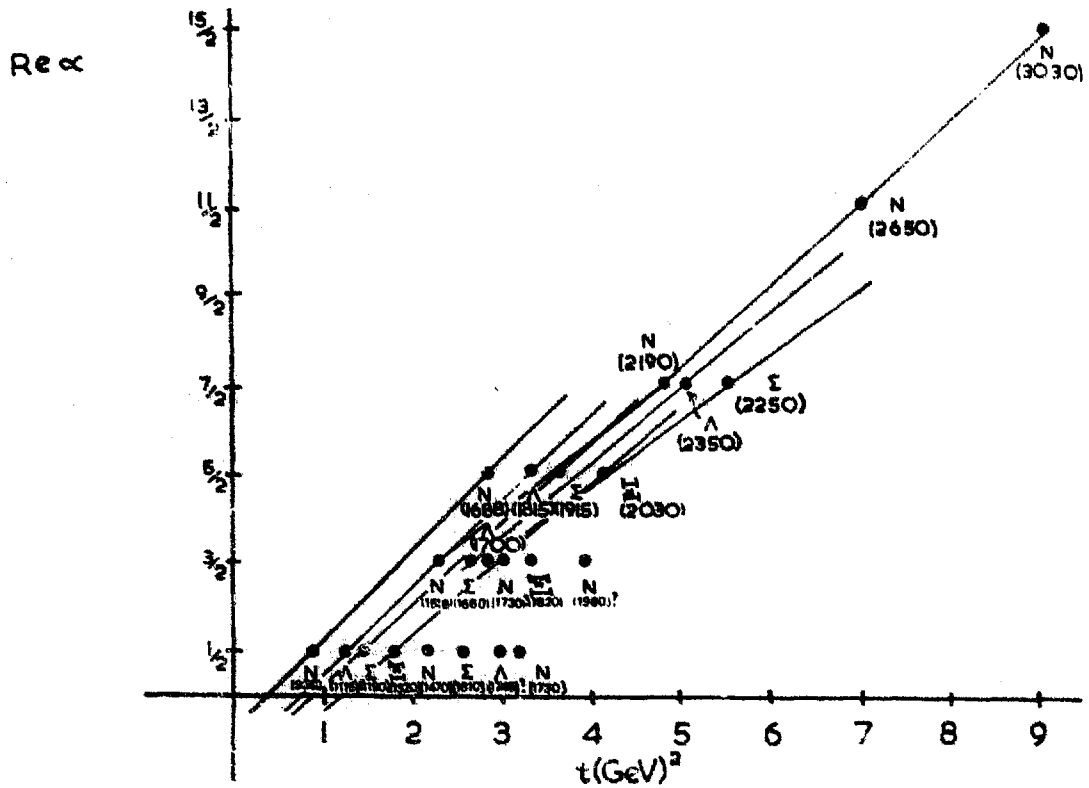


Fig. 8. The Chew-Frautschi plot for the natural parity octet baryons.

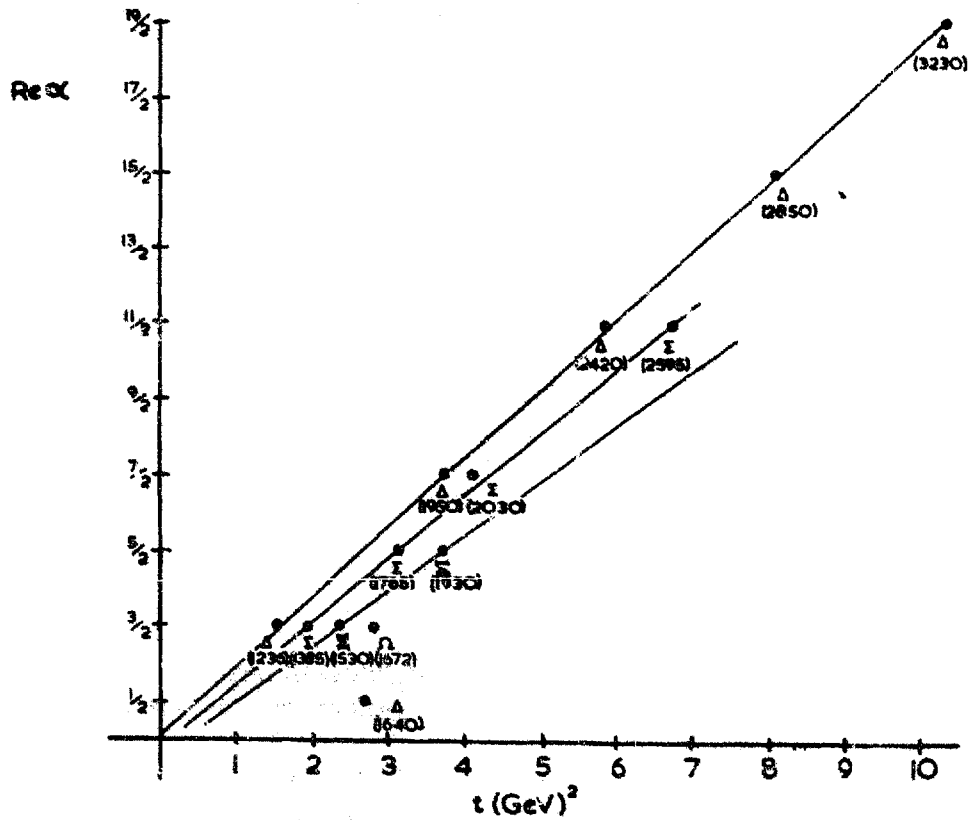


Fig. 9. The Chew-Frautschi plot for the unnatural parity decuplet baryons.

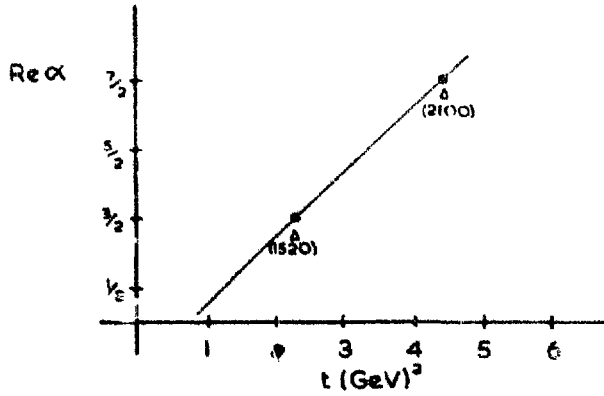


Fig. 10. The Chew-Frautschi plot for the natural parity singlets.

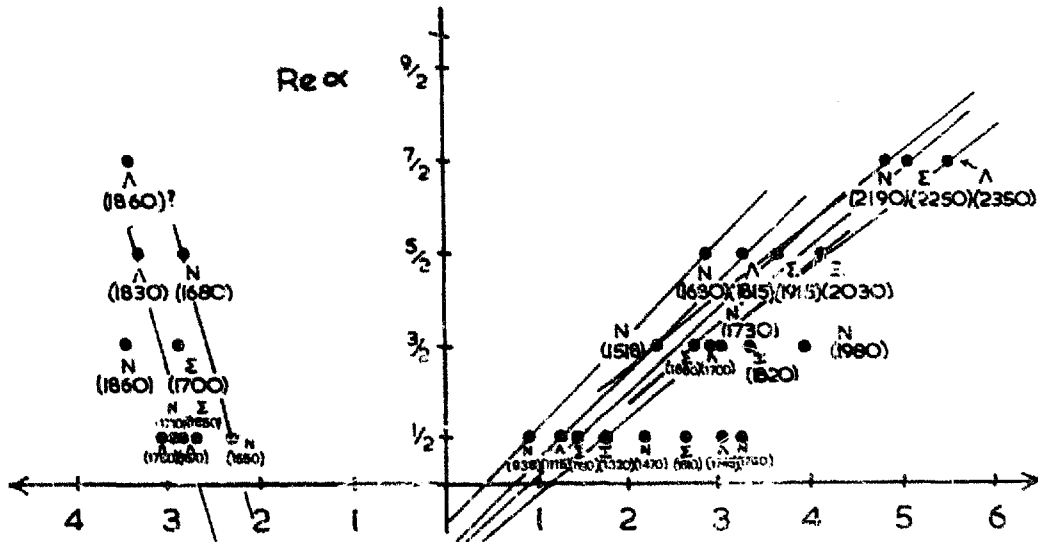


Fig. 11. Octet states of both parities, showing the deficiency of unnatural parity states on the left-hand side.

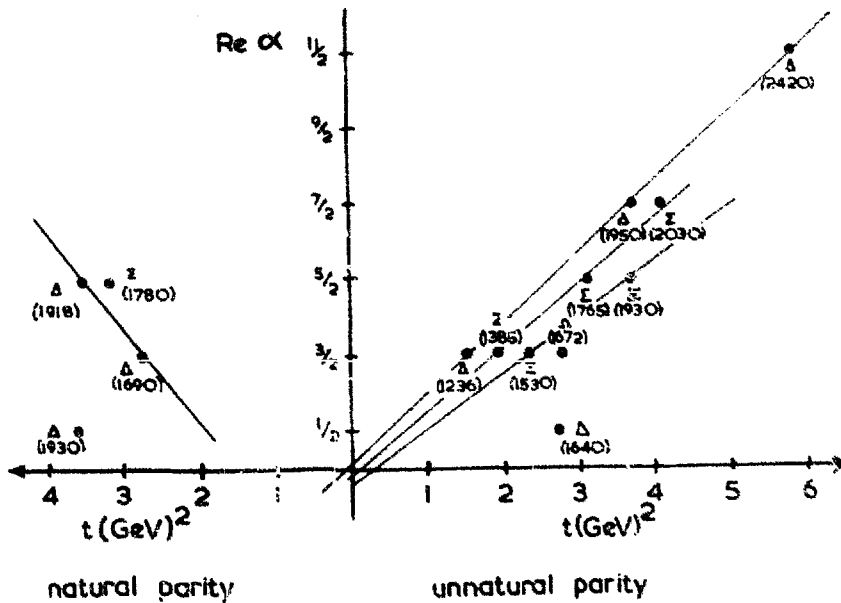


Fig. 12. Decuplet states of both parities.

Since the widths of the baryon states are reasonably well known it is possible to determine $\text{Im } \alpha$ using (3.8). Some examples for the dominant trajectories are presented in fig. 13 [59]. Evidently $\text{Im } \alpha(t)$ is a more or less linear function of t , but with a much smaller slope than $\text{Re } \alpha$. If this behaviour is substituted in (3.16) we again find that the integral is very small, and the straightness of $\text{Re } \alpha$ is due to the dominance of the two subtraction terms.

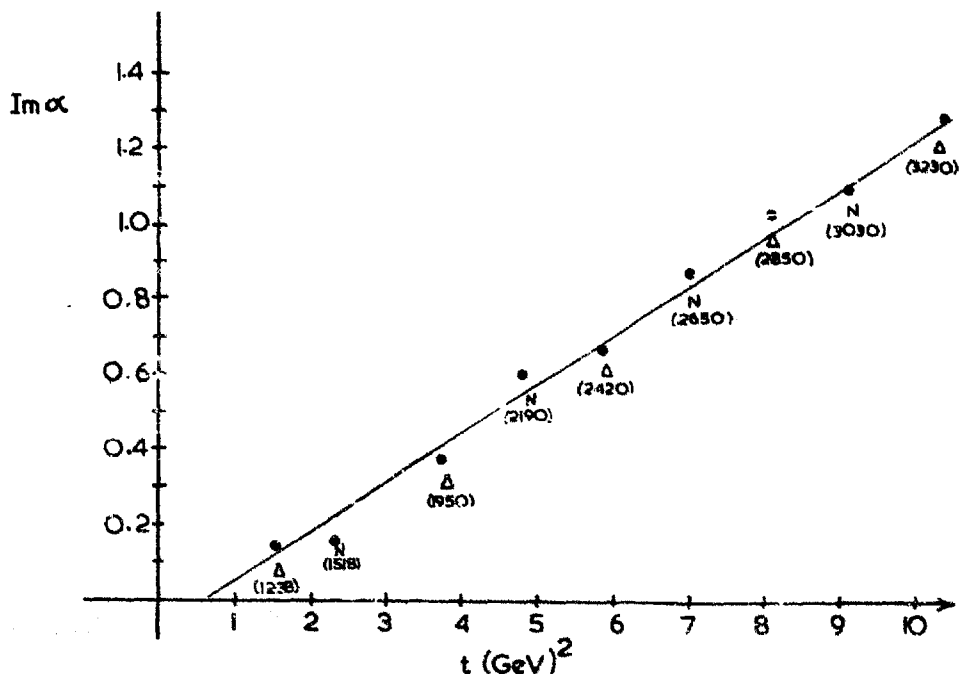


Fig. 13. A plot of $\text{Im } \alpha$ against t for the two baryon trajectories which have the greatest number of established resonances.

If we wish to find the residue of the trajectory we need to know the elasticity of the resonance. (Remember in (3.8) Γ is the total decay width to all channels, not the partial decay width.) If we define the elasticity in terms of the decay width of the resonance to the elastic channel Γ_{el} as

$$x \equiv \Gamma_{\text{el}}/\Gamma,$$

the elastic residue in $13 \rightarrow 13$ is then

$$\beta_{\text{el}}(t) = \frac{x \sqrt{t}}{2q_{t13}} \text{Im } \alpha(t).$$

So the behaviour of the residue depends strongly on the behaviour of the elasticity as one goes up a trajectory. The evidence for baryon trajectories is that x is an exponentially decreasing function of t which we may write as

$$\beta_{\text{el}}(t) \underset{t \rightarrow \infty}{\approx} \text{const. } e^{-d \text{Re } \alpha(t)},$$

where d is a constant ≈ 0.5 . (See refs. [60, 61].)

CHAPTER 4 PROPERTIES OF REGGE POLES

4.1. *Introduction*

In the previous chapter we looked at the resonance interpretation of a Regge trajectory for positive energies. However, much more information can be obtained about a trajectory through its contribution to the asymptotic behaviour of the crossed-channel amplitude, for which we shall develop general expressions in this chapter.

First we discuss the kinematical singularities and zeros of the residue functions, which are required by the analytic properties of the helicity amplitudes. There are kinematical constraints on the helicity amplitudes which may require corresponding constraints in the residues of a given trajectory at the various thresholds and pseudothresholds. There are also constraints at $t = 0$ between helicity amplitudes of different parities, and these may (but need not) require 'conspiracies' between trajectories of opposite parity.

Then in section 4 we briefly examine the problem of unequal mass kinematics when the Regge pole terms have unwanted $t = 0$ singularities. These may be cancelled by 'daughter' trajectories which are spaced at integer units of angular momentum below the 'parent'. The conspiracy and daughter ideas have also been examined by many authors from a group-theoretical viewpoint, and, although it does not add anything essential to the earlier discussions, we briefly review this approach in section 5.

The requirements on a Regge residue do not end with these kinematical considerations, however, for there are also conditions on the behaviour of the residue function whenever a trajectory passes through a nonsense value of J . These are due to the peculiarities of the Froissart-Gribov projection at these points, and may (but need not) result in dips in various differential cross sections. These dips are one of the most interesting aspects of Regge phenomenology.

Because of the complexity of the singularities and constraints in t of a t -channel helicity amplitude, some authors have preferred to work with s -channel amplitudes, which are free of them. We derive an approximate expression for a t -channel Regge pole in an s -channel helicity amplitude, valid to first order in t/s , in section 7.

With all these various factors accounted for we give a general prescription for the contribution of a Regge trajectory in section 8, and discuss some of its characteristic features, and experimental consequences. The reader who is not concerned with the details may like to skip straight to this section, and refer back as necessary.

4.2. *Kinematical singularities and Regge residues*

The residue of a Regge pole is given by (see (3.9))

$$\beta_H(t) = \frac{1}{2\pi i} \int dJ A_{HJ}^{\sigma\eta}(t), \quad (4.1)$$

where the integration contour is taken round the pole at $J = \alpha(t)$. It follows from (4.1) that $\beta_H(t)$ inherits the t singularities of $A_{HJ}(t)$, except that (as we found for the trajectory function in section 3.3) there is no left-hand cut, and of course no pole $(J - \alpha(t))^{-1}$. Thus $\beta_H(t)$ will have both the dynamical right-hand cut of $A_{HJ}(t)$.

beginning at the t -channel threshold, and also its kinematical t singularities. It is these kinematical singularities which concern us in this section.

There have been many papers devoted to finding these singularities [23-25, 62]. One method, devised by Hara [62] and fully exploited by Wang [23], uses the fact that the only kinematical t -singularities of the s -channel amplitudes stem from the half-angle factors $\xi_{\mu\mu'}(z_s)$ (analogous to (2.20)). Hence the only other t -singularities of a t -channel helicity amplitude are those arising from the helicity crossing matrix (2.12). Alternatively general methods have been devised to construct invariant amplitudes free of kinematical singularities (and constraints) which may then be related to helicity amplitudes [24-65]. This procedure is difficult for high spin particles, though it is the usual method for πN and $K N$ scattering, and the photo-production of pions. More recently a very simple and physical interpretation of these singularities has been given [25] and our (necessarily brief) account will exploit this fact. A good general account is that of ref. [64], and a good introductory review may be found in ref. [12].

For our general t -channel process $1+3 \rightarrow 2+4$ there may be kinematical singularities at the thresholds $t = (m_1 + m_3)^2$ and $t = (m_2 + m_4)^2$, and at the pseudo-thresholds $(m_1 - m_3)^2$ and $(m_2 - m_4)^2$, and at $t = 0$. We assume initially that $m_1 > m_3$ and $m_2 > m_4$. Equal masses are considered later.

The threshold singularities stem from the threshold behaviour of the partial-wave amplitudes. For example, if we consider the $1+3$ threshold the behaviour must be

$$A_{HJ}^{\sigma\eta}(t) \sim_{q_{13} \rightarrow 0} (q_{13})^{L_m}, \quad (4.2)$$

where L_m is the lowest possible orbital angular momentum given that J is the total angular momentum; i.e. we expect the usual non-relativistic behaviour. We would expect $L_m = J - (\sigma_1 + \sigma_3)$ except that this value may be incompatible with the parity of the state, in which case we have to increase it by 1. This condition may be written [25]

$$L_m = J - (\sigma_1 + \sigma_3) + \frac{1}{2} [1 - \eta_1 \eta_3 (-1)^{\sigma_1 + \sigma_3 - \nu}] \equiv J - Y_{13}^+ \text{ (say)}. \quad (4.3)$$

But the behaviour (4.2) is not automatically obtained from the Froissart-Gribov projection (as it would be for spinless scattering). Instead since

$$z_t = \frac{t^2 + 2st - t(m_1^2 + m_2^2 + m_3^2 + m_4^2) + (m_1^2 - m_3^2)(m_2^2 - m_4^2)}{4t q_{t13} q_{t24}} \quad (4.4)$$

and

$$q_{t13} = \frac{[t - (m_1 + m_3)^2]^{\frac{1}{2}} [t - (m_1 - m_3)^2]^{\frac{1}{2}}}{2t^{\frac{1}{2}}} \equiv T_{13}^+ T_{13}^- (2t^{\frac{1}{2}})^{-1} \text{ (say)}, \quad (4.5)$$

we find that as $t \rightarrow (m_1 + m_3)^2$, $q_{t13} \rightarrow 0$ and $z_t \rightarrow \infty$; and so in (2.39) $e_{\lambda\lambda'}^J(z_t) \sim z_t^{-J-1}$ from (2.34), and $\xi_{\lambda\lambda'}(z_t) \sim z_t^M$, and $dz_t = ds(2t q_{t13} q_{t24})^{-1}$, giving

$$A_{HJ}^{\sigma\eta}(t) \sim_{q_{t13} \rightarrow 0} (T_{13}^+)^{J-M}. \quad (4.6)$$

The discrepancy between (4.6) and (4.2) must already be present as a kinematical singularity in $A_{HJ}(s, t)$, and hence in $D_{SII}(s, t)$ in (2.39). So we need

$$A_{HJ}(s, t) \underset{T_{13}^+ \rightarrow 0}{\sim} (T_{13}^+)^{M-Y_{13}^+} \quad (4.7)$$

Similar remarks apply at the other thresholds and the pseudothresholds, except that the effective parity of the lighter particle (say m_3) at the pseudothreshold is [25] $\eta_3(-1)^{2\sigma_3}$, so we end up with

$$A_{HJ}(s, t) \propto (T_{13}^+)^{M-Y_{13}^+} (T_{13}^-)^{M-Y_{13}^-} (T_{24}^+)^{M-Y_{24}^+} (T_{24}^-)^{M-Y_{24}^-}, \quad (4.8)$$

where $Y_{13}^\pm = \sigma_1 + \sigma_3 - \frac{1}{2} [1 - \eta_1 \eta_3 (-1)^{\sigma_1 - \sigma_3 - \nu}]$, and Y_{13}^+ is defined in (4.3) above.

If say $m_1 = m_3 \equiv m$, then the pseudothreshold moves to $t = 0$, a point which will be discussed later. Precisely similar conclusions hold if $m_2 = m_4$. And, of course, if $m_1 = m_2 = m_3 = m_4$ both pseudothresholds move to $t = 0$.

These facts allow us to write the threshold behaviour for any masses in the form

$$A_{HJ}^{\sigma\eta} \propto K_{\lambda\lambda'}(t) (q_{t13} q_{t24})^{J-M}, \quad (4.9)$$

where $K_{\lambda\lambda'}(t)$ is given in table 1, and so from (4.1)

$$\rho_{H^{\lambda\lambda'}}^{(\sigma)} = K_{\lambda\lambda'}(t) \left(\frac{q_{t13} q_{t24}}{s_0} \right)^{\alpha(t)-M} \bar{\beta}_H(t), \quad (4.10)$$

where $\bar{\beta}_H(t)$ is free of singularities at the thresholds and pseudothresholds. The scale factor s_0 is arbitrary, but is to be measured in the same units as t so that the units of $\bar{\beta}_H(t)$ can remain constant as $\alpha(t)$ varies. We shall discuss this further in section 8.

Unfortunately this does not exhaust the problem connected with the thresholds because there are also constraints between the different helicity amplitudes at these points. This is because at threshold only the lowest allowed orbital state, $L = 0$ or 1 , is non-vanishing, so the various partial-wave helicity amplitudes are related to each other (at least in the physical region) by the Clebsch-Gordan coefficients which connect them to this L state [63, 64, 2]. These constraints must also relate the residues of a given trajectory in the different helicity amplitudes. They are important from a theoretical point of view because if a Regge contribution is written with the residues having the singularities of (4.10) but not the constraints, the resulting differential cross section (2.14) will have kinematical t -singularities. We know such singularities should not occur because they can not present in (2.9). In practice, however, the thresholds are usually rather far from the s -channel physical region ($t < 0$) where we are interested in using the formulae, and practical difficulties only arise in cases like $\pi N \rightarrow \pi \Delta$ where the $t = (m_\Delta - m_N)^2$ pseudothreshold is near to $t = 0$.

These threshold constraints have been derived by several authors [24, 25, 63-65] and their implications for Regge theory have been extensively discussed by Jackson and Hite [25]. Probably the most elegant derivation is that due to Trueman [64], which is reviewed with several useful examples in ref. [12]. Here we shall content ourselves with giving just one illustrative example in detail, the t channel amplitude for $\pi\pi \rightarrow NN$.

Table 1

The threshold kinematical factor $K_{\lambda\lambda}(t)$.

a) $m_1 \neq m_2, m_3 \neq m_4$ (UU scattering)

$$K_{\lambda\lambda}(t) = (T_{13}^+)^{M-Y_{13}^+} (T_{13}^-)^{M-Y_{13}^-} (T_{24}^+)^{M-Y_{24}^+} (T_{24}^-)^{M-Y_{24}^-}$$

where

$$T_{ij}^+ = [t - (m_i + m_j)^2]^{\frac{1}{2}}; \quad T_{ij}^- = [t - (m_i - m_j)^2]^{\frac{1}{2}}$$

$$Y_{ij}^{\pm} = \sigma_i + \sigma_j - \frac{1}{2} [1 - \eta_i \eta_j (-1)^{\sigma_i \pm \sigma_j - \nu}]$$

where the σ_i is the particle spin, η_i the intrinsic parity, and we are assuming $m_j < m_i$. The other cases can be obtained from this by setting the masses equal and ignoring the pseudothreshold at $t = 0$, thus

b) $m_1 = m_2 = m, m_3 \neq m_4$ (EU)

$$K_{\lambda\lambda}(t) = (t - 4m^2)^{\frac{1}{2}} (M - Y_{13}^+) (T_{24}^+)^{M - Y_{24}^+} (T_{24}^-)^{M - Y_{24}^-}$$

where

$$Y_{13}^+ = 2\sigma_1 - \frac{1}{2} [1 - \eta]$$

c) $m_1 = m_2 = m_3 = m_4 = m$ (EE)

$$K_{\lambda\lambda}(t) = (t - 4m^2)^{M - 2\sigma}$$

In the above we have assumed that if $m_i = m_j$ then the two particles have the same spin and parity.

The two independent helicity amplitudes have the kinematical singularities

$$A_{++,00}(s,t) = \hat{A}_{++,00}(s,t) (t - 4m^2)^{-\frac{1}{2}},$$

$$A_{+-,00}(s,t) = \hat{A}_{+-,00}(s,t) t^{\frac{1}{2}} (t - 4\mu^2)^{\frac{1}{2}} (1 - z_t^2)^{\frac{1}{2}}, \quad (4.11)$$

where $\pm \equiv \pm \frac{1}{2}$, m is the mass of the nucleon and μ that of the pion, and \hat{A} is free of kinematical singularities. There is a constraint at the $N\bar{N}$ threshold which takes the form

$$(A_{++,00} + iA_{+-,00}) \propto (t - 4m^2)^{\frac{1}{2}}. \quad (4.12)$$

If each of these amplitudes is expressed in terms of a single Regge pole (see section 4 for the details) we put

$$A_{++,00}(t) = \gamma_1(t) (t - 4m^2)^{-\frac{1}{2}} (s/s_0)^{\alpha(t)}, \quad (4.13)$$

$$A_{+-,00}(t) = \gamma_2(t) [t(t - 4\mu^2)]^{\frac{1}{2}} (1 - z_t^2)^{\frac{1}{2}} (s/s_0)^{\alpha(t) - 1}. \quad (4.14)$$

where $\gamma_1(t)$ and $\gamma_2(t)$ are kinematical-singularity free residues. When we take the asymptotic form of z_t for large s the latter amplitude becomes,

$$A_{+-,00}(t) \underset{s \rightarrow \infty}{\sim} i\gamma_2(t) t^{\frac{1}{2}} (t - 4m^2)^{-\frac{1}{2}} (s/s_0)^{\alpha(t)}, \quad (4.15)$$

so both (4.13) and (4.15) are singular at $t = 4m^2$. However the constraint (4.12) reads

$$\gamma_1(4m^2) = \gamma_2(4m^2) 2m, \quad (4.16)$$

which we can ensure by putting

$$2m\gamma_2(t) \equiv \gamma_1(t) + \gamma_3(t) [(4m^2 - t)/4m^2], \quad (4.17)$$

where $\gamma_1(t)$ and $\gamma_3(t)$ are unconstrained and singularity free. Putting (4.17) in (4.15) we get, from (2.14)

$$\frac{d\sigma}{dt} = \frac{1}{64\pi s} \frac{1}{q_s^2} \frac{1}{4m^2} \left\{ \gamma_1^2(t) - \frac{t}{4m^2} [2\gamma_1(t)\gamma_3(t) + \gamma_3^2(t) (1 - \frac{t}{4m^2})] \right\} \left(\frac{s}{s_0}\right)^{2\alpha(t)} \quad (4.18)$$

which has no singularity.

In principle such a constraint should be included in any Regge pole fit, but in practice had we used (4.15) instead of (4.17) the singularity at $t = 4m^2$ would not have made much difference. This is fortunate as it is very tedious to have invent parameterizations which take care of all the constraints in processes with high spin.

We come now to the behaviour at $t = 0$ [66], and consider first the unequal mass case $m_1 \neq m_2 \neq m_3 \neq m_4$. From (4.4) we find that as $t \rightarrow 0$, $z_t \rightarrow \epsilon$ where $\epsilon = \pm 1$ according as $(m_1 - m_3)(m_2 - m_4) \geq 0$. Hence the half-angle factor (2.20) has the behaviour

$$\xi_{\lambda\lambda'}(z_t) \underset{t \rightarrow 0}{\sim} t^{|\lambda - \epsilon\lambda'|/2} \quad (4.19)$$

and so from (2.25)

$$\hat{A}_{H_t}(s, t) \sim t^{-|\lambda - \epsilon\lambda'|/2} \quad (4.20)$$

and from the definition (2.47)

$$\hat{A}_{H_t}^\eta(s, t) = \hat{A}_{H_t}(s, t) \pm \eta \hat{A}_{H_t}(s, t) \approx t^{-|\lambda - \epsilon\lambda'|/2} F_1(s, t) \pm \eta t^{-|\lambda + \epsilon\lambda'|/2} F_2(s, t), \quad (4.21)$$

where F_1 and F_2 are regular at $t = 0$. Hence we conclude that $\hat{A}_{H_t}^\eta$ has a singularity of the form

$$\hat{A}_{H_t}^\eta \underset{t \rightarrow 0}{\approx} \frac{F^\eta}{t^{\frac{1}{2} \max\{|\lambda + \lambda'|, |\lambda - \lambda'|\}}} = \frac{F^\eta}{t^{(M+N)/2}}, \quad (4.22)$$

where M, N are defined in (2.16) and (2.19), and F^η is regular at $t = 0$. However such a singular behaviour is not permitted to a single Regge pole, for if we put

$$A_{H_t}(s, t) \equiv \xi_{\lambda\lambda'}(z_t) \hat{A}_{H_t}(s, t) \underset{t \rightarrow 0}{\sim} t^{|\lambda - \epsilon\lambda'|/2} \frac{1}{2} \left[\frac{F^\eta}{t^{(M+N)/2}} \mp \eta \frac{F^{-\eta}}{t^{(M+N)/2}} \right], \quad (4.23)$$

the result is singular unless $F^\eta = \pm F^{-\eta}$, except when $\lambda = \lambda' = 0$. Such an equality of F^η and $F^{-\eta}$ at $t = 0$ is in fact readily deducible by combining (4.21) and (4.22). However this relation can obviously only be satisfied if we have two trajectories of opposite parity. Here we are assuming that there is only one trajectory so we must use instead of (4.22)

$$\hat{A}_H^\eta \underset{t \rightarrow 0}{\sim} \frac{F^\eta}{t^{\frac{1}{2} \ln \{ |\lambda + \lambda'|, |\lambda - \lambda'| \}}} = \frac{F^\eta}{t^{(M-N)/2}} \quad (4.24)$$

(Note that for boson-fermion scattering N is not an integer and we are not allowed to multiply by a half integer power of t . We discuss this problem in section 3.)

In addition to the singularity (4.24), it is evident from (4.5) that if we use the form (4.10) for $\beta_H(t)$ we shall introduce a further singularity $t^{M-\alpha(t)}$. We shall find in section 4 that the $(q_t 13 q_t 24)^{\alpha(t)}$ behaviour of the residue will cancel with that of the leading order term in the asymptotic expansion of

$$a_{\lambda\lambda'}^\alpha(z) \sim z_t^\alpha \sim \left(\frac{s}{2q_t 13 q_t 24} \right)^\alpha, \quad (4.25)$$

but the t^M factor remains, so combining (4.10) with (4.24) we end up with

$$\beta_H(t) = t^{-(M+N)/2} K_{\lambda\lambda'}(t) \left(\frac{q_t 13 q_t 24}{s_0} \right)^{\alpha(t)-M} \gamma_H(t), \quad (4.26)$$

where $\gamma_H(t)$ is free of kinematical singularities. However even this will not do for

$$\beta_H(t) \underset{t \rightarrow 0}{\sim} t^{-\alpha} t^{(M-N)/2} \quad (4.27)$$

is not factorizable between the different helicity amplitudes. We know from (2.67) that we must be able to write β_H as a product of the two vertices independently

$$\beta_{\lambda\lambda'}(t) = \beta_\lambda(t) \beta_{\lambda'}(t). \quad (4.28)$$

The simplest way of satisfying this is to put $\beta_H(t) \sim t^{-\alpha} t^{(M+N)/2}$ so we end up with [66, 67, 37]

$$\beta_H(t) = t^{-(M-N)/2} K_{\lambda\lambda'}(t) \left(\frac{q_t 13 q_t 24}{s_0} \right)^{\alpha(t)-M} \gamma_H(t), \quad (4.29)$$

where $\gamma_H(t)$, the 'reduced residue', is free of kinematical singularities etc., but may have to satisfy constraints like (4.16).

If one pair of masses is equal, say $m_1 = m_3$, then $z_t \sim t^{\frac{1}{2}}$, while if $m_2 = m_4$ as well z_t is finite at $t = 0$, so the \hat{A}_H have just the same singularities as the A_H . These $t = 0$ singularities stem from the fact that $t = 0$ is a pseudothreshold; or (equivalently under crossing) because with one mass pair equal the crossing matrix (2.12) is singular at $t = 0$, while for both pairs equal the line $t = 0$ is the boundary of the s -channel physical region where the s -channel amplitudes must satisfy

$$A_{H_S}(s, t) \sim t^{(|\mu| - |\mu'|)/2}. \quad (4.30)$$

The resulting singularities are [67]

$$A_{H_t} \sim t^{n/2} \quad \text{where } n = [1 - (-1)^{\lambda+\lambda'}]/2 \text{ for EE,}$$

$$A_{H_t} \sim t^{-\sigma_1+z} \quad \text{where } z = [1 - \eta(-1)^{2\sigma_1+\lambda+\lambda'+M}]/4 \text{ for EU,} \quad (4.31)$$

where EE means both $m_1 = m_3$ and $m_2 = m_4$, while EU means $m_1 = m_2$, $m_3 \neq m_4$.

Since q_{t13} is finite if $m_1 = m_3$, and q_{t24} is if $m_2 = m_4$, the threshold factor in (4.10) has the behaviour t^0 for EE and $t^{(M-\alpha)/2}$ for EU, so we end up with $\beta_H \sim t^{n/2}$ for EE and $\beta_H \sim t^{(M-\alpha)/2-\sigma_1+z}$ for EU. However both forms are incompatible with factorization, and if we also take into account the need for

$$(\beta_{EU})^2 = \beta_{EE} \beta_{UU}$$

at $t \approx 0$, with β_{UU} given by (4.29), we end up with

$$\beta_H(t) = t^\delta K_{\lambda\lambda'}(t) \left(\frac{q_{t13} q_{t24}}{s_0} \right)^{\alpha(t)-M} \bar{\gamma}_H(t), \quad (4.32)$$

with δ given in table 2. We discuss alternative forms to this in the next section.

Table 2

The exponent of t in a Regge pole residue (with evasion). For the different mass configurations the $t = 0$ behaviour is t^δ where

- a) UU $\delta = -\frac{1}{2}(M-\Lambda)$
- b) EU $\delta = \frac{1}{2}[|\lambda| - M] + \frac{1}{4}[1 - \eta(-1)^\lambda]$
- c) EE $\delta = \frac{1}{4}[1 - \eta(-1)^\lambda] + \frac{1}{4}[1 - \eta(-1)^{\lambda'}]$

where $\lambda = (\lambda_1 - \lambda_3)$ is the helicity change at the equal mass end in (b).

4.3. Conspiracies

In obtaining the $t = 0$ behaviour of the Regge residue function (4.32) we supposed that there was only a single Regge trajectory (of a given parity), and so we were forced to give the residue the behaviour (4.34) which was less singular than that allowed for the amplitude (4.22). This has the consequence that if we use the residue (4.32) the contribution of the Regge pole vanishes at $t = 0$ for all $A_{H_t}(s, t)$ with $N \neq 0$.

This is because, as is evident from (4.23), the definite parity amplitudes satisfy the constraint equation

$$\hat{A}_{H_t}^{\eta}(s, t) \mp \eta \hat{A}_{H_t}^{-\eta}(s, t) = O(t^N). \quad (4.33)$$

With the behaviour (4.32) we say that the single Regge pole 'evades' this constraint by having an extra t^N factor in its residue.

An alternative solution to this constraint, however, would be for two Regge poles of opposite particles (\pm) to 'conspire' together to satisfy (4.33) by having equal trajectories, $\alpha_+(0) = \alpha_-(0)$, and equal residues

$$\beta_H^+(t) \mp \beta_H^-(t) = O(t^N) \quad (4.34)$$

with all the other quantum numbers (apart from parity) the same [60-66]. With this most singular behaviour we have

$$\beta_H^\eta(t) \sim t^{-\alpha} t^{(M-N)/2}, \quad (4.35)$$

but obviously one can have a less singular behaviour than this without completely evading the constraint.

Unfortunately (4.35) is not compatible with factorization, but we can define the Toller quantum number of a given trajectory, Λ , such that the residue has the most singular behaviour allowed by analyticity for that helicity amplitude, A_{H_t} which has $\lambda = \lambda' = \Lambda$; so putting $\beta_H^\eta = \beta_{\lambda\lambda'}^\eta$, we have

$$\beta_{\Lambda\Lambda}^\eta \approx F_{\Lambda\Lambda}^\eta t^{-\alpha}. \quad (4.36)$$

So for the case (4.35) $\Lambda = N$; and from (4.36) we find

$$\beta_{\Lambda\lambda'}^\eta \approx F_{\Lambda\lambda'}^\eta t^{-\alpha} t^{(\Lambda - |\lambda'|)/2}. \quad (4.37)$$

And in general if we apply factorization we get

$$\beta_{\lambda\lambda'}^\eta \approx F_{\lambda\lambda'}^\eta t^{-\alpha} t^{|\Lambda - |\lambda'||/2} t^{|\Lambda - |\lambda||/2} \quad (4.38)$$

and the constraint analogous to (4.34) is

$$F_{\lambda\lambda'}^\eta \neq \eta F_{\lambda\lambda'}^{-\eta} \sim t^{(|\lambda + \lambda'| - |\Lambda - \lambda'| - |\Lambda - \lambda|)/2} \text{ or } \sim 1, \quad (4.39)$$

whichever is the less singular. The residues $\beta_{\Lambda\Lambda}$, $\beta_{\Lambda\lambda'}$ and $\beta_{\lambda\Lambda}$ have the most singular allowed behaviour, but the others are less singular.

The effect of such a conspiracy can be looked at from the viewpoint of the corresponding s -channel helicity amplitudes [69, 70]. We have

$$A_{H_S}(s, t) = \xi_{\mu\mu'}(z) \hat{A}_{H_S}(s, t) \sim (-t)^{\|\mu_1 - \mu_2\| - \|\mu_3 - \mu_4\|/2} \quad (4.40)$$

and, as required by angular momentum conservation, only amplitudes with no net helicity flip do not vanish in the forward direction. (As $s \rightarrow \infty$, $t = 0$ becomes the forward direction where $z_S = 1$.) The crossing angles χ_i in (2.13) behave like

$$\sin \chi_1 \sim \frac{2m_1 |t|^{1/2}}{s \rightarrow \infty |m_1^2 - m_3^2|} \text{ etc.}, \quad (4.41)$$

and $d_{\lambda_1 \mu_1}^{\sigma_1}(\chi_1) \sim \chi_1^{|\lambda_1 - \mu_1|}$ as $\chi \rightarrow 0$; and so, since the residue (4.38) the t -channel amplitude behaves like

$$A_{H_t}(s, t) \sim t^{\|\Lambda - \lambda'\| + \|\Lambda - \lambda\|/2}, \quad (4.42)$$

we have

$$A_{H_S}(s, t) \sim (-t)^{\frac{1}{2} \min \{ |\lambda_1 - \mu_1| + |\lambda_2 - \mu_2| + |\lambda_3 - \mu_3| + |\lambda_4 - \mu_4| + |\Lambda - |\lambda_1 - \lambda_3|| + |\Lambda - |\lambda_2 - \lambda_4|| \}} \quad (4.43)$$

when the minimum is taken over all $\lambda_1 \lambda_2 \lambda_3 \lambda_4$ in the sum (2.11). So we end up with

$$A_{H_S}(s, t) \sim (-t)^{(|\Lambda - |\mu_1 - \mu_3| + |\Lambda - |\mu_2 - \mu_4||)/2}$$

Thus only amplitudes which have the same helicity flip at both vertices, i.e.

$$|\mu_1 - \mu_3| = |\mu_2 - \mu_4| = \pm \Lambda \tag{4.45}$$

do not vanish in the forward direction. In the case of evasion $\Lambda = 0$, and only amplitudes with no net helicity flip are finite at $t = 0$.

A precisely similar discussion can be given for the EE and EU mass cases except that now there are also kinematical singularities of $A_H(s, t)$ of the form $t^{-\sigma}$ which give us the maximum allowed singularity at each vertex. The result is [69, 70] that the $t = 0$ behaviour of the residue becomes t^δ , with δ given by table 3 instead of table 2.

Table 3

The exponent of t in a Regge pole residue for a Regge pole of Toller number Λ . For the different mass configurations the $t = 0$ behaviour is t^δ where

- a) UU $\delta = \frac{1}{2} \{ |\Lambda - M| + |\Lambda - N| \} - M$
- b) EU $\delta = \frac{1}{2} \{ |\Lambda - |\mu|| - M + [1 + \eta\bar{\eta}(-1)^\Lambda] + \epsilon(\Lambda - 2\sigma_1) \}$
- c) EE $\delta = \frac{1}{2} \{ 2 + \eta\bar{\eta}(-1)^\Lambda + \eta\bar{\eta}(-1)^{\Lambda'} + \epsilon(\Lambda - 2\sigma_1) + \epsilon(\Lambda - 2\sigma_2) \}$

where $\eta = (-1)^{\Lambda+1}$ or $(-1)^{2\sigma-1}$ for $2\sigma \geq t$
 and $\epsilon(\Lambda - 2\sigma) = \Lambda - 2\sigma$ for $\Lambda - 2\sigma > 0$
 $= 0$ for $\Lambda - 2\sigma \leq 0$.

If we were to insert a more zero behaviour than that of table 3, i.e. $A_H(t) \sim t^{\delta+n}$, $n = 1, 2, 3 \dots$ then we have

$$A_{H_S}(s, t) \sim (-t)^{(|\Lambda - |\mu_1 - \mu_2| + |\Lambda - |\mu_2 - \mu_4||)/2+n} \tag{4.46}$$

which vanishes for all helicities. This is known as trivial evasion [66].

For boson-fermion scattering (in the t -channel) λ and λ' are half-odd-integers. So if we were to multiply the amplitude by t^N as in (4.24) we should be introducing a spurious square-root branch point. The amplitudes are analytic in \sqrt{t} and s [23], and one of the amplitudes in (4.21) changes sign on the replacement $\sqrt{t} \rightarrow -\sqrt{t}$, so we have

$$A_{H_t}^\eta(s, \sqrt{t}) = -(-1)^{\lambda-\lambda'} A_{H_t}^{\bar{\eta}}(s, -\sqrt{t}) \tag{4.47}$$

This in the generalized MacDowell symmetry [45] referred to in chapter 3. It means that for fermions there has to be a conspiracy between opposite parity trajectories such that

$$\alpha^-(\sqrt{t}) = \alpha^-(-\sqrt{t}) \quad \text{and} \quad \beta_H^+(\sqrt{t}) = -(-1)^{\lambda-\lambda'} \beta_H^-(-\sqrt{t}) \tag{4.48}$$

This solution corresponds to taking $\Lambda = \frac{1}{2}$ in (4.33), which from (4.44) is obviously necessary if all the s -channel amplitudes are not to vanish at $t = 0$. A conspiracy is thus essential for fermion trajectories.

Although in principle such conspiracies can occur in any process involving particles with spin there are only a few cases where they are likely to be important experimentally. The reason for this is that if an evasive pole can contribute to a helicity amplitude with $\lambda = \lambda' = 0$ then its contribution to $(d\sigma/dt)$ at $t = 0$ will not vanish. It will thus look very similar to a trajectory with Toller number Λ contributing to the $\lambda = \lambda' = \Lambda$ amplitude. Since there is usually not enough polarization information to determine the spin structure of a process in detail it is only really in those processes where a particle can not couple to a non-flip amplitude that a clear distinction can be made. The leading trajectories f , A_2 , ρ etc. are known to evade.

There is, however, a possibility that the pion takes part in a conspiracy in $\gamma p \rightarrow \pi^+ n$ [71] and $np \rightarrow pn$ [72]. In the first case there are no amplitudes with $\lambda = 0$ since $\lambda_\gamma = \pm 1$ only, and $\lambda_\pi = 0$. In the second case the pion couples equally to only two s -channel amplitudes, A_{++}^S and A_{+-}^S , and since the latter involves helicity flip and must vanish at $t = 0$, so must the whole pion contribution. But in both these processes if the pion has $\Lambda = 1$ its contribution can remain finite (in the latter case because the natural parity conspirator trajectory cancels the pion contribution to the flip amplitude and leaves it finite in the no-flip) see section 7.4. As we shall discuss in chapter 7 there is a forward peak associated with the pion in these processes which might seem to favour the conspiracy mechanism, but such conspiracies seem to be incompatible with factorization (see ref. [73]) quite apart from the fact that no suitable scalar trajectory is known, and explanation involving Regge cuts are now preferred.

There is in fact no evidence that any trajectory has anything except the minimum possible Toller number, $\Lambda = 0$ for bosons, and $\Lambda = \frac{1}{2}$ for fermions.

4.4. Daughter trajectories

If we consider the Regge pole term given in (3.3) and take the asymptotic form of the rotation function (2.51), and the residue from (4.32), we get

$$\hat{A}_{H_t}^{\gamma}(s, t) = -\bar{\beta}_H(t) \left(\frac{q_{t13} q_{t24}}{s_0} \right)^{\alpha(t)-M} \left[\frac{e^{-i\pi(\alpha-v)} + s}{2 \sin \pi(\alpha-v)} \right] \gamma_H(\alpha) (z_t/2)^{\alpha-M}, \quad (4.49)$$

where

$$\bar{\beta}_H(t) = 16\pi (2\alpha(t) + 1) t^\delta K_{\lambda'}(t) \gamma_H(t) (-1)^{(\lambda-\lambda' - |\lambda-\lambda'|)/2} \quad (4.50)$$

and

$$\gamma_H(\alpha) = \frac{(2\alpha)!}{[(\alpha+M)!(\alpha-M)!(\alpha+N)!(\alpha-N)!]^{\frac{1}{2}}}. \quad (4.51)$$

Then if we make the replacement

$$z_t \underset{s \rightarrow \infty}{\sim} \frac{s}{2q_{t13} q_{t24}},$$

we obtain

$$A_{H_t}(s, t) = -\beta_{H_t}(t) \left[\frac{e^{-i\pi(\alpha-v)} + s}{2 \sin \pi(\alpha-v)} \right] f_H(\alpha) \xi_{\lambda\lambda}(z_t) \left(\frac{s}{4s_0} \right)^{\alpha-M} \quad (4.52)$$

and with $\xi_{\lambda\lambda}(z) \sim s^M$ we end up with $A_{H_t}(s, t) \sim s^{\alpha(t)}$, the expected Regge behaviour

However it is evident from (4.4) that this derivation goes wrong at $t = 0$ for unequal mass kinematics. For since from (4.5) $q_t \sim t^{-\frac{1}{2}}$ we have $z_t \rightarrow 1$ for all s , and the usual asymptotic behaviour seems to fail at $t = 0$. But this result is rather hard to believe because we know that the scattering amplitude is not singular at $t = 0$ and so it should have a uniform asymptotic behaviour.

The problem is further illuminated if we expand $\hat{a}_{\lambda\lambda}^{\sigma\eta}(z_t)$ in powers of s . We put (from (4.4))

$$z_t = \frac{s}{2q_t 13 q_t 24} (1 + \Delta/s),$$

where

$$\Delta = \frac{1}{2t} [t^2 - t \Sigma + (m_1^2 - m_3^2)(m_2^2 - m_4^2)] \quad (4.53)$$

and expand

$$\hat{a}_{\lambda\lambda}^{\sigma\eta}(z_t) = f(\alpha) [(z_t/2)^{\alpha-M} + a_1(\alpha)(z_t/2)^{\alpha-M-2} + \dots], \quad (4.54)$$

where $a_1(\alpha)$ is a known function. This gives

$$A_{H_t}(s, t) = -\beta_{H_t}(t) \left[\frac{e^{-i\pi(\alpha-v)} + s}{2 \sin \pi(\alpha-v)} \right] f_H(\alpha) \xi_{\lambda\lambda}(z_t) \times \left\{ (s/4s_0)^{\alpha-M} + \Delta(\alpha-M) 4s_0 (s/4s_0)^{\alpha-M-1} + \left[(\alpha-M)(\alpha-M-1)/2 (4s_0 \Delta)^2 + a_1(\alpha) \left(\frac{q_t 13 q_t 24^2}{s_0} \right) \right] (s/4s_0)^{\alpha-M-2} + \dots \right\} \quad (4.55)$$

Thus the term of order $(s/4s_0)^{\alpha-M-n}$ has a singularity t^{-n} . It is this singularity of the Regge pole term which destroys the asymptotic behaviour at $t = 0$.

But we know that the amplitude as a whole is analytic, so something must cancel this unwanted singularity. One suggestion, first broached in ref. [74] and discussed in some detail in chapter 3 of ref. [15] is that the cancellation may come from the background integral in (2.54). There is a difficulty in that the background should be $< O(s^{-\frac{1}{2}})$, but in ref. [15] it is shown that the non-uniform asymptotic behaviour of the Regge pole term can be matched precisely by that of the background, which satisfies the above bound for all $t \neq 0$. The J -plane interpretation of such a background is unclear, however.

An alternative, and much more popular suggestion has been that one should invoke further Regge poles, known as 'daughters' [75] which have singular residues which precisely cancel the singularities produced by the original or 'parent' trajectory. Thus the first daughter has a trajectory $\alpha_1(t)$ such that

$$\alpha_1(0) = \alpha(0) - 1 \quad (4.56)$$

and a residue

$$\beta_1(t) \underset{t \rightarrow 0}{\rightarrow} \beta(0) \frac{\Delta'(\alpha(0) - M)4s_0}{t} + (\text{non-singular term}) ;$$

$$\Delta' = (m_1^2 - m_3^2)(m_2^2 - m_4^2) . \quad (4.57)$$

We need a sequence of such daughters with $\alpha_k(0) = \alpha(0) - k$, $k = 1, 2, 3, \dots$ and with residues whose singular parts are determined by the singularities of (4.55). (Note that β_2 has to cancel the first singularity of α_1 as well as the second term of (4.55), etc.) The non-singular parts of the daughter residues are not determined, however; and the relations (4.56) and (4.57) hold only at $t = 0$ and tell us nothing about the behaviour of the daughters at other t values.

If there is a conspiracy the situation is more complicated than this because the relationship between the trajectories of opposite parity taking part in the conspiracy also has to be maintained; and because of (2.49) a trajectory of unnatural parity can contribute to a natural parity amplitude to non-leading order, and vice-versa. Since for a conspiracy with Toller number Λ an equality of the form (4.39) has to be satisfied not only are the positions of the daughter and conspirator trajectories and the singular parts of their residues determined at $t = 0$, but also the first $(\Lambda - 1)$ derivatives [68]. This limits the possible deviation of the daughter trajectory from the position $\alpha_k(t) = \alpha(t) - k$ as we move away from $t = 0$.

If one pair of masses is equal, say $m_1 = m_3$, $m_2 \neq m_4$, then $\Delta' = 0$ in (4.57) and so the first term is non-singular, and only the even-order daughters are required. And if both mass pairs are equal the q 's are not singular either, and the daughters are not needed. Factorization will demand their presence in such reactions of course, but with non-singular residues.

The final result is that if there is an infinite sequence of daughter trajectories the asymptotic behaviour $A_{H_t}^{\eta}(s, t) \sim s^{\alpha(t) - M}$ is maintained for all t . However at $t = 0$ the ε_t in $\xi_{\lambda\lambda'}(z_t) \rightarrow 1$ we we find that

$$A_{H_t}(s, 0) \sim s^{\alpha(0) - M} \quad (4.58)$$

rather than the usual behaviour $s^{\alpha(0)}$. Since we have chosen Λ to be the helicity ($\lambda = \lambda' = \Lambda$) of the t -channel amplitude which has the normal kinematical behaviour at $t = 0$ (and whose contribution to the differential cross section, therefore, does not vanish) we have the maximum power behaviour $A_{H_t}(s, 0) \sim s^{\alpha(0) - \Lambda}$. Such a behaviour holds only for a very small region round $t = 0$, however (vanishingly small as $s \rightarrow \infty$), which may not include the s -channel physical region, and at larger $|t|$ the usual behaviour still occurs (see ref. [25]).

Thus an infinite sequence of daughter trajectories is needed each having the same quantum numbers as the parent, except that the odd numbered daughters must have opposite signature, so that their signature factors will be identical at $t = 0$, i.e. we need for the k th daughter

$$1 - \sigma_k e^{i\pi\alpha(0) - k} = 1 + \sigma e^{i\pi\alpha(0)} , \quad (4.59)$$

so $\sigma_k = \sigma (-1)^k$. Since the parity of the daughters must be natural or unnatural corresponding to that of the parent the actual parity of the odd daughters' particles will be opposite to those of the parent.

We have already noted in chapter 3 that there is very little evidence for the existence of such daughter trajectories at physical J values for $l > 0$, though they can certainly not be excluded, and there is no reason to expect that (2.58) will hold for larger l .

One way of trying to find out what happens for $l = 0$ is to construct dynamical models for the daughter trajectories. For example one may solve the Bethe-Salpeter equation with unequal masses [76], or represent the Regge poles as sums of ladder Feynman diagrams [77]. Freedman and Wang in their original work on daughter trajectories [75] noted that the Bethe-Salpeter equation must produce daughters, but more recent work [76] has shown that the trajectories do not usually run parallel to the parent, but gyrate wildly in the region of the negative J -axis. An example is shown in fig. 14. This makes one feel that if they exist the daughters may well be rather unimportant objects serving merely to maintain the $s^{\alpha(t)-M}$ behaviour at $l = 0$ but having nothing to do with physical particles.

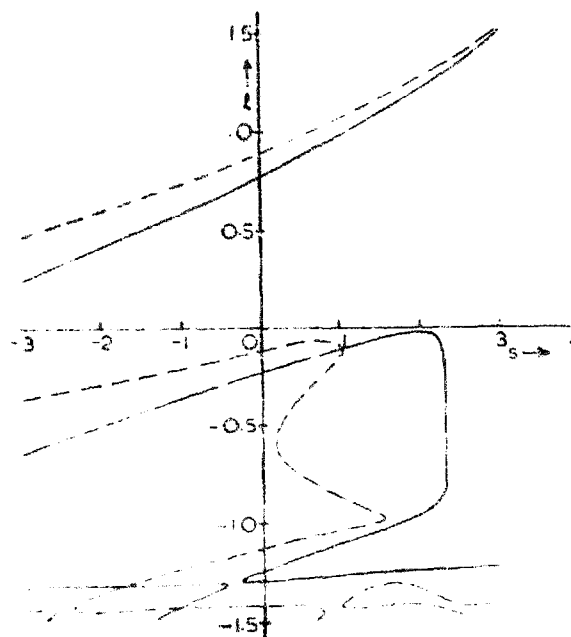


Fig. 14 The Regge trajectories obtained in ref. [76] using the Bethe-Salpeter equation using a potential with a repulsive core. The continuous and dashed curves correspond to different coupling strengths. The strange behaviour of the daughters will be noted.

It should be noted that if the daughters simply cancel the singularities of the leading Regge pole there is no need to include them explicitly in a Regge fit where only the leading power is used. If the daughters have non-singular parts to their residues additional $s^{\alpha(t)-1-M}$ contributions may be present, but the other complications of the J -plane (secondary trajectories, cuts etc.) make them difficult to detect in the experimental data.

4.5. Group theoretical methods

The conspiracy and daughter problems indicate that $l = 0$ is a difficult point for Regge theory. Indeed the singularities which prompted the introduction of daughters strongly suggest that the rotation functions $d_{\lambda\lambda'}^J(z)$ are inappropriate here. The work of Toller [78] and his many followers attempts to rectify this by adopting a more general point of view with regard to the meaning of a partial-wave decomposition.

The partial wave series in the t -channel (2.15) with which we began our discussion of Regge theory involves a decomposition of the amplitude in terms of representation functions of the three dimensional rotation group $SO(3)$ (or, since we include half-integer spins), the covering group $SU(2)$. This rotation group is the 'little group' of the inhomogeneous Lorentz group (or Poincaré group) \mathcal{P} (see e.g. ref. [79]), i.e. it is the group of transformations which leaves invariant the total four-momentum of the incoming (or outgoing) particles

$$P_\mu \equiv (p_{1\mu} + p_{3\mu}) = (p_{2\mu} + p_{4\mu}), \quad \mu = 1, \dots, 4. \quad (4.60)$$

The angular momentum J^2 is of course the eigenvalue of the Casimir operator of this little group.

However, $SO(3)$ is only the little group for $\mathcal{P}_\mu P_\mu^2 = t > 0$. Wigner [80] showed that there are four distinct classes of representations of \mathcal{P} characterized by different values of the Casimir operator P^2 . These are

- | | | |
|--|---|-------------------------|
| (i) Timelike $t > 0$ | ; | little group $SO(3)$ |
| (ii) Spacelike $t < 0$ | ; | little group $SO(2, 1)$ |
| (iii) Lightlike $t = 0$ and $P_\mu \neq 0$ | ; | little group $E(2)$ |
| (iv) Null $t = 0$ and $P_\mu = 0$ | ; | little group $SO(3, 1)$ |

The representations of $SU(2, 1)$ have been studied by Bargman [81], and he showed (theorem 9) that a function which is square integrable on the group manifold can be expanded in terms of the principle and discrete series of representations; the representation functions being again the $d_{\lambda\lambda}^J(z)$, but with z , taking the unphysical values appropriate to $t < 0$. The representation of the scattering amplitude on this basis has the form [82, 83]

$$A_{H_f}(s, t) = -\frac{16\pi}{2i} \int_{-\frac{1}{2}-i\infty}^{-\frac{1}{2}+i\infty} dJ \frac{2J+1}{\sin \pi(J+\lambda')} A_{HJ}(t) d_{\lambda-\lambda'}^J(z) + (\text{nonsense terms}) \quad (4.61)$$

i.e. precisely the same as (2.54) without any Regge poles or cuts in $\text{Re } J > -\frac{1}{2}$. The square-integrability condition in fact amounts to the requirement that

$$A_{H_f}(s, t) = O(s^{-\frac{1}{2}}), \quad (4.62)$$

so the absence of such singularities is obvious. It thus appears that there is a mathematical analogy between making the Sommerfeld-Watson transform and representing the amplitude in terms of its little group for $t < 0$. It should be noted, however, that the Sommerfeld-Watson representation is valid for all s and t , while this little group representation applies only to $t < 0$, so there is by no means a complete equivalence between them. What is more there is nothing very special about the line $\text{Re } J = -\frac{1}{2}$ in (2.54) and we are free to move the contour as we wish, whereas (4.61) can only embrace Regge singularities in the right-half J -plane by analytic continuation. In non-relativistic potential scattering $SO(3)$ is still the little group for the time-like region, but for $t < 0$ the little group is $E(2)$ [84] whose representations are quite unlike those of $SO(2, 1)$ and do not give a satisfactory basis

for continuation in J [85]. Since we know that the Sommerfeld-Watson transform can be performed in potential scattering this is a further indication of the need for caution in assuming the physical equivalence of (2.54) and (4.61).

Bearing these qualifications in mind one can examine what happens at $t = 0$. Because of the mass-shell conditions $p_1^2 = m_1^2$, $p_2^2 = m_2^2$ etc., the fact that $t^2 - (p_1 + p_3)^2 - (p_2 + p_4)^2 = 0$ implies that $P_\mu = 0$ only if $m_1 = m_3$ and $m_2 = m_4$. Thus whether the little group will be $O(3, 1)$ or $E(2)$ depends on whether or not the masses are equal. If they are equal one can try, in analogy with the above, to represent the amplitude on the basis of $SO(3, 1)$ representations, denoted by $d_{TT'\lambda T'}^{\Lambda\sigma}(z_t)$. These have been derived by Toller and Sciarrino [86] (see also ref. [83]) and depend on two Casimir operators one of which, the Toller number Λ , is discrete (taking on values $0, 1, 2, 3 \dots$ or $\frac{1}{2}, \frac{3}{2}, \frac{5}{2} \dots$) and the other, σ , is pure imaginary ($-\infty < i\sigma < \infty$). This extra Casimir operator appears because there are two degrees of freedom in satisfying $P^2 = 0$ with equal masses. (The other corresponds to the variation of s .)

The partial-wave expansion can be written [78, 83]

$$A_{H_t}(s, t=0) = \delta_{\lambda\lambda'} \sum_{TT'} \sum_{\Lambda = -T_M}^{\Lambda + T_M} \int_{-i\infty}^{i\infty} d\sigma (\Lambda^2 - \sigma^2) A_{TT'\lambda}^{\Lambda\sigma}(t) d_{T\lambda T'}^{\Lambda\sigma}(z_t), \quad (4.63)$$

where the $A_{TT'\lambda}^{\Lambda\sigma}$ are suitably defined 'partial-wave' amplitudes, $T_M \equiv \min(T, T')$ and in the summation

$$|\sigma_1 - \sigma_2| \leq T \leq \sigma_1 + \sigma_2 \quad \text{and} \quad |\sigma_3 - \sigma_4| \leq T' \leq \sigma_3 + \sigma_4. \quad (4.64)$$

The hypothesis is then made that one can insert a Toller pole into the σ variable just as one normally inserts a Regge pole into the J integral of (2.54). So if there is a pole at $\sigma = \alpha$ say we have

$$A_{H_t}(s, 0) = (4.63) + \delta_{\lambda\lambda'} \sum_{TT'} g_{TT'} (\Lambda^2 - \alpha^2) d_{T\lambda T'}^{\Lambda\alpha}, \quad (4.65)$$

where Λ is the Toller number of the pole which is restricted by (4.64). The asymptotic behaviour of (4.65) can be deduced from the fact that

$$d_{T\lambda T'}^{\Lambda\sigma}(z_t) \sim (z_t)^{\sigma-1-|\Lambda-\lambda|}, \quad (4.66)$$

so we find

$$A_{H_t}(s, 0) \sim \delta_{\lambda\lambda'} (z_t)^{\alpha-1-|\Lambda-\lambda|}. \quad (4.67)$$

If we compare this with (4.58) we see that it is the same as the asymptotic behaviour of a Regge pole with $\alpha(0) = \alpha - 1$ and Toller number Λ . In fact if one decomposes the $SO(3, 1)$ representations in terms of the $d_{\lambda\lambda'}^j(z_t)$'s one finds [86] that the single Toller pole (4.65) corresponds to an infinite sequence of Regge poles with

$$\alpha_k(0) = \alpha(\Lambda, 0) - k - 1, \quad k = 0, 1, 2, \dots \quad (4.68)$$

In fact it is completely equivalent to a conspiring daughter sequence of Toller number Λ . Away from $t = 0$ of course we lose the $SO(3, 1)$ symmetry so there is no need for the daughters to be parallel to the parents.

Unfortunately a similar argument can not be carried through for unequal masses, because then the little group is $E(2)$, and as has already been mentioned it does not seem to have much connection with Regge theory. It is thus necessary to use arguments based on continuation in the masses to justify the use of Toller poles in this case [87].

The question arises as to whether nature uses this extra degree of freedom at $t = 0$ and contains conspiring daughter sequences, or whether it chooses to ignore it and evade the $t = 0$ constraints. Just as a single Toller pole corresponds to a conspiracy of Regge poles so a single Regge pole corresponds to a 'counter-conspiracy' of Toller poles. The real question is thus which one should regard as primary, the J -plane or the Toller σ -plane. There does not seem to be any way of answering this question a priori, but various models have been suggested. We have already mentioned, in the previous section, that the Bethe-Salpeter equation exhibits the $SO(3, 1)$ symmetry for unequal masses [75]. Of course with unequal masses this symmetry is only to be found off the mass shell. But whether such a model can be taken seriously at the daughter level remembering the peculiar results presented in fig. 14 is doubtful. Other dynamical models, such as those based on the N/D method, which continue on shell two-body unitarity down to $t = 0$ do not possess the extra degree of freedom needed for this symmetry.

The question of the significance of Toller poles can of course only finally be resolved by confrontation with experiment. We have already noted the lack of evidence for daughter trajectories, and the absence of the parity doublets which are needed for conspiracies, and unless a lot more resonant states are found one will be forced to conclude that little trace of the $SO(3, 1)$ symmetry persists in the t -channel physical region. But a more direct test is whether or not conspiring trajectories are needed to fit experimental data. We shall find in chapter 7 that the leading P, P', ρ, ω, A_2 etc. trajectories do not conspire, and we have already noted that the best test of conspiracy, that of the pion in $\gamma p \rightarrow \pi^+ n$ and $pn \rightarrow \pi^+ p$ no longer seems viable. There is thus no evidence for trajectories with $\Lambda > \frac{1}{2}$, and the prospects for Toller poles seem poor at present.

4.6. Nonsense zeros

We have found in section (2.9) that the behaviour of $e_{\lambda\lambda'}^J(z_t)$ at nonsense points introduces various singularities into the partial wave amplitudes, and of course, from (4.1), these must also appear in the residue function.

The story so far is that we may write our Regge pole term either with first type functions as in (2.54) or second type as in (2.58). If we take the asymptotic z_t forms of these functions (either (2.51) or (2.34)), give the residue the kinematical singularities of (4.32), and use the arguments of section 4 to replace z_t by $(s-u)/4q_t$ for all t , $s \rightarrow \infty$, we end up with

$$A_{H_f}(s, t) = -(-1)^{(\lambda-\lambda' - |\lambda-\lambda'|)/2} 16\pi [2\alpha(t) + 1] t^\delta K_{\lambda\lambda'}(t) \bar{\gamma}_H(t) \\ \times \left[\frac{e^{-i\pi(\alpha(t)-v)}}{2 \sin \pi [\alpha(t) - v]} \right] \left\{ \frac{(2\alpha)!}{[(\alpha+M)!(\alpha-M)!(\alpha+1)!(\alpha-N)!]^{1/2}} \right\} \left(\frac{s-u}{8s_0} \right)^{\alpha(t)-M} \xi_{\lambda\lambda'}(z_t), \quad (4.69)$$

where $\bar{\gamma}_H(t)$ is a kinematical singularity free residue function. (Note that to obtain this result from (2.58) it is necessary to use

$$\Gamma(\alpha) = \pi [\sin \pi \alpha \Gamma(1-\alpha)]^{-1}. \quad (4.70)$$

The expression in braces $\{ \} = f_H(\alpha)$ has various singularities which can not be present in the amplitude, and so we require that $\bar{\gamma}_H(t)$ should cancel them. Firstly since

$$(2\alpha)! \frac{2^{2\alpha+1} \alpha! (\alpha + \frac{1}{2})!}{\pi^{\frac{1}{2}} (2\alpha + 1)},$$

we can rewrite

$$f_H(\alpha) = \frac{2^{2\alpha+1}}{\pi^{\frac{1}{2}}} \frac{(\alpha)! (\alpha + \frac{1}{2})!}{[(\alpha + M)! (\alpha - M)! (\alpha + N)! (\alpha - N)!]^{\frac{1}{2}}} \frac{1}{(2\alpha + 1)}.$$

The last factor cancels with that in (4.69). There are poles at $\alpha = -\frac{1}{2}, -\frac{3}{2} \dots$ from the $(\alpha + \frac{1}{2})!$, or at $\alpha = -1, -2, -3$ from the $(\alpha)!$, depending on whether M and N are integers or half integers. Such poles are not expected in the amplitude, and in fact violate the Mandelstam symmetry (2.57), so we need $\bar{\gamma}_H(t) \sim [(\alpha + \frac{1}{2} - \nu)]^{-1}$ to cancel them. Such a behaviour is in fact guaranteed by the behaviour of $\epsilon_{\lambda\lambda'}^J(z_t)$ (see (2.33)) in the Froissart-Gribov projection (2.39) for $A_{HJ}^J(t)$ (as long as it converges). The remaining part of (4.69) has the form

$$\propto \frac{(\alpha + \nu)!}{\sin \pi(\alpha - \nu) [(\alpha + M)! (\alpha - M)! (\alpha + N)! (\alpha - N)!]^{\frac{1}{2}}},$$

which behaves, as $\alpha \rightarrow J_0$, where $J_0 - \nu$ is an integer, like

$$\begin{aligned} (\alpha - J_0)^{-1} & \text{ for } J_0 \geq M & \text{ and } \nu > J_0 > -N \\ (\alpha - J_0)^{-\frac{1}{2}} & \text{ for } M > J_0 \geq N & \text{ and } -N > J_0 > -M \\ \text{finite} & \text{ for } N > J_0 \geq \nu & \text{ and } J_0 > -M. \end{aligned}$$

the branch point $(\alpha - J_0)^{-\frac{1}{2}}$ at the sense-nonsense (sn) points (see section (2.5) for his terminology) must not appear in the amplitude, so we need either $\bar{\gamma}_H(t) \sim (\alpha - J_0)^{-\frac{1}{2}}$ or $\sim (\alpha - J_0)^{\frac{1}{2}}$. The former behaviour would be expected from the Froissart-Gribov projection except that, as described in section (2.9), we expect a superconvergence relation to hold in order to remove the resulting fixed infinite singularity (neglecting the third-double-spectral-function effects at wrong-signature points). So we end up with $\bar{\gamma}_H(t) \sim (\alpha - J_0)^{\frac{1}{2}}$, at least at right signature points. The poles in the ss. region $J_0 \geq M$ correspond of course to the physical particle poles so we should normally expect $\bar{\gamma}_H(t)$ finite here. Then using the factorization requirement (4.28) we must have

$$\beta_{ss} \beta_{nn} = (\beta_{sn})^2 \propto (\alpha - J_0), \tag{4.71}$$

so the nn. residues must vanish like $(\alpha - J_0)$. This is known as the choosing-sense mechanism in that the trajectory couples to the ss. amplitude and decouples from the nn. amplitude. If this behaviour occurs at every nn. point we end up with [25]

$$\bar{\gamma}_H(t) \propto \left[\frac{(\alpha + M)! (\alpha + N)!}{(\alpha - M)! (\alpha - N)!} \right]^{\frac{1}{2}}. \tag{4.72}$$

Combining this with our earlier requirements we can put

$$\bar{\gamma}_H(t) = \gamma_H(t) \frac{2^{2M+1}}{\pi^{\frac{1}{2}}} \frac{1}{(\alpha + \frac{1}{2} - v)!} \left[\frac{(\alpha+M)!(\alpha+N)!}{(\alpha-M)!(\alpha-N)!} \right]^{\frac{1}{2}} \quad (4.73)$$

and we obtain

$$A_{H_f}(s, t) = -(-1)^{(\lambda-\lambda' - |\lambda-\lambda'|)/2} 16\pi t^\delta K_{\lambda\lambda'}(t) \gamma_H(t) \left[\frac{e^{-i\pi(\alpha-v)}}{2 \sin \pi(\alpha-v)} \right] \\ \times \frac{(\alpha+v)!}{(\alpha-M)!(\alpha-N)!} \left(\frac{s-u}{2s_0} \right)^{\alpha-M} \xi_{\lambda\lambda'}(z_f), \quad (4.74)$$

where the residue $\gamma_H(t)$ is free of all kinematical requirements (except possibly threshold constraints).

This expression has the following behaviour at right-signature points

- (1) Poles $(\alpha - J_0)^{-1}$ for $J_0 \geq M$
- (2) Finite for $M > J_0 \geq N$
- (3) Zeros $(\alpha - J_0)$ for $N > J_0 \geq v$ and $J_0 < 0$.

At wrong signature points there is an extra zero, $(\alpha - J_0)$, coming from the signature factor so the behaviour is finite at (1), zero at (2), double zero at (3) (if we neglect the third double spectral function).

There are however three considerations which may complicate this comparatively simple picture:

a) *Ghost-killing factors.* If a trajectory passes through a right-signature sense point for $t < 0$ the residue must vanish. Otherwise for our sense choosing amplitude we should have a particle pole of negative t , i.e. negative (mass)². Since the Froissart bound requires $\alpha(t) < 1$ for $t < 0$ this is only a problem for even signature trajectories, such as the P, f and A₂, at $\alpha = 0$. Such an extra zero will then also have to appear in the other amplitudes because of (4.71). The use of such a zero is sometimes called the 'Chew mechanism' [88].

b) *Choosing nonsense.* At any given nonsense point the trajectory may choose to satisfy (4.71) by having β_{nn} finite and $\beta_{ss} \propto (\alpha - J_0)$. Although it is hard to think of a dynamical mechanism which will cause this to happen it is an equally good solution [33]. We then have $\bar{\gamma}_H(t) \propto [(\alpha - J_0)(\alpha + J_0 + 1)]^{\frac{1}{2}}$ for $N \leq J_0 < M$ as above, but $\bar{\gamma}_H(t) \propto (\alpha - J_0)(\alpha + J_0 + 1)$ for some sense points, say for $s > J_0 > M$, where $s - v$ is an integer $> M$. So we have

$$\bar{\gamma}_H(t) \propto \frac{(\alpha+s)!}{(\alpha-s)!} \left[\frac{(\alpha-M)!(\alpha-N)!}{(\alpha+M)!(\alpha+N)!} \right]^{\frac{1}{2}} \quad (4.75)$$

instead of (4.72). The resulting pole in the nn. amplitude can not correspond to a physical particle of course, and so it must be cancelled (or compensated) by another trajectory. However the asymptotic behaviour of $e_{\lambda\lambda'}^{-\alpha} 1(z_f)$ at a nn. point J_0 is $\sim z_f^{\alpha - J_0 - 1}$ not $\sim z_f^\alpha$ the compensating trajectory should pass through $-J_0 - 1$. This is often called the 'Gell-Mann mechanism'.

If we wish to avoid the need for such a compensating trajectory we can insert an extra zero in the nn. residue. Then by (4.71) an extra zero will also appear in the ss. residue. This is known as the 'no compensation mechanism'

c) *Wrong-signature fixed poles.* Because of the third double spectral function, fixed poles (or infinite square root branch points) may be expected in the signatured amplitudes at wrong-signature points. These do not give rise to poles in the physical amplitudes because they are cancelled by the zero of the signature factor. However if such poles are present in the residues of Regge poles they will cancel the signature factor's zero which we assumed above. There are two points to note about this, however. Firstly these fixed poles may simply be additional to the Regge poles and so not present in their residues (see ref. [89]). And secondly, even if they do multiply the residue, the fact at the nonsense point the residue has contributions only from the third double spectral function, whereas at all other points it has contribution from all three double spectral functions, means that one would certainly expect a zero near to this point.

The resulting behaviour of the residue and of the amplitude at the ss., sn. and nn. points corresponding to these various possibilities is summarized in table 4.

It will be noted that for some choices a zero is expected in various helicity amplitudes at the nonsense points. The classic example of this is the differential cross section for $\pi^-p \rightarrow \pi^0$ which is believed to be controlled near the forward direction by the ρ pole. From fig. 5 we see that $\alpha_\rho(t) = 0$ for $t \approx -0.6 \text{ GeV}^2$. If we consider the two amplitudes for $\pi^- \pi^0 \rightarrow \bar{p}n$ given in (4.11), $\alpha = 0$ is a ss. point for A_{++00} , but a sn. point for A_{+-00} . Hence we see from table 4 that if the ρ chooses sense and there is no wrong signature pole, A_{+-00} vanishes at $t = -0.6$ while A_{++00} remains finite. On the other hand if it chooses nonsense both vanish, while if the residue contains the fixed pole both are finite. The data shown in fig. 15 exhibit a dip but not a zero. This would seem to favour the choosing sense mechanism, though other possibilities can not be ruled out. We shall mention an alternative explanation of this dip, involving cuts, in section (5.6).

Table 4
The behaviour of the residue and amplitude as a trajectory passes through a nonsense point, J_0 .

		Residue			Amplitude			
		nn	sn	ss	Mechanism	nn	sn	ss
Right signature	}	$(\alpha - J_0)$	$(\alpha - J_0)^{\frac{1}{2}}$	1	Sense choosing	$(\alpha - J_0)$	1	$(\alpha - J_0)^{-1}$
		1	$(\alpha - J_0)^{\frac{3}{2}}$	$(\alpha - J_0)$	Nonsense choosing	1	1	1
		$(\alpha - J_0)^{-1}$	$(\alpha - J_0)^{\frac{3}{2}}$	$(\alpha - J_0)$	Chew mechanism	$(\alpha - J_0)^2$	$(\alpha - J_0)$	1
		$(\alpha - J_0)$	$(\alpha - J_0)^{\frac{3}{2}}$	$(\alpha - J_0)^2$	No compensation	$(\alpha - J_0)$	$(\alpha - J_0)$	$(\alpha - J_0)$
Wrong signature	$(\alpha - J_0)^{-1}$	$(\alpha - J_0)^{-\frac{1}{2}}$	1	Fixed pole	1	1	1	

In the above we have assumed the presence of a fixed pole in the residue at the wrong signature point. If this is absent the residue behaves in the same way as at the corresponding right-signature point, and the amplitude is the same except for an extra $(\alpha - J_0)$ from the signature factor.

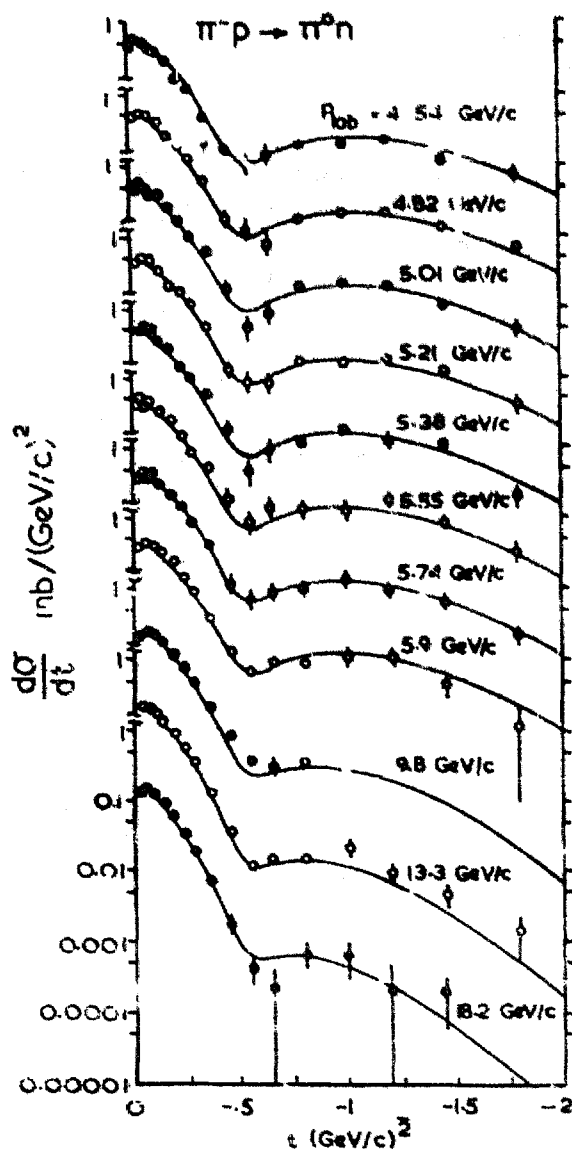


Fig. 15. Data on $d\sigma/dt$ for $\pi^-p \rightarrow \pi^0n$ at various energies. The lines are a fit with ρ and ρ' trajectories from ref. [189].

4.7. Regge poles in s -channel amplitudes

In discussing the contribution of a t -channel pole it has been essential to work with t -channel helicity amplitudes. This is rather unfortunate because, as we have seen, we are involved with several t -channel singularities and constraints, but when finally we combine the helicity amplitudes to give the differential cross section (2.14) all these kinematical singularities cancel out. This must be so since we know that we could equally well use (2.9), and the s -channel amplitudes have no t -singularities except those from $\xi_{\mu\mu'}(z_s)$ in the forward direction, $\phi(s, t) = 0$. Because of this it is clear that there would be many advantages in working with the t -channel poles in s -channel helicity amplitudes instead [69, 70]. In doing this the points we need to take care of are:

- (i) The extra t factors at $t = 0$ required by parity conservation and factorization.
- (ii) The general factorization of the residue for different t -channel helicities λ, λ'

(iii) The various nonsense factors required by the t -channel amplitudes. It turns out that (i) and (ii) can readily be accommodated if we work only to first order in (t/s) , and that the only problem concerns (iii).

One begins by writing

$$A_{H_S}(s, t) = \left(\frac{s}{s_0} \frac{1-z_S}{2}\right)^{|\mu-\mu'|/2} \left(\frac{1+z_S}{2}\right)^{|\mu+\mu'|/2} \left[\frac{e^{-i\pi\alpha-v} + \sigma}{2 \sin \pi(\alpha-v)} \right] \left(\frac{s}{s_0}\right)^{\alpha(t)} \beta_{H_S}(t) \quad (4.76)$$

This has the t singularities required by angular-momentum conservation, and the required Regge behaviour. Now as $s \rightarrow \infty$

$$\left(\frac{s}{s_0} \frac{1-z_S}{2}\right)^{|\mu-\mu'|/2} \rightarrow \left(\frac{-t}{s_0}\right)^{|\mu-\mu'|/2} \quad (4.77)$$

which is independent of s , as required, but it does not satisfy the t -channel factorization condition. To obtain a proper factorized form we make use of the result (4.44) for the $t = 0$ behaviour of a s -channel amplitude due to an evasive ($\Lambda = 0$) pole, and put

$$A_{H_S}(s, t) = \left(\frac{-t}{s_0}\right)^{(|\mu_1-\mu_3| + |\mu_2-\mu_4| - |\mu-\mu'|)/2} \times \left\{ \left(\frac{s}{s_0} \frac{1-z_S}{2}\right)^{|\mu-\mu'|/2} \left(\frac{1+z_S}{2}\right)^{|\mu+\mu'|/2} \left[\frac{e^{-i\pi\alpha-v} + \sigma}{2 \sin \pi(\alpha-v)} \right] \left(\frac{s}{s_0}\right)^{\alpha(t)} \gamma_{H_S}(t) \right\} \quad (4.78)$$

where $\gamma_{H_S}(t)$ is factorizable in terms of s -channel helicities, i.e.

$$\gamma_{\mu_1\mu_2\mu_3\mu_4} = g_{\mu_1\mu_3} g_{\mu_2\mu_4} \quad (4.79)$$

Although we have deduced (4.78) using the result (4.44) it must in fact be valid for any mass combinations since A_{H_S} has no t singularities which depend on the masses.

The factorization (4.79) in terms of s -channel helicities stems from the factorization of the crossing matrix (2.12), but (4.78) is valid only to first order in t/s from (4.77). Hence one must not extrapolate (4.78) too far from the forward peak, but in view of its simplicity it has much to recommend it.

It is not difficult to generalize the above result to include conspiring trajectories except that one needs to construct combinations of s -channel amplitudes corresponding asymptotically to definite parity in the t -channel (see ref. [69]). One then deduces from (4.44) the form

$$A_{H_S}^{\eta}(s, t) = \left(\frac{-t}{s_0}\right)^{|\Lambda - (|\mu_1-\mu_3| + |\mu_2-\mu_4| - |\mu-\mu'|)|} \times \{4.78\} \quad (4.80)$$

where the 'good parity' amplitudes are

$$A_{H_S}^{\eta}(s, t) = A_{\mu_1\mu_4\mu_1\mu_2} + \eta \sigma \eta_2 \eta_4 (-1)^{\sigma_4 - \sigma_2 + \mu_4 - \mu_2} A_{\mu_3\mu_4\mu_1\mu_2} \quad (4.81)$$

and constraints like (4.33) hold. This reduces to (4.78) if $\Lambda = 0$.

As we noted above the chief problem with this method arises when we consider

the nonsense factors. For suppose that in some process just one t -channel helicity amplitude A_{H_t} vanishes like $(\alpha - J_0)$ for $t < 0$. Then using the crossing relation (2.11) we deduce that there must be a constraint on the s -channel amplitudes of the form

$$\sum_{H_s} M(H_s H_t)^{-1} A_{H_s}(s, t) \propto (\alpha(t) - J_0), \quad (4.82)$$

which is not easy to parameterize. But from table 4 it can be seen that if the trajectory chooses nonsense there are no zeros in the t -channel amplitudes at the right signature points. (Remember the nn. pole will be compensated.) Similarly if there are fixed poles in the residues at wrong-signature points there are no zeros in any of the amplitudes. So for these two cases there is no problem. The choosing sense, and Chew mechanisms have zeros in some amplitudes and not in others, however, and there is no alternative to using the crossing matrix as in (4.82).

4.8. Regge poles and asymptotic behaviour

From the earlier sections of this chapter we have ended up with a Regge pole asymptotic form (4.74) which contains the various kinematical factors discussed in sections 2 and 3, (which depend on the external masses and whether or not a conspiracy occurs) and which assumes that the trajectory chooses sense. We have also mentioned various alternative α factors which occur if the trajectory chooses nonsense, if there are fixed poles, or ghost-killing factors, etc. We now wish to discuss the general characteristics of (4.74).

a) Power behaviour. Evidently

$$A_{H_t}(s, t) \underset{s \rightarrow \infty}{\sim} \left(\frac{s-u}{2s_0}\right)^{\alpha(t)} \sim \left(\frac{s}{s_0}\right)^{\alpha(t)}$$

for all t except for unequal mass kinematics when $z_t = -1$ at $t = 0$ and there is instead an $((s-u)/2s_0)^{\alpha-M}$ behaviour as we approach $t = 0$. But since $t = 0$ is outside the physical region this is not usually very important. See ref. [25] for a thorough discussion. Apart from this the pure power behaviour is characteristic of a pole. To non-leading order in (s/s_0) there will be many corrections, due to the non-leading terms in the expansion of $d_{\lambda\lambda'}^{\alpha}(z_t)$, and due to daughter trajectories and trajectories of opposite parity, quite apart from more subtle corrections needed because a single Regge pole has the wrong singularities in s (see e.g. chapter 3 of ref. [15]). This should warn us against trying to work too far below the leading singularity in a Regge fit. With such a power behaviour we predict from (2.14)

$$\frac{d\sigma}{dt} \sim \left(\frac{s}{s_0}\right)^{2\alpha(t)-2} \quad (4.83)$$

and from the optical theorem (2.8)

$$\sigma^{\text{tot}}(s) \sim \left(\frac{s}{s_0}\right)^{\alpha(t)-1} \quad (4.84)$$

if a single trajectory dominates.

b) *Trajectory dominance.* If there are several trajectories present, the leading trajectory, the one with the largest $\text{Re } \alpha(t)$, will be dominant asymptotically. The value of s above which this occurs depends partly on the ratio of the two couplings,

but particularly on the value of s_0 . In most Regge fits s_0 is held fixed at $\approx 1 \text{ GeV}^2$, but this is mainly a matter of 'folklore' as we have no theoretical way of determining what it should be (see however section (6.5)). On the other hand if the correct value were much larger than this it would be hard to understand why a smooth Regge behaviour is observed in most amplitudes for $s > 2-3 \text{ GeV}^2$.

c) *Connection with particles.* The trajectory functions should of course pass through physical particles for $t > 0$ and we can obtain a good idea of what they will be simply by continuing the straight lines of figs. 5-12 to $t < 0$. The dominant boson trajectories will be those of the vector and tensor nonets with intercepts between about 0 and $\frac{1}{2}$, plus of course the Pomeron with $\alpha(0) = 1$. We discuss fits much more fully in chapter 7, and here we will give just one illustration based on the $\pi^-p \rightarrow \pi^0n$ data in fig. 15. A simple fit of the equation

$$\log(d\sigma/dt) = [2\alpha(t) - 2] \log(s) + \text{constant} \tag{4.85}$$

at different t values gives the curve for $\alpha(t)$ shown in fig. 16. This extrapolates almost through the ρ particle, though of course there is no reason why the trajectory should be exactly straight.

A fixed power behaviour, $\alpha(t) = J_0$ (a constant), would correspond either to a fixed J plane pole (which does not give rise to a t plane pole and hence is not a particle) or to a Kronecker-delta term in the J -plane

$$A_{HJ}(t) = \delta_{JJ_0} \frac{g^2}{t - m^2}, \tag{4.86}$$

which would correspond to an elementary particle of spin J_0 . Except possibly in photoproduction (see chapter 7) such fixed power behaviours are not found.

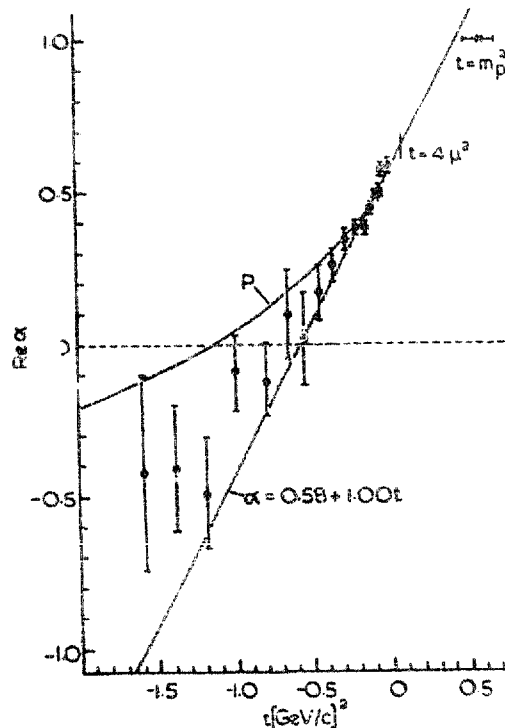


Fig. 16. The ρ trajectory as deduced from a single pole fit to the $\pi^-p \rightarrow \pi^0n$ differential cross section in ref. [184]

tion. We shall find in chapter 7 that in those cases where it has been possible to test this relation it is reasonably well verified. It is not really a test of Regge pole dominance however since it follows directly from dispersion relations and the power behaviour $s^{\alpha(t)}$. For example with a once subtracted dispersion relation we have at fixed t

$$\text{Re} A(s, t) = s \frac{P}{\pi} \int_{\text{RH}}^{\infty} \frac{\text{Im} A(s', t)}{(s' - s)s'} ds' + s \frac{P}{\pi} \int_{\text{LH}}^{-\infty} \frac{\text{Im} A(s', t)}{(s' - s)s'} ds' \quad (4.90)$$

and if $\text{Im} A(s, t) \sim s^{\alpha(t)}$ for $s > 0$, and we use

$$\frac{P}{\pi} \int_0^{\infty} \frac{ds'}{s' - s} s'^{\alpha-1} = -s^{\alpha-1} \cot \pi\alpha$$

and

$$\frac{1}{\pi} \int_0^{\infty} \frac{ds'}{s' + s} s'^{\alpha-1} = -s^{\alpha-1} \text{cosec} \pi(\alpha - 1)$$

the result (4.89) follows. The same result is found for any number of subtractions. Thus any success of the phase-energy relation is really just a test of the power behaviour and analyticity rather than of Regge pole dominance.

The other important fact about (4.74) is that the phase is the same for all helicity amplitudes. Since polarization phenomena depend on helicity amplitudes having different phases (see (7.1)) a single Regge pole can not give rise to polarization. Thus for example the fact that there is a polarization of 10-15% in $\pi^-p \rightarrow \pi^0n$ shows that there must be some other exchange besides the ρ trajectory contributing despite the success of the fit in fig. 16. It is of course not difficult to think of other contributions which can interfere with the ρ trajectory to produce the polarization (see chapter 7).

f) *Factorization*. We have already noted that a Regge residue has to factorize, (2.67), so if only a single Regge pole is involved in a given set of processes we deduce (see fig. 1)

$$\left(\frac{d\sigma}{dt}\right)_{12 \rightarrow 34}^2 = \left(\frac{d\sigma}{dt}\right)_{11 \rightarrow 33} \left(\frac{d\sigma}{dt}\right)_{22 \rightarrow 44} \quad (4.91)$$

Unfortunately it is not easy to test this directly because there are not enough different processes available (p or n have always to be used as the target). Moreover it depends crucially on the dominance of just a single trajectory. We shall mention some tests in chapter 7. It is however an important constraint on Regge residues.

Another application of factorization is that since $1+2 \rightarrow 3+4$ has the same t -channel poles as $1+\bar{4} \rightarrow 3+\bar{2}$ (i.e. we just rotate the right-hand side of fig. 1) the contribution of a given pole to these two processes must be the same apart from a possible \pm sign. So if a single trajectory dominates these two cross sections are predicted to be identical. This is known as 'line reversal' symmetry. Thus for example the P contribution to $p\bar{p} \rightarrow p\bar{p}$ must be the same as that for $p\bar{p} \rightarrow p\bar{p}$. This also follows from the Pommeranchuk theorem however (see chapter 7).

g) *Dips*. We have found that Regge pole amplitudes may vanish at nonsense points (section 6), but that there is some ambiguity about this depending on the presence of fixed poles, etc. We shall see in chapter 7 that some but by no means

tion. We shall find in chapter 7 that in those cases where it has been possible to test this relation it is reasonably well verified. It is not really a test of Regge pole dominance however since it follows directly from dispersion relations and the power behaviour $s^{\alpha(t)}$. For example with a once subtracted dispersion relation we have at fixed t

$$\text{Re} A(s, t) = s \frac{P}{\pi} \int_{\text{RH}}^{\infty} \frac{\text{Im} A(s', t)}{(s' - s)s'} ds' + s \frac{P}{\pi} \int_{\text{LH}}^{-\infty} \frac{\text{Im} A(s', t)}{(s' - s)s'} ds' \quad (4.90)$$

and if $\text{Im} A(s, t) \sim s^{\alpha(t)}$ for $s > 0$, and we use

$$\frac{P}{\pi} \int_0^{\infty} \frac{ds'}{s' - s} s'^{\alpha-1} = -s^{\alpha-1} \cot \pi\alpha$$

and

$$\frac{1}{\pi} \int_0^{\infty} \frac{ds'}{s' + s} s'^{\alpha-1} = -s^{\alpha-1} \text{cosec} \pi(\alpha - 1)$$

the result (4.89) follows. The same result is found for any number of subtractions. Thus any success of the phase-energy relation is really just a test of the power behaviour and analyticity rather than of Regge pole dominance.

The other important fact about (4.74) is that the phase is the same for all helicity amplitudes. Since polarization phenomena depend on helicity amplitudes having different phases (see (7.1)) a single Regge pole can not give rise to polarization. Thus for example the fact that there is a polarization of 10-15% in $\pi^-p \rightarrow \pi^0n$ shows that there must be some other exchange besides the ρ trajectory contributing despite the success of the fit in fig. 16. It is of course not difficult to think of other contributions which can interfere with the ρ trajectory to produce the polarization (see chapter 7).

f) *Factorization*. We have already noted that a Regge residue has to factorize, (2.67), so if only a single Regge pole is involved in a given set of processes we deduce (see fig. 1)

$$\left(\frac{d\sigma}{dt}\right)_{12 \rightarrow 34}^2 = \left(\frac{d\sigma}{dt}\right)_{11 \rightarrow 33} \left(\frac{d\sigma}{dt}\right)_{22 \rightarrow 44} \quad (4.91)$$

Unfortunately it is not easy to test this directly because there are not enough different processes available (p or n have always to be used as the target). Moreover it depends crucially on the dominance of just a single trajectory. We shall mention some tests in chapter 7. It is however an important constraint on Regge residues.

Another application of factorization is that since $1+2 \rightarrow 3+4$ has the same t -channel poles as $1+\bar{4} \rightarrow 3+\bar{2}$ (i.e. we just rotate the right-hand side of fig. 1) the contribution of a given pole to these two processes must be the same apart from a possible \pm sign. So if a single trajectory dominates these two cross sections are predicted to be identical. This is known as 'line reversal' symmetry. Thus for example the P contribution to $p\bar{p} \rightarrow p\bar{p}$ must be the same as that for $p\bar{p} \rightarrow p\bar{p}$. This also follows from the Pommeranchuk theorem however (see chapter 7).

g) *Dips*. We have found that Regge pole amplitudes may vanish at nonsense points (section 6), but that there is some ambiguity about this depending on the presence of fixed poles, etc. We shall see in chapter 7 that some but by no means

all the expected dips occur. Unfortunately there are also other possible explanations of these dips involving Regge cuts, so there is some uncertainty, and the correct explanation is still unclear.

h) *Exchange degeneracy*. In chapter 3 we noted evidence for the degeneracy of opposite signature. It is obvious from (2.39) that the identity of $A_{HH}^J(t)$ and $A_{HH}^{\bar{J}}(t)$ implies that there is no exchange force, i.e. no u -channel discontinuity. This would mean that the residues were identical as well as the trajectories. Obviously the difference between two such exchange degenerate trajectory contributions is proportional to

$$\left[\frac{e^{-i\pi(\alpha-v) + \sigma}}{2 \sin \pi(\alpha-v)} \right] - \left[\frac{e^{-i\pi(\alpha-v) - \sigma}}{\sin \pi(\alpha-v)} \right] = \frac{2\sigma}{\sin \pi(\alpha-v)}, \quad (4.92)$$

which is purely real. We shall see in chapter 6 that there are some theoretical grounds for expecting this sort of cancellation to occur.

Exchange degeneracy also implies the absence of fixed poles (since there is no third double spectral function), and that the trajectories will choose nonsense. This is because e.g. an even signature trajectory must have a ghost-killing zero at $\alpha = 0$ in a sense amplitude, which must therefore also be present in the exchange degenerate odd-signature trajectory.

i) *The Regge pole parameters*. It is evident from the above discussion that there are several characteristic features of Regge pole exchange which we can hope to observe in the data. But there are many ambiguities, both from the presence of other secondary trajectories and cuts, and from the various choices as to conspiracy or evasion, sense or nonsense coupling, etc. Even when we have decided about these there are the free parameters of the trajectory function $\alpha(t)$ and the reduced residues $\gamma_H(t)$. The former can be predetermined to some extent from the position of the resonances, particularly if one is prepared to limit oneself to linear trajectories, but the behaviour of $\gamma_H(t)$ is almost wholly arbitrary. In a few cases the residues of the particle poles are known coupling constants, but even then there is no unique prescription for analytic continuation. It is usual to adopt a hypothesis of simplicity, and suppose that once the essential kinematical and dynamical factors have been taken care of the reduced residue will be either a constant or a slowly varying function. One factor which will greatly affect this t -dependence is the choice made for s_0 , since varying it is equivalent to including an extra exponential t factor in the residue. It is obvious that if the residue is given too much arbitrary structure the fit loses its conviction, but how many parameters one should permit oneself is very much a matter of taste.

This concludes our survey of the properties of Regge poles, but before we can confront these predictions with experiment we need to know about the other types of J -plane singularities which may be present, in particular the branch cuts.

CHAPTER 5 REGGE CUTS

5.1. Introduction

In the preceding chapter we discussed the exchange of a Regge pole, which corresponds to the exchange of a single particle. The subject of this chapter is Regge cuts which, speaking roughly, correspond to the simultaneous exchange of two or

more particles. But whereas we have been able to describe the properties of poles with some confidence all that one can say with certainty about cuts is that they must exist, and they have known positions.

In chapter 2 cuts were invoked to remove the incompatibility of the Gribov-Pomeranchuk fixed pole with the unitarity equation. Other solutions to this problem have been suggested, such as that the poles become like essential singularities when they are iterated with unitarity [93, 94], but all such suggestions run into the problem that such a singularity at a nonsense point $J = J_0$ would lead to an s^{J_0} behaviour of the scattering amplitude, which is incompatible with the Froissart bound for $J_0 > 1$. A simple pole is allowed because it is cancelled by the zero of the signature factor and so does not contribute to the asymptotic behaviour.

The confidence that cuts can be invoked to shield the fixed poles rests mainly on Mandelstam's argument [95] which we shall discuss in the next section. This demonstrates that the same sort of Feynman diagrams that contribute to the third double spectral function, and hence to the fixed poles, also give rise to cuts. There are still two problems, however. One is that there are some Feynman diagrams which likewise appear to produce cuts (the so-called Amati-Fubini-Stanghellini, AFS, cuts [96]) but whose cuts are known to be cancelled by other diagrams. They appear on unphysical sheets and do not contribute to the asymptotic behaviour. One can thus not be completely sure that Mandelstam's cuts are not similarly cancelled, though the fixed-pole argument gives good reason to believe that they are not. The other problem is that we still only know how to evaluate the magnitude of the cut discontinuity in terms of Feynman diagram models. Since few people nowadays suppose that Lagrangian field theory is ever likely to be the basis of a viable theory of strong interactions this means that there is no agreed method to calculate cuts.

However, some models which do permit one at least to estimate the cuts given the input pole parameters have been suggested, and we shall describe and comment on two of these (the absorption and eikonal models) in sections 4 and 5. Then we discuss some of the general characteristics of cuts as indicated by such models. In particular we introduce the as yet unsolved problem of whether the cuts are strong enough to interfere with the poles in such a way as to produce the various dips observed in differential cross sections, or whether these dips are, as discussed in section (4.6), due to nonsense zeros.

In addition to these dynamical Regge cuts there may also be fixed cuts which we give a brief mention in section 7.

5.2. Regge singularities and Feynman diagrams

The calculation of the asymptotic behaviour of Feynman diagrams has been discussed by several authors, and comprehensively reviewed in refs. [97, 98]. In this section we shall mainly just quote some of the relevant results, and the reader who is interested in the details should consult ref. [97] or the original works.

We consider a diagram consisting of scalar meson lines of mass m with vertex coupling constant g . The contribution of such a diagram to the scattering amplitude is given by (neglecting normalization factors)

$$A(s, \hat{\theta}) = \lim_{\epsilon \rightarrow 0} g^n \int \frac{d^4 k_1 \dots d^4 k_l}{\prod_{r=1}^n (q_r^2 - m^2 + i\epsilon)}, \quad (5.1)$$

where the q_γ are the four-momenta of the n internal lines; the k_i are the internal loop momenta (that is independent linear combinations of the q_γ), and there are m vertices. The particles in such a theory are of course elementary, and since they are scalar they contribute a Kronecker delta's to the s -channel partial wave amplitudes of the form

$$A_J(s) = \delta_{J0} \frac{g^2}{s - m^2} \tag{5.2}$$

However if we consider an infinite sequence of ladder diagrams such as fig. 17 it can be shown (ref. [99]) that the diagram with n rungs contributes at large s

$$A^n(s, t) \sim \frac{g^2}{s} \frac{[K(t) \log s]^{n-1}}{(n-1)!} \tag{5.3}$$

where $K(t)$ is a known function (given by the box diagram). So, if we are justified in supposing that the limit of the sum of the diagrams is the sum of the limits, the sequence gives

$$A(s, t) \sim \frac{g^2}{s} \sum_{n=1}^{\infty} \frac{[K(t) \log s]^{n-1}}{(n-1)!} = g^2 s^{\alpha(t)} \tag{5.4}$$

where $\alpha(t) = -1 + K(t)$. So the sum gives us a Regge pole behaviour with a trajectory functions which begins at -1 for $t \rightarrow \infty$, and which is cut above the t threshold. This is exactly the same as the behaviour of a trajectory in Yukawa potential scattering which it closely resembles, and the fact that the trajectory end point is at -1 is due to the $1/s$ behaviour of (5.2).



Fig. 17. An infinite sequence of ladder diagrams which sum to give a t -channel Regge pole.

General rules for the asymptotic behaviour of more complex diagrams have been given [98]. In particular it turns out that for all planar diagrams (i.e. diagrams which can be drawn in a plane without crossing lines) the behaviour is always of the form

$$s^{-n}(\log s)^m \quad \text{with} \quad n \geq 1, m \geq 0 \tag{5.5}$$

This knowledge is not much use to use since, as we have just seen, the Regge behaviour comes from summing infinite sets of diagrams. But it does indicate that if we were to treat the sides of the ladders in fig. 17 as composite particles we should still probably get a Regge pole.

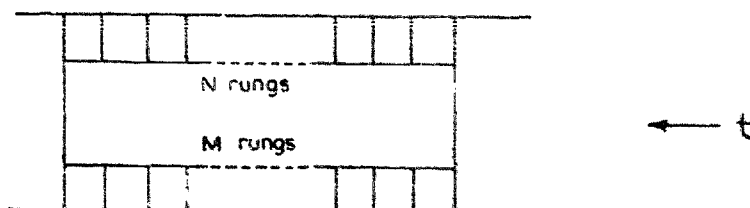


Fig. 18. One of an infinite sequence of double-ladder diagrams which might be expected to give rise to a Regge cut, but does not.

The Regge cuts are supposed to stem from the exchange of two or more Regge poles, so we might try a model such as fig. 18. However it can be shown that each such diagram has an asymptotic behaviour $\sim s^{-3} \log s$ independent of N and M , so this should also be the behaviour of the sum. This gives us a fixed-cut like behaviour with $\alpha_c(t) = -3$ for all t .

At first sight this result is rather surprising since if we take each of the ladder sums in fig. 18 as giving us a Regge pole behaviour, and then apply elastic unitarity in the s -channel to find the discontinuity across the two particle cut (fig. 19a), we get [96]

$$\text{Disc}_2 A(s, t) = \frac{q_s}{32\pi^2 \sqrt{s}} \int A_1(s, t_1) A_2^*(s, t_2) d\Omega_s \quad (5.6)$$

and if we put each $A_i(s, t) \sim s^{\alpha_i(t)}$ this gives

$$\text{Disc}_2 A(s, t) \sim s^{\max[\alpha_1(t_1) + \alpha_2(t_2)] - 1}, \quad (5.7)$$

where t_1 and t_2 are subject to the constraint

$$\delta(t, t_1, t_2) = -(t^2 + t_1^2 + t_2^2) + 2t_1 t_2 + 2t t_1 + 2t t_2 > 0. \quad (5.8)$$

(We shall perform this sort of calculation explicitly below, section 4.) These are the AFS cuts. They are cancelled by the contributions of the other unitary dissections which can be made through fig. 19a, such as that shown in fig. 19b. Thus the on mass shell AFS cuts are cancelled by the off mass shell parts of the Feynman integration, and the cuts are spurious.

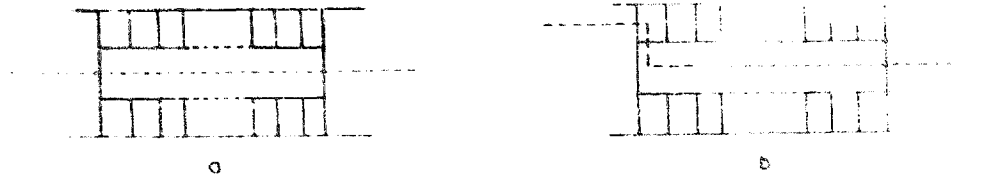


Fig. 19. (a) The two-particle unitarity section of fig. 18. (b) A different partition of fig. 18 which involves 3 particle unitarity.

If we wish to avoid this cancellation we must turn to non-planar diagrams [95]. The simplest is shown in fig. 20 where we have Reggeon ladders connected by crosses at each end. Because of the crosses this diagram has a third (su) double spectral function and so it is also involved in the t -channel Gribov-Pomeranchuk fixed poles. Since it requires a minimum of 4 particles in the s -channel it will obviously not be present in potential scattering. This has only Regge poles for suitable potentials like the Yukawa.

In order to demonstrate more explicitly that fig. 18 does not have a cut and fig. 19 does, one can make use of the Reggeon calculus invented by Gribov [100] which allows one to work with mixed Feynman-Regge pole diagrams. Here we shall briefly outline this method [101, 102].

Consider the diagram fig. 21 where R_1 and R_2 are Regge pole amplitudes. In terms of the Feynman rules this may be written (neglecting normalization factors)

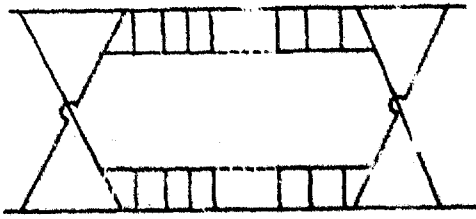


Fig. 20. An example of a type of diagram which, when summed over all possible numbers of rungs, does give rise to a Regge cut.

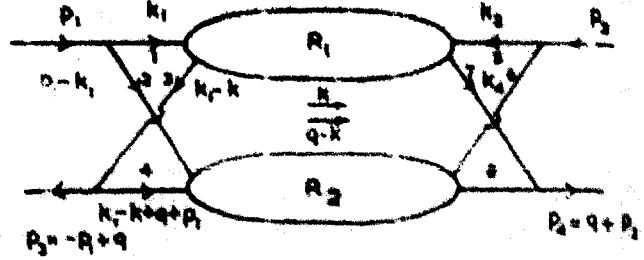


Fig. 21. The Feynman diagram of fig. 20 with the ladders replaced by Regge poles R_1 and R_2 .

$$A(s, t) = i\lambda^2 \int d^4k \frac{d^4k_1 d^4k_2 R_1(k_1, k_2, k) R_2(p_1 - k_1, p_2 - k_2, q - k)}{s \prod_{m=1} d_m}, \quad (5.9)$$

where d 's are the denominators corresponding to the internal lines

$$d_1 = k_1^2 - m^2 + i\epsilon,$$

$$d_2 = (p_1 - k_1)^2 - m^2 + i\epsilon, \text{ etc.} \quad (5.10)$$

We then introduce the four-vectors

$$p'_1 = p_1 - (m^2/s) p_2,$$

$$p'_2 = p_2 - (m^2/s) p_1. \quad (5.11)$$

which have the property that

$$p'^2_1 = p'^2_2 = 0 + O(1/s^2); \quad 2p'_1 p'_2 = s. \quad (5.12)$$

As usual $s = (p_1 + p_2)^2$ and $t = (p_1 - p_3)^2 = q^2$, and we can write

$$q = \frac{t}{s} (p'_2 - p'_1) + Q, \quad (5.13)$$

where Q is a vector perpendicular to the plane containing p_1 and p_2 . Then following Sudakov [103] we write each of the internal momenta in terms of their component in the plane of p'_1 and p'_2 , and those perpendicular to it, i.e.

$$k = \alpha p'_2 + \beta p'_1 + k_\perp,$$

$$k_1 = \alpha_1 p'_2 + \beta_1 p'_1 + k_{1\perp},$$

$$k_2 = \alpha'_2 p_1 + \beta p'_1 + k_{2\perp}. \quad (5.14)$$

We then express each of the denominators (5.10) in terms of these variables:

$$d_1 = \alpha_1 \beta_1 s + k_{1\perp}^2 - m^2 + i\epsilon ,$$

$$d_2 = (\alpha_1 - m^2/s)(\beta_1 - 1)s + k_{1\perp}^2 - m^2 + i\epsilon , \text{ etc.} \quad (5.15)$$

and the integration volume elements are

$$d^4k = \frac{1}{2} |s| \, d\alpha d\beta d^2k_{\perp} \text{ etc.} \quad (5.16)$$

We then assume, and this is the crucial simplification, that $R_1(k_1 k_2 k)$ is large only when the energy variable $s_1 \equiv (k_1 + k_2)^2 \approx 2k_1 k_2 = \beta_1 \alpha_2 s$ is large (i.e. of order s), and when the momentum transfer k^2 , and the 'masses' k_1^2, k_2^2 are small (i.e. of order m^2); and similarly for R_2 . Thus we are assuming that the Regge amplitude is peripheral, and that its form factors vanish $\sim (k_i^2)^{-1}$ (see ref. [95]). Hence the only important region of integration in (5.9) is when

$$k_{1\perp}^2, k_{2\perp}^2, k_{\perp}^2 \sim m^2 ; \quad \alpha, \beta, \alpha_1 \sim m^2/s ; \quad \text{and} \quad \beta_1, \alpha_2 \sim 1 . \quad (5.17)$$

We then take a factorized form for the Regge amplitudes

$$R_1(k_1, k_2, k) = g_1 [k_1^2, (k - k_1)^2, k^2] g_2 [k_2^2, (k + k_2)^2, k^2] \xi_{J_1}(2k_1 k_2)^{J_1(k^2)} ,$$

$$R_2(p_1 - k_1, p_2 - k_2, q - k) = g'_1 ((p_1 - k_1)^2, (p_1 - k_1 - q + k)^2, (q - k)^2)$$

$$\times g'_2 ((p_2 - k_2)^2, (p_2 - k_2 + q - k)^2, (q - k)^2) \xi_{J_2}[2(p_1 - k_1)(p_2 - k_2)]^{J_2((q - k)^2)} , \quad (5.18)$$

where ξ_{J_i} are the signature factors, and we have used J_i for the positions of the poles (to avoid confusion with the Feynman parameters α). When these are substituted in (5.9), and the restrictions (5.17) are noted, the integrations over $\alpha_1, \alpha_2, \beta_1, \beta_2, \alpha, \beta, k_{1\perp}$ and $k_{2\perp}$ can be carried out separately, and we end up with

$$A(s, t) = \frac{1}{|s|} \int d^2k_{\perp} N_{J_1 J_2}(q, k_{\perp}) s^{J_1 + J_2} \xi_{J_1} \xi_{J_2} , \quad (5.19)$$

where

$$N_{J_1 J_2} = \int d^2k_{\perp} d\beta_1 d\alpha_1 d\alpha \frac{s^2 \lambda^2 g_1 g'_2 \beta_1^{J_1} (1 - \beta_1)^{J_2}}{4 \prod_{m=1}^d m} . \quad (5.20)$$

The function $N_{J_1 J_2}$ is the Feynman integral over the cross on the left of fig. 21, and it appears squared because the right-hand side gives an identical result.

In order to determine the J -plane structure of (5.19) we must make a Froisart-Gribov projection, which for spinless scattering is

$$A_J(t) = \frac{1}{\pi} \int_{-\infty}^{\infty} D_S(s, t) Q_J(z_i) . \quad (5.21)$$

Now from (5.19)

$$D_S(s, t) = \frac{1}{|s|} \int d^2k_{\perp} N_{J_1 J_2}^2(q, k_{\perp}) s^{J_1 + J_2} \text{Re} \{ \xi_{J_1} \xi_{J_2} \} \quad (5.22)$$

and using the fact that $Q_J(z_f) \sim s^{-J-1}$ we have

$$A_J(t) \propto \int d^2k_{\perp} \frac{\text{Re} \{ \xi_{J_1} \xi_{J_2} \}}{J+1 - J_1(k^2) - J_2[(q-k)^2]} \quad (5.23)$$

This gives us the expected cut, and its position is the same as that of the AFS cut (5.7).

It is fairly straightforward in principle to apply this technique to more complicated diagrams where there are larger numbers of Regge poles connected by Feynman propagators. One is still left with the problem however that one needs to be able to perform the Feynman integration (5.20) which involves the form factors of the Reggeons, since the couplings g_i, g'_i are functions of the masses k_i^2 . It is not possible to evaluate the cuts using just the on mass shell properties of the Regge poles.

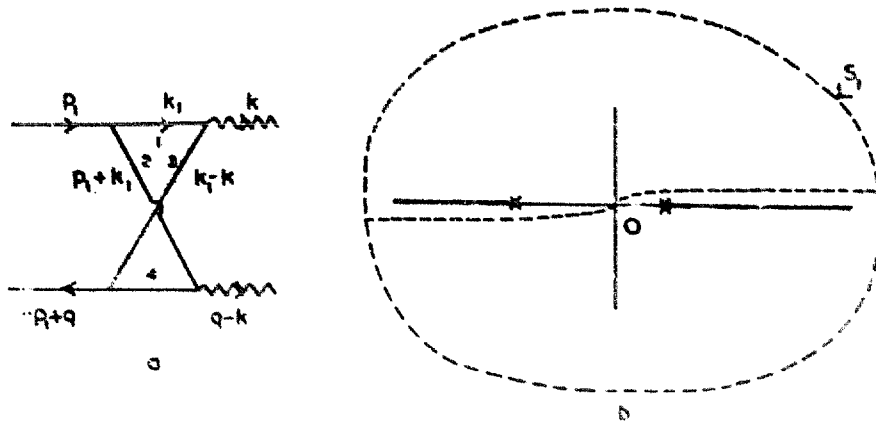


Fig. 22. (a) The Feynman amplitude for the left side of fig. 21, with two Reggeon external lines. (b) The contour of integration along the real s_1 axis in (5.24). The contour may be closed either above or below, but in either case it encloses one of the unitary cuts of A_1 .

The integral for $N_{J_1 J_2}$ is essentially an integral over the Feynman amplitude shown in fig. 22a. If we express it in terms of invariants it becomes

$$N(t, t_1 t_2) = \int_{-\infty}^{\infty} ds_1 A_1(s_1, ; t_1, t_2), \quad (5.24)$$

where

$$A_1(s_1, t; t_1, t_2) = \int_0^1 d\beta_1 \beta_1^{J_1} (1-\beta_1)^{J_2} \int_{-\infty}^{\infty} \frac{d\tau_1 dk_{1\perp} s'_1 s'_2}{4 \prod_{m=1}^{\infty} \epsilon'_m} \quad (5.25)$$

is the amplitude of fig. 22a apart from the J 's in the numerator. These are due to the spins of the Reggeons and it can be shown that they do not affect the singularity

structure of A_1 . The integral in (5.24) is carried out at fixed t over s_1 , and one can now see why it is important that the diagram should have a cross. For the presence of the cross means that A_1 will have both a right-hand cut corresponding to the s_1 thresholds, and a left-hand one corresponding to the u_1 thresholds ($s_1 + u_1 + t = 4m^2$). So the integration contour will be as in fig. 22b. Since this diagram $\sim 1/s_1^2$ for large s_1 , if there were only a right-hand cut or only a left-hand cut one would be able to close the contour by a semicircle in the upper or lower half plane (respectively) without enclosing any singularities and so conclude that $N = 0$. It is only the fact that A_1 has both cuts that gives us a finite answer. In fact if we distort the contour to enclose say the right-hand cut we get (since A_1 is real analytic)

$$N(t, t_1, t_2) = 2i \int_{4m^2}^{\infty} \text{Im} A_1(s_1, t, t_1, t_2) ds_1. \quad (5.26)$$

It is now fairly obvious that one can generalize the above discussion and obtain the amplitude for the Regge cut in a general two Reggeon diagram like fig. 23 provided that both the amplitudes A_1 and A_2 have both left- and right-hand cuts. But unfortunately there is then no reason to expect that the integral (5.26) will converge if the amplitude A_1 has Regge behaviour.



Fig. 23. A general two Reggeon exchange amplitude, which will give rise to a Regge cut provided A_1 and A_2 both contain crosses, as in fig. 21.

5.3. *Physical interpretation*

So far this has just been mathematics, and we must now try to understand the physical meaning of these requirements on A_1 and A_2 . We can get some idea about deuteron-deuteron scattering. We expect that to a good approximation this can be represented by the scattering of the neutrons and protons separately. If we represent each of the interactions by the exchange of a single Reggeon we get diagrams like fig. 24. But fig. 24b where two Reggeons are exchanged between the same pair of particles, becomes very unlikely at high energy because the two nucleons do not stay together long enough. This diagram has no third double spectral function and does not give a cut (only an AFS cut). On the other hand fig. 24c where the two Reggeons come from different nucleons can occur at high energies, and this diagram has precisely the structure of fig. 21. One may thus conclude that in general the existence of a cut depends on the structure of the scattering particles - they must break up and reform, virtually [104].

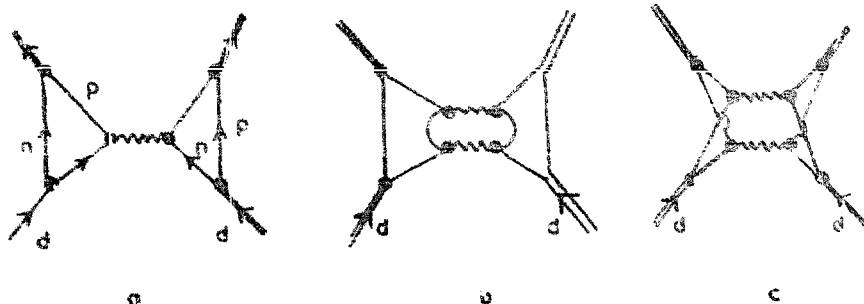


Fig. 24. Deuteron-deuteron scattering. (a) A single interaction between the nucleons represented by a Regge pole exchange. (b) Double Regge pole exchange between the same pair of nucleons. (c) Double Regge pole exchange between different pairs of nucleons.

There is obviously some relation between the above discussion and Glauber theory [105], but in fact the relation turns out to be a very complicated one. For example if one considers πd scattering, Glauber theory gives (fig. 25)

$$A_{\pi d} = G(t) (A_{\pi p} + A_{\pi n}) + \int G(p^2) A_{\pi p} A_{\pi n} d^2 p, \quad (5.27)$$

where G is the deuteron form factor (and represents the fact that the nucleons are off the mass shell). The first terms are the single scatterings on the proton and neutron, while the second term is the shadow correction, and represents the fact that for part of the time one nucleon is behind the other and so invisible to the pion. This must obviously make the amplitude smaller than the sum of the single scattering terms. It was shown by Gell-Mann and Udgaonkar [106] that the second term of (5.27) has a cut like behaviour, and this has been analysed in greater detail by Abers et al. [107]. However the diagram fig. 25c does not have a real cut, only an AFS cut, if the particles are on the mass shell. In order to get a Regge cut we should have to regard the pion as a composite object too. This does not mean that Glauber theory is wrong, at least at low energies, only that it does not give a valid result at asymptotic energies. In fact one can estimate that it will break down when the energy is of the order of $m_\pi(m_N/\delta)^{1/2}$ where δ is the binding-energy of the deuteron [108].

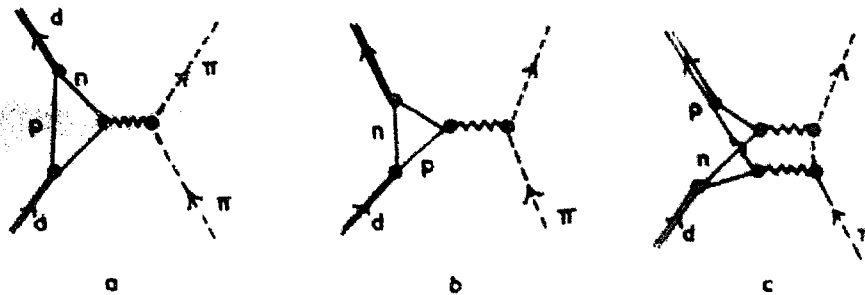


Fig. 25. Diagrams with single and double scattering for pion-deuteron scattering.

The situation is further complicated by the fact that the iteration of the potential (the Regge pole) corresponds both to diagrams like fig. 26a in which the potential acts several times between the same pair of particles, and ones like fig. 26b in which the ordering of the interactions is different, and which involve multiple scattering [109, 110]. This appears to contradict what was said above about the improbability of multiple scattering between the same pair of particles, but since in Glauber theory the energy of the incident particle is high, and any changes in it due to scattering very small (otherwise the deuteron would break up), we have a cer-

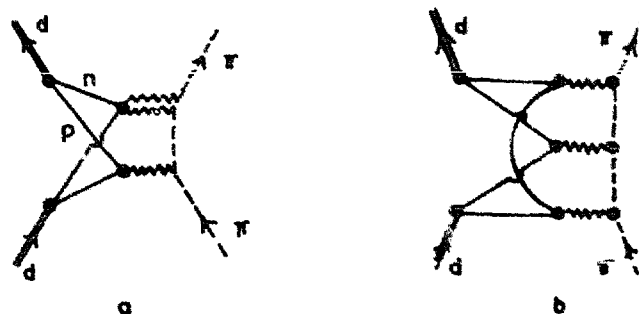


Fig. 26. Two examples of diagrams which involve three Reggeon exchanges, but which have a different time ordering of the interactions.

tainty in the energy which implies an uncertainty in the time ordering of the interaction. So figs. 26a and 26b are equivalent, and the Glauber correction already includes some of the multiple (more than two) scattering corrections, but only to the extent that the π , n and p can be regarded as elementary objects incapable of virtual break up. Glauber theory is thus an essentially low energy approximation, and does not seem to provide much of a guide as to what one should expect for Regge cuts.

But at least one can see that the cuts depend on the scattering particles having a composite structure, just as the Regge pole exchange reflects the compositeness of the exchanged particle. However, it is one thing to be convinced of this, and quite another to turn it into a model for calculating cuts, particularly in circumstances where the composite structure of the particles is a good deal less obvious than it is for the deuteron. See ref. [108].

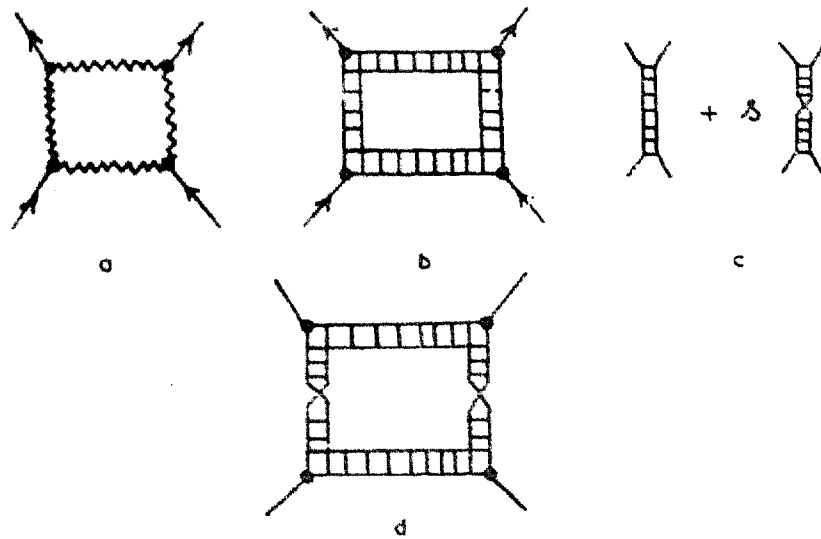


Fig. 27 (a) The Reggeon-box diagram, (b) represented by ladders, (c) Each Reggeon may be represented by a sum of ladders plus twisted ladders when signature is taken into account, so giving rise to the twisted diagrams like (d).

One approach has been to take into account the Regge pole nature of the scattering particles by drawing a Reggeon box [104, 111] as in fig. 27a. If these poles were simply represented by ladders as in fig. 27b we should have only a planar diagram and no cut. But if we remember that the Regge pole has a signature so that the s -channel poles should be represented by fig. 27c i.e. the sum of a ladder and a twisted ladder, then part of what is represented by fig. 27a is fig. 27d which does have a cut. This is held by some authors [101, 104] to justify the replacement of the s -channel poles by the sum of all the particles lying on its trajectory as in fig. 28. These diagrams of course have only AFS cuts, and the author has been unable to understand how this step is justified. It does, however, as we shall see in the next

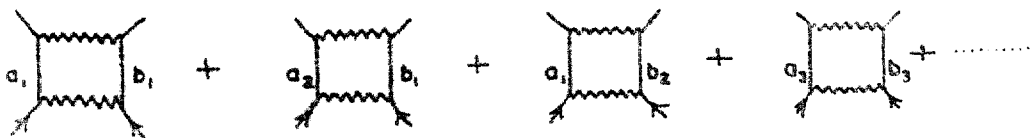


Fig. 28 Some of the terms involved in fig. 27(a) when the two direct channel Reggeons are represented by the particles which lie on them, i.e. particles a_1, a_2, a_3, \dots and b_1, b_2, b_3, \dots respectively.

sections, lead to a definite prescription for calculating cuts which can be compared with experiment.

So far we have described the behaviour of the cuts in the J plane, but of course they can also be interpreted in the t -plane [112]. If they are to shield the Gribov-Pomeranchuk fixed poles we require that the branch point should be at the leading wrong-signature nonsense point (say J_0) for $t = t_0$, the t -channel threshold, i.e. $a_c(t_0) = J_0$. Thus for example for the scattering of two identical spinless particles of mass m , lying on a trajectory $\alpha(t)$ such that $\alpha(m^2) = 0$, the highest nonsense point is at $J = -1$, so we must have

$$a_c(4m^2) = -1. \quad (5.28)$$

The condition (5.7) for two identical trajectories leads to (see (5.87))

$$a_c(t) = 2\alpha(t/4) - 1, \quad (5.29)$$

which satisfies (5.28). With unequal masses the cut structure is more complicated however (see refs. [113, 114]).

In the t plane we have the inverse function to $a_c(t)$, namely $t_c(J)$ defined such that

$$a_c[t_c(J)] = J. \quad (5.30)$$

From (5.28) $t_c(-1) = 4m^2$. As J is increased from -1 , t_c moves along the elastic branch cut until the first inelastic branch point t_1 (say) is reached. At this point $t_c(J)$ passes through the inelastic branch point onto the unphysical sheet, its work of preventing the elastic unitarity equation (2.61) from generating an essential singularity being complete [112], and so $a_c(t)$ has a branch point at J_1 , where $t_c(J_1) = t_1$. This means that the cut discontinuity $\Delta(J, t)$ of (2.54) has the inelastic branch point. If the elastic unitarity equation is to hold Δ must vanish as $t \rightarrow t_c$ e.g.

$$\Delta(J, t) \sim [t - t_c(J)]^\delta \quad \delta > 0. \quad (5.31)$$

Inverting this result we get

$$\Delta(J, t) \sim [J - a_c(t)]^\delta, \quad (5.32)$$

which means that the cut discontinuity must be singular and vanish at the end point of integration in (2.54). Hence the leading asymptotic behaviour of the cut term will be (see section 2.7)

$$A^{\text{cut}}(s, t) \sim (s/s_0)^{\alpha_c(t)} [\log(s/s_0)]^{-1-\delta}. \quad (5.33)$$

Note that this relation depends on unitarity in the t -channel whereas the cuts themselves are generated by unitarity in the s -channel. The incorporation of t -channel unitarity requires adding all the iterations of fig. 21 as shown in fig. 29. In fact such a series is also strictly necessary to eliminate the Gribov-Pomeranchuk singularity properly, and the problem of calculating such a sum is described in ref. [115].



Fig. 29. The sum of iterated, crossed boxes which results when *t*-channel unitarity is applied to fig. 24.

5.4. The Reggeized absorption model

The Reggeized absorption model [104, 116, 117] may be used for any inelastic reaction involving the exchange of quantum numbers. One uses a Regge pole to carry the quantum numbers, but also includes the modifications caused by elastic scattering in the initial and final states, as in fig. 30. Since the elastic amplitudes are predominantly imaginary the effect is to reduce the contributions of the lower partial waves, which corresponds physically to the absorption of the incoming or outgoing particles into channels other than the one being considered. One may of course use the elastic scattering amplitude, if it is known, directly, but for our purposes it is more illuminating to represent it by its Regge pole, the Pomeron. Fig. 30 then looks like a two-Reggeon cut (albeit an AFS one).

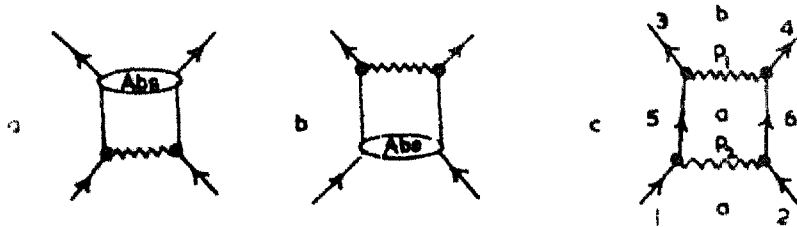


Fig. 30. The absorptive correction to a single Regge pole exchange, representing (a) final state interactions or (b) initial state interactions. (c) gives the labels used for the particles in (5.37), P_1 being the Regge pole, and P_2 the Pomeron exchange amplitude

In detail the hypothesis is that one may write for the *s*-channel partial wave amplitude for the process channel *a* (particles 1 + 2) → channel *b* (particles 3 + 4) in the form of a matrix product in the space of *s*-channel helicity states

$$A_J^{ab}(s) = (S_J^{aa}(s))^{\frac{1}{2}} A_J^{abP_1}(s) (S_J^{bb}(s))^{\frac{1}{2}} \quad (5.32)$$

where $A_J^{abP_1}(s)$ is the partial wave projection into the *s*-channel of the *t*-channel Regge pole carrying the quantum numbers, and S^{aa} is the partial wave *s*-matrix for elastic scattering in the incoming channel, etc. If we put

$$S_J^{aa}(s) \approx 1 + 2i \rho^{aa}(s) A_J^{aaP_2}(s), \quad (5.35)$$

where $\rho^{aa}(s) = 2q_s 12/s^{\frac{1}{2}}$ is the kinematical factor, and $A_J^{aaP_2}$ is the partial wave projection of the P_2 exchange amplitude (and use a similar expression for S^{bb}), we get, expanding the square roots

$$A_J^{ab}(s) = A_J^{abP_1}(s) + i \rho^{aa}(s) A_J^{aaP_2}(s) A_J^{abP_1}(s) + i \rho^{bb}(s) A_J^{abP_1}(s) A_J^{bbP_2}(s) \quad (5.36)$$

The first term represents the Regge pole exchange while the second and third are two particle cuts due to the exchange of the Regge pole with a Pomeron. From say the first the first of these the full cut contribution is (writing out the helicity explicitly - see fig. 30c)

$$A_{HS}^{cut}(s, t)$$

$$= i\rho^{aa}(s) 16\pi \sum_J (2J+1) \sum_{\mu_5\mu_6} A^{aaP_2}_{\mu_1\mu_2\mu_5\mu_6}(s) A^{abP_1}_{\mu_5\mu_6\mu_3\mu_4}(s) d_{\mu\mu'}^J(z_s), \quad (5.37)$$

where

$$\mu = \mu_1 - \mu_2 \quad \text{and} \quad \mu' = \mu_3 - \mu_4. \quad (5.38)$$

If we perform the partial wave projection of the pole amplitudes (dropping the channel labels for simplicity) we get

$$A_{HS}^{cut}(s, t) = \sum_{\mu_5\mu_6} i\rho(s) 16\pi \sum_J (2J+1) d_{\mu\mu'}^J(z_s) \frac{1}{32\pi} \int_{-1}^1 A^{P_1}_{\mu_1\mu_2\mu_5\mu_6}(s, z_1) \times d_{\mu\mu'}^J(z_1) dz_1 \frac{1}{32\pi} \int_{-1}^1 A^{P_2}_{\mu_5\mu_6\mu_3\mu_4}(s, z_2) d_{\mu''\mu'}^J(z_2) dz_2, \quad (5.39)$$

where $\mu'' = \mu_5 - \mu_6$ and z_1 and z_2 are the cosines of the scattering angles between the initial and intermediate, and intermediate and final states, respectively, which therefore satisfy the addition theorem

$$z_1 = z z_2 + (1-z^2)^{\frac{1}{2}} (1-z_2^2)^{\frac{1}{2}} \cos \phi_1,$$

where ϕ_1 is the azimuthal angle between the directions of motion in the initial and intermediate states (fig. 31). But [104]

$$\sum_J (2J+1) d_{\mu\mu'}^J(z_s) d_{\mu\mu''}^J(z_1) d_{\mu''\mu'}^J(z_2) = \frac{2}{\pi} \frac{\theta(\Delta)}{\Delta^{\frac{1}{2}}} \cos(\mu\phi_1 + \mu'\phi_2 + \mu''\phi_3), \quad (5.40)$$

where

$$\Delta = 1 - z_s^2 - z_1^2 - z_2^2 + 2z_s z_1 z_2, \quad (5.41)$$

$\theta(\Delta)$ is the step function, and the azimuthal angles ϕ_i satisfy

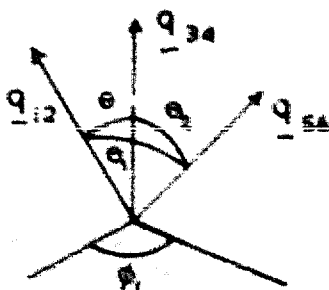


Fig. 31. The angles between the incoming centre of mass momentum q_{12} , the intermediate state momentum q_{56} , and the final state momentum q_{34} . This latter is taken as the axis about which the azimuthal angle ϕ between q_{12} and q_{56} is measured.

$$\begin{aligned}
 e^{i\phi_2} &= (z_1 - z z_2 + i\Delta^{\frac{1}{2}}) (1 - z_2^2)^{-\frac{1}{2}} (1 - z^2)^{-\frac{1}{2}} \\
 e^{i\phi_1} &= (z_2 - z z_1 + i\Delta^{\frac{1}{2}}) (1 - z^2)^{-\frac{1}{2}} (1 - z_1^2)^{-\frac{1}{2}} \\
 e^{i\phi_3} &= (-z + z_1 z_2 - i\Delta^{\frac{1}{2}}) (1 - z_1^2)^{-\frac{1}{2}} (1 - z_2^2)^{-\frac{1}{2}},
 \end{aligned}
 \tag{5.42}$$

so (5.39) simplifies to

$$\begin{aligned}
 A H_S(s, t) &= \sum_{\mu_5 \mu_6} \frac{1 \rho(s)}{32\pi^2} \int_{-1}^1 dz_1 \int_{-1}^1 dz_2 A_{\mu_1 \mu_2 \mu_5 \mu_6}^{P1}(s, z_1) A_{\mu_5 \mu_6 \mu_1 \mu_2}^{P2}(s, z_2) \\
 &\quad \times \frac{\theta(\Delta)}{\Delta^{\frac{1}{2}}} \cos(\mu \phi_1 + \mu' \phi_2 + \mu'' \phi_3).
 \end{aligned}
 \tag{5.43}$$

This gives us a complete prescription for the cut amplitude in terms of the pole amplitudes.

There are several ways of approximating (5.43) to give simple analytic expressions for the cuts. For large s and small t we may write for each z in (5.43)

$$z \approx 1 + 2t/s, \quad z_1 \approx 1 + 2t_1/s, \quad z_2 \approx 1 + 2t_2/s
 \tag{5.44}$$

and if we express the Regge pole terms as exponentials in t we can use the fact that [118]

$$\int_{-s}^0 dt_1 \int_{-s}^0 dt_2 e^{\delta_1 t_1 + \delta_2 t_2} \frac{\theta(K)}{K^{\frac{1}{2}}} = \pi \frac{A}{A} e^{-\frac{1}{2} \delta (b_1 + b_2) \left[\frac{A s}{2} - \frac{A s}{2} \right]},
 \tag{5.45}$$

where

$$K = -(t^2 + t_1^2 + t_2^2) + 2(t t_1 + t t_2 + t_1 t_2) + 4t t_1 t_2 / s
 \tag{5.46}$$

and

$$A = [b_1^2 + b_2^2 + 2b_1 b_2 z_s]^{\frac{1}{2}}.
 \tag{5.47}$$

To first order in t/s this gives

$$(5.45) \approx \pi \frac{e^{h_1 b_2 t / (b_1 + b_2)}}{(b_1 + b_2)}.
 \tag{5.48}$$

The introduction of say a factor t , into the integrand of (5.45) is equivalent to differentiating it with respect to b_1 and so the integral is just the right-hand side of (5.48) differentiated with respect to b_1 . So in general if the integrand is written as a polynomial times an exponential we have [119]

$$\int_{-s}^0 dt_1 \int_{-s}^0 dt_2 \sum_{n, m} a_{nm} t_1^n t_2^m e^{\delta_1 t_1 + \delta_2 t_2} \frac{\theta(K)}{K} \approx \pi \sum_{n, m} a_{nm} \frac{\partial^n}{\partial b_1^n} \frac{\partial^m}{\partial b_2^m} \left[\frac{e^{h_1 b_2 t / (b_1 + b_2)}}{b_1 + b_2} \right].
 \tag{5.49}$$

This is sufficiently general to embrace all the cases likely to be of interest except when there is a pole very close to $t = 0$. In practice this applies only to the pion - for which see ref. [104].

To first order in t/s , $\phi_1 + \phi_2 = -\phi_3$. The dominant terms in the sum over $\mu_5 \mu_6$ will be those for which there is no helicity flip in the elastic amplitude, i.e. $\mu' = \mu''$, and so do not vanish in the forward direction. If we keep just these terms the cosine factor in (5.43) becomes just $\cos(\mu - \mu') \phi_2$.

If for example we consider a non-flip amplitude $\mu = \mu' = \mu'' = 0$ and write the pole terms in the form

$$A_{H_S}^{P1}(s, z_1) = -G_1 e^{b_1 t_1} \left(\sum_n a_n^1 t_1^n \right) e^{-\frac{1}{2} i \pi \alpha_1(t_1)} (s/s_0)^{\alpha_1(t_1)} \quad (5.50)$$

(where we have absorbed all the t dependence of the residue into an exponential times a polynomial in t , but have included the phase of the signature factor explicitly) and a similar term for A^{P2} , and use a linear approximation for the trajectories

$$\alpha_i(t) = \alpha_i(0) + \alpha'_i t \quad (5.51)$$

we find

$$A_{H_S}^{\text{cut}}(s, t) \sim \frac{i}{16\pi s_0} G_1 G_2 \left(\frac{s}{s_0} \right)^{\alpha_1(0) + \alpha_2(0) - 1} \sum_{n, m} a_n^1 a_m^2 \frac{\partial^n}{\partial c_1^n} \frac{\partial^m}{\partial c_2^m} \times \frac{e^{c_1 c_2 t / (c_1 + c_2)}}{c_1 + c_2} e^{-\frac{1}{2} i \pi (\alpha_1(0) + \alpha_2(0))}, \quad (5.52)$$

where

$$c_i \equiv b_i + \alpha'_i [\log(s/s_0) - \frac{1}{2} i \pi]. \quad (5.53)$$

The large s dependence of this expression is

$$A_{H_S}^{\text{cut}}(s, t) \sim \left(\frac{s}{s_0} \right)^{\alpha_c(t)} \left[\log \left(\frac{s}{s_0} \right) \right]^{-1}, \quad (5.54)$$

where the position of the cut is

$$\alpha_c(t) = \alpha_1(0) + \alpha_2(0) - 1 + \frac{\alpha'_1 \alpha'_2}{\alpha'_1 + \alpha'_2} t. \quad (5.55)$$

The reader may readily convince himself that this corresponds to (5.7) i.e.

$$\alpha_c(t) = \max[\alpha_1(t_1) + \alpha_2(t_2) - 1], \quad (5.56)$$

where t_1, t_2 and t are related by the solid angle condition (5.46) in the limit $s \rightarrow \infty$, i.e. $\mathfrak{B}(t, t_1, t_2) = 0$ (see (5.8)) or

$$\sqrt{-t_1} + \sqrt{-t_2} = \sqrt{-t} \quad (5.57)$$

and when the trajectories have the linear form (5.51).

If the slopes of the trajectories are the same we get

$$\alpha_c(t) = \alpha_1(0) + \alpha_2(0) - 1 + \frac{1}{2}\alpha't, \tag{5.58}$$

so the slope of the cut is smaller than that of the pole. Since for the Pomeron we have $\alpha_2(0) = 1$ the cut is

$$\alpha_c(t) = \alpha_1(0) + \frac{1}{2}\alpha't, \tag{5.59}$$

so the cut coincides with the pole at $t = 0$, and lies above if for $t < 0$. Since all other poles have $\alpha(0) < 1$ the dominant cut in any reaction will always be that generated by the Pomeron together with the pole which carries the quantum numbers.

We also notice from (5.52) that the asymptotic phase of the amplitude is given by the product of the phases of the poles at $t = 0$. This is in agreement with the results of the Reggeon calculus (5.19). In fact since $A^{\text{Pole}}(-s, t) = \sigma A^{\text{P}}(s, t)$ from the signature factor, it is clear from (5.43) that the signature of the cut is

$$\sigma_c = \sigma_1 \cdot 2. \tag{5.60}$$

This also follows from (5.19).

This result for the phase is to be contrasted with that of the AFS cuts (5.6), which arise if fig. 30 is interpreted as a unitarity diagram. We then get instead of (5.36) [120]

$$\text{Im } A_J^{\text{cut } ab}(t) = \text{Re } \rho^{aa}(s) [A_J^{aa P_2}(s)] \cdot A_J^{ab P_1}(s). \tag{5.61}$$

Since the elastic amplitude is almost pure imaginary for $t \approx 0$ the complex conjugation in (5.61) changes the sign of the imaginary part of the amplitude relative to (5.36). This sign is clearly of great importance if we are to obtain a destructive interference between pole and cut to produce dips. The sign (5.36) is supported by the Reggeon diagram technique.

If the elastic amplitude is approximated by the Pomeron with $\alpha(0) = 1$ we may write

$$A_H^{P_2}(s, t) = i s_0 \sigma^{\text{tot}} \left(\frac{s}{s_0}\right)^{\alpha_c t}, \tag{5.62}$$

where we have used the optical theorem (2.8) to relate the imaginary part of the amplitude to the total cross section. This gives, from (5.52),

$$A_H^{\text{cut}}(s, t) = \frac{\sigma^{\text{tot}}}{16\pi} G_1 \left(\frac{s}{s_0}\right)^{\alpha_1(0)} \sum_n a_n \frac{\partial^n}{\partial c_1^n} \left[\frac{c_1 c_2 t / e^{(c_1+c_2)t}}{c_1 + c_2} \right] e^{-\frac{1}{2}i\pi \alpha_1(0)}. \tag{5.63}$$

This is a very convenient analytic approximation for many purposes.

Of course (5.43) gives us the cut amplitude directly. If we want to know the cut discontinuity we can write the Sommerfeld-Watson transform (leaving out various factors - compare (2.54)) as

$$A_H^{\text{cut}}(s, t) = 16\pi \int^{\alpha_c} dJ \Lambda_H(J, t) (-s/s_0)^J \tag{5.64}$$

and putting

$$A^{\text{Pole}}(s, t) = G(t) (s/s_0)^{\alpha(t)} \quad (5.65)$$

in (5.43) we get

$$\Delta_H(J, t) = \frac{16(s)}{32\pi^2} \int_{-1}^1 dz_1 \int_{-1}^1 dz_2 G_1(t_1) G_2(t_2) \times \frac{\theta(\Delta)}{\Delta^{\frac{1}{2}}} \cos(\mu \phi_1 + \mu' \phi_2 + \mu'' \phi_3) \delta(J - \alpha_1(t) - \alpha_2(t)) . \quad (5.66)$$

Note that in general this discontinuity does not satisfy the t -channel unitarity condition (5.32).

Although the absorption model has produced for us a cut which has the phase and position which we anticipated from the Reggeon calculus, the diagram fig. 30 from which we started is definitely planar, and so the model only makes sense if we remember that the sides of fig. 30 are supposed to correspond to the twisted propagators of fig. 27. The Reggeons in the direct channel will presumably carry other particles besides the intermediate state 5 + 6 (as in fig. 28). In principle one should try and include these by adding the corresponding diagrams individually, but a commonly employed approximation [104, 116] is simply to multiply the right-hand side of (5.43) by some number $\lambda > 1$ to represent the addition of these other graphs. But these other diagrams have higher thresholds and it would seem that λ should really be an increasing function of s . If it were, however, this additional s dependence would alter the cut position (5.55). And indeed there is no reason to expect the sum (5.26) to converge [108].

There are also other worries, such as the fact that we have to take the complete fig. 30, not just the part corresponding to the twisted propagator fig. 27d. Also since the Regge pole term by itself has an imaginary part it must already include some absorption (in the sense of an optical potential, see ref. [111]). Thus although the absorptive prescription has the merits of precision and simplicity, with a physical-seeming interpretation in terms of Glauber rescattering, as well as giving cuts of the expected position and phase, there does not seem to be any compelling reason to accept it as giving a reliable quantitative estimate of the magnitude of a cut.

It also suffers from the disadvantage of being suitable only for inelastic processes, and gives only a two Reggeon cut. The eikonal model of the next section suggests a way of overcoming both these restrictions, however.

5.5. The eikonal model

This model [111] makes use of the semi-classical impact parameter technique which is appropriate for elastic scattering processes at high energies when large numbers of partial waves are involved.

The s -channel partial wave series

$$A_{HS}(s, t) = 16\pi \sum_{J=M}^{\infty} (2J+1) A_{HJ}(s) d_{\mu\mu'}^J(z_s) \quad (5.67)$$

may be approximated at high energies and small angles ($s \gg t$) and large J by making the replacement (see ref. [121])

$$q_{\mu\mu'}^J(\theta) \approx J_{\mu}^-(\left(J + \frac{1}{2}\right)\theta), \tag{5.68}$$

where $\mu = |\mu - \mu'|$ and J_{μ}^- is a Bessel function. Since $\cos \theta \approx 1 + t/2q_s^2$ we can put $\theta \approx (-t/q_s^2)^{1/2}$. We introduce the impact parameter b by the expression

$$J = q_s b - \frac{1}{2}. \tag{5.69}$$

Classically this corresponds to the closeness of approach of a particle with angular momenta J to the target centre (see fig. 32). If we then make the replacement

$$\sum_J = \int_0^{\infty} q_s db \tag{5.70}$$

(5.67) becomes

$$A_{H_S}(s, t) = 16\pi \int_0^{\infty} q_s db 2q_s b A_{HJ}(s) J_{\mu}^-(b\sqrt{-t}). \tag{5.71}$$



Fig. 32. The impact parameter b at which a particle, momentum q_s , passes through the target.

Then we can write the partial wave amplitudes in terms of the phase shift $\delta_J(s)$

$$A_{HJ}(s) = e^{\frac{2i\delta_J(s)}{2i\mu\lambda}} - 1 \tag{5.72}$$

and define the eikonal phase χ , i.e. the phase shift for scattering at a given impact parameter, by

$$\chi(s, b^2) \equiv 2\delta_{q_s b - \frac{1}{2}}(s). \tag{5.73}$$

Physically this means that we are supposing that each part of the incident particle's wave front passes straight through the scattering potential at its impact parameter, and is altered only in phase, not direction. This is why the result is only valid for large energies near the forward direction.

Combining (5.71), (5.72) and (5.73) we get

$$A_{H_S}(s, t) = 16\pi q_s \sqrt{s} \int_0^{\infty} b db [1 - e^{i\chi(s, b^2)}] J_{\mu}^-(b\sqrt{-t}). \tag{5.74}$$

Note that this is not the same as a Fourier-Bessel transform since χ is not the exact eikonal phase but is given by (5.73). Finally we expand the exponential in (5.74) in powers of χ and get

$$A_{H_S}(s, t) = 8\pi q_s \sqrt{s} \int_0^{\infty} b db \left[\chi + \frac{i\chi^2}{2} - \frac{\chi^3}{3!} \dots - i \frac{(i\chi)^n}{n!} \dots \right] J_{\mu}^-(b\sqrt{-t}). \tag{5.75}$$

The crucial step in connecting this with Regge theory is then to identify the Regge pole exchange amplitude with the first term of (5.75), i.e.

$$A_{H_S}^P(s, t) = 8\pi q_S \sqrt{s} \int_0^\infty b db \chi(s, b^2) J_{\bar{\mu}}(b \sqrt{-t}). \quad (5.76)$$

The Fourier-Bessel inverse of this gives us the eikonal phase

$$\chi(s, b^2) = \frac{1}{8\pi q_S \sqrt{s}} \int_{-\infty}^0 \frac{1}{2} dt J_{\bar{\mu}}(b \sqrt{-t}) A_{H_S}^P(s, t), \quad (5.77)$$

so χ is determined by the Regge pole parameters.

The two particle exchange cut is then given by the second term of (5.75) i.e.

$$A_{H_S}^{\text{cut}(2)}(s, t) = i 4\pi q_S \sqrt{s} \int_0^\infty b db \chi^2(s, b^2) J_{\bar{\mu}}(b \sqrt{-t}), \quad (5.78)$$

which when we substitute (5.77) for χ becomes (remembering the helicity summation, see (5.39))

$$A_{H_S}^{\text{cut}(2)}(s, t) = \frac{i}{16\pi q_S \sqrt{s}} \sum_{\mu''} \int_{-\infty}^0 \frac{1}{2} dt_1 \int_{-\infty}^0 \frac{1}{2} dt_2 \int_0^\infty b db J_{|\mu - \mu''|}(b \sqrt{-t_1}) \\ \times A_{H_S}^P(s, t_1) J_{|\mu'' - \mu'|}(b \sqrt{-t_2}) A_{H_S}^P(s, t_2) J_{\bar{\mu}}(b \sqrt{-t}). \quad (5.79)$$

Usually for elastic scattering we are interested mainly in non-flip amplitudes, since these do not vanish in the forward direction, and we can use the equivalent result to (5.40), viz. [104]

$$\int_0^\infty b db J_0(b \sqrt{-t_1}) J_0(b \sqrt{-t_2}) J_0(b \sqrt{-t}) = \frac{2}{\pi} \frac{\theta(\delta)}{\delta^{\frac{1}{2}}}, \quad (5.80)$$

where δ is defined in (5.8), so we end up with

$$A_{H_S}^{\text{cut}(2)}(s, t) = \frac{i}{32\pi^2 q_S \sqrt{s}} \int_{-\infty}^0 dt_1 \int_{-\infty}^0 dt_2 A_{H_S}^P(s, t_1) A_{H_S}^P(s, t_2) \frac{\theta(\delta)}{\delta^{\frac{1}{2}}}. \quad (5.81)$$

This is identical with the absorptive prescription (5.43) in the limit (5.44), $s \rightarrow \infty$ and $\mu = \mu' = \mu'' = 0$.

What is more (5.75) tells us how to calculate the cut stemming from the exchange of any number of poles. For instance for 3 poles we have

$$A_{H_S}^{\text{cut}(3)}(s, t) = - \frac{8\pi q_S \sqrt{s}}{3!} \int_0^\infty b db \chi^3 J_{\bar{\mu}}(b \sqrt{-t}), \quad (5.82)$$

which substituting (5.81) for the χ^2 part and (5.77) for χ , and using (5.80) again, gives

$$A_H^{\text{cut}(3)}(s, t) = \frac{2i}{3!} \frac{i}{16\pi^2 q_S \sqrt{s}} \int_{-\infty}^0 dt_1 \int_{-\infty}^0 dt_2 \frac{\theta(\delta)}{\delta^{\frac{1}{2}}} A_H^{\text{cut}(2)}(s, t_1) A_H^P(s, t_2). \quad (5.83)$$

And this process can obviously be repeated for any number of poles. Thus if we approximate the single pole amplitude by

$$A_{H_S}^P(s, t) = G(s/s_0)^{\alpha(0)} e^{ct} e^{-\frac{1}{2}t\alpha(0)},$$

with c given by (5.53) we get for the n -particle cut

$$\begin{aligned} A_H^{\text{cut}(n)}(s, t) &= (-1)^{n+1} \frac{1}{nn!} \left(\frac{G}{i6\pi\sqrt{s}q_{sc}} \right)^{n-1} G \left(\frac{s}{s_0} e^{-\frac{1}{2}i\pi} \right)^{n\alpha(0)} e^{(c/n)t} \\ &\underset{s \rightarrow \infty}{\sim} \frac{(-1)^n}{nn!} G^n [8\pi s_0 c' \sqrt{s/s_0}]^{-n+1} (s/s_0)^{\alpha_c^n(t)} e^{-\frac{1}{2}i\pi\alpha_c^n(t)}, \end{aligned} \quad (5.84)$$

where the position of the cut is

$$\alpha_c^n(t) = n\alpha(0) + \frac{\alpha'}{n} t - n + 1. \quad (5.82)$$

For the dominant Pomeron we have

$$\alpha_c^n(t) = 1 + \frac{\alpha'}{n} t, \quad (5.83)$$

so all the P-exchange branch points coalesce at $t = 0$, and the cut slopes get smaller as n is increased. And using (5.62) we get

$$A^{\text{cut}(n)}(s, t) = \frac{is\sigma^{\text{tot}}}{nn!} \left(\frac{-\sigma^{\text{tot}}}{8\pi c} \right)^{n-1} e^{(c/n)t}, \quad (5.84)$$

so the sign of the various cuts alternates.

It is interesting to estimate the size of these cuts relative to the P pole. For example in NN elastic scattering we can take $\sigma^{\text{tot}} \approx 40$ mb and $c \approx 5 \text{ GeV}^{-2}$ at machine energies, so the ratio is

$$A^P : A^{\text{cut}(2)} \approx 5 : 1 \quad \text{at} \quad t = 0$$

and the 3-particle cut is only about 0.5% of the pole. Hence at $t = 0$ we can expect the pole to dominate. But the different t dependences of the various terms means that the magnitude of the cut is comparable to that of the pole at $t \approx -0.65 \text{ GeV}^2$ [118].

If we combine the absorptive idea for quantum number exchange, with this eikonal method for multi-Pomeron exchange we can calculate the cuts due to the exchange of any number of poles whether identical or not. Note that there are two cut terms in (5.36) i.e. figs. 30a and 30b, and one must add all the possible permutations of the P's and the other Regge poles to get consistent results.

Unfortunately the justification for the eikonal method is no clearer than it is for the absorption method, however. In potential scattering the eikonal phase is given by inserting the Born approximation for the pole in (5.77) [111]. Thus the eikonal method rests on the identification of the Regge pole amplitude with a relativistic Born-approximation. It has been demonstrated [122] (at least to some approximation) that the eikonal expansion corresponds, in a field-theoretic sense, to the ladder sum of diagrams with and without crossed rungs, as in fig. 33, where the rungs represent the Born approximation. Thus part of each contribution would seem to come from uncrossed diagrams which do not contribute to the cuts, and

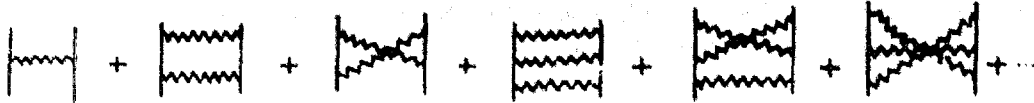


Fig. 33. The sequence of crossed and uncrossed Feynman graphs which are summed in the sikonal approximation according to ref. [122].

should presumably be contained instead in the Regge poles. The validity of the identification of the Regge pole with the Born approximation thus seems doubtful.

5.6. General properties of Regge cuts

Even if we can not have complete confidence in the models of the previous sections, they do permit us to draw some reasonably firm conclusions about the nature of Regge cuts:

a) *Position.* The position of the branch point due to the exchange of n Reggeons $\alpha_i(t)$ $i = 1 \dots n$ is at

$$\alpha_c^{(n)}(t) = \max \left\{ \sum_{i=1}^n \alpha_i(t_i) - n + 1 \right\}, \quad (5.85)$$

where the t_i are related by the addition theorem generalization of (5.57)

$$\sum_{i=1}^n \sqrt{-t_i} = \sqrt{-t}. \quad (5.86)$$

If the trajectories are identical this becomes

$$\alpha_c^n(t) = n \alpha(t/n) - n + 1, \quad (5.87)$$

while if they are linear

$$\alpha_c^n(t) = n \alpha(0) - n + 1 + \frac{\alpha'}{n} t. \quad (5.88)$$

b) *Phase.* The signature of the cut is the product of the signatures of the poles (see (5.60))

$$\sigma_c = \prod_{i=1}^n \sigma_i \quad (5.89)$$

and if all the poles are identical the asymptotic $\log s \rightarrow \infty$ phase is $e^{-\frac{1}{2}i\pi \alpha_c^n(t)}$.

c) *General form.* There is a logarithmic factor $[\log(s/s_0)]^{-n+1}$ for each pole so that the contributions of the higher order cuts vanish relative to those of the lower order by some power of $\log s$. However this factor must be wrong for $n = 2$ because it violates t -channel unitarity (see (5.33)), but the required correction δ is not known.

From this we can deduce a general expression for a cut contribution from n identical trajectories

$$A_{H_S}^{\text{cut}(n)}(s, t) = \xi_{\mu\mu'}(z_S) F(t) (s/s_0)^{\alpha_c(t)} e^{-\frac{1}{2}i\pi \alpha_c(t)} [\log(s/s_0) + d]^{-n+1}, \quad (5.90)$$

where $F(t)$ is an arbitrary function free of kinematical singularities, d is a constant, and $\alpha_c^n(t)$ is given by (5.87).

The mixed eikonal/absorptive prescription gives a specific model for $F(t)$ and d in terms of the pole parameters which may or may not be satisfactory.

d) *Condensation*. We have found that the Pomeron with $\alpha(0) = 1$ generates an infinite sequence of Regge cuts which condense on $\alpha(0)$ at $t = 0$. Similarly if we exchange some pole $\alpha_1(t)$ together with any number of Pomerons all the cuts will arrive at $\alpha_1(0)$ at $t = 0$. These cuts will dominate over others due to the exchange of two or more lower-lying trajectories.

We noted in chapter 3 that the theorem on the reality of the trajectory function below threshold breaks down when Regge singularities collide, and it is possible that all trajectories are complex for $t < 0$ because of these cuts. But although this possibility has elicited some comment in the literature [123, 124] there is no evidence to support it. Regge fits with $\alpha(t)$ real seem to be satisfactory though of course there is no really crucial test.

Gribov [100, 125] has pointed out further difficulties which arise from applying the diagram technique to Pomerons. When Reggeon loops are calculated divergences occur which require renormalization, but this is hard to achieve consistently for Pomerons. So though the diagram technique gives useful insights it can not be taken too literally.

e) *Cuts and dips*. An important property of the cuts is that their fall with increasing $|t|$ is slower than it is for the poles so that if a single pole behaves like e^{ct} , the exchange cut from n such poles behave like $e^{(c/n)t}$. When this fact is combined with the alternating sign from multiple P exchange (5.84) we see that though the poles dominate at $t = 0$ the 2-particle cut is likely to be strong enough to cancel the pole term at some larger $|t|$. Similarly the 3-particle cut will interfere with these at still larger $|t|$. The amplitudes are complex, however, and the interference will result in dips rather than zeros, and even these dips may be washed-out at very large $|t|$ [116].

We have already noted that there can be dips due to the nonsense factors in the Regge pole amplitudes provided there are no wrong-signature fixed poles in the residues. But there is now the possibility of an alternative mechanism in which the poles do not have zeros, but the amplitudes have dips due to pole-cut interference. In fact it has been shown [104, 116] that if the enhancement factor λ (see section 4) is allowed to be ≈ 2 many of the observed dips can be explained in this way. Since the integral (5.81) is heavily weighted towards $t_1, t_2 = 0$ the strength of the cuts, and hence the nearness of this dip, will depend greatly on whether or not the pole terms have zeros. If in a given s-channel amplitude the pole terms have no zeros except for the kinematical one needed in the forward direction ($\sim (1 - s/s_0)^{\frac{1}{2}} |\mu - \mu'|$) then the dips are found to occur systematically at $t \approx -0.2, -0.6$ and -1.2 GeV^2 for amplitudes with $|\mu - \mu'| = 0, 1$ and 2 respectively [116]. The one at $t = -0.6$ is obviously in the right place to explain the dip in $\pi^- p \rightarrow \pi^0 n$, e.g. and we shall see in chapter 7 that the others are also just where they are needed for some processes. So fixing the arbitrary parameter λ puts several different dips in about the right place, though the fact that it has to be so large is rather worrying.

Since both the fixed poles and the cuts come from the third double spectral function, both the nonsense-zero and the pole-cut interference explanations are equally consistent from a theoretical standpoint. The former requires small (or no) fixed poles and small cuts while the latter requires strong fixed poles (so strong that not even a sizeable dip is seen in the pole term) and strong cuts. Both points of view have their protagonists - sometimes known as the Argonne [126-128] and Michigan [104, 116] schools (respectively) - and we shall try to review some of

the experimental evidence in chapter 7. At the moment neither viewpoint seems to have overwhelming merit, and it may well be that (as so often) the truth lies somewhere in between, i.e. the poles have some wrong-signature zeros, and the cuts are of importance in generating some dips, and especially in filling in unwanted dips.

f) *Conspiracies*. Another important aspect of a cut is that it is an essentially s -channel phenomenon, that is to say it depends on unitarity in s -channel amplitudes. This plus the absence of a factorization requirement means that the only kinematical factors required are those essential to angular momentum conservation i.e.

$$A_{H_S}(s, t) \sim \xi_{\mu\mu'}(z_S) \sim (1 - z_S)^{\frac{1}{2}} |\mu - \mu'| \quad (5.91)$$

So if we take such a cut contribution and apply the crossing relation (inverse to (2.11)) to re-express it in terms of t -channel helicity amplitudes we shall find that the various conspiracy relations are satisfied automatically, since a cut is of mixed t -channel parity in general. Cuts can thus provide a natural explanation of those cases where conspiring poles have been tried but found wanting. Thus for the problem concerning the pion in $\gamma p \rightarrow \pi^+ n$ and $p n \rightarrow n p$ mentioned in section (4.3), the π - P cut, which contains parts of both even and odd parity and remains finite at $t = 0$, can provide a ready solution. Since this cut has the same asymptotic behaviour as the pion pole (apart from $\log s$ factors) a fit just as good as with π + conspirator can be made [116]. It is found that very large cuts, with $\lambda \approx 3.55$ are needed, however. If conspiracies between poles are regarded as implausible this is one of the best places to try and determine the magnitude of cut effects.

5.7. Fixed cuts

So far our discussion has concentrated on moving Regge cuts, but there may also be fixed cuts, and these deserve a brief mention.

We have already noted a kinematical source for one type of fixed cut in section (2.9). It is found that square root branch points occur in each helicity amplitude at the sense-nonsense points, and so there are fixed branch cuts running along the real J axis from $\sigma_T - 1$ to $-\sigma_T$ where $\sigma_T \equiv \max\{\sigma_1 + \sigma_3, \sigma_2 + \sigma_4\}$. Since the $d_{\lambda\lambda'}^J$'s have complementary branch-points these cuts do not contribute to the asymptotic behaviour of the amplitude. They could however permit the existence of fixed poles at nonsense points with $J < \sigma_T - 1$. There is no evidence that they do, but most of the processes which are studied have spins which are too low for $\sigma_T - 2$ to be a sense-nonsense point. There has been some discussion [129] of the possibility that if one considers high spin intermediate states, say particles 5 + 6 with the 5 + 6 threshold below that for $1 + 2 \rightarrow 1 + 2$, then such poles can exist at nonsense points with $J < \sigma_5 + \sigma_6 - 1$. But in fact extended unitarity, which allows one to write a unitarity like equation for the discontinuity across the $1 + 2$ threshold branch point separately, rules this out [130].

A second, and quite different, type of fixed cut has been suggested by Carlitz and Kislinger [131] in order to remove the embarrassment caused by the MacDowell symmetry for fermions, which we discussed in sections (3.3) and (4.3). They suggest that the scattering amplitude should have a fixed cut at $J = \alpha_0$, where α_0 is the intercept of the fermion trajectory at $t = 0$. It can then be arranged that the negative parity trajectory moves behind this cut on an unphysical J -plane sheet for positive \sqrt{t} , so that there are no physical particles on the trajectory.

Specifically, for the nucleon trajectory in $\pi N \rightarrow \pi N$ they write

$$A_{HJ}^{\sigma\eta}(t) = \beta(t) \frac{\alpha'^{\frac{1}{2}} \sqrt{t} + \eta(J - \alpha_0)^{\frac{1}{2}}}{J - \alpha_0 - \alpha' t} \frac{1}{(J - \alpha_0)^{\frac{1}{2}}}, \quad (5.92)$$

where as usual $\eta = \pm$ for natural/unnatural parity. (Ref. [131] uses u for t which is more appropriate for backward scattering.) This expression has a pole at $J = \alpha_0 + \alpha' t$ and a fixed square root branch point at $J = \alpha_0$. The constraint (4.47) is satisfied by construction. However the pole in the $\eta = -$ amplitude moves through the cut onto an unphysical sheet as \sqrt{t} increases through zero, so there are no poles for positive \sqrt{t} . If (5.92) is substituted in the Sommerfeld-Watson transform we get

$$A_{Hl}^{\sigma\eta}(s, t) = -16\pi^2 \frac{2\alpha(t) + 1}{\sin \pi\alpha(t)} \beta(t) d_{\lambda\lambda'}^{\sigma\eta}(\alpha(t), z_l) + \int^{\alpha_0} dJ(2J + 1) \frac{\beta(t)}{\sin \pi(J + \lambda')} \hat{d}_{\lambda\lambda'}^{\sigma\eta}(J, z_l) \frac{\alpha'^{\frac{1}{2}} \sqrt{t} + \eta(\alpha_0 - J)^{\frac{1}{2}}}{(J - \alpha_0 - \alpha' t)(\alpha_0 - J)^{\frac{1}{2}}}, \quad (5.93)$$

where the contour of integration is round the cut branch point, and $\alpha(t) = \alpha_0 + \alpha' t$. This sort of expression has been used to fit backward πN scattering with the N_α and Δ_8 poles [132]. The results are reasonably satisfactory in that some spurious wide angle dips produced by the exchange poles alone (see chapter 7) are removed, but an unreasonably large nucleon residue is needed because the cut discontinuity is too large near $t = 0$. This is not really surprising because the infinite type singularity $(J - \alpha_0)^{-\frac{1}{2}}$ is in conflict with partial-wave unitarity, but giving the cut a non-singular discontinuity ruins the fit.

CHAPTER 6 DUALITY

6.1. High and low energies

In chapter 2 we showed that the Sommerfeld-Watson transform provides an exact representation of the scattering amplitude for all s and t in terms of t -channel J -plane singularities. The main use which we have made of it, however, is in high energy approximations when only the leading poles and cuts are needed. If we wish to go to lower energies we must expect more terms to become relevant.

At low energies it is often more convenient to represent the scattering amplitude by its partial waves in the direct- (s -) channel, i.e.

$$A_{H_S}(s, t) = 16\pi \sum_{J_S = M}^{\infty} (2J_S + 1) A_{HJ_S}(s) d_{\lambda\lambda'}^{J_S}(z_S). \quad (6.1)$$

The advantage lies in the fact that at low energies only a few partial waves will be non-zero, and it is often quite a reasonable approximation to represent each partial wave as a sum of resonance poles

$$A_{HJ_S}(s) = \sum_r \frac{g_r(s)}{s_r - s}, \quad (6.2)$$

where s_r is the (complex) resonance position. The partial-wave series only converges in a region round the s -channel physical region (the Lehman ellipse) of course.

Since both (6.1) and (2.54) are exact representations of the amplitude it is natural to wish to try and understand the relationship between approximations like (6.2) and the Regge representation. This is particularly important in the intermediate energy region ($\approx 1.5 - 3$ GeV) where the known resonances seem to be dying out but the amplitude has not yet settled down to its smooth asymptotic behaviour.

The first point to note is that t -channel Regge poles and cuts do not contain poles in s . This means that a finite number of them can never give rise to an s -channel resonance, so either an infinite number is needed or the resonances are in the background integral. On the other hand the resonance poles lie on unphysical sheets (except for bound states) and one does not know how to continue the Regge pole terms (defined on the physical sheet) to the resonance position. The Regge poles and cuts do not individually contain the s -channel threshold behaviour either, so again, since the representation (2.54) must contain this behaviour, there must either be an infinite number of them, or it must stem from the background integral, however far back one may push the integration contour.

Where an s -channel pole will appear in the t -channel J -plane depends on the behaviour of its residue $g(s)$. If g is real and constant as $s \rightarrow \infty$ then the $1/s$ behaviour of (6.2) will give rise to a fixed J -plane pole at $J = -1$. On the other hand if $g(s)$ decreases exponentially with s the resonance will never appear in the J -plane however far back we push the integration contour, but will always be part of the background integral. If there are many poles there may be a mutual cancellation

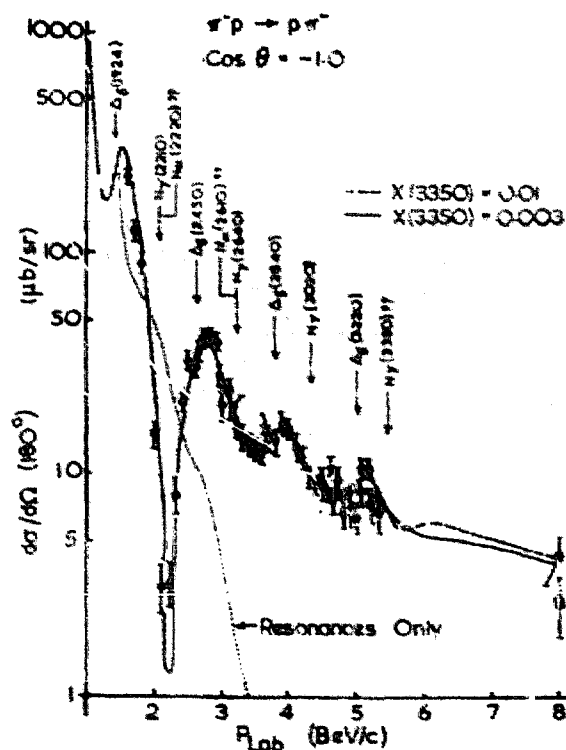


Fig. 34. The differential cross section for backward $\pi^+p \rightarrow \pi^+p$ scattering, showing the interference pattern and its interpretation in refs. [57, 58] in terms of resonances interfering with a smooth Regge exchange background.

between them so that even with constant g 's the asymptotic behaviour is faster than $1/s$, but if the s -channel poles are ever to give rise to the asymptotic behaviour of a t -channel Regge pole an infinite number will be needed.

It is thus not possible to give a simple a priori answer to the question of how to cope with the intermediate energy range, because we do not know how to continue the Regge pole and cut terms down to low energies, or the resonance pole terms to higher energies. The answer depends on the dynamics of the particular amplitude.

One suggestion is that one can simply add the leading trajectories and the resonance poles [57, 58], so that

$$A_H(s, t) = A_H^{\text{Regge}}(s, t) + A_H^{\text{Res}}(s, t), \quad (6.3)$$

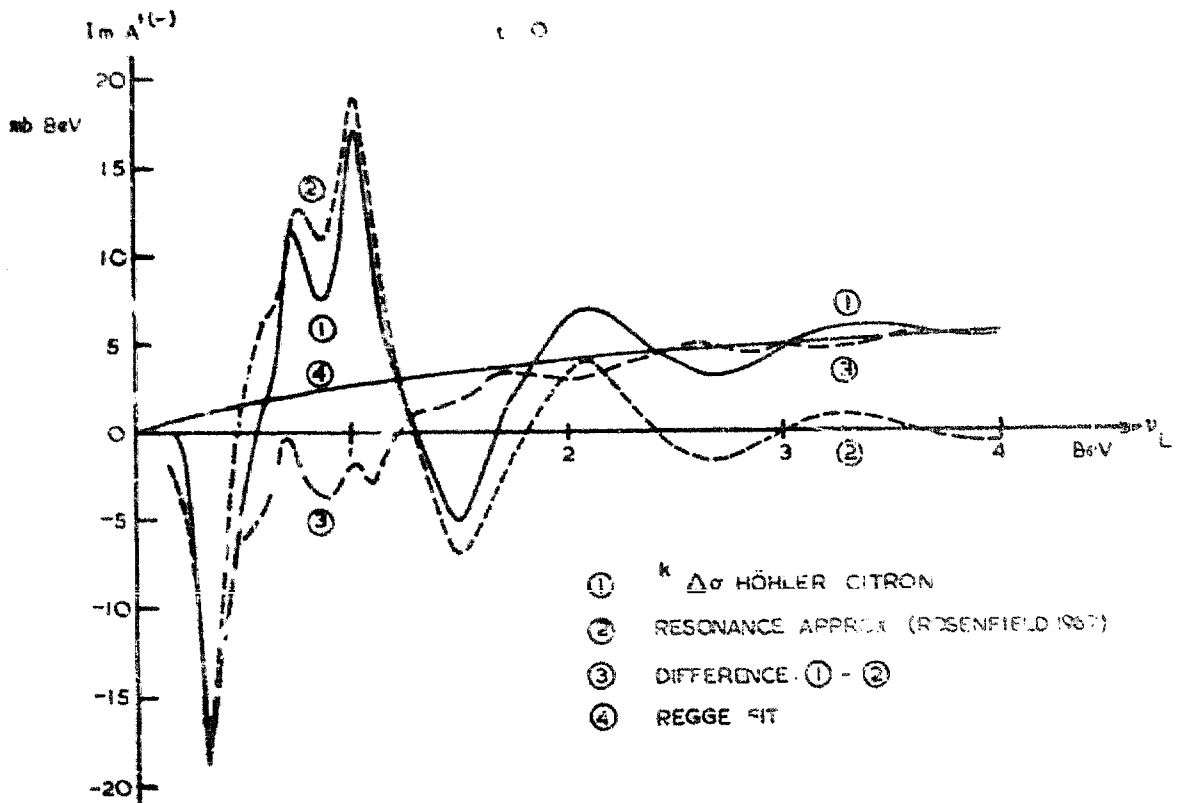
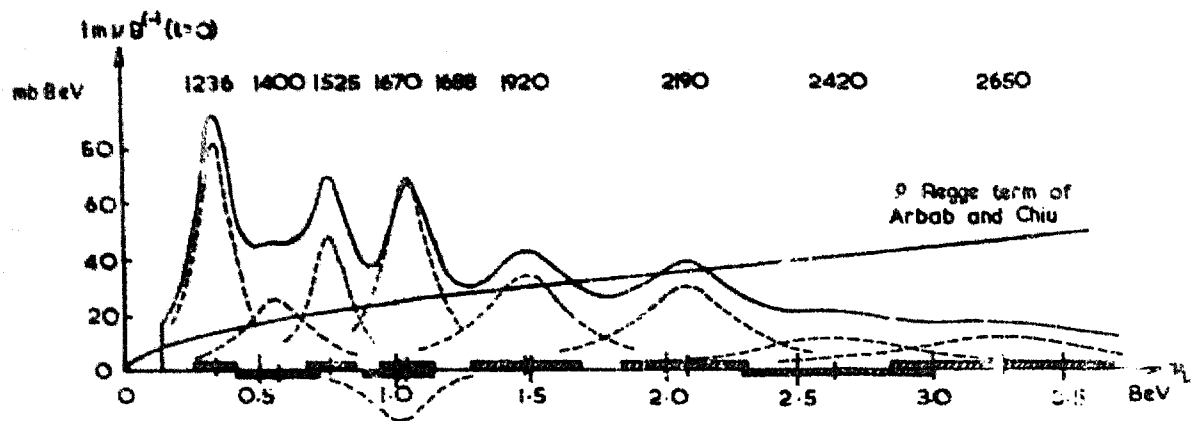


Fig. 3. The resonance and Regge pole contributions to $\text{Im} A^{-1}$ and $\text{Im} (\nu B)$ in $\pi^- p \rightarrow \pi^0 n$ at $t = 0$; from ref. [133].

i.e. the Regge poles give a smooth background to the resonances, and the resonances are part of the background integral below the leading poles. The Regge and resonance amplitudes are both complex of course, and the resulting interference pattern, a bumpy resonance structure superimposed on the Regge asymptotic behaviour, was used by Langer and Cline [57, 58] to identify resonances, for example by looking at backward πN data (see fig. 34).

However this 'interference model' was criticised in a now classic paper by Dolen, Horn and Schmid [133] on the grounds that the resonances may already be included in the Regge terms, at least to some extent, so that double counting may occur. In particular they found that in $\pi^- p \rightarrow \pi^0 n$ if they added the known resonances to the ρ trajectory obtained from a high energy fit the result was much larger than the amplitude (fig. 35).

This in itself is not conclusive, however. Firstly it is not difficult to think of different parameterizations of the Regge pole terms, such as $[(s - s_f)/s_0]^{\alpha(t)}$ instead of $(s/s_0)^{\alpha(t)}$ for example, which greatly reduce the magnitude of the Regge term at low energy (near the arbitrary point s_f) without altering the asymptotic behaviour. The branch point at $s = s_f$ would be spurious of course, but then so is the one at $s = 0$ in the usual Regge term - it comes from the approximation (4.25) and is inconsistent with the analyticity of the amplitude.

Secondly the size of the resonance contribution is ambiguous. The usual method of identifying a resonance in partial-wave analysis is to make an Argand diagram plot of the phase of the amplitude varying with energy. An inelastic Breit-Wigner term of the form

$$A_J(s) = \frac{\Gamma x \sqrt{s_f}}{s_f - s - i \Gamma \sqrt{s_f}}, \quad (6.4)$$

(where Γ is the width and x the elasticity) would produce an anticlockwise loop in this Argand diagram, as in fig. 36, and so the resonance parameters may be established by trying to fit the loop with such a Breit-Wigner formula [134]. The parameters are chosen so as to saturate the amplitude at the resonance point, but the contribution of an inelastic resonance can be made much smaller by giving its residue a phase $e^{i\phi}$. (Reality of the residues is required only for elastic resonances without background [135].) Low energy, fairly elastic, resonances usually produce bumps in the amplitude, and their identification is not in doubt, but in the

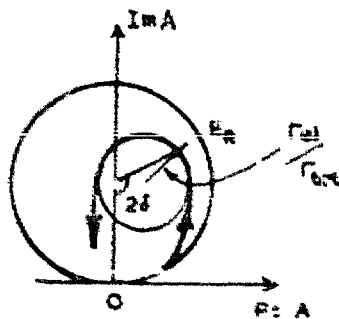


Fig. 36. Showing the behaviour of the partial-wave Argand diagram when an inelastic resonance occurs. For a range of energies near the resonance energy E_R the curve follows the circle due to the Breit-Wigner term, but this circle is smaller than the unitarity circle because of the inelasticity, and it is pushed over to one side, and the phase at resonance is rotated from $\frac{1}{2}\pi$ by the background.

intermediate energy region there can be little certainty about their existence and strength. In fact, as we shall discuss below, perfectly good fits to the data can be made using the interference model (6.3), with phases for the resonance residues [196].

Despite this there have been several theoretical developments which have led many people to believe that the double-counting of the interference models is serious, and it is these developments which form the subject of this chapter. But first we must introduce another tool which has been much used in recent Regge phenomenology, finite energy sum rules.

6.2. Finite energy sum rules

Finite energy sum rules (FESR) are akin to the SCR of section 2, but they differ in that they are not restricted to cases where the amplitude is convergent at infinity [193]. It is only necessary that the amplitude should have a known asymptotic behaviour. Most of the applications have been restricted to situations where only Regge poles are expected to be important in the high-energy behaviour, and we shall make this simplification in our presentation. The inclusion of cuts is mentioned in the final section.

A scattering amplitude is expected to obey a fixed t dispersion relation (2.26)

$$\hat{A}_{H_i}(s, t) = \frac{1}{\pi} \int_0^\infty \frac{D_S(s', t)}{s' - s} ds' + \frac{1}{\pi} \int_{u_0}^\infty \frac{D_U(u', t)}{u' - u} du' . \tag{6.5}$$

Since we are supposing that there are only Regge poles we can write

$$\hat{A}_{H_i}(s, t) \sim \sum_{s \rightarrow \infty} G_i(t) \frac{e^{-i\pi(\alpha_i - \nu) + \sigma_i}}{2 \sin \pi(\alpha_i - \nu)} \left(\frac{\nu}{s_0}\right)^{\alpha_i(t) - M} , \tag{6.6}$$

where we have defined

$$\nu \equiv (s - u)/2 \tag{6.7}$$

and the residue $G_i(t)$ may be found by comparing with (4.74). We will suppose that the sum (6.6) includes all the poles with $\text{Re } \alpha(t) > -k$ (say). From (6.6)

$$D_S(s, t) \sim \sum_{s \rightarrow \infty} G_i(t) (\nu/s_0)^{\alpha_i(t) - M} \tag{6.8}$$

and

$$D_U(s, t) \sim \sum_{s \rightarrow \infty} \sigma_i G_i(t) (\nu/s_0)^{\alpha_i(t) - M} (-1)^{M - \nu} . \tag{6.9}$$

Hence we may write

$$\begin{aligned} \hat{A}_{H_i}(s, t) - A_{H_i}^{\text{Regge}}(s, t) &= \frac{1}{\pi} \int_{\nu_t}^\infty \frac{D_S(\nu', t) - \sum_i G_i(t) (\nu'/s_0)^{\alpha_i(t) - M}}{\nu' - \nu} d\nu' \\ &+ \frac{1}{\pi} \int_{\nu_t}^\infty \frac{D_U(\nu', t) - (-1)^{M - \nu} \sum_i \sigma_i G_i(t) (\nu'/s_0)^{\alpha_i(t) - M}}{\nu' + \nu} d\nu' , \end{aligned} \tag{6.10}$$

where ν_t is the threshold expressed in terms of ν , and the integrals will converge.

As $s \rightarrow \infty$

$$\hat{A}_{H_t}(s, t) - \hat{A}_{H_t}^{\text{Regge}}(s, t) \sim 1/\nu^k, \quad (6.11)$$

since all the higher contributions to the asymptotic behaviour of the amplitude are included in \hat{A}^{Regge} . So taking the limit of (6.10) as $\nu \rightarrow \infty$ we conclude that the coefficient of $(\nu)^{-1}$ on the right-hand side of (6.10) must vanish, i.e.

$$\int_{\nu_t}^{\infty} \{D_S(\nu', t) - D_U(\nu', t) - \sum_i [1 - \sigma_i(-1)^{M-\nu'}] G_i(t) (\nu'/s_0)^{\alpha_i(t)-M}\} d\nu' = 0. \quad (6.12)$$

Now since the Regge poles contain the asymptotic behaviour of $D_S(\nu, t)$ the integrand will vanish for $\nu > N$ say, if N is chosen to be sufficiently large, so we can write

$$\int_{\nu_t}^N \{D_S(\nu', t) - D_U(\nu', t)\} d\nu' = \sum_j \frac{2s_0 G_j(t) (N/s_0)^{\alpha_j(t)-M+1}}{\alpha_j(t) - M + 1}, \quad (6.13)$$

where we have performed the integral over the Regge pole (and taken its contribution from the lower limit of integration ν_t to negligible relative to that from the upper limit N). It must be noted that only poles with signature $\sigma_j = (-1)^{M-\nu+1}$ contribute to (6.13).

This expression gives us a relation between the imaginary part of the scattering amplitudes at low energies ($< N$), and the Regge pole terms which fit the high energy amplitude ($> N$). It depends only on the analytic properties of the amplitude and the asymptotic behaviour, and is exact to the extent that Regge pole dominance is valid.

We can generalize (6.13) by writing a dispersion relation for

$$[\hat{A}_{H_t}(s, t) - \hat{A}_{H_t}^{\text{Regge}}(s, t)] \left(\frac{\nu}{s_0}\right)^{2n}, \quad (6.14)$$

instead of (6.10). As long as $2n < k$ the coefficient of the $1/\nu$ term must vanish and so we have

$$\int_{\nu_t}^N \{D_S(\nu', t) - D_U(\nu', t)\} \left(\frac{\nu'}{s_0}\right)^{2n} d\nu' = \sum_j \frac{2s_0 G_j(t) (N/s_0)^{\alpha_j(t)-M+2n+1}}{\alpha_j(t) - M + 2n + 1}. \quad (6.15)$$

If an odd power of (ν/s_0) were used in (6.14) only the poles with $\sigma_k = (-1)^{M-\nu}$ would contribute giving

$$\int_{\nu_t}^N \{D_S(\nu', t) + D_U(\nu', t)\} \left(\frac{\nu'}{s_0}\right)^{2n-1} d\nu' = \sum_k \frac{2s_0 G_k(t) (N/s_0)^{\alpha_k(t)-M+2n}}{\alpha_k(t) - M + 2n}. \quad (6.16)$$

An alternative, and perhaps more elegant, way of deriving these results is to use Cauchy's theorem to write (6.5) as

$$\int_c \hat{A}_{H_t}(\nu', t) d\nu' = 0, \quad (6.17)$$

where c is a contour round the threshold branchpoints as shown in fig. 37. Hence we have

$$2i \int_{\nu_t}^N \{D_S(\nu', t) - D_U(\nu', t)\} d\nu' = - \int_{c'} \hat{A}_{H_t}(\nu', t) d\nu', \quad (6.18)$$

where c' is the circle at $|\nu| = N$. If we then replace the amplitude at $|\nu| = N$ by (6.6) and perform the integration round the circle by putting $\nu = N e^{i\phi}$, and take suitable care of the discontinuity of the Regge term at the branch cuts, we obtain the same result as (6.13).

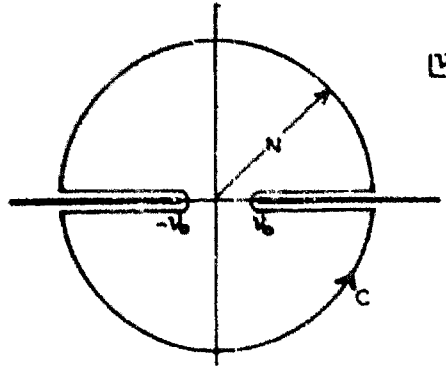


Fig. 37. The contour of integration in the complex ν plane used in (6.17).

These sum rules involve only the imaginary part of the low energy amplitude. It is possible to include arbitrary mixtures of the real and imaginary parts by writing a dispersion relation for [137]

$$A_{H_t}(\nu, t) \left(\frac{\nu_t^2 - \nu^2}{s_0^2} \right)^{\beta/2}, \quad (6.19)$$

where β is a continuously variable parameter. We then get instead of (5.13)

$$\int_{\nu_t}^N [\cos(\pi\beta/2) \text{Im} \hat{A}_{H_t}(\nu', t) - \sin(\pi\beta/2) \text{Re} \hat{A}_{H_t}(\nu', t)] \left(\frac{\nu'^2 - \nu_t^2}{s_0^2} \right)^{\beta/2} d\nu' \\ = \sum_j \frac{2s_0 G_j(t) (N/s_0)^{\alpha_j(t)+\beta+1} \cos \frac{1}{2}\pi [\alpha_j(t) + \beta]}{\alpha_j(t) + \beta + 1 \cos \frac{1}{2}\pi \alpha_j(t)} \quad (6.20)$$

again neglecting terms of order ν_t/N . However only in a few cases is the real part of an amplitude known directly (e.g. from Coulomb interference), and usually the real parts are determined from dispersion relations, in which case they do not of course give independent information about the high-energy behaviour.

These sum rules have had a wide variety of applications [138]. For example [139] if we consider the amplitude for $\pi^-p \rightarrow \pi^0n$, where the negative signature ρ^- Regge pole is expected to be the dominant contribution, we find (using the usual A and B notation for the amplitudes - see e.g. ref. [12] for the relation of these to helicity amplitudes), setting $s_0 = 1$

$$\int_{\nu_t}^N \text{Im} A^{(-)}(\nu', t) d\nu' = G_A(t) \frac{N^{\alpha(t)+1}}{\alpha(t)+1}, \quad \int_{\nu_t}^N \nu' \text{Im} B^{(-)}(\nu', t) d\nu' = G_B(t) \frac{N^{\alpha(t)+1}}{\alpha(t)+1} \quad (6.21)$$

where the $G_i(t)$ are the independent residues in the A' and B amplitudes, and the (-) sign indicates that the anti-symmetric isospin combinations have been taken (see e.g. ref. [12]). These relations have been used to find the ρ trajectory and residue functions, by inserting the phase shift results for the low energy amplitudes. Since phase-shift analyses have only been carried out at low energies it is unavoidable that N should be taken rather low $\approx 1-1.5 \text{ GeV}^2$. This is rather too low for one to have confidence that the asymptotic behaviour has been reached. None-the-less the resulting Regge parameters are in fairly good agreement with those found in high energy fits.

Since there are two Regge parameters $\alpha(t)$ and $G_i(t)$ in each of the relations (6.21) they do not have a unique solution. But it is possible to deduce $\alpha(t)$ from the ratios of different moment sum rules directly. Thus if we define [133]

$$S_n(t) = \frac{1}{N^{n+1}} \int_0^N \nu^n \text{Im} A_i^{(-)}(\nu, t) d\nu = \frac{G_A(t) N^{\alpha(t)}}{\alpha(t) + n + 1} \quad (6.22)$$

then we have

$$\frac{S_n(t)}{S_m(t)} = \frac{\alpha(t) + m + 1}{\alpha(t) + n + 1}. \quad (6.23)$$

So $\alpha(t)$ can be deduced by taking the first two non-vanishing moments, and then inserted in (6.21) to give the $G_i(t)$. The trajectories obtained agree well with those of high energy fits, the residues rather less well. The various resonance contributions to the low energy integrals have different t dependences due to their different spins; in fact they oscillate like $d_{\lambda\lambda'}^\sigma(z_s)$. The result is that the integrals have zeros at various t -values. It is found that $G_A(t)$ changes sign at $t \approx -0.15 \text{ GeV}^2$ and $G_B(t)$ at $t \approx -0.6 \text{ GeV}^2$. This latter point is of course just where we expect a nonsense zero in the ρ residue at $\sigma_\rho(t) = 0$. The former we shall identify in chapter 7 as the 'cross-over' zero of πN scattering.

In principle the presence of secondary trajectories can also be determined by these sum rules. Thus if there is a secondary ρ' trajectory below the ρ with a trajectory function $\alpha_1(t)$ we can deduce

$$\frac{S_1(t) - G_A(t) N^{\alpha(t)}}{S_3(t) - \frac{\alpha(t)+1}{\alpha(t)+3} G_A(t) N^{\alpha(t)}} = \frac{\alpha_1(t) + 3}{\alpha_1(t) + 1}. \quad (6.24)$$

In ref. [133] it is found that $\alpha_1(t) \approx 0.3 + 0.8t$ which is much higher than one would expect, and it can not really be taken very seriously because of the large errors.

The higher moment sum rules weight the integral more towards the upper limit of integration where the amplitudes are less well known. In fact if one takes N large enough the sum rule becomes just the same as a Regge fit at N . The sum rule can be used to predict the high energy behaviour from low energy data only if N is taken large enough, but if N is really in the asymptotic region a high energy fit is really just as good. In either case because of the limited accuracy of the data the results obtained will depend very much on the assumptions which are made as to the number of input trajectories etc. With data of finite accuracy there is no possibility of a unique analytic extrapolation.

There is, however, one crucial advantage of the FESR method over conventional fits, namely that the input amplitudes (e.g. the A' and B πN amplitudes above) are already decomposed into their spin components whereas, the high-en-

ergy ν data only enables us to find $|A'|^2$ and $|B|^2$, and the signs of the amplitudes can not be determined. In fact in the old fits of πN scattering the sign of $B^{(+)}$ was opposite to the value subsequently obtained from FESR. The FESR sign has recently been confirmed by measuring spin-rotation parameters [139].

Another interesting aspect of FESR is the possibility they offer of finding fixed poles at wrong-signature points. These do not contribute to the asymptotic behaviour, of course, and so can not be obtained directly in fits. But if we take amplitudes of definite signature (2.39), which have the dispersion relations

$$A'_H(s, t) = \frac{1}{\pi} \int_{s_0}^{\infty} \frac{D_{Hs}(s', t)}{s' - s} ds' + (-1)^{M-\nu} \int_{u_0}^{\infty} \frac{D_{Hu}(s', t)}{s' - s} ds' \quad (6.25)$$

and follow the procedure (6.5) to (6.16) we find

$$\int_{\nu_t}^N [D_{Hs}(\nu', t) + (-1)^{M-\nu} D_{Hu}(\nu', t)] (\nu'/s_0)^n d\nu' = \sum_i \frac{2s_0 G_i(t) (N/s_0)^{\alpha_i(t) - M + n + 1}}{\alpha_i(t) - M + n + 1} \quad (6.26)$$

These coincide with (6.15) or (6.16) only for alternate moments. The mistake in (6.26) is that we have neglected the fixed poles in the signated amplitude at wrong-signature nonsense points. If there were no fixed poles (6.26) would hold, and to the extent that they are small it may still be approximately valid, but otherwise we need to add them to the right-hand side of (6.26). Thus if we consider the negative signature ρ contribution to the spin-flip amplitude B with $M = 1$, and for which $J = 0$ is a wrong signature point, it is found [133] that for the zeroth moment

$$\int_{\nu_t}^N \text{Im } B^{(-)}(\nu', t) d\nu' = G_B(t) \frac{N^{\alpha(t)}}{\alpha(t)} + g(t), \quad (6.27)$$

where $g(t)$ is almost independent of t . This constant is due to the dominance of the s -channel nucleon born term on the left-hand side of (6.27), whose $1/\nu$ tail gives rise to the fixed power behaviour. It may be interpreted as a fixed pole at $J = 0$.

However, our main interest in FESR in this chapter is that they led Dolen, Horn and Schmid [133] to the conclusion that the interference model commits double counting. The point is that essentially the whole of $\text{Im } A'$ and $\text{Im } B$ at low energies is given by the s -channel poles. Hence we have approximately

$$\int_{\nu_t}^N \text{Im } A'^{(-)\text{Pole}}(\nu, t) d\nu = G_A(t) \frac{N^{\alpha(t)+1}}{\alpha(t)+1} \text{ etc.} \quad (6.28)$$

In other words the average of the direct channel poles is equal to the Regge pole term. This gives one definition of duality - so called 'average duality' - the resonance poles are dual to the Regge poles in this average sense. The authors of ref [133] suggested that instead of the interference model (6.3) a better representation of the amplitude would be given by

$$A_H(s, t) \approx A_H^{\text{Regge}}(s, t) + A_H^{\text{Res}}(s, t) - (A^{\text{Res}}(s, t)). \quad (6.29)$$

The final term represents the average of the resonance terms. Whether or not this is very different from the interference model depends whether the resonances tend to add, as they appear to do in $B^{(-)}$ and $A'^{(-)}$, or cancel as they do in $A'^{(-)}$ and $B^{(-)}$.

However, as we have already mentioned, the work of ref. [136] indicates that since we do not know a priori the phase of an inelastic resonance contribution it is possible to make either prescription work in any amplitude. But if (6.28) is accepted it leads to a new sort of bootstrap-like principle in which the direct channel resonances determine the cross-channel Regge poles. It is very different of course from the conventional form of bootstrap in which unitarity is used to generate the resonances from the crossed-channel potential, and in particular, as we shall see in section 5, the solutions of the FESR conditions are in no way unique. Because of this we would prefer to use the term 'FESR consistency condition' to describe this duality idea, and preserve the word 'bootstrap' with its former meaning.

It should be noted that the resonances dominate the imaginary part of the amplitude but not the real part (the real part of a Breit-Wigner formula vanishes at the resonance position). A common approximation is to represent the imaginary part as a sum of delta-functions at the resonance positions

$$D_S(s, t) = \sum_r R(s, t) \delta(s - s_r). \quad (6.30)$$

The reason why the FESR gives such a strong constraint is evident from this approximation. For substituted in the dispersion relation (6.5) the form (6.30) gives

$$A(s, t) = \sum_r \frac{R(s_r, t)}{s - s_r} \sim \frac{1}{s}, \quad (6.31)$$

but we have assumed that $A - A^{\text{Regge}} < O(1/s)$ so the resonances must be contained in the Regge term.

6.3. Schmid loops

The form of a Regge pole amplitude presents us with a further possible source of ambiguity in identifying inelastic resonances. We have mentioned that the method used in phase-shift analysis is to look for anti-clockwise loops in the partial-wave Argand diagram, but it was shown by Schmid [140] that the crossed-channel Regge pole term may also give rise to such loops because of the phase variation given by the signature factor.

For example in a spinless scattering amplitude with the exchange of a single Regge trajectory $\alpha(t) = \alpha(0) + \alpha't$, and equal mass kinematics,

$$z_s = 1 + \frac{t}{2q_s^2}; \quad q_s^2 = \frac{s - 4m^2}{4}, \quad (6.32)$$

the phase of the s -channel partial wave projection depends on [141]

$$\int_{-1}^1 e^{-i\pi\alpha(t)} P_J(z_s) dz_s = e^{-i\pi[\alpha(0) - 2\alpha_s^2 \alpha']} i^J j_J(-2q_s^2 t), \quad (6.33)$$

where $j_J(x)$ is the spherical Bessel function. Thus as the energy (or q_s^2) increases the phase of the partial-wave amplitude rotates anti-clockwise. And if we identify the point s_r , where the phase reaches $\pi/2$, as a 'resonance' position, then there will be another 'resonance' at

$$s'_\gamma = s_\gamma + 1/\alpha' \text{ etc.} \quad (6.34)$$

and every partial wave resonates at these same values of s . So the form of the partial waves is similar to that for a set of trajectories. The parent trajectory is linear with slope α' , with a sequence of daughter trajectories such that in each partial wave the resonances are spaced by $1/\alpha'$. (There are also trajectories above the parent which we discuss later.) The t dependence of all the other factors in the Regge pole term will obviously alter the shapes and sizes of the loops, but the phase variation must retain the pattern indicated above as long as $\alpha(t)$ and t are real. The reason for this structure is of course that the oscillating phase of the Regge term matches the oscillations in z_s of the Legendre polynomials representing the spins of the 'resonances'. Since $P_l(z_s) \rightarrow 1$ as $z_s \rightarrow 1$ all the 'resonances' add in the forward direction corresponding to the peripheral forward peak of the Regge term.

How should these loops be interpreted? We know that the Regge pole term is a smooth function of s and does not contain any poles, but on the other hand we only know the form of the Regge term on the physical sheet and the resonance poles are on unphysical sheets. Remembering the average duality suggested by FESR analyses it seemed natural to Schmid [140] to identify the loops with a set of overlapping resonances. The difference is that now the duality is local - the matching of the resonances with the Regge pole holds at each s point without any need of averaging. The sum of the poles gives rise to a smooth Regge behaviour because as one partial wave reaches its maximum at a resonance others are at minima. The fact that the resonance has been projected from a smooth function guarantees this cooperation between the partial waves. Obviously such a cooperation is a good deal less than perfect in the actual physical amplitudes at low energies because we see bumps, but it may be supposed that the smooth high energy behaviour represents the onset of local duality.

This would mean that at any energy one could use either the s -channel resonance prescription (6.2) or the t -channel Regge pole description (2.54). At low energies, where the resonance poles are well separated, the s -channel description is to be preferred since a large number of Regge poles are needed to produce the bumps; while at high energies the s -channel prescription becomes complicated, requiring many overlapping resonances, but the t -channel prescription requires only a few Regge poles.

The failure of the s -channel partial-wave series outside the Lehman ellipse should make one cautious about pressing the equality of the two descriptions too far, however. An equally good interpretation [142] of what is happening would seem to be that the Argand loops at high energies do not correspond to resonances at all but are simply the result of the phase variation caused by the crossed-channel Regge poles. For example it is certainly the case that if one takes a high energy fit to say πN scattering, and continues it down to lower energies, and makes a partial-wave projection, the Argand loops obtained are very similar to those found in low energy partial-wave analyses [142, 143]. This obviously must be so to the extent that the continued Regge poles give a reasonable fit to the low energy data. The loops are more complicated than in the discussion above because the phase of the amplitude at any point is the sum of the phases of several different Regge poles. And of course if one chooses not to interpret the loops as resonances the whole case for duality crumbles, and the interference model may be re-instated.

The only way of distinguishing these two hypotheses is to try and find some criterion for the existence of inelastic resonances apart from Argand loops. When a resonance produces a strong bump in some amplitude its existence is very plausible because a small number of Regge terms can not produce such a bump, but at higher energies where the amplitudes are smooth there does not seem to be any simple criterion that can be applied. A resonance pole exists on an unphysical sheet, and there is no unique way of analytically continuing the experimental data from the real axis.

In order to make such a continuation one requires a dynamical model. The Breit-Wigner formula is one such model but it is by no means unique, and in fact ought not to be applied in situations where the resonance may have a large background [135]. If we had an adequate dynamical model for inelastic resonances (based for example on many channel N/D equations) one could try to confirm the presence of such resonances properly, but as we are still very far from having satisfactory models only the low mass resonances can be regarded as well established at present.

There is one other important property of a resonance pole, that it should appear in all communicating channels, which at first sight might seem to offer hope of distinguishing true resonances from Regge pole effects. Put in another way, since the Regge poles must factorize in the t -channel, and the resonances must factorize in the s -channel, if Regge generated loops are to be interpreted as resonances they must factorize in both s and t , which is hardly possible. This is only true for single trajectory exchanges, however, and we shall find in the next section that very often either there are cancellations between different trajectories, or a closely related set of poles can be exchanged in the various communicating channels such that similar circles are produced in each. This only confounds the problem of the existence of high mass resonances, but it also means that if one believes in dual models one must place various restrictions on the trajectories which can be exchanged which have very interesting consequences for Regge phenomenology.

6.4. Dual models [144]

The first thing to note about the suggested equivalence of crossed-channel Regge poles and resonances is that it can not be made to work for the Pomeron (P). For example, as far as we know K^+p scattering does not give rise to any resonances. If there were such doubly charged strange baryons they would not fit into any of the $SU(3)$ multiplets discussed in chapter 3, and could not be made up from three quarks as the other baryons can. For this reason K^+p is known as an 'exotic' channel. But, of course, like other elastic scattering processes $K^+p \rightarrow K^+p$ is expected to be controlled at high energy by the exchange of the P trajectory. We shall see in chapter 7 that there have been many successful fits of this kind. Since there is no other trajectory known which is high enough to cancel the P we would expect to find Schmid loops in K^+p scattering, but these would not correspond to resonances.

The most popular way out of this dilemma [145, 146] is to suppose, not implausibly, that the P is quite unlike other Regge singularities. We have already noted, in chapter 5, the condensation of cuts which results from multiple P exchange, and it may well be that the singularity which has been represented by the P pole in Regge fits is really a complicated superposition of cuts. Alternatively it can be argued that the P may have a very small slope, so that its phase oscillations are

slow, and will only produce loops at high energies if at all. In fact at one time an almost zero slope for the P seemed to be favoured in Regge fits, and the more recent Serpukhov data seem to favour $\alpha'_P \approx 0.5$ which is only about half that of other trajectories. Thus the P may not give rise to loops (or perhaps to very weakly coupled, sometimes exotic, ones), and its main function may be to give a predominantly imaginary background to the resonances produced by all the other exchanged trajectories. In K^+p these other exchanges are ρ , ω , f and A_2 , but we have already found that these have roughly degenerate trajectories, and if we suppose that this degeneracy holds for the residues too, these contributions to the imaginary part of the amplitude will cancel (see (4.92)) leaving only the P. This suggestion is born out by the flatness of the K^+p total cross section (see section 7.6) which can be fitted by the P alone. In fact quite generally the total cross sections for those processes which do contain resonances, such as $\pi^\pm p$, $K^- p$, $K^- n$, $\bar{p}p$ and $\bar{p}n$, are decreasing at high energies so the lower trajectories must contribute, while in processes with no known resonances, like K^+p , K^+n , pp and pn , the cross sections are more-or-less constant above about 2 GeV (below which threshold effects may be important). One also finds that exotic processes have smooth differential cross sections, while those with resonances exhibit dips in $d\sigma/dt$ characteristic of Regge pole exchanges.

These facts suggest that, if one first subtracts the Pomeron from all the amplitudes to which it can contribute, it may be possible to fit the remaining amplitudes with just the lower lying trajectories, and that these trajectories will be dual to non-exotic resonances only. One is thus postulating a solution to the FESR consistency condition which contains only poles (direct channel resonances = crossed channel Regge poles).

To see how such a model fits together we start with $\pi\pi$ scattering. When the P has been removed we are left with only the ρ and f from among the dominant trajectories. The $I = 2$ $\pi^+\pi^+$ and $\pi^-\pi^-$ states are exotic, and if they are to contain no resonances we require that the ρ and f exchanges should be exchange degenerate and cancel each other, i.e. $\alpha_\rho(t) = \alpha_f(t)$ and $\beta_{\rho\pi\pi} = \beta_{f\pi\pi}$. Then in $\pi^+\pi^-$ scattering the sign of the ρ contribution is opposite (due to charge conjugation) and the required resonances do occur in the $I = 0$ and $I = 1$ channels. Then in $K\bar{K}$ scattering we can exchange the $I = 0$ f and ω , and the $I = 1$ ρ and A_2 . The absence of resonances in the exotic K^+K^- and K^+K^0 channels requires $\alpha_f = \alpha_\omega$, $\alpha_\rho = \alpha_{A_2}$, $\beta_{fKK} = \beta_{\omega KK}$ and $\beta_{\rho KK} = \beta_{A_2 KK}$. And in πK scattering, where we have the exchange degenerate K^* , K^{**} trajectory, the $I = \frac{3}{2}$ channel is exotic, and we require that the ρ and f should be exchange degenerate with $\beta_{\rho KK} = \beta_{fKK}$.

In fact we can express all these requirements in terms of octet-octet scattering with SU(3) symmetry [147]. However, the symmetry can not be exact for we need $\beta_{\rho KK} = \beta_{\omega KK}$, while SU(3) gives $\sqrt{3}\beta_{\rho KK} = \beta_{\omega KK}$. But if we introduce a mixing between the ϕ and ω , so that the physical ω particle is a mixture of the octet and singlet $I = 0$ states,

$$|\omega\rangle = \cos\theta|\omega_8\rangle + \sin\theta|\omega_1\rangle,$$

we can satisfy the duality requirement with a mixing angle $\cos\theta = (\frac{1}{3})^{-\frac{1}{2}}$, i.e. $\theta \approx 35^\circ$. This angle is the one obtained from the quark model if the ϕ consists only of strange quarks (= $\lambda\bar{\lambda}$) - the so called 'ideal' mixing angle - and is in rough agreement with the experimental value obtained from the mass splitting, $\theta \approx 40^\circ$ [48]. This same angle is needed for f, f' mixing if the f' is to decouple from $\pi\pi$ scattering so as not to spoil the above picture, and experimentally it is found that for the 2^+ nonet $\theta \approx 30^\circ$ [48].

If we proceed to examine forward meson-baryon scattering, exactly the same restrictions are needed - in fact we have already noted that the above degeneracy of ρ , f , ω and A_2 is also needed to ensure no exotic resonances in K^+p . New results come from backward scattering however since the u channel trajectories can also give Schmid loops. The absence of K^+p resonances requires a degeneracy of the $\Lambda_{\alpha,\beta}$ and $\Sigma_{\beta,\gamma}$ trajectories [148]. (There are many Y^* states but the others are weakly coupled, and may presumably be neglected to some approximation.) Similarly in $K^-p \rightarrow \Sigma^+\pi^-$ the Δ resonances in the u channel ($K^+\Sigma^+ \rightarrow p\pi^+$) are dual to the K^* , K^{**} $I = \frac{1}{2}$ trajectories, and there has to be a degeneracy between the Λ and Σ trajectories in order to avoid $I = \frac{3}{2}$ K^* 's. So generalized to SU(3) we need a degeneracy between the various singlet, octet and decuplet trajectories having the same (or related) quantum numbers [146]. This is partly substantiated by some of the best cases shown in fig. 38, but is not well satisfied in general.

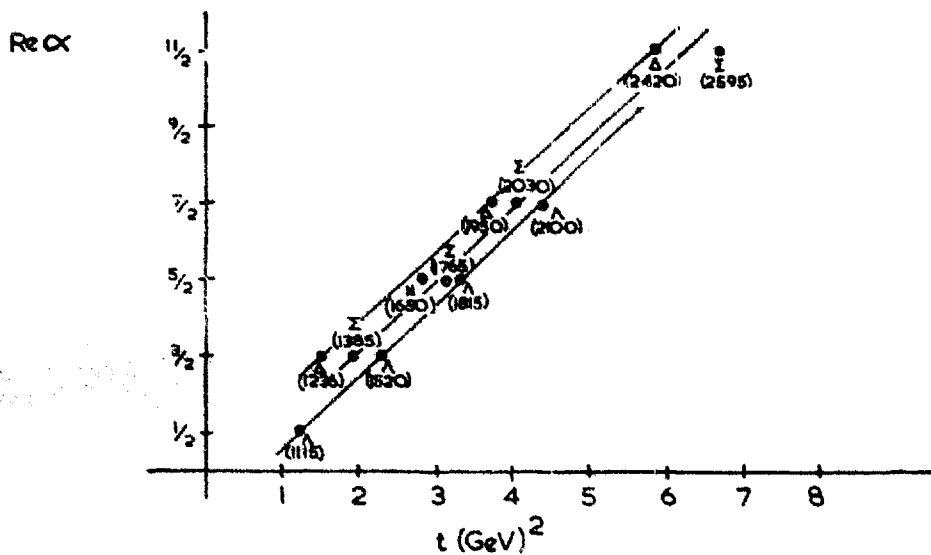


Fig. 38. Some examples of exchange degenerate baryon trajectories. These are the best examples. The trajectory splitting is much greater for other baryons.

The idea of duality thus produces an impressive set of predictions - that resonances fall into singlets, octets and decuplets only with no exotics, that the 2^+ and 1^- mesons, and the octet and decuplet baryons, are exchange degenerate, and that the 2^+ and 1^- mixing angles are about 35° . All these results may be expressed very simply with the 'duality diagrams' of Harari [149] and Rosner [150], in which each external particle is represented by lines corresponding to the quarks (p , n , λ) of which it is composed. The quarks maintain their identity throughout the process, and this tells one what the intermediate states in either channel are. Thus three quarks travelling in the same directions give a baryon, while two travelling in opposite directions give a meson, and only diagrams with 2 or 3 quark intermediate states are allowed (see fig. 39). Diagrams with crossing lines or more than this number of quarks are 'illegal'. These rules embody SU(3), no exotic states, and the mixing angle.

There are, however, some serious problems with this duality scheme. The first concerns baryon-anti-baryon scattering. Here we have 3 quark lines in each direction (fig. 39) which is illegal so we predict that there are no meson resonances in the $B\bar{B}$ channel. One might think of altering the rules to include them but it does

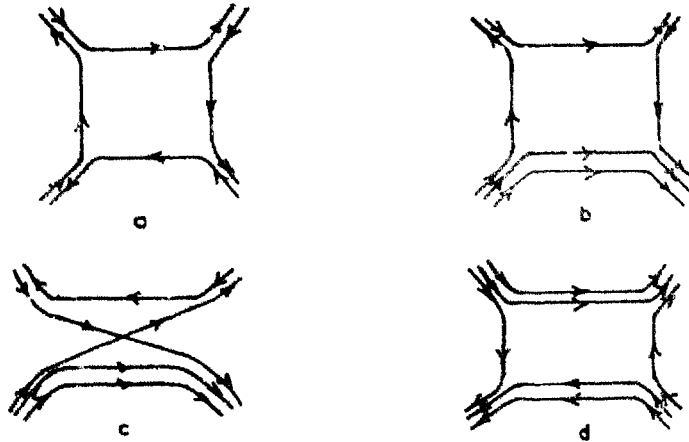


Fig. 39. Duality diagrams for (a) meson-meson and (b) meson-baryon scattering. (c) is an 'illegal' meson-baryon diagram because the quark lines cross. (d) The diagram for baryon-anti-baryon scattering showing the four quarks in the $B\bar{B}$ intermediate state.

not seem to be possible to do this consistently [151]. For example in $\Delta\bar{\Delta}$ scattering there are $I = 0, 1, 2, 3$ channels, and only $I = 0, 1$ should contain resonances. Imposing no exotics in $I = 2, 3$ in both the s and t channels requires that all the amplitudes should vanish. Another problem stems from the fact that the 0^- mesons do not have the ideal mixing angle, but rather $\theta \approx 10^\circ$ [48], so there is no consistent solution to the duality requirements for processes in which these trajectories can be exchanged, such as pseudoscalar-scalar, or pseudoscalar-vector scattering. And although we have found a solution with three groups of degenerate trajectories $\alpha_\rho = \alpha_\omega = \alpha_f = \alpha_{A_2}$, $\alpha_{K^*} = \alpha_{K^{**}}$ and $\alpha_\phi = \alpha_{f'}$, if one considers simultaneously the three reactions $\pi^+p \rightarrow \pi^+p$, $\pi^+p \rightarrow K^+\Sigma^+$ and $K^+\Sigma^+ \rightarrow K^+\Sigma^+$, all of which contain Δ 's in the s channel, but which exchange members of different groups in the t channel, one must require all the trajectories to be degenerate [152]. That is to say we need complete SU(3) degeneracy, despite the fact that we also need a mixing angle. Also the attempts which have been made to fit amplitudes by a sum of the P plus direct channel resonances have not been all that impressive quantitatively [153, 154], and in chapter 7 we shall show evidence that the exchange degeneracy of residues seems to be violated by factors of 2 and more.

So one must conclude that these dual models involving just poles bear at best only a rather partial resemblance to the real world, though they do seem to have several merits as a first approximation. But so far we have only considered the construction of dual models in terms of their internal quantum numbers. We must now think about the construction of functions which satisfy the requirements of duality.

6.5. The Veneziano model

The Veneziano model [155, 156] is a simple analytic function which satisfies most of the requirements of duality in a model involving poles only.

As an example we consider the amplitude for $\pi^+\pi^- \rightarrow \pi^+\pi^-$ which has poles in the s and t channels, but the u channel is exotic ($I = 2$). Once the P contribution has been removed we expect the leading contribution to be the ρ -f exchange degenerate trajectory in both channels. Duality requires that the sum of an infinite number of s -channel poles should be re-expressible as a sum of an infinite number of t -channel poles, in such a way that either sum gives the complete amplitude. And the

asymptotic behaviour must correspond to that of the leading trajectory exchanged, in either channel.

The simplest functional form which has an infinite set of s channel poles lying on a trajectory $\alpha_s(s)$, with the poles appearing when $\alpha_s =$ positive integer, is $\Gamma[1 - \alpha_s(s)]$. Since we require an identical behaviour in the t -channel we might try

$$A(s, t) = \Gamma[1 - \alpha_s(s)]\Gamma[1 - \alpha_t(t)], \tag{6.35}$$

but this would have a double pole at every s - t point where both α_s and α_t are integral [157]. (In our case α_s and α_t are the same function, but in more general amplitudes this need not be true.) We can easily remove these poles by dividing by $\Gamma[1 - \alpha_s(s) - \alpha_t(t)]$ so we end up with the Veneziano formula

$$V(s, t) = g \frac{\Gamma[1 - \alpha_s(s)] \Gamma[1 - \alpha_t(t)]}{\Gamma[1 - \alpha_s(s) - \alpha_t(t)]}, \tag{6.36}$$

where g is an arbitrary constant giving the scale of the couplings. This function has pole lines at fixed s and at fixed t , where the α 's are integers, and lines of zeros running diagonally through the intersections of the poles, as shown in fig. 40.

Its asymptotic behaviour may be obtained from Stirling's formula:

$$\Gamma(x) \xrightarrow{x \rightarrow \infty} (2\pi)^{\frac{1}{2}} e^{-x} x^{x-\frac{1}{2}}, \tag{6.37}$$

except along the negative x axis where the poles occur. If we combine (6.37) with (4.70) we find that for large s , assuming $\alpha(s)$ is an increasing function of s as $s \rightarrow \infty$

$$V(s, t) \rightarrow \frac{\pi [\alpha_s(s)]^{\alpha_t(t)}}{\Gamma[\alpha_t(t)] \sin \pi \alpha_t(t)} e^{-i\pi \alpha_t(t)}. \tag{6.38}$$

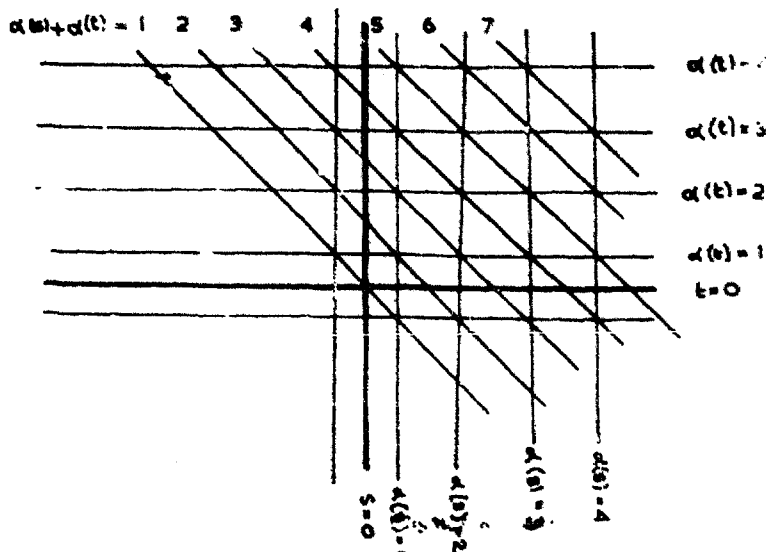


Fig. 40. The Veneziano amplitude in the s - t plane. The poles occur where $\alpha(s)$ and $\alpha(t)$ pass through positive integers, and the lines of zeros connect the pole intersections diagonally in order to prevent there being double poles.

So if $\alpha_S(s)$ is a linear function of s , $\alpha_S(s) = \alpha(0) + \alpha' s$ we end up with Regge behaviour, $V(s, t) \sim (\alpha' s)^{\alpha(t)}$. Comparing this with (4.74) we see that we obtain $\alpha' = 1/s_0$. We have noted that s_0 is usually taken to be $\approx 1 \text{ GeV}^{-2}$ which agrees with the trajectory slopes, and this model provides the only known connection between these two quantities; in fact it is the only prediction of s_0 in any theory known to the author. There is a problem, however, in that the asymptotic behaviour does not hold within a wedge along the real s axis because of the accumulation of s poles there.

Since, if $\alpha(s) = \text{integer } J$ (say) for some $s = s_J$ we have

$$\Gamma[1 - \alpha_S(s)] \underset{s \rightarrow s_J}{\sim} \frac{(-1)^J}{(J-1)! \alpha'(s - s_J)} \tag{6.39}$$

and the expression $\Gamma[1 - \alpha_t(t)] \{\Gamma[1 - J - \alpha_t]\}^{-1}$ can be written as a polynomial in $t [= -2q_S^2(1 - z_S)]$ of order J , we find that the residue of the pole at s_J is

$$g(\alpha')^{J-1} \frac{(2q_S^2)^J}{(J-1)!} (z_S)^J + O(z_S^{J-1}). \tag{6.40}$$

And if this polynomial in z_S is expressed as a sum of Legendre polynomials in z_S the highest term is $P_J(z_S)$, so the pole corresponds to a degenerate sequence of resonances of spins $J, J-1, \dots, 0$ i.e. a daughter sequence [158].

For $\pi\pi$ scattering the coupling factor g may be determined by ensuring that the residue of the rho meson pole on the leading trajectory at $J = 1$ corresponds to the known $\rho \rightarrow \pi\pi$ decay width. Once this is done the whole $\pi^+\pi^-$ amplitude (apart from the P) is fixed. The full $\pi\pi$ amplitude for all isospins may then be found by adding $V(s, u)$ and $V(t, u)$ terms in accordance with the crossing matrix and the absence of $l = 2$ resonances (see e.g. ref. [159]). The resulting resonance spectrum is shown in fig. 41 with the degenerate daughter trajectories below each of the parents. Unfortunately most of the required states are not known, as we have already seen in chapter 3. Similar Veneziano constructions can be made for other processes.

It is clear that since the Veneziano model is an analytic function of s and t containing just poles, and having the correct asymptotic behaviour, it must provide a solution of the FESR consistency condition (6.28) [155, 160]. It has, however, a very serious deficiency in that the resonance poles all lie on the real axis and have

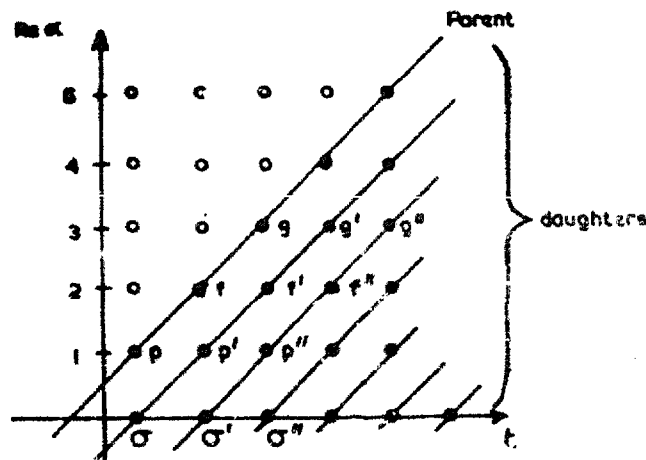


Fig. 41. The $\sigma, \rho, f, g \dots$ states required in the Veneziano model for $\pi\pi$ scattering. The open circles above the parent trajectory represent the positions where ancestors occur if complex α 's are used.

zero width. This prevents there being Regge behaviour on the real axis, and of course it is incompatible with the unitarity condition. It also means that it is not possible to compare the formula directly with experiment.

The trajectories should obviously have an imaginary part above threshold generated by unitarity, and if this is inserted into (6.36) the poles are moved off the real axis. But this has the undesirable side-effects, that all the resonances at a given s value (all the daughters) have the same width (though they have different residues, and hence different elasticities), and that the residues of the poles cease to be polynomials in s and so there are resonances of arbitrarily high spin at every s_T point. The trajectories generated in this way which lie above the parent trajectory are called 'ancestors' [161] (fig. 41). (We have already noted a similar problem with Schmid loops.) Despite the fact that these trajectories lie higher than the parent the asymptotic behaviour of the amplitude is still given by the parent (i.e. is $s^{\alpha(t)}$) by construction. This indicates that an amplitude with ancestors fails to satisfy the conditions for Carlson's theorem, and does not have a Sommerfeld-Watson representation. Even if we are prepared to ignore these ancestors this procedure still does not give very good agreement with experiment because the resulting Argand diagram loops are very poorly correlated with the resonances [162], and the amplitude is very oscillatory at intermediate energies and does not achieve a smooth Regge behaviour until very large s (≈ 20 GeV) is reached unless $\text{Im } \alpha(t)$ is made to grow very rapidly with s . In this case the resonances rapidly become so wide as to disappear [162, 163], unlike fig. 13.

Although there has been a large literature [164] on more sophisticated methods of unitarizing the Veneziano model all the different suggestions seem either to have serious mathematical defects or to impose unitarity in such a way that the original duality properties of the model get lost in the process. The basic problem is that the Veneziano model is independent of the external particle masses whereas the unitarity cuts depend directly on these masses. It thus seems more-or-less inevitable that unitarity must break the duality between the poles, and that this sort of dual model will only provide a non-unitary first approximation. And all attempts to confront dual models with experiment necessarily involve approximations which destroy some of their essential features.

There is also a lot of ambiguity in the precise form the Veneziano model should take. The particular form (6.36) is only one of a whole class of functions satisfying our requirements, and we can write more generally

$$A(s, t) = \sum_{lmn} C_{lmn} V_{lmn}(s, t), \quad (6.41)$$

where the C 's are arbitrary expansion coefficients and

$$V_{lmn}(s, t) \equiv \frac{\Gamma[1 - \alpha_S(s) + l] \Gamma[1 - \alpha_T(t) + m]}{\Gamma[1 - \alpha_S(s) - \alpha_T(t) + n]}, \quad (6.42)$$

where l, m, n are positive integers (or zero). Terms like (6.42) are known as Veneziano satellites. They differ from (6.36) in that the first pole in s lies at $\alpha_S(s) = l+1$ not 1, etc., and the asymptotic behaviour is $s^{\alpha_T(t) + m - n}$, etc. Thus (6.42) provides a perfectly good solution to the FESK constraints which need to give no relation what-so-ever between the leading singularities in the s and t channels [165, 166]. Only if both sets of leading singularities appear in the same Veneziano term are

they correlated. This sort of ambiguity highlights the difference between the FESR consistency condition and a true bootstrap whose uniqueness depends on satisfying unitarity as well as the analyticity requirements.

The fact that the trajectories all appear in exchange degenerate pairs means that there are no fixed poles in the residues, and the Regge pole amplitudes have wrong-signature zeros. It also means that the trajectories decouple from the sense as well as the nonsense amplitudes. Thus for example in πN scattering the ρ trajectory must decouple from the sense amplitude at $\alpha = 0$ in order to avoid a ghost, so by exchange degeneracy the ρ decouples as well. In other words the trajectories all choose nonsense in the nomenclature of section (4.6). The Veneziano amplitudes themselves contain fixed poles [167], however, because they contain (essentially) a third double spectral function (except in cases where there are exotic channels with no resonances). These are unshielded by cuts of course, but since we do not apply the unitarity condition this does not matter.

Experimental applications of the Veneziano model require that we should be able to deal with particles having spin. This has not been done in a completely satisfactory way for arbitrary spins, because there are the usual problems of the parity doubling of straight Fermion trajectories, and the fact that the daughter sequences in the Veneziano model do not correspond to those of a Toller pole means that in order to satisfy the conspiracy relations etc. infinite sums of Veneziano terms with parity degeneracy are needed to give the Toller pole behaviour. Nonetheless such processes as πN and KN scattering have been treated by several authors, who represent the A and B invariant amplitudes by Veneziano models containing the appropriate trajectories [168, 169].

A comprehensive fit has been attempted by Berger and Fox [169], who find that sizeable satellite terms are needed, so that the duality between the leading trajectories in the various channels is broken. Also the Δ exchange residue does not extrapolate to the known $\pi N \Delta$ coupling constant at the Δ pole. This and other examples would seem to prove that although the Veneziano model may be a very interesting toy it is not in any sort of quantitative agreement with the two-particle \rightarrow two-particle scattering data.

One reason for its continuing popularity is that it can readily be generalized to processes involving many particles [170]. Thus we may rewrite (6.36) as

$$V(s, t) = B_4[-\alpha_s(s) - \alpha_t(t)] (1 - \alpha_s(s) - \alpha_t(t)) , \quad (6.43)$$

where

$$B_4(x_1, x_2) \equiv \int_0^1 du_1 u_1^{x_1} u_2^{x_2} ; \quad u_2 = 1 - u_1 \quad (6.44)$$

is the Euler beta function. The generalization to the five point function is then [171]

$$B_5(x_1, x_2, x_3, x_4, x_5) = \int_0^1 du_1 \int_0^1 du_4 \frac{1}{u_5} u_1^{x_1} u_2^{x_2} u_3^{x_3} u_4^{x_4} u_5^{x_5} , \quad (6.45)$$

with $u_1 = 1 - u_5 u_2$, $u_2 = 1 - u_1 u_3$ etc. It is outside the scope of this article to discuss Regge fits to many particle production processes [172], but it is evident that this representation provides a convenient way of coping with Regge behaviour in amplitudes depending on many variables. There is no reason to expect good quan-

titative fits with only single Veneziano terms because we know they can not be achieved for the 4-point function, but given the very approximate nature of the most of the multiple production data a few terms may be enough. Though reasonably good fits have been achieved they do not really tell us very much about duality, or (except in a very crude way) about the validity of multi-Regge models. For reviews see refs. [172, 173].

These many-particle models also give us further insight into how to cope with spin. For example if one is interested in a four-point amplitude in which one of the external particles has spin, one can go to the corresponding five-point function and take the residue of the pole corresponding to this particle. This residue gives the required four-point function, which will be a sum like (6.41) with determined coefficients. This has opened up exciting possibilities for dealing with multiparticle intermediate states in bootstrap problems [174], but so far neither the self-consistency of the approach nor the validity of the basic postulates has been established. See ref. [175]. One important consequence of such models is that factorization demands that many of the trajectories should be multiple [176]. Thus if the leading parent trajectory is single, the first daughter is doubled and the second daughter 5 fold. These multiple trajectories do not necessarily have multiple poles at the lowest spin values but they do at the higher ones. There is of course no real evidence for such a multiplicity of resonances except perhaps for the splitting of the A_2 .

6.6. *The problem of duality*

It will be evident from the preceding discussion that the precise status of the duality concept is unclear. It seems to be possible to construct an ideal dual world consisting of an infinite number of parallel Regge trajectories with zero width resonances which satisfy exchange degeneracy, exact SU(3) symmetry, and the ideal mixing angle between the singlet and octet isosinglets, with no Pomeron. But such a model can not be compared directly with experiment because among other things it violates unitarity. However, if we relax the strict duality requirements by giving the resonances finite widths and ignore the ancestor problem, put in SU(3) breaking for the trajectory functions and ignore the factorization problem, and include the P, we find a world which it can plausibly be claimed bears a strong qualitative resemblance to the real world. Indeed it provides the only 'explanation' of many facts (or seeming facts) such as the absence of exotic resonances, the magnitude of the mixing angle, exchange degeneracy, and $\alpha' \approx 1/s_0$.

The agreement with experiment is far from being quantitative, but it is not clear whether this is (a) because duality is only valid to an approximation; or (b) because we have not succeeded in constructing dual models for the real world, where unitarity applies, SU(3) and exchange degeneracy are broken, and cuts, and perhaps weak exotic resonances, exist; or (c) because duality is completely false. Obviously unitarity must make quite a large difference because among other things it will interrelate the P with other trajectories, require the presence of new trajectories (such as those which appear at $L = -\frac{1}{2}, -\frac{3}{2}, \dots$ which we normally choose to ignore) and will require cuts to shield the fixed poles. The failures of Regge fits involving just poles, such as the factorization problems which arise with conspiracies and at the cross-over point (see chapter 7), and the need for cuts to explain some of the $d\sigma/dt$ dips, make it obvious that if dual models are to have any hope of succeeding some way must be found to incorporate cuts. To give just one example, if the pion conspiracy explanation of the forward peak in $\gamma p \rightarrow \pi^+ n$ is rejected because of fac-

torization problems, this peak must be due to a cut. However in terms of the s -channel this peak is produced by the resonances, in particular the nucleon Born term [177]. So the nucleon pole must be dual to a Regge cut in this process, not a trajectory.

It has been suggested that the Veneziano model should be regarded as a sort of Born approximation for strong interactions [174], and that if some sort of unitarity iteration were applied the physical S -matrix would result. But quite apart from the difficulties of carrying out such a unitarization program it is by no means clear that the final amplitudes will obey duality just because their Born approximation does.

What is worse we have seen that if duality is not accepted at the outset then the criteria used for identifying resonances by partial wave analysis are inconclusive, and the existence of a resonance can only finally be decided when we have a dynamical model (involving unitarity) which tells us how to continue onto the physical sheets. One can not tell by looking at experimental data alone, except in the case of very strongly coupled elastic resonance like the Δ . Thus even if the observed 'resonances' (Argand loops) can be made to saturate the amplitude this still does not prove that duality is true because we do not know if they really are resonances.

The author is thus led to the somewhat pessimistic conclusion that the duality idea will only really become experimentally verifiable if a dynamical model which incorporates it can be constructed. Until then it will remain a suggestive but tantalisingly imprecise idea whose meaning is unclear, and whose application to phenomenology is fraught with ambiguities. On the other hand if such a dynamical model can be found it may well be able to explain most of what we now know, or think we know, about strong interactions.

CHAPTER 7 HIGH ENERGY PHENOMENOLOGY

7.1. Exchange models

The principal aim of Regge phenomenology is to try and identify the exchange forces which control elementary particle scattering. We have discussed the main features of the Regge pole and cut exchanges in chapters 4 and 5, and in this chapter we shall give a rather brief survey of the successes and failures of Regge models.

The dominant singularities in any reaction are those which lie right-most in the complex J -plane. In constructing exchange models one must of course bear in mind the restrictions of charge, baryon number, strangeness, and G -parity conservation, and charge conjugation invariance, as well as the $SU(2)$ isospin symmetry. The trajectories exchanged must correspond to the known particles, as discussed in chapter 3, and the various residues of a given pole must be related by factorization. We may also try to add the additional restrictions of $SU(3)$ symmetry for the residues, and exchange degeneracy. Though the cuts are much less restricted, we have seen in chapter 5 how their power behaviour is related to that of the poles, and that there are various models which can be used, at least tentatively, to try and estimate the magnitude of the cuts.

We shall see that some features of the Regge model, such as the fact that the energy dependence of the amplitudes close to the forward and backward directions

should correspond to the highest trajectory which can be exchanged, are very well verified. But there is rather more freedom at larger angles due to the alternative choices of sense or nonsense, etc., the arbitrariness in the behaviour of the residue functions, and the uncertainty in the magnitude of the cuts.

The experimental information available is greatly restricted because the only high energy beams available for experiments are π^\pm , K^\pm , p , \bar{p} and γ , and the only elementary particle targets are the p and the n . (The n is sufficiently loosely bound in the deuteron for one to be able to deduce neutron scattering from deuteron scattering with some confidence.) Since isospin relates $\pi^+p \equiv \pi^-n$ and $\pi^-p = \pi^+n$ this means that there are just 12 possible incident channels. Fortunately there is a much greater variety of two-body final states because one can measure resonance production processes such as $\pi N \rightarrow \pi \Delta \rightarrow \pi \pi N$ with reasonable accuracy. Table 5 contains a list of most of the two-body processes which have been analysed, together with the trajectories which can be exchanged.

We anticipate that elastic scattering will be dominated by the Pomeron, P , with $\alpha(0) \approx 1$ (see section 4.8), but there are also the f (assuming this to be different from the P) and the f' trajectories. Each of these has vacuum quantum numbers, which means that they can also be exchanged in quasi-elastic processes (i.e. no quantum number exchange). There are also the $I = 0$ ω and ϕ trajectories which involve no exchange of internal quantum numbers, but which have negative G parity, so their coupling to processes involving mesons is restricted. Because they are so similar it is usually impossible to separate their contributions which are lumped together. The neutral members of the $I = 1$ ρ and A_2 trajectories are also present in many elastic processes, but these trajectories also dominate charge exchange processes, which demand an $I = 1$ exchange. The $I = 1$ pion is a much lower trajectory than any of the above (see fig. 5), but because of its strong coupling, and the nearness of the exchanged pion pole to the direct-channel physical region, it is often essential for explaining the data near the forward direction. We therefore treat pion exchange processes separately in table 5. Processes with strangeness exchange require K^* and K^{**} trajectories, and also, where quantum numbers allow, the K . For baryon exchange processes (i.e. the backward direction in meson baryon scattering) we may need the N_α , N_γ and Δ_δ trajectories, depending on the amount of charge exchanged, or, if strangeness is also exchanged, the Λ and Σ trajectories will be used.

With this set of leading trajectories, i.e. P , f , $\omega(\phi)$, ρ , A_2 , π , K^* , K^{**} , K , N_α , N_γ , Δ_δ , Λ_α , Λ_γ , Σ_α , Σ_β , Σ_γ and Σ_δ , we can hope to fit all the various two-body processes. There may be complications due to the presence of secondary trajectories with the same quantum numbers (referred to with primes, e.g. f' , ρ'), but fig. 6 suggests that these are all much lower than the leading trajectories and will not be very important unless they have very strong couplings or small slopes. There will also be cuts, but the dominant cuts in any process are always those stemming from the highest trajectory which can be exchanged together with the Pomeron, and these will have the same quantum numbers (except parity) and the same intercept, as the leading trajectory (see section 5.6). Other cuts produced by the exchange of two or more Reggeons other than the P will have a lower intercept than the leading trajectory and are unlikely to be very important except in those processes where no single trajectory can be exchanged. We discuss some examples below. Other trajectories such as the A_1 ($I = 1$, $J^{PC} = 1^{++}$) and B ($I = 1$, $J^{PC} = 1^{+-}$) are sometimes invoked, but they are likely to be rather low lying. The main reason for using them in the past has been to obtain a contribution of opposite parity to that

Table 5
Regge fits.

Process	Trajectories	References to fits
Charge exchange processes		
$\pi^-p \rightarrow \pi^0n$	ρ	[104, 182-201, 206, 281, 357, 361]
$\pi^-p \rightarrow \eta^0n$	A_2	[128, 190, 195, 196, 199, 202, 206, 281-284, 357, 361]
$K^-p \rightarrow \bar{K}^0p$	$\rho + A_2$ }	[183, 190, 195, 196, 199, 203, 204, 206, 242, 281, 287, 288, 357, 358, 361]
$K^+p \rightarrow K^0p$		
$\pi^+p \rightarrow \pi^0\Delta^{++}$	ρ	[205, 206, 281, 289-291]
$\pi^+p \rightarrow \eta\Delta^{++}$	A_2	[205, 206, 281, 291]
$K^+p \rightarrow K^0\Delta^{++}$	$\rho + A_2$ }	[203-206, 289]
$K^-n \rightarrow \bar{K}^0\Delta^-$		
$\pi N \rightarrow \omega N$	ρ	[206, 292, 293]
$\pi N \rightarrow \omega\Delta$	ρ	[216, 292-294, 296, 326]
$\pi N \rightarrow A_2\Delta$	ρ	[206, 294]
$\gamma p \rightarrow \pi^0p$	$\rho + \omega$	[128, 207-210, 216, 294, 297, 299-303]
$\gamma p \rightarrow \eta p$	$\rho + \omega$	[209-210, 294]
Hypercharge exchange processes		
$\pi^-p \rightarrow K^0\Lambda$	$K^* + K^{**}$	[203, 204, 213, 281, 304, 357]
$\pi^-p \rightarrow K^0\Sigma^0$	$K^* + K^{**}$	[203, 204, 213, 281, 289, 304, 357]
$\pi^+p \rightarrow K^+\Sigma^+$	$K^* + K^{**}$	[213, 281, 304, 357, 358]
$K^-p \rightarrow \pi^0\Lambda$	$K^* + K^{**}$	[204, 305, 357]
$K^-n \rightarrow \pi^-\Lambda$	$K^* + K^{**}$	[203, 213, 304]
$K^-p \rightarrow \pi^-\Sigma^+$	$K^* + K^{**}$	[203, 204, 213, 289, 304, 357, 358]
$K^-n \rightarrow \pi^-\Sigma^0$	$K^* + K^{**}$	[213, 304]
$K^-p \rightarrow \pi^-\Sigma^{*-}(1385)$	$K^* + K^{**}$	[203, 306]
Pseudoscalar meson exchange processes		
$\pi p \rightarrow \rho N$	$\pi + A_2 + \omega$	[104, 206, 244, 294, 307]
$\pi p \rightarrow f_0 N$	$\pi + A_2$	
$\pi p \rightarrow A_2 \Lambda$	π	[206]
$\pi p \rightarrow \rho\Delta$	$\pi + A_2$	[104, 225, 299, 308-310, 326]
$\pi p \rightarrow f_0\Delta$	π	[310]
$pn \rightarrow np$	$\pi + \rho + \omega + A_2$	[215, 217, 220, 248, 311, 312]
$pp \rightarrow N\Delta$	$\pi + \rho + \omega + A_2$	[216, 218, 219]
$pp \rightarrow \Delta\Delta$	$\pi + \rho + \omega + A_2$	
$pp \rightarrow n\bar{n}$	$\pi + \rho + \omega + A_2$	[104, 215, 217, 220, 311]

Table 5 (continued)

Process	Trajectories	References to fits
Pseudoscalar meson exchange processes		
$p\bar{p} \rightarrow \Delta\bar{\Delta}$	$\pi + \rho + \omega + A_2$	[216, 218, 310]
$\gamma p \rightarrow \pi^+ n$	$\pi + \rho + A_2$	[71, 104, 207, 214, 216, 218, 221, 299, 313-319]
$\gamma n \rightarrow \pi^- p$	$\pi + \rho + A_2$	
$\gamma p \rightarrow \pi^- \Delta^{++}$	$\pi + \rho + A_2$	
$p\bar{p} \rightarrow \Lambda\bar{\Lambda}(\Sigma\bar{\Sigma})$	$K + K^* + K^{**}$	[213, 229]
$\gamma p \rightarrow K^+ \Lambda(\Sigma^0)$	$K + K^* + K^{**}$	[71, 207, 228, 312, 314]
$\gamma p \rightarrow K^{*+} \Lambda(\Sigma^0)$	$K + K^* + K^{**}$	
Baryon exchange processes		
$\pi^- p \rightarrow p\pi^-$	$\Delta\delta$	[132, 320, 321, 235, 236, 238, 321, 350]
$\pi^+ p \rightarrow p\pi^+$	$N_\alpha + N_\gamma + \Delta\delta$	
$K^- n \rightarrow \Lambda\pi^-$	$N_\alpha + N_\gamma$	[237, 238]
$pp \rightarrow \pi^+ d$	$N_\alpha + N_\gamma$	[234]
$\gamma p \rightarrow n\pi^+$	$N_\alpha + N_\gamma + \Delta\delta$	[231, 233, 235, 322, 323]
$\gamma p \rightarrow p\pi^0$	$N_\alpha + N_\gamma + \Delta\delta$	
$\gamma p \rightarrow p\eta$	$N_\alpha + N_\gamma$	[235]
$\gamma p \rightarrow p\rho$	$N_\alpha + N_\gamma + \Delta\delta$	[235, 323]
$\gamma p \rightarrow \Delta^{++}\pi^-$	$\Delta\delta$	[324]
$\pi^- p \rightarrow \Lambda K^0$	$\Sigma_\alpha + \Sigma_\beta + \Sigma_\gamma + \Sigma_\delta$	[241]
$K^+ p \rightarrow pK^+$	$\Lambda_\alpha + \Lambda_\gamma$	[240, 325, 350]
Elastic processes		
$\pi^- p \rightarrow \pi^- p$	$P + f + \rho$	[133, 136, 153, 154, 169, 183, 189, 196-198, 242, 245-247, 250, 255, 258, 260, 327-336, 337, 343]
$\pi^+ p \rightarrow \pi^+ p$	$P + f - \rho$	
$K^- p \rightarrow K^- p$	$P + f + \rho + \omega + A_2$	[127, 153, 169, 183, 196, 242, 250, 254, 255, 258-260, 284, 286, 288, 327, 337-343]
$K^- n \rightarrow K^- n$	$P + f - \rho + \omega - A_2$	
$K^+ p \rightarrow K^+ p$	$P + f - \rho - \omega + A_2$	
$K^+ n \rightarrow K^+ n$	$P + f + \rho - \omega - A_2$	
$pp \rightarrow pp$	$P + f - \rho - \omega + A_2$	[220, 243, 252, 255, 260, 263, 344-349]
$pn \rightarrow pn$	$P + f + \rho - \omega - A_2$	
$\bar{p}p \rightarrow \bar{p}p$	$P + f + \rho + \omega + A_2$	
$pn \rightarrow pn$	$P + f - \rho + \omega - A_2$	
$\gamma p \rightarrow \gamma p$	$P + f + \rho + \omega + A_2$	
		[267, 351-354]

Table 5 (continued)

Process	Trajectories	References to fits
Quasi-elastic processes		
$\pi p \rightarrow \pi N^*(1400)$ etc.	$P+f+\rho$	[268, 274]
$\gamma p \rightarrow \rho^0 p$	$P+A_2+\pi$	[216, 226, 314, 355, 356]
$\gamma p \rightarrow \omega p$	$P+A_2+\pi$	[216, 226, 314, 355, 356]
$\gamma p \rightarrow \phi p$	$P+A_2+\pi$	[226, 269, 270, 314, 355, 356]
Exotic exchange processes		
$\pi^- p \rightarrow K^+ \Sigma^-$	(ρK^*)	
$K^- p \rightarrow K^+ \Sigma^-$	(ρK^*)	
$K^- p \rightarrow K^0 \Sigma^0$	$(K^* K^*)$	
$\pi^- p \rightarrow \pi^+ \Delta^-$	$(\rho \rho)$	
$K^- p \rightarrow \pi^+ \Sigma^-$	(ρK^*)	
$K^- p \rightarrow \rho^+ \Sigma^+$	(ρK^*)	
$\bar{p} p \rightarrow \Sigma \bar{\Sigma}$	(ρK^*)	
$K^- p \rightarrow \rho K^-$	$(K^* \Delta)$	
$K^- p \rightarrow n \bar{K}^0$	$(K^* \Delta)$	
$\bar{p} p \rightarrow \Lambda \bar{\Lambda}, \Sigma \bar{\Sigma}$	$(N \Lambda), (N \Sigma)$	

provided by the leading trajectories, especially in conspiracy models. Such opposite parity contributions are also provided by cuts, however, since they do not have definite parity (thus the B is similar to a ρP cut, and the A_1 to a πP cut), and it is probable that they will not be necessary if strong cuts are included.

If we are to try and isolate the contributions of the various singularities it is obviously desirable to start with processes where only a few trajectories can be exchanged, and for this reason we begin our discussion with quantum-number exchange reactions before proceeding to the more complicated elastic scattering processes. This is the reason for the grouping in table 5.

This table also includes a representative set of references to some of the more recent fits so that the reader can compare for himself the various Regge models. From these papers it should be possible to trace the earlier literature where necessary. We have certainly not attempted to mention all (or even most) of the fits to a given process (the author is aware of some 70 papers on fitting $\pi^- p \rightarrow \pi^0 n$ for example), nor can we hope to be completely up to date. The discussion which follows is concentrated on what we feel are some of the most interesting problems, and we can only plead for the indulgence of the authors of neglected papers, and remind the reader that other thorough reviews have been given recently in refs. [15-17, 178-181].

7.2. Charge exchange processes

a) $\pi^-p \rightarrow \pi^0n$. Table 5 shows that only one of our set of Regge poles, the ρ , can be exchanged in this process, and because of this it has been subjected to very close scrutiny, and fitted by many kinds of Regge models.

We have already presented some of the data, and a simple one pole fit in figs. 15 and 16. In fact it is possible to obtain a very good representation of the data if the ρ chooses sense [182-185], and has a zero in the sense-nonsense amplitude $A_{+-,00}$ (see section 4.6) at $\alpha = 0$, i.e. there is no wrong signature fixed pole in the residue. (We use the amplitudes (4.11).) The forward dip is explained by the dominance of the spin flip amplitude, which of course has to vanish in the forward direction, and the dip at $t \approx -0.6$ is accounted for by the nonsense zero in this amplitude.

Unfortunately this nice simple picture became untenable when it was discovered that there is a substantial polarization (shown in fig. 42). The polarization of particle 3 normal to the scattering plane, P , is given by

$$P \frac{d\sigma}{dt} = \sum_{H_S} [(\sigma_3 + \mu_3)(\sigma_3 - \mu_3 + 1)]^{\frac{1}{2}} \text{Im}[\langle \mu_3 - 1 \mu_4 | A | \mu_1 \mu_2 \rangle \langle \mu_3 \mu_4 | A | \mu_1 \mu_2 \rangle^*] \quad (7.1)$$

and so depends on there being a phase difference between the amplitudes. We have noted that a single Regge pole gives the same phase to all amplitudes (assuming α and γ are real) and so the single pole fit must be wrong.

However it is not difficult to think up other contributions which might interfere with the ρ to produce this phase difference. One possibility is interference with direct channel resonances [186-188], though this explanation is in conflict with duality which requires that these poles should already be included in the Regge poles. The presence of another trajectory, the ρ' , is suggested by the work of ref. [133] (see section 6.2), and has been used by several authors [189-192]. The ρ' so obtained has quite a large intercept (≈ 0 in ref. [189]) and is much above the daughter value ($\alpha_{\rho'}(0) = \alpha_{\rho}(0) - 1$). Another suggestion, inspired by the fact that the A_2 with which the ρ may be exchange degenerate is known to be split [48], and by the multiplicity of trajectories found in multi-particle dual models (see section 6.5), is that the ρ trajectory is doubled. A small separation $\alpha_{\rho'} - \alpha_{\rho} \approx 0.1$ can ex-

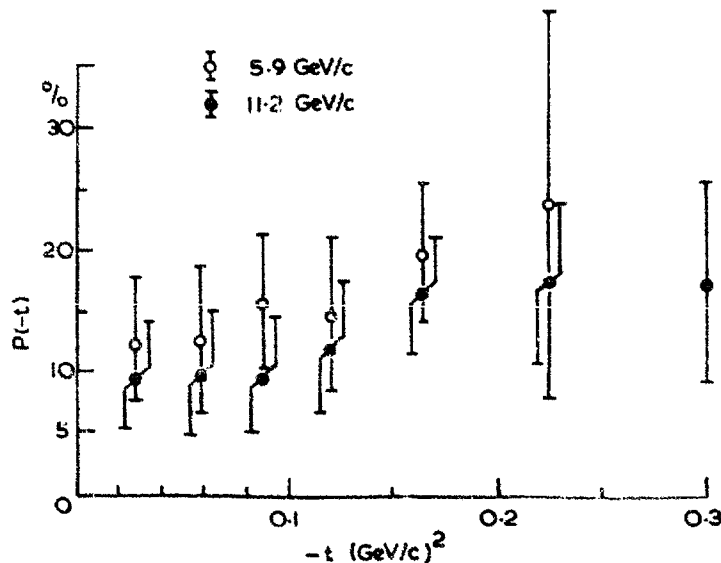


Fig. 42. The polarization in $\pi^-p \rightarrow \pi^0n$ from Bonamy et al., Phys. Letters 23 (1966) 501.

plain the polarization [193]. Models have also been suggested in which the secondary ρ' trajectory is a $\Lambda = 1$ conspirator [191-192, 194-195], which has the advantage of explaining the zero in the non-flip amplitude at $t \approx 0.15$. This 'cross-over' zero is not apparent in simple fits to the high-energy charge-exchange differential cross section because of the dominance of the flip amplitude, but it is needed to explain the fact that in πN elastic scattering the difference

$$\left[\frac{d\sigma}{dt} (\pi^-p) - \frac{d\sigma}{dt} (\pi^+p) \right]$$

changes sign at this point (see section 6 below), and it is also demanded in the charge exchange process by FESR [133], a fact which we noted in section 6.2. There have been many papers applying FESR to determine the pole parameters following the work of ref. [133].

Once one includes some such additional contribution besides the ρ pole one can if one wishes allow the ρ residue in the non-flip amplitude to vanish at $\alpha = 0$ along with the flip amplitude without there being a zero of $d\sigma/dt$. This means that equally good fits can be obtained with the ρ choosing nonsense instead of sense [196]. This choice of nonsense is of course required if the ρ is to be exchange degenerate with the f . The energy dependence in the region of the dip is not very different from other t values, however, so the additional contribution can not be much lower in the J -plane than the ρ .

An obvious way to obtain such a secondary contribution is of course from cuts. These can readily fill in the dip with the right sort of energy dependence, and may also account for the cross-over zero [197-199], though in practice it seems to be difficult to get this zero in the right place - it tends to want to be nearer to the pole zero, say at $t = -0.3 - -0.4$. A more radical suggestion is that (as discussed in section 5.6) the cuts are very strong and interfere with the ρ pole to produce the dip at $t = -0.6$ without there being a zero of the pole amplitude; i.e. there is a strong fixed pole in the ρ residue at $\alpha = 0$. Fits of this type have been obtained [200], though there is some difficulty in fitting the data for $|t| > 0.6$ because the smaller slope of the cut tends to make the shrinkage of the differential cross section too small at these larger t values [178]. A plot of the effective trajectory, α_{eff} , due to the sum of the cut and pole in this model, which makes this problem rather evident, is presented in fig. 43. It will be easier to assess the severity of this problem when higher-energy data are available. The existence of a strong fixed pole, which therefore requires a strong cut, is certainly suggested by the FESR analysis of ref. [133] (see also ref. [201]).

This brief discussion highlights both the successes and the failures of Regge theory. Fig. 16 is certainly excellent evidence for the dominance of a moving Regge singularity associated with the ρ pole. But despite the reasonably good data we can not even be sure whether the pole is finite in both $A_{+-,00}$ and $A_{++,00}$ at $t = -0.6$ (and there is strong cut) or is finite in $A_{++,00}$ but not $A_{+-,00}$ (i.e. chooses sense), or vanishes in both (chooses nonsense). And the secondary contribution may be an additive pole, the ρ' , or a cut (strong or weak) or direct channel resonances; fairly good fits can be obtained with any of these hypotheses. Of course some additional information can be obtained by examining other processes to which the ρ also contributes, but the ambiguities persist. In fact we shall find that it is quite impossible to arrive at an agreed set of Regge parameters for any process; the parameters obtained always depend on the model which has been used for the fit.

One can of course invoke additional principles such as exchange degeneracy

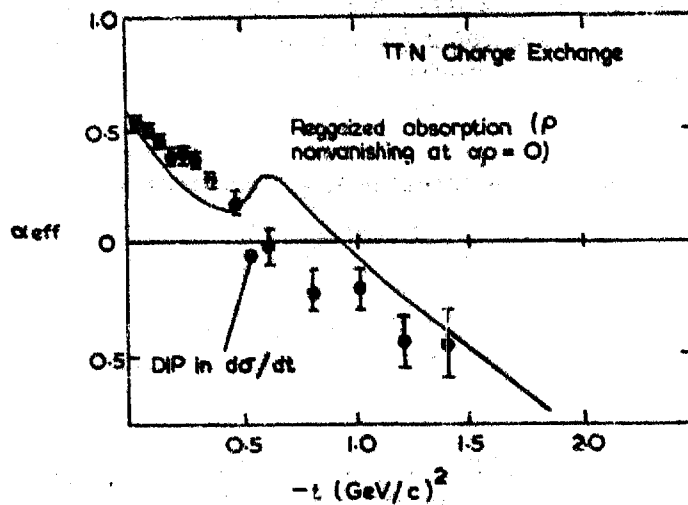


Fig. 43. The effective trajectory in the strong cut model for $\pi^-p \rightarrow \pi^0n$ compared with the experimental values, from ref. [178].

which requires all poles to choose nonsense, or, at the other extreme, suppose that all dips are due to cuts interfering with the poles just because some of the dips predicted by the nonsense factors in poles do not occur. But the unbiased observer has to admit that at the moment almost any of the above models can be made to give a reasonable fit with sufficient ingenuity, and none has an overwhelming advantage for all processes. We shall therefore not go into much detail below in describing the parameters of the fits but will leave the reader to look up those in which he is interested.

b) $\pi^-p \rightarrow \eta n$ and KN charge exchange. The process $\pi^-p \rightarrow \eta n$ is very similar to the above except that the A_2 rather than the ρ is the only pole from our list which can be exchanged. The basic features also seem to be quite similar in that the spin flip amplitude appears to dominate (though the forward dip is less evident), but there is no dip at $t = -0.6$. This means that the slope of the trajectory is harder to determine.

The early fits used a rather small slope [202], principally because they assumed the Chew mechanism (see section 4.6) which gives a dip at $\alpha = 0$ due to the vanishing of the flip amplitude. (Of course the sense amplitude remains finite as the residue zero is cancelled by the pole). However if the trajectory chooses nonsense both amplitudes are finite (see table 4) and there is no difficulty in fitting with a trajectory similar to that of the ρ [185]. But even this is not conclusive, for if the non-flip residue is given the change of sign at $t \approx -0.15$ suggested by the cross-over effect a good fit with the Chew mechanism and a normal slope for the A_2 is possible because of an interference between the two amplitudes. If the ρ and A_2 trajectories are exchange degenerate of course both must choose nonsense.

Since this process is kinematically very similar to $\pi^-p \rightarrow \pi^0n$ the strong cut model would also expect a dip, and its absence has to be explained by a smaller value of λ [180], or by non-degenerate couplings [361].

The processes $K^-p \rightarrow \bar{K}^0n$ and $K^+n \rightarrow K^0p$ are related to the above in that they require both the ρ and A_2 with same couplings at the nucleon end. In fact if one assumes SU(3) for the residues one can predict them directly from the fits $\pi^-p \rightarrow \pi^0n$ and ηn . Equally good fits can be obtained with either the sense or nonsense choosing mechanism so there is no resolution of this ambiguity [185].

These processes can also provide a test of exchange degeneracy because if the ρ and A_2 are exactly exchange degenerate the $K^+n \rightarrow K^0p$ amplitude must be purely real (see (4.92)) while that for $K^-p \rightarrow \bar{K}^0n$ has the $e^{i\pi\alpha(t)}$, and two differential cross sections should be exactly equal. In fact the K^+n data is larger than K^-p at low energies (< 5 GeV), but they seem to be equal at higher energies [203, 358, 360]. Various suggestions have been made to account for the discrepancy at low energy, such as a splitting of the trajectories [204] (the A_2 is heavier than the f), secondary trajectories [204], or cuts [358]. However the leading cut (generated by the P) produces an effect in the wrong direction, and pole-pole cuts must be blamed [358].

c) *Other hadronic charge-exchange processes.* The remaining charge exchange processes in table 5 all involve resonance production. This fact introduces further ambiguities both because the data are less accurate, and because with the higher spins there are more residue parameters to juggle with. The set of processes $\pi^+p \rightarrow \pi^0\Delta^{++}$, $\pi^+p \rightarrow \eta\Delta^{++}$, $K^+p \rightarrow K^0\Delta^{++}$ and $K^-n \rightarrow \bar{K}^0\Delta^-$ are similar to those discussed above in requiring ρ , A_2 and $\rho+A_2$ exchanges respectively, while $\pi N \rightarrow \omega N$, $\pi N \rightarrow \omega\Delta$ and $\pi N \rightarrow A_2\Delta$ require only the ρ . Fits to various combinations of these processes have been attempted [205, 206] using some of the different types of models described above. There is of course no difficulty in fitting, but no narrowing of the range of possibilities either.

d) *Neutral pseudoscalar-meson photoproduction.* This is a convenient point at which to discuss two photoproduction processes which though they do not involve charge exchange should be controlled by the non-strange vector mesons ρ and ω , i.e. $\gamma p \rightarrow \pi^0p$ and $\gamma p \rightarrow \eta p$.

The data for $\gamma p \rightarrow \pi^0p$ shown in fig. 44 are in fact consistent with an effective trajectory which is fixed at zero [178], which may perhaps indicate a non-Regge behaviour. But it is not too difficult to reproduce this effect (within the rather large errors) by a suitable combination of singularities. Fixed poles are ruled out by unitarity, but of course a fixed power behaviour may be obtained from a δ_{J0} term in the J -plane, and various fixed power fits have been suggested.

The differential cross section has a forward dip followed by a further dip at $t \approx -0.5$, which is suggestive of an ω or ρ nonsense zero. The dip appears to be filling up with energy, however. Cross sections for scattering by polarized photons have been measured, and it is found that perpendicular polarization dominates. This is controlled asymptotically by natural parity exchange, so it confirms the dominance of the ρ and ω trajectories, and shows that the dip is not filled in by a negative parity object such as the B which was used in earlier fits [207]. If one makes use of the $\gamma n \rightarrow \pi^0n$ data it is possible to make an isospin decomposition as well, and it is found that some isovector ρ contribution is definitely needed along with the isoscalar ω . A model with ω and ρ together with ωP and ρP cuts appears to fit the data fairly well [208], but as usual it is not clear whether the cuts should be strong enough to produce the dip [209], or merely to fill in to some extent the dip produced by the poles.

The process $\gamma p \rightarrow \eta p$ has exactly the same exchange, and it is rather surprising that there is no corresponding dip at $t = -0.5$. Presumably ρ exchange dominates, and it has been argued that the absence of a dip can only naturally be explained by a strong cut model [209, 210], though the B trajectory has been invoked [211] as an alternative way of fitting it. Higher energy data should be able to distinguish between these explanations.

It has been noted [117, 212] that the presence or absence of dips in some of these processes can be explained in terms of the rule enunciated in section 5.6e, that a

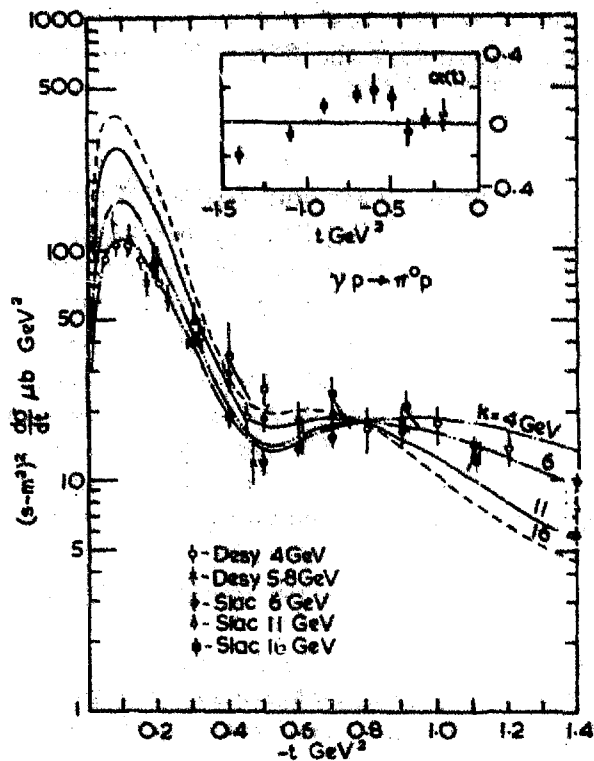


Fig. 44. The differential cross section, and $\alpha_{\text{eff}}(t)$ for $\gamma p \rightarrow \pi^0 p$ from ref. [224].

cut-pole interference gives a dip at $t \approx -0.6$ if the dominant amplitude has helicity flip $\Delta h \equiv |\mu_1 - \mu_3| - |\mu_2 - \mu_4| = \pm 1$. The ω coupling to NN is predominantly electric, $|\mu_2 - \mu_4| = 0$, while the ρ coupling to NN or $N\Delta$ is predominantly magnetic, $|\mu_2 - \mu_4| = 1$. Since $SU(3)$ predicts $\gamma_{\omega\pi\gamma} > \gamma_{\rho\pi\gamma}$, and $\gamma_{\rho\pi\gamma} > \gamma_{\omega\pi\gamma}$ we find the helicity flips shown in table 6. Those with $|\Delta h| = 1$ are the ones with dips, and the fact that this rule works so well must be regarded as good evidence for the strong cut model.

Table 6
Processes with and without dips at $t \approx -0.6$.

Process	Dip?	Exchange	Δh
$\gamma N \rightarrow \pi^0 N$	yes	$\omega(\rho)$	1
$\gamma N \rightarrow \eta N$	no	$\rho(\omega)$	0, 2
$\gamma N \rightarrow \pi^\pm N$	no	ρ	0, 2
$\pi N \rightarrow \omega N$	no	ρ	0, 2
$\pi^- p \rightarrow \gamma^0 p$	yes	ρ	1
$\pi N \rightarrow \omega \Delta$	no	ρ	0, 2
$\pi N \rightarrow \pi \Delta$	yes	ρ	1
$\pi N \rightarrow \rho N$	yes	ω	1

7.3. Hypercharge exchange processes

These may conveniently be divided, as in table 5, into those processes where the K can be exchanged and those where it can not. Where it can not the dominant trajectories should be the exchange degenerate (?) K^* , K^{**} . If the degeneracy were exact should expect an equality of the moduli of the pairs of amplitudes such as $(\pi^-p \rightarrow K^0\Lambda, K^-p \rightarrow \pi^0\Lambda)$, $(\pi^+p \rightarrow K^+\Sigma^+, K^-p \rightarrow \pi^-\Sigma^+)$ and $(K^-p \rightarrow \pi^-\Sigma^+(1385), \pi^+p \rightarrow K^+\Sigma^+(1385))$. The agreement is in fact very poor [203]. The lack of equality can be blamed either on a splitting of the degeneracy [204], or on cuts [358], but as with the charge exchange processes the effect seems to be in the wrong direction. A detailed fit of recent data including absorptive cuts and SU(3) residues has been given in ref. [213]. The results are moderately good given the rather few parameters, but the data do not have any distinctive features (dips etc.) to constrain the fit strongly. Unfortunately there does not seem to be very good agreement with such little polarization data as are available. One can hope that good polarization data will be available soon using the weak decay of the hyperon.

7.4. Pseudo-scalar-meson exchange processes

The group of processes in table 5, in which the pion can be exchanged present a particular problem for Regge theory. The reason is that many of these reactions exhibit sharp forward spikes or dips (see table 7), which have a width $\approx m_\pi^2$ and so seem quite clearly to be associated with the pion, and yet an evasive pion is decoupled in the forward direction (see section 4.3). There are two possible solutions to this problem; either there is a pion conspiracy or there are very strong cuts.

Table 7
Processes with dips and spikes near $t = 0$ due to π exchange.

Process	Structure
$\pi^-p \rightarrow \rho^0n$	Dip
$\pi^+n \rightarrow \rho^0p$	Dip
$\pi^\pm p \rightarrow \rho^\pm p$	Dip
$\pi^+p \rightarrow \rho^0\Delta^{++}$	Spike
$\pi^+p \rightarrow f^0\Delta^{++}$	Spike
$\pi^+n \rightarrow f^0p$	Dip
$\gamma p \rightarrow \pi^+n$	Spike
$\gamma n \rightarrow \pi^-p$	Spike
$\gamma p \rightarrow \pi^-\Delta^{++}$	Dip
$\gamma n \rightarrow \pi^+\Delta^-$	Dip
$K^\pm p \rightarrow K^{*\pm}p$	Dip
$K^-p \rightarrow K^*n$	Dip
$K^\pm p \rightarrow K^*\Delta$	Spike

The way in which the conspiracy works in photoproduction can be understood by writing the differential cross section for small $|t|$ in terms of invariant amplitudes which are free of kinematical singularities and constraints [214], i.e.

$$\frac{d\sigma}{dt} \propto \{[|A_1|^2 + |t||A_4|^2] + [|A_1 + tA_2|^2 + |t||A_3|^2]\}, \quad (7.2)$$

where the first term in square brackets correspond to natural parity, $\eta = 1$, and the second to $\eta = -1$. At $t = 0$ only A_1 is finite and must contain equal contributions from both parities. The pion couples only to A_2 and so vanishes unless the residue takes the form a_2/t . However A_2 can not be singular so we need a conspirator trajectory with a singular coupling $A_2 \underset{t \rightarrow 0}{\approx} -a_2/t$. However the conspirator has even parity and so does not contribute to $(A_1 + tA_2)$, so its contribution to A_1 is finite, $a_1 = a_2$. Hence the natural parity A_1 amplitudes is finite at $t = 0$ and has the same residue as the pion.

There were several successful fits of processes such as $pn \rightarrow np$, $\bar{p}n \rightarrow \bar{n}p$, $\gamma p \rightarrow \pi^+ n$ [71, 72, 216, 217] making use of such a conspiracy. Since there is no known scalar particle with the pion mass it is generally assumed that the conspirator chooses nonsense, and so has vanishing coupling at $\alpha = 0$, though a very flat trajectory is also a possibility. In order to get a fit a very rapid variation of the pion residue is required such that it vanishes for $t \approx -m_\pi^2$. This rather strange behaviour is found in all the three reactions above, and is confirmed by FESR. Factorization then implies that all the $\pi N \bar{N}$ vertices must vanish at this point. (Some authors have connected this with PCAC.)

However it was shown by Le Bellac [73] that this sort of conspiracy is incompatible with factorization. Thus if we consider the t -channel amplitudes for $\pi\rho \rightarrow N\bar{N}$, $A_{\frac{1}{2}\frac{1}{2}, 00}$ must vanish like $t^{\frac{1}{2}}$, and no conspiracy is possible. And by factorization

$$\left(\beta_{\frac{1}{2}\frac{1}{2}, 00}^{\pi\rho \rightarrow N\bar{N}}\right)^2 = \beta_{00, 00}^{\pi\rho \rightarrow \pi\rho} \beta_{\frac{1}{2}\frac{1}{2}, \frac{1}{2}\frac{1}{2}}^{N\bar{N} \rightarrow N\bar{N}},$$

so if there is a conspiracy in $pn \rightarrow np$ and the latter residue is non-vanishing then $\beta_{00, 00}^{\pi\rho \rightarrow \pi\rho}$ must vanish like t . If we then look at $\pi N \rightarrow \rho\Delta$ we have

$$\left(\beta_{\frac{1}{2}\frac{1}{2}, 00}^{\pi\rho \rightarrow N\bar{\Delta}}\right)^2 = \beta_{00, 00}^{\pi\rho \rightarrow \pi\rho} \beta_{\frac{1}{2}\frac{1}{2}, \frac{1}{2}\frac{1}{2}}^{N\bar{\Delta} \rightarrow N\bar{\Delta}}$$

and since the residue on the left-hand side is kinematically finite it must have a dynamical zero (it can not have a $t^{\frac{1}{2}}$ singularity). This means that the forward $\pi N \rightarrow \rho\Delta$ cross section is predicted to vanish, and so is $N\bar{N} \rightarrow \Delta\bar{\Delta}$. There is some difficulty in testing these predictions because the Δ is a broad resonance (which 'fuzzes' the kinematics) but the evidence is definitely against it [218].

This argument leaves us with cuts as the only way of getting the forward peaks. The rapid variation near $t = 0$ is explained naturally by an interference between the smooth cut and the evasive pion pole, and no zero is needed in the pion residue. Cut models of $\gamma p \rightarrow \pi^+ n$, $\pi N \rightarrow \rho N$, $\pi N \rightarrow \rho\Delta$, $p\bar{p} \rightarrow n\bar{n}$, $np \rightarrow pn$ and $pp \rightarrow n\Delta^{++}$ are available [200, 209, 219, 220], and all require very strong cuts, stronger than in most other processes; and in particular for $\gamma p \rightarrow \pi^+ n$ the enhancement factor λ is found to be 3.55 [209]. This makes one feel a bit uneasy, particularly as really all one is trying to do is to reproduce the forward peak obtained from a gauge invariant Born term [221],

$$A_2 = \frac{eg}{(s - m_N^2)(t - m_\pi^2)}. \quad (7.3)$$

In fact as in $\gamma p \rightarrow \pi^0 p$ there is some evidence in both $\gamma p \rightarrow \pi^+ n$ and $\gamma p \rightarrow \pi^- \Delta^{++}$ of an effective α approximately constant, ≈ 0 [178]. It has been suggested that this may be a fixed J -plane pole [222], but unless something totally unexpected is happening

this is ruled out by unitarity (higher order electromagnetic corrections ensure that the trajectory has a slope $\alpha' = 0$ ($\frac{1}{137}$) at least). In any case such a fixed pole can not be correlated with the pion (a fixed J pole does not give a t -plane and so does not correspond to a particle) and is completely at invariance with vector dominance which relates the photoproduction amplitudes with those of purely hadronic reactions involving vector mesons.

There is a further problem with the pion coupling to $\gamma p \rightarrow \pi^+ n$, namely that if one applies the usual rules of Reggeization (chapters 2 and 4) there is no pion pole at all [223]. The reason for this is that the exchanged pion is at the t -channel $\gamma\pi$ threshold, and if one inserts the usual threshold behaviour the pole is cancelled by a kinematical factor. Since the pion manifestly is present it is essential to find some way of rectifying this. One possibility is simply to neglect the unitarity problem and invoke a fixed pole, but an alternative which seems preferable in some ways is to suppose that the $\gamma\pi$ threshold does not give rise to the usual threshold behaviour, perhaps because there is no non-relativistic limit for photon processes. Normally if one were to alter the threshold behaviour one would introduce a kinematical singularity, but in this case it does not happen because the sn. factor $\alpha_\pi(t)$ has just the form needed to cancel the singularity at $t = m_\pi^2$. This problem only arises because of the identity of the external and internal pions, and does not occur in any other process, except Compton scattering, which we shall discuss below.

The very good data on $\gamma p \rightarrow \pi^+ n$ and $\gamma n \rightarrow \pi^- p$ present an interesting challenge to Regge theorists. As for neutral pion photoproduction, data with polarized photons make a complete experimental isospin and parity decomposition possible. If we assume that an evasive π plus πP cuts gives the extreme forward peak, one still needs the ρ and A_2 to explain the larger angle data. The π^+/π^- ratio falls rapidly from unity indicating the presence of the positive G -parity ρ . Unlike neutral photoproduction there is no dip at $t = -0.6$ so one must assume that the dip is filled by a wrong-signature fixed pole and cuts. Both the Michigan and Argonne models seem to be able to reproduce this effect.

In $\gamma p \rightarrow \pi^- \Delta^{++}$ $d\sigma/dt$ is of the same magnitude as $\gamma p \rightarrow \pi^+ n$ at $t = 0$, then rises to a large maximum at $t \approx -m_\pi^2$, after which descends to follow the $\gamma p \rightarrow \pi^+ n$ data at larger $|t|$. Again a gauge invariant Born term can give a good fit near the forward direction [224]. A Regge pole model with a pion conspiracy plus the ρ and A_2 is possible, but since the conspiracy is now ruled out one must expect strong cuts to be present. The related processes $\gamma p \rightarrow \pi^+ \Delta^0$, $\gamma n \rightarrow \pi^+ \Delta^-$, and $\gamma n \rightarrow \pi^- \Delta^+$ have also been studied experimentally, and seem to indicate the need for an $I = 2$ exchange as well as the ρ and A_2 [224]. If this is confirmed it could be evidence for a ρ - ρ cut. If one is to have any hope of disentangling the pole and cut contributions one needs to look at several processes simultaneously and use the extra constraint provided by factorization. So far this has only been attempted on any scale for these processes with purely pole models (e.g. refs. [225, 226]).

In general whether one gets a peak or a dip from a π exchange reaction depends on whether the helicity amplitude which dominates has zero helicity flip or not. One can account for the results of table 7 by supposing that the π coupling to say particles 1 and 3 favours the minimum possible helicity change [227], i.e. $\min |\lambda_1 - \lambda_3|$, though of course for the $\bar{N}\bar{N}$ vertex we must have $|\lambda_1 - \lambda_3| = 1$. Thus in $\gamma p \rightarrow \pi^- p$ there is one unit of helicity flip in both the $\gamma\pi\pi$ and $\bar{N}N\pi$ vertices, and $\Delta h \equiv |\lambda_1 - \lambda_3| - |\lambda_2 - \lambda_4| = 0$ and a forward peak results. On the other hand for $\gamma p \rightarrow \pi^- \Delta^{++}$ there is one unit of flip at the $\gamma\pi$ end but none at the $\bar{N}\Delta$ end so we have

$\Delta h = 1$ and a narrow dip results, while for $\pi p \rightarrow \rho N$ the meson vertex conserves helicity and the baryon one does not, so $\Delta h = 1$ and there is a forward dip.

Most of the corresponding K exchange processes listed in the table do not have good enough data for convincing fits to be possible. The photoproduction processes $\gamma p \rightarrow K^+ \Lambda$ and $\gamma p \rightarrow K^+ \Sigma^0$ can be fitted with a K conspiracy similar to that for the pion [71], but because the K pole is so much further from the forward direction there is a forward dip rather than the peak of pion exchange processes. Again cuts can be invoked instead of the conspiracy [228].

The $\gamma_{KN\Lambda}$ coupling seems to be much larger than $\gamma_{KN\Sigma}$, and new data on $\gamma n \rightarrow K^+ \Sigma^-$ indicates the need for $I = \frac{3}{2}$ exchanges as well as $I = \frac{1}{2}$. This could be a ρK^* cut [224]. The Λ^* and Σ^* photoproduction processes are very similar. In general the strange particle couplings seem to be much smaller relative to the non-strange ones than one would expect from SU(3) [224]. In $p\bar{p} \rightarrow \Lambda\bar{\Lambda}$ some forward K contribution seems to be needed, which again could in principle be produced by a conspiring pole or a cut [229].

7.5. Baryon exchange processes

Near the backward direction of meson-nucleon scattering processes we expect the u -channel baryon exchanges to dominate, so backward scattering data can give us insight into a quite different set of trajectories. This is particularly useful as we already have quite a lot of information about these trajectories for $u > 0$ from figs. 8-12.

There is the complication that we must expect a $\Lambda = \frac{1}{2}$ conspiracy between opposite parity trajectories, so for pseudoscalar-meson-baryon scattering the differential cross section is

$$\frac{d\sigma}{du} = \frac{1}{64\pi^2 q_s \sqrt{s}} \left\{ \left| \beta^+ \left(\frac{1 + e^{-i\pi\alpha^+ - \frac{1}{2}}}{\cos \pi\alpha^+} \right) \left(\frac{s}{s_0} \right)^{\alpha^+ - \frac{1}{2}} \right|^2 + \left| \beta^- \left(\frac{1 + e^{-i\pi\alpha^- - \frac{1}{2}}}{\cos \pi\alpha^-} \right) \left(\frac{s}{s_0} \right)^{\alpha^- - \frac{1}{2}} \right|^2 \right\}, \quad (7.4)$$

where \pm correspond to natural and unnatural parity poles, which satisfy (4.48). Thus at fixed u we have

$$\frac{d\sigma}{du} = f(u) \left(\frac{s}{s_0} \right)^{\alpha^+(\sqrt{u}) + \alpha^-(\sqrt{u}) - 2} \quad (7.5)$$

and any odd $u^{\frac{1}{2}}$ terms in α do not contribute to the amplitude (see (3.27)). The residues β must take the form $[(\alpha - \frac{1}{2})!]^{-1}$ to kill the poles at $\alpha = -\frac{1}{2}, -\frac{3}{2}, \dots$ provided there are no fixed poles at the wrong-signature nonsense points. The $\pi^{\pm}p$ backward data are shown in fig. 45. We expect N_α , N_γ and Δ_0 exchanges, and the dip in π^+p at $u = -0.15$ can be explained by a nonsense zero where $\alpha_N = -\frac{1}{2}$, provided the N_γ contribution is small [230]. If the N_γ were exchange degenerate with the N_α the dip would be completely filled in. The lack of a corresponding dip in the $\pi^-p \rightarrow p\pi^-$ data is explained by the dominance of the Δ_0 contribution. The trajectories needed to fit agree well with those of figs. 8 and 9, but a dip is to be expected in π^-p at $\alpha_\Delta = -\frac{3}{2}$, i.e. $u \approx -1.9 \text{ GeV}^2$. This dip is not observed, but its absence can be explained by a fixed pole, a cut, or by the trajectory bending so that it does not pass through $-\frac{3}{2}$ within the region of a fitted [230, 231]. The residues are given the form

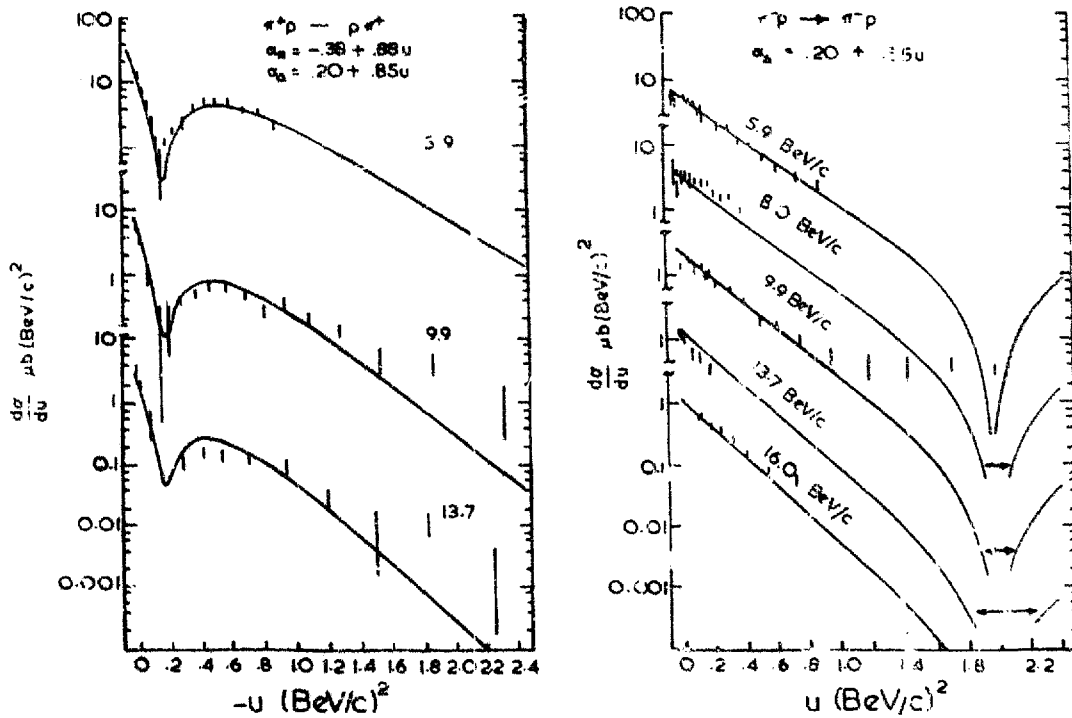


Fig. 45. The differential cross sections for $\pi^{\pm}p \rightarrow p\pi^{\pm}$ compared with the Regge pole fit of ref. [230].

$$\beta(u) = [\alpha(\sqrt{u} + M) + b(u - M^2)] e^{cu} \frac{1}{(a - \frac{1}{2})!} \quad (7.6)$$

which vanishes at $\sqrt{u} = -M$, where M is the mass of the exchanged particle (N or Δ), in order to kill the first particle on the parity doublet trajectory. The resulting trajectories are $\alpha_N = -0.38 + 0.91u$ and $\alpha_{\Delta} = 0.21 + 0.84u$. The N_{Δ} residue function extrapolated to the N pole gives good agreement with the πNN coupling constant, but the Δ_{δ} residue disagrees with the Δ width, being much too small. This suggests that a more complex parameterization is called for. In fact if the Δ chooses nonsense at $\alpha_{\Delta} = \frac{1}{2}$ ($u \approx 0.35$) and so changes sign there, the extrapolation is much improved [232].

If we next turn our attention to the photoproduction processes $\gamma p \rightarrow p\pi^0$ and $\gamma p \rightarrow n\pi^+$ we find that there is no corresponding dip at $\alpha_N = -\frac{1}{2}$, and that the ratio of $p\pi^0$ to $n\pi^+$ is u dependent so the $I = \frac{1}{2}$ and $I = \frac{3}{2}$ contributions must have different u dependence. In a pure pole fit it is necessary to incorporate the N_{γ} degenerate with N_{ρ} in order to fill the dip [233]. This is very embarrassing since the two trajectories are certainly not degenerate for $u > 0$ (see fig. 8), and it is hard to see why N_{γ} should contribute strongly here, and not at all in backward πN . This process also shows little shrinkage, in fact it is consistent with a fixed power behaviour at $\alpha = -0.5$ [178]. This can be explained away by a Δ_{δ} contribution which is small at $u = 0$ and becomes large at larger $|u|$, however.

The N_{ρ} and N_{γ} trajectories also contribute to backward $pp \rightarrow \pi^+d$ and the (so far rather poor) data show little structure, and so are compatible with exchange degeneracy [234]. If the couplings are degenerate here then they must also be in πN by factorization, and it becomes impossible to explain the dip by a nonsense zero.

The obvious way round this problem is to assume that where there is dip struc-

ture it is due to pole cut interference rather than the vanishing of the poles. A comprehensive fit of all these processes with strong cuts has been reported in ref. [235]. The fit is fairly satisfactory given the rather few parameters, but, as would be expected, the discrepancy is worst for the $\pi N \rightarrow N\pi$ processes which are the ones best accounted for by poles alone. On the other hand the Δ width comes out right. A recent comparison [236] of all possible Regge pole and/or cut models for $\pi N \rightarrow N\pi$ concludes that all can be made to work with equal ease, and there is no reason to favour any.

Drago et al. [237] have used $K^-n \rightarrow \Lambda\pi^-$, which also has a dip at $u = -0.2$, to try and distinguish between the Argonne and Michigan cut models, but both seem to be equally satisfactory. If pole dominance is accepted the N_α exchange in $\pi N \rightarrow N\pi$ and $K^-n \rightarrow \Lambda\pi^-$ enables one to determine the ratio of the πNN and KNA coupling constants by extrapolating the fits to the pole. A recent determination [238] gives $\gamma_{KNA} = 15.5 \pm 5$, which is within the range predicted by $SU(3)$ (unlike some other estimates from dispersion relations [239]).

Of the strange baryon exchange processes $K^+p \rightarrow pK^+$ has no dip structure, a fact which can readily be explained [240] by $\Lambda_\alpha\Lambda_\gamma$ exchange degeneracy with $\alpha = -0.7 + 0.96u$, while $\pi^-p \rightarrow \Lambda K^0$ requires Σ exchanges, and a fit with Σ_α and Σ_γ trajectories which are degenerate in α (see fig. 38) but not in residue has been made [241]. It accounts well for the polarization. One should expect an important contribution from the higher lying $\Sigma_\beta, \Sigma_\delta$ as well, however.

7.6. Elastic scattering

There is of course more data on elastic scattering than other processes but there are also more problems, mainly because of the need for the Pomeron which is not necessarily associated with any known particle, but also because of the number of lower lying trajectories which contribute.

Many good fits using just poles have been achieved for all the processes in table 5, as well as some which include cuts. In recent years it has become common to combine both high and low energy data by using FESF techniques, (see section 6.2). However all of the older fits are in substantial disagreement with the new high energy data on $\pi^-p, \pi^-n (= \pi^+p), K^-p$ and $\bar{p}p$ cross sections obtained at Serpukhov. This is not really surprising as the new data do not extrapolate in any simple way from the old. Since the Serpukhov data must be regarded as preliminary, in the sense that there is as yet no confirmation from another experiment, we shall first discuss the pre-Serpukhov fits, and then go on to some of the attempts which have been made to understand the newer data.

Data on total cross sections are shown in fig. 46. The signs of the contributing trajectories in table 5 depend partly on the fact that particles of even charge conjugation, P, f, A_2 , contribute with the same sign to $1+2$ and $1+\bar{2}$ scattering ($\bar{2}$ is the antiparticle of 2) while those of odd C , i.e. ρ, ω , contribute oppositely. Similarly the isovector ρ and A_2 contributions change sign under $\pi^+ \rightarrow \pi^-, K^+ \rightarrow K^-$ or $p \rightarrow n$, while the isoscalars are unchanged. The absolute signs within a given group of processes are not determined, however. If we use the signs given in the table, and we have exact exchange degeneracy i.e. $\rho = \omega = f = A_2$ then the exotic channels (see section 6.2) K^+p , and $\bar{p}p$ are given solely by the P . This accounts for the flatness of their cross sections compared to the other processes. But asymptotically all the total cross sections should be controlled by the P so we predict $\sigma(\pi^+p) = \sigma(\pi^-p)$, $\sigma(K^+p) = \sigma(K^-p)$ and $\sigma(\bar{p}p) = \sigma(pp) = \sigma(pn) = \sigma(\bar{p}n)$ as $s \rightarrow \infty$, in accordance with the Pomeron theorem (discussed below).

Similarly if we take the differences $\Delta(\pi p) \equiv \sigma(\pi^-p) - \sigma(\pi^+p)$, $\Delta(K^+p) - \Delta(K^+n) \equiv$

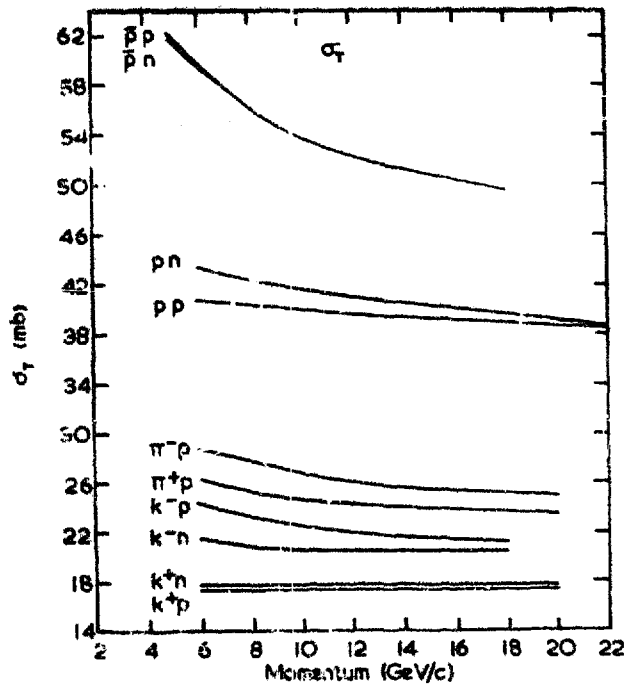


Fig. 46. The total cross sections below Serpukhov energies, from ref. [15].

$\sigma(K^-p) - \sigma(K^+p) - \sigma(K^+n) + \sigma(K^-n)$, and $\Delta(\pi p) - \Delta(\pi n) \equiv \sigma(pp) - \sigma(p\bar{p}) - \sigma(pn) + \sigma(\bar{p}n)$, these combinations are given solely by the ρ . The very small difference between $\sigma(\pi p)$ and $\sigma(\pi n)$ for example indicates the smallness of the ρNN non-flip coupling.

The charge exchange processes are related to the elastic amplitudes by the isospin relations

$$\begin{aligned} \sqrt{2} A(\pi^-p \rightarrow \pi^0n) &= A(\pi^+p) - A(\pi^-p) \\ A(K^-p \rightarrow \bar{K}^0n) &= A(K^-p) - A(K^-n) \\ A(K^+n \rightarrow Kp) &= A(K^+p) - A(K^+n) \\ A(p\bar{p} \rightarrow \bar{n}n) &= A(p\bar{p}) - A(\bar{p}n) \\ A(pn \rightarrow np) &= A(pp) - A(pn) \end{aligned} \quad (7.7)$$

so it is useful to have fitted the charge exchange processes first in order to pin down the ρ and A_2 parameters before trying the elastic amplitudes.

Some recent pole fits have been made [189, 242, 243] using secondary f' , ρ' and ω' trajectories in addition to those of table 5. They are very impressive considered purely as descriptions of the data. In particular the structure of the polarizations are very well accounted for. The trajectory parameters [189] are $\alpha_{\rho} = 1 + 0.37t$, $\alpha_{\rho} = \alpha_{f'} = 0.56 + 0.9t$, $\alpha_{\rho'} = \alpha_{f'} = t$. The ρ chooses sense and its spin-flip residue vanishes at $t = -0.6$, and the f' chooses nonsense so both its residues vanish at this point. The secondary trajectories are needed to fit the FESR, and the ρ' is also required to fit the charge exchange polarization. The cross-over phenomenon referred to in section 2 (i.e. the fact that

$$\left[\frac{d\sigma}{dt}(\pi^-p) - \frac{d\sigma}{dt}(\pi^+p) \right]$$

changes sign at $t \approx -0.15 \text{ GeV}^2$) requires a zero of the ρ residue in the non-flip amplitude. KN and NN show the same cross-over, and a corresponding zero is required in the ω residue at $t = -0.15$. Such a zero does not occur in other related processes such as $\pi p \rightarrow \rho N$ and $\gamma p \rightarrow \pi^0 p$, however, as it should by factorization [244], so this procedure can not be regarded as satisfactory. But provided one does not mind the small P slope this cross-over zero is really the only problem with purely pole fits.

Various attempts have been made to test the hypothesis that these processes can be fitted by a sum of a flat P plus the direct channel poles, as required by duality [153, 154, 245]. Moderately good fits can be obtained, but the ambiguities in the resonance contributions make them unconvincing, at least to this author. There have also been generally rather unsuccessful attempts to fit πN and KN and NN with Veneziano models [169, 246-248].

If one invokes cuts one can explain, at least in principle, both the cross-over zero (by the usual pole-cut interference) and why the shrinkage is less than would be expected from a P of slope $\approx 1 \text{ GeV}^{-2}$. Early fits were made with cuts generated by a flat P (the so called hybrid model) [249-251] but more recently a P of normal slope has been used [252]. The P can not be the only vacuum trajectory, however, because the change of slope of $d\sigma/dt$ from the steepness of the pole to the less steep cut should occur at lower t as the energy increases whereas in fact the opposite occurs [178]. To explain this one still needs include the secondary f trajectory etc. The position of the cross-over zero is hard to explain on the weak cut (Argonne) model (see section 5.6). The ω pole gives a zero at $t \approx -0.6$ and it is not possible for the cut to move it to $t \approx -0.15$ [252]. The Michigan strong cut model has less trouble [116].

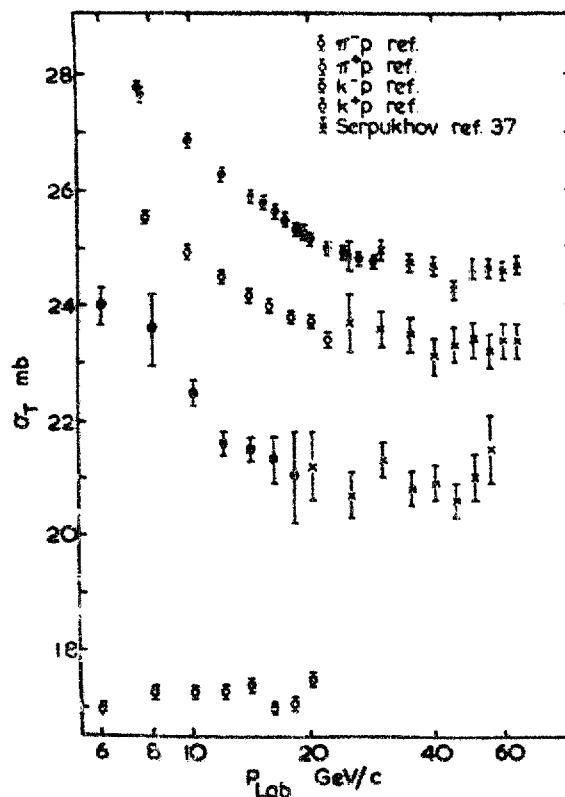


Fig. 47. The total cross sections at high energies, from ref. [138].

As we have mentioned all the earlier fits failed to predict the Serpukhov data on πN and KN scattering shown in fig. 47. It is easy to understand why if one notes the discontinuity of slope between the old data < 30 GeV and the new data, 30-70 GeV. What is worse the new K^+p data appears to be running parallel to the K^+p data (still only available at low energy) instead of meeting it as the Pomeranchuk theorem [253], and all simple Regge pole and cut models, require. Similarly the π^-p data are not approaching those for π^+p . However, the latter are deduced from πd scattering by Glauber theory (using $\pi^-n \equiv \pi^+p$) and so are in some doubt.

As usual there has been a wide variety of explanations suggested. They fall into three classes. The first is to suppose that the errors in the data are rather larger than claimed by the experimenters, in which case Regge poles (with slightly different parameters from the previous ones) still fit [254]. Or one may accept the data but suppose that despite fig. 48 the $\pi^\pm p$ and $K^\pm p$ data will eventually meet at ∞ . In this case the cross sections must rise again above 70 GeV. A simple way to obtain such a rising behaviour is to use cuts [255], since we have seen (section 5.6) that the PP cut is negative and decreases logarithmically to leave a dominant P pole. An example of such a fit is shown in fig. 48, and we see that very large asymptotic cross sections are predicted.

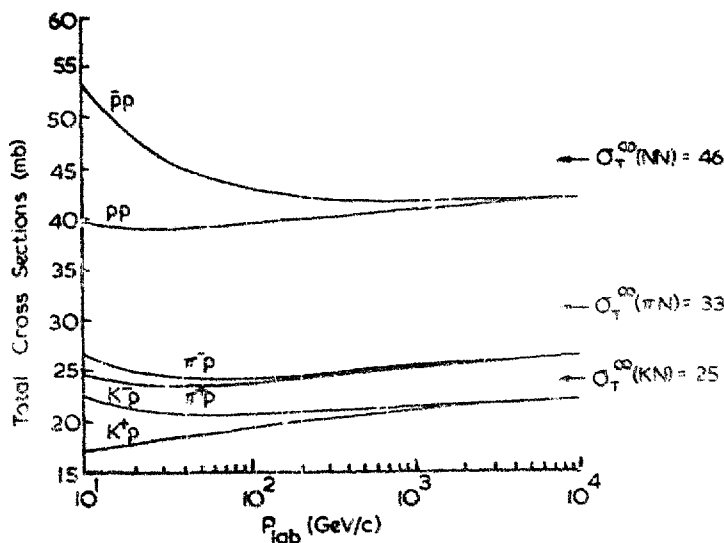


Fig. 48. A fit to the Serpukhov data with Regge cuts in which the asymptotic cross sections are predicted to be well above the currently measured values, from ref. [255].

The third possibility is that the Pomeranchuk theorem [253] itself is false. This states that the particle and anti-particle cross sections on a given target must become equal at high energy, and its proof depends on assuming that the amplitudes become imaginary at high energy, i.e.

$$\frac{\text{Im } A / \text{Re } A}{s} \rightarrow \infty, \quad s \rightarrow \infty$$

If instead they become dominantly real the theorem breaks down and the particle and anti-particle cross sections can be different [256, 257]. An alternative derivation for πN scattering is to use (7.7) and require the vanishing of the inelastic charge exchange process, but this does not work for KN etc.

It is not possible to construct Regge pole models which violate this theorem.

(Indeed it was just because it does satisfy the Pommeranchuk theorem that the Pommeranchon received its name [55].) The reason for this is that in order to get a constant asymptotic behaviour at ∞ we need $\alpha(0) = 1$. But the difference $[A(K^+p) - A(K^-p)]$ (say) is given by an odd signature trajectory (by crossing symmetry) and an odd signature trajectory with $\alpha = 1$ is purely real and so does not contribute to the total cross section. Cuts are no good either because they have the same signature properties and vanish asymptotically.

Two ways of violating the Pommeranchuk theorem which have been suggested are to introduce J -plane dipoles [258] or other more complicated singularities [259] which can give a finite contribution to the imaginary part, or to make the odd signature trajectory complex [260], which produces an oscillating cross section. The first is unpleasant because the singularity has no obvious explanation as a particle exchange effect, and tends to produce logarithmically increasing cross sections, while the second has even less intuitive meaning.

The pp differential cross sections continue to shrink at high energies and are consistent with a P slope of about 0.5 GeV^{-2} for $-0.1 < t < 0$ [261]. This revives the idea that the P is associated with the f particle, which would require a trajectory $\alpha_P = 1 + 0.64t$. In this case the P' trajectory, presumably contains the $f'(1514)$. It has been pointed out [262] that the f seems to have zero NN flip coupling, which if true for the whole trajectory would explain why the πN helicity flip amplitudes seem to be very small. However cuts generated by a P with slope 1 can reproduce the effective slope of $\frac{1}{2}$ just as well [263].

All in all we find that the results of the first Serpukhov experiments are so unexpected that one is unwilling to put too much weight on them until they are independently confirmed. It will be a very unfortunate coincidence if nature has chosen to change the slopes of the total cross sections just at the maximum energy of the previous generation of accelerators, as fig. 49 suggests.

The final elastic process in our list, Compton scattering, presents a particular difficulty for Regge theory [214]. One expects of course a constant cross section controlled by the P , but because of the helicity of the photon ($\lambda_\gamma = \pm 1$) $\alpha = 1$ is a wrong-signature nonsense point. Hence the P coupling would have to vanish at $\alpha = 1$, i.e. $t = 0$, if there were not a wrong-signature fixed pole [265]. But it is rather peculiar that Compton scattering should be controlled by the third double spectral function in this way. An alternative way out of the dilemma [223] is to note that $t = 0$ is the $\gamma\gamma$ threshold and if one is willing to alter the threshold behaviour on the grounds that the photon has no non-relativistic limit (just like the $\gamma\pi$ threshold in $\gamma p \rightarrow \pi^+ n$ discussed above) the nonsense decoupling factor $(\alpha(t)-1)$ can replace the required kinematical zero and leave a finite coupling. Also because this process has two electromagnetic vertices the usual theorem against the presence of a fixed pole (which still applies in photoproduction) breaks down [266]. Fits to the γp total cross section data combined with dispersion relations suggest the presence of a real part unconnected with the Regge terms, and of magnitude roughly equal to the Thomson limit ($= -1/137 m_N$) [267]. This could be interpreted as a fixed pole at $J = 0$.

7.7. Quasi-elastic scattering

In view of our uncertainty about the nature of the P required in elastic scattering, it is important to try and test whether quasi-elastic processes (i.e. processes which are inelastic but involve no exchange of quantum numbers) are also controlled by this trajectory, and hence have constant cross sections.

In fig. 49 we show the cross sections for $\pi p \rightarrow \pi N^*$, where the N^* 's are various $I = \frac{1}{2}$ nucleon resonances [268]. The data are not particularly good, but clearly indicate constancy at high energy. This is to be contrasted with the decline of the cross sections for production of $I = \frac{3}{2} N^*$ resonances which are controlled by the ρ

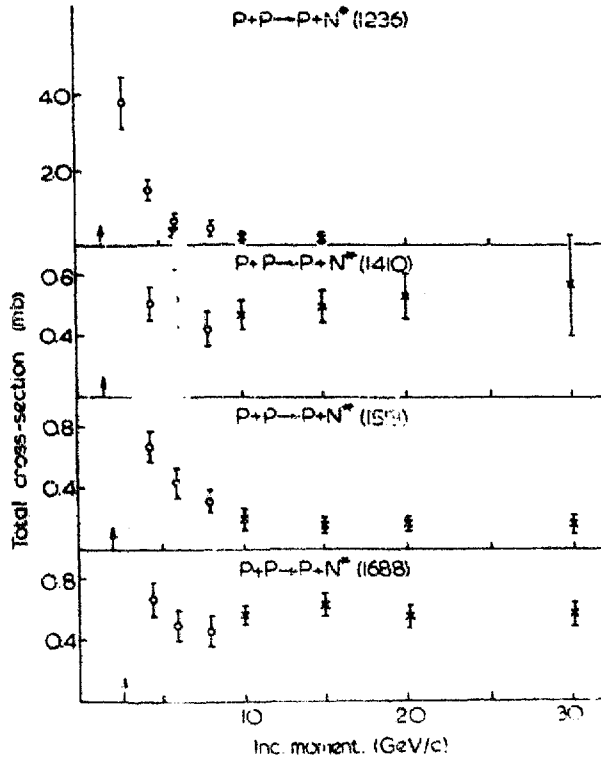


Fig. 49. The total cross sections for the production of some N^* resonances, from ref. [268].

The vector-meson photoproduction processes also provide a useful test, and again the cross sections seem to be compatible with constancy, at least for the ρ and ω [224]. There is a large slope in the ω cross section at low energies which can be attributed to π -exchange since one expects from SU(3) that the $\omega\pi\gamma$ coupling will be much larger than the $\rho\pi\gamma$. It has recently been pointed out by Barger and Cline [269] that the reaction $\gamma p \rightarrow \phi p$ may offer a particularly good chance of observing the P trajectory unencumbered by the P' (or f?) which complicates the analysis of other reactions. The reason for this is that because of the mixing angle (section 6.4) the ϕ is decoupled from non-strange hadrons (it is made up of $\lambda\lambda$ quarks) so that in $\phi N \rightarrow \phi N$ (in which only $I = 0$ states can be exchanged) the ϕ should decouple from the f leaving just P exchange. According to the vector dominance hypothesis

$$\frac{d\sigma}{dt}(\gamma p \rightarrow \phi p) = \frac{e^2}{4\gamma_\phi^2} \frac{d\sigma}{dt}(\phi_{tr} p \rightarrow \phi p),$$

where ϕ_{tr} means a transversely polarized ϕ meson, and γ_ϕ is the $\phi\gamma$ coupling. The rather poor data on $\gamma p \rightarrow \phi p$ suggest a P slope of about $\frac{1}{2}$, but because of the possibility that one is really observing a set of multiple P cuts this only represents a lower bound to the slope. In fact a cut analysis suggests $\alpha_P \approx 1 \text{ GeV}^{-2}$ [270]. A P with such a large slope is rather difficult for the duality hypothesis be-

cause it will produce Schmid loops in exotic channels, and so requires the introduction of exotic states. Also if the P is identified with the f , the $\rho f A_2$ degeneracy, which is essential for pole duality (see section 6.4), is destroyed.

7.8. No single particle exchange possible

An important test of the consistency of our theory is that those processes where no known trajectory can be exchanged should not give rise to prominent forward or backward peaks. Some examples are given in table 5, none of which have any significant structure (in fact several are too small to measure). This confirms the association of peaks with particle exchanges, and once that is granted, shows that there are no strongly coupled exotic trajectories in the channels considered. There should, however, be contributions from multiple trajectory exchanges, and the two Reggeon cuts which one would expect to dominate (given the rules of section 5.6) are shown in the table. A determination of the energy dependence and magnitudes of these amplitudes could provide a good deal of information about these cuts. Unfortunately experiments on $\pi^- p \rightarrow \bar{K}^+ +$ (missing mass) show no amplitude at all [271], while $K^- p \rightarrow p K^-$ shows a strong decrease $\sim s^{-9}$ at low energies (the resonance region) [272]. There should be a $K^* \Delta$ cut with an s^{-3} dependence but this is not seen. A model of this cut has been suggested [273], but it is well below the bounds of the present high energy experiments. It must be hoped that much better data on this sort of process will be available before too long.

7.9. Factorization

The question of the factorization of Regge poles deserves a more general mention.

We have used arguments based on factorization to decide against the existence of a cross-over zero in the ρ and ω trajectories at $t \approx -0.15$, and against the conspiracy explanation of n dominated reactions. But one ought also to ask whether there is any direct experimental evidence in favour of factorization. In fact it is very hard to obtain because one can not do the necessary experiments; e.g. one can look at πN and NN scattering but not $\pi\pi$. One fairly direct test [274] for the P is to test the equality

$$\frac{\frac{d\sigma}{dt} (NN \rightarrow NN)}{\frac{d\sigma}{dt} (\pi N \rightarrow \pi N)} = \frac{\frac{d\sigma}{dt} (NN \rightarrow NN^*)}{\frac{d\sigma}{dt} (\pi N \rightarrow \pi N^*)},$$

where the N^* is any $I = \frac{1}{2}$ nucleon resonance. The left-hand side is 2.7 at $t = 0$ and the right-hand side is 3.2 and 2.9 for the $N^*(1400)$ and $N^*(1688)$ respectively (with errors of ± 0.6 on each). This is some, but not very strong, evidence for factorization. Bari and Razihi [275] have looked at the ratio

$$\frac{d\sigma}{dt} (\pi N \rightarrow \pi N) \Big/ \frac{d\sigma}{dt} (NN \rightarrow \pi NN)$$

for a range of πN final-state energies and find good agreement with factorization despite the fact that there will be $I = \frac{3}{2}$ contamination (dropping with increasing energy of course).

The absence of more direct tests of factorization permits the (? fleeting) thought that perhaps all trajectories are multiple, as suggested by the split A_2 and multi-particle Veneziano models [276]. A small splitting can explain several

of the problems of the simple pole model (such as $\pi^-p \rightarrow \pi^0 n$ polarization (see section 2) and the cross-over zero) but not the π conspiracy. However, since we know that non-factorizable cuts must also be present it seems most natural to blame any failures of factorization on them.

CHAPTER 8 SOME CONCLUSIONS

The discussions of the preceding chapters should be sufficient to vindicate the claim made in the introduction, that Regge theory provides a most successful approach to high-energy scattering, and that J -plane analysis is an essential tool for understanding strong interactions.

Despite the many ambiguities we have been able to draw some reasonably firm conclusions about Regge poles. Most trajectories seem to be essentially straight, parallel lines, with a slope about 1 GeV^{-2} , and many of the dominant trajectories are approximately exchange-degenerate. We have found no evidence that trajectories take part in conspiracies, but all seem to have Toller number $\Lambda < 1$. There is a problem with regard to the baryons in that one does not find approximately degenerate pairs of opposite parity trajectories. This is incompatible with the straightness of the baryon trajectories unless there is some mechanism to make the residues vanish for every integer on the odd parity side; or some singularity like the Carlitz-Kislinger cut (discussed in section 5.7) is invoked. There is very little evidence for daughter trajectories, and it seems likely that if they exist they stay in the left-half J -plane, serving merely to preserve analyticity at $l = 0$, and do not produce physical particles. Their status may be similar to that of the many unimportant low-lying trajectories in potential scattering, such as those which occur at thresholds at $L = -\frac{1}{2}, -\frac{3}{2}, \dots$

The nature of the Pomeron is still uncertain. The fact that the pp data continue to shrink at Serpukhov energies requires a moving singularity, and we do not know of a mechanism which can produce cuts with $\alpha_c(0) = 1$ if there are not also poles with $\alpha(0) = 1$; but whether the P has the slope indicated by the pp data (≈ 0.5) and so perhaps passes through the f , or has a similar slope to other trajectories (≈ 1) but is partially masked by the cuts, remains unclear.

We have found no evidence for fixed J -plane singularities (apart from the nonsense wrong-signature fixed poles), except possibly in some photoproduction processes, but even here the evidence seems to be against them at larger $|t|$.

Poles alone are not able to fit the data, however, because in particular the cross-over zero and the pion conspiracy are incompatible with factorization, and to explain these effects we must use cuts. We know on theoretical grounds that cuts are needed to explain how the Gribov-Pomeranchuk fixed poles are shielded from the unitarity equation, but unfortunately we do not have a reliable model to calculate their magnitudes because they depend (at least in Feynman diagram models) on continuing the Reggeon couplings off the mass shell. The various on-mass-shell prescriptions, such as the absorptive and eikonal models, do not have any very compelling theoretical backing; indeed both seem to involve planar diagrams which should not give rise to cuts.

The absence of a reliable method of estimating cut magnitudes is the principal problem of Regge phenomenology at present. It has not so far been possible to distinguish experimentally between the so called strong (or Michigan) cut model in

which pole-cut interference is responsible for the various dips in the differential cross sections, and the weak (or Argonne) model in which the poles themselves have zeros at wrong-signature nonsense points, and the cuts serve merely to move or fill in these zeros. But it seems likely that better data, particularly on polarizations may enable a choice to be made. It must be born in mind, however, that since neither model has a very sound theoretical status it is quite possible that neither will be found to work in all processes. At present $\gamma p \rightarrow \pi^+ n$ seems to require very strong cuts (even by the standards of the Michigan model) while $\pi^- p \rightarrow \pi^0 n$ would be quite happy with almost negligible ones.

The plea for better data is of course perennial among theorists, but so much has been learned by fitting two body processes that one feels justified in asking for more data on resonance production processes so that tests of factorization can be made; more high energy polarization measurements so that the spin structure of amplitudes can be determined with greater confidence; and of course the more data there is on any process at large s and t the better, since the different pole and cut models become more readily distinguishable at higher energies and wider angles. It seems that more is likely to be learned in the near future from quasi two-body production experiments than from more complex final states which are so much harder to analyse.

Dual models, which have enjoyed such a vogue in recent years, pose some very difficult theoretical problems. We have seen in chapter 6 that the ideal dual world where every amplitude is saturated by narrow resonances which fall into non-exotic $SU(3)$ multiplets with exchange degenerate trajectories bears only a partial, and by no means quantitative, relation to nature. Once one attempts to make corrections for unitarity, $SU(3)$ breaking, etc., the whole edifice seems to crumble. The model becomes too imprecise to test because there are so many ambiguities in determining the existence and magnitude of inelastic resonances, and in how to continue a Regge pole term to low energies. One can not decide what is meant by 'broken duality' until one has a clear idea of what exact duality means (if anything) outside a world of narrow resonances. It seems to the author that little if any progress can be expected unless and until some fairly precise prescription can be given for constructing dual models with resonances of finite width, so that there is a definite prescription for continuing the amplitude onto the unphysical sheets to the poles. The Veneziano models provides no help in this, and not surprisingly it does not fit two-body processes at all well.

Most of the problems really stem from the fact that duality is too vague to be a fundamental principle itself, and yet it is hard to see from what more basic concept an approximate duality could derive. At the moment it is a purely ad hoc notion. Probably the chief current interest in dual models is that they provide a convenient framework for constructing many-particle amplitudes which have the required poles and multi-Regge behaviour, rather than in duality itself.

Though Regge phenomenology has made great progress in the last few years the same can not be said for our understanding of the basic dynamical principles on which this success presumably depends. In particular both the straightness of the trajectories, and exchange degeneracy, are completely unexpected, and seem quite at variance with the potential scattering ideas which motivated the introduction of Regge poles into particle physics. In potential scattering [4, 5, 14] the leading trajectories satisfy dispersion relations of the form

$$\alpha(t) = \alpha(\infty) + \frac{1}{\pi} \int_{t_0}^{\infty} \frac{\text{Im } \alpha(t')}{t' - t} dt' \quad (8.1)$$

and are strongly curved, their real parts reaching a maximum not far above threshold when $\text{Im } \alpha$ becomes sizeable, and then turn down again. Exchange degenerate trajectories occur only in the absence of an exchange (Majorana) force.

None of the attempts which have been made to calculate Regge trajectories from 'equivalent potentials' [15, 277] have been able to reproduce such straight, degenerate trajectories. The lack of curvature is in fact strong evidence that the channels which control the dynamics are of very high mass [278]. This is clear from (8.1) in that if the threshold, t_0 , in (8.1) is very far away we can approximate the integral by a pole

$$\alpha(t) = \alpha(\infty) + R/(t_p - t) \quad \text{for } |t| \ll t_0, \quad (8.2)$$

where $t_p \gg t_0$. Then $\alpha'(0) = R/t_p^2$ and $\alpha''(0) = 2R/t_p^3$ so we get $\alpha' \gg \alpha''$ (prime = d/dt) and the trajectory is nearly straight for small $|t|$.

The dominance of such a high mass channel is strongly suggestive of the heavy quark model of course, and this can also explain why the trajectories are exchange degenerate in that there will be no particle-exchange forces in the exotic qq channel, but only in the $q\bar{q}$ channel. But, it should be noted that the observed residues will not be exchange degenerate in this model, for what we see are the couplings to low mass channels, and it is only in the unobserved qq channel that the residues will be degenerate [279]. There is a difficulty with this quark model however [278], for if the trajectory is to obey (8.2) with $\alpha(0) = \frac{1}{2}$ and $\alpha'(0) = 1 \text{ GeV}^{-2}$, we have

$$\alpha(\infty) = \frac{1}{2} - t_p \text{ GeV}^{-2}.$$

Now t_p is above the qq threshold at $4m_q^2$, so if the quarks have masses of about 10 GeV say then $\alpha(\infty) < -400$. In potential scattering (say for a Yukawa potential $V(r) = g e^{-\lambda r}/r$) the leading trajectories have $\alpha(\infty) = -1$ because the potential Born term $g/(s - \lambda^2)$ corresponds to a fixed pole in the t -channel J -plane at -1 . To remove this pole we must require that the potential obey SCR (like section 2.9). In configuration space these SCR correspond to zeros in the potential at the origin, say $V(r) = g r^n e^{-\lambda r}$, and we require $n \approx 400$. It is hard to see how such a potential can be strong enough to produce highly bound states (though of course the analogy with potential scattering could break down completely). Very similar remarks apply even if we do not require the existence of real quarks but simply use them to simulate the coupling to many-particle channels. In any such model the trajectories are CDD trajectories as far as the low mass channels are concerned, and it is hard to see how Regge behaviour can hold for $s \ll m_Q^2$.

An alternative possibility is that the trajectory obeys the twice subtracted dispersion relation (3.15). We have seen that this is in good accord with the observed behaviour of $\text{Im } \alpha$, at least for mesons. But in this case α' is not determined by unitarity at all (which simply determines $\text{Im } \alpha$), and the two subtraction parameters $\alpha(\infty)$ and α' are arbitrary. The trajectories are now CDD trajectories in all channels. Since in fact α' is observed to be approximately the same for all trajectories we can speculate that it represents a fundamental constant of strong interactions, and that unitarity (via $\text{Im } \alpha$) simply determines the small deviation of α' from this uni-

versal value in individual trajectories. However, this takes us so far from potential scattering that it becomes hard to see why there should be any application of Regge theory to particle physics at all.

We conclude therefore that the straightness of Regge trajectories is one of the most baffling, and most important, problems of elementary particle theory. But if it can be solved then we shall probably be well on the way to a complete understanding of strong interaction dynamics.

ACKNOWLEDGEMENTS

I am very grateful to many of my colleagues in Durham, especially Professor E. J. Squires and Dr. R. C. Johnson for their comments on this article. It has also benefitted from correspondence with Drs. M. Jacob, E. L. Berger, G. L. Kane, J. K. Storrow, G. Ringland and R. J. N. Phillips.

REFERENCES

- [1] T. Regge, *Nuovo Cimento* 14 (1959) 951.
- [2] T. Regge, *Nuovo Cimento* 18 (1960) 947.
- [3] A. Bottino, A. M. Longhoni and T. Regge, *Nuovo Cimento* 23 (1962) 954.
- [4] E. J. Squires, *Complex angular momentum and particle physics* (Benjamin, New York, 1963).
- [5] R. G. Newton, *The complex J plane* (Benjamin, New York, 1964).
- [6] G. F. Chew and S. C. Frautschi, *Phys. Rev. Letters* 7 (1961) 394.
- [7] R. Blankenbecler and M. L. Goldberger, *Phys. Rev.* 126 (1962) 766.
- [8] S. C. Frautschi, M. Gell-Mann and F. Zachariasen, *Phys. Rev.* 125 (1962) 2204.
- [9] G. F. Chew, *Rev. Mod. Phys.* 34 (1962) 394.
- [10] G. F. Chew, *The dynamical S-matrix* (Benjamin, New York, 1966).
- [11] H. Pilkuhn, *The interactions of hadrons* (North-Holland, Amsterdam, 1967).
- [12] A. D. Martin and T. D. Spearman, *Elementary particle theory* (North-Holland, Amsterdam, 1970).
- [13] H. Burkhardt, *Dispersion relation dynamics* (North-Holland, Amsterdam, 1969).
- [14] V. De Alfaro and T. Regge, *Potential scattering* (North-Holland, Amsterdam, 1967).
- [15] P. D. B. Collins and E. J. Squires, *Regge poles in particle physics* (Springer, Berlin, 1968).
- [16] J. D. Jackson, *Rev. Mod. Phys.* 42 (1970) 12.
- [17] G. E. Hite, *Rev. Mod. Phys.* 41 (1969) 669.
- [18] V. Barger and D. Cline, *Phenomenological theories of high energy scattering* (Benjamin, New York, 1969).
- [19] S. Mandelstam, *Phys. Rev.* 112 (1958) 1344; 115 (1959) 1741; 115 (1959) 1752.
- [20] See any introductory book, e.g. refs. [11-13 or 15] above, for the kinematics, and an explanation of the idea of crossing.
- [21] M. Jacob and G. C. Wick, *Ann. Phys.* 7 (1959) 404.
- [22] T. L. Trueman and G. C. Wick, *Ann. Phys.* 26 (1964) 322.
- [23] L. L. C. Wang, *Phys. Rev.* 142 (1966) 1187.
- [24] G. Cohen-Tannoudji, A. Morel and H. Navelet, *Ann. Phys.* 46 (1963) 239.
- [25] J. D. Jackson and G. E. Hite, *Phys. Rev.* 169 (1968) 1248.
- [26] A. R. Edmonds, *Angular momentum in quantum mechanics* (Princeton University, 1957).
- [27] H. Lehmann, *Nuovo Cimento* 10 (1958) 579.
- [28] M. E. Rose, *Elementary theory of angular momentum* (Wiley, New York, 1957).
- [29] M. Andrews and J. G. Wilson, *J. Math. Phys.* 5 (1964) 1391.
- [30] W. Drechsler, *Nuovo Cimento* 53A (1968) 115.

- [31] W. Drechsler, Complex angular momentum theory in particle physics, Trieste report IC/69/39 (1969), unpublished.
- [32] E. C. Titchmarsh, The theory of functions, 2nd ed. (Oxford University, 1939) p. 1-6.
- [33] M. Gell-Mann et al., Phys. Rev. 133 (1964) B146; 133 (1964) P161.
- [34] S. Mandelstam, Ann. Phys. 19 (1962) 254.
- [35] M. Froissart, Phys. Rev. 123 (1961) 1053.
- [36] J. M. Charap and E. J. Squires, Phys. Rev. 127 (1962) 1387.
- [37] F. Arbab and J. D. Jackson, Phys. Rev. 176 (1968) 1796.
- [38] V. N. Gribov and L. Y. Pomeranchuk, Proc. 1962 CERN Conf. on high energy physics, p. 522.
- [39] H. Cheng, Phys. Rev. 130 (1963) 1283.
- [40] A. O. Barut and D. E. Zwanziger, Phys. Rev. 127 (1963) 974.
- [41] J. R. Taylor, Phys. Rev. 127 (1962) 2257.
- [42] V. N. Gribov and L. Y. Pomeranchuk, Phys. Rev. Letters 9 (1962) 238.
- [43] B. R. Desai and R. G. Newton, Phys. Rev. 129 (1963) 1445.
- [44] R. R. Desai and B. Sakita, Phys. Rev. 136 (1964) B226.
- [45] S. MacDowell, Phys. Rev. 116 (1959) 774.
- [46] P. Carruthers, Introduction to unitary symmetry (Interscience, New York, 1966).
- [47] M. Gourdin, Unitary symmetries (North-Holland, Amsterdam, 1967).
- [48] Particle Data Group, Rev. Mod. Phys. 42 (1970) 87.
- [49] M. Roos, Nuovo Cimento Letters 3 (1970) 257.
- [50] D. Crennell et al., Phys. Letters 28B (1968) 136.
- [51] J. D. Jackson and C. Quigg, Private communication in ref. [156].
- [52] G. McClellan et al., Phys. Rev. Letters 23 (1969) 718.
- [53] M. N. Focacci et al., Phys. Rev. Letters 17 (1966) 890.
- [54] P. D. B. Collins, R. C. Johnson and E. J. Squires, Phys. Letters 26B (1968) 223.
- [55] G. F. Chew and S. C. Frautschi, Phys. Rev. Letters 7 (1961) 394.
- [56] R. C. Johnson, Nucl. Phys. B5 (1968) 673.
- [57] V. Barger and D. Cline, Phys. Rev. Letters 16 (1966) 913.
- [58] V. Barger and D. Cline, Phys. Rev. 155 (1967) 1792.
- [59] R. M. Spector, Phys. Rev. 173 (1967) 1671.
- [60] H. Goldberg, Phys. Rev. Letters 19 (1967) 1391.
- [61] R. M. Spector, Wayne State University, unpublished report (1969).
- [62] Y. Hara, Phys. Rev. 136 (1964) 507.
- [63] J. Franklin, Phys. Rev. 170 (1968) 1606.
- [64] I. L. Fruehan, Phys. Rev. 173 (1968) 1684; erratum Phys. Rev. 181 (1969) 2154.
- [65] J. P. Ader, M. Capdeville and H. Navelet, Nuovo Cimento 66A (1968) 315.
- [66] E. Leader, Phys. Rev. 166 (1968) 1599.
- [67] A. Capella, J. Tran Thanh Van and A. P. Contogouris, Nucl. Phys. B12 (1969) 167.
- [68] J. M. Wang and L. L. Wang, Phys. Rev. D1 (1970) 663.
- [69] G. Cohen-Tannoudji, Ph. Salin and A. Morel, Nuovo Cimento 55A (1969) 412.
- [70] M. Le Bellac, Nuovo Cimento 55A (1968) 318.
- [71] J. S. Ball, W. R. Frazer and M. Jacob, Phys. Rev. Letters 20 (1968) 518.
- [72] R. J. N. Phillips, Nucl. Phys. B2 (1967) 657.
- [73] M. Le Bellac, Phys. Letters 25B (1967) 524.
- [74] M. L. Goldberger and C. E. Jones, Phys. Rev. 150 (1966) 1269.
- [75] D. Z. Freedman and J. M. Wang, Phys. Rev. 153 (1967) 1596.
- [76] R. E. Cutkosky and J. S. Deo, Phys. Rev. Letters 19 (1967) 1286.
- [77] A. R. Swift, J. Math. Phys. 8 (1967) 2420;
- V. Chung and D. R. Snider, Phys. Rev. 162 (1967) 1639.
- [78] M. Toller, Nuovo Cimento 37 (1965) 631; 53A (1967) 671.
- [79] V. E. Britten and A. O. Barut (Eds.), Lectures in theoretical physics, Vol. 7A (University of Colorado Press, 1964).
- [80] E. P. Wigner, Ann. Math. 40 (1939) 159.
- [81] V. Bargmann, Ann. Math. 48 (1947) 568.
- [82] H. Joos in ref. [79].
- [83] J. C. Boyce, J. Math. Phys. 8 (1967) 675;
- J. C. Boyce, R. Delbourger, A. Salam and J. Strathdee, Trieste preprint IC/67/9, 1967 (unpublished).
- [84] E. Inonu and E. P. Wigner, Nuovo Cimento 9 (1952) 707.

- [85] J.-M. Levy-Leblond, *Nuovo Cimento* 45 (1966) 772.
- [86] H. Sciarrino and M. Toller, *J. Math. Phys.* 8 (1967) 1252.
- [87] G. Domokos and G. L. Tindle, *Phys. Rev.* 165 (1968) 1906;
K. M. Bitar and G. L. Tindle, *Phys. Rev.* 175 (1968) 1835;
P. K. Kuo and P. Suranyi, *Phys. Rev. D1* (1970) 3416, 3424.
- [88] G. F. Chew, *Phys. Rev. Letters* 16 (1966) 60.
- [89] R. Oehme, *Phys. Letters* 28B (1968) 122.
- [90] A. N. Diddens et al., *Phys. Rev. Letters* 9 (1962) 108, 111.
- [91] J. Foley et al., *Phys. Rev. Letters* 10 (1963) 376.
- [92] K. Igi, *Phys. Rev.* 130 (1963) 820.
- [93] E. J. Squires, *Phys. Letters* 7 (1963) 363.
- [94] D. Atkinson and A. P. Contogouris, *Nuovo Cimento* 39 (1965) 1082, 1102.
- [95] S. Mandelstam, *Nuovo Cimento* 30 (1963) 1127, 1148.
- [96] D. Amati, S. Fubini and A. Stanghellini, *Phys. Letters* 1 (1962) 29.
- [97] R. Oehme, in: R. G. Moorhouse (Ed.), *Strong interactions and high energy physics* (Oliver and Boyd, London, 1964).
- [98] R. J. Eden, P. V. Landshoff, D. I. Olive and J. C. Polkinghorne, *The analytic S-matrix* (Cambridge University, 1966).
- [99] J. C. Polkinghorne, *J. Math. Phys.* 4 (1963) 503.
- [100] V. N. Gribov, *JETP (Sov. Phys.)* 26 (1968) 414.
- [101] C. Risk, Lawrence Radiation Lab. preprint UCRL-19453 (1970).
- [102] G. A. Winbow, *Phys. Rev.* 177 (1969) 2533.
- [103] V. V. Sudakov, *JETP* 30 (1956) 87.
- [104] F. Henyey, G. L. Kane, J. Pumplin and M. H. Ross, *Phys. Rev.* 182 (1969) 1579.
- [105] R. J. Glauber, in: *Lectures in theoretical physics*, Vol. 1 (Wiley, New York, 1959).
- [106] M. Geil-Mann and B. M. Udgankar, *Phys. Rev. Letters* 8 (1962) 346.
- [107] E. S. Abers, H. Burkhardt, V. L. Teplitz and C. Wilkin, *Nuovo Cimento* 42 (1966) 365.
- [108] P. V. Landshoff, *Phys. Rev.* 177 (1969) 2531; *Acta Physica Austriaca, Suppl.* VII (1970) 145.
- [109] D. R. Harrington, *Phys. Rev. D1* (1970) 260.
- [110] C. Wilkin, *Lecture at the Summer School on diffractive processes*, McGill University (1969) (unpublished).
- [111] R. C. Arnold, *Phys. Rev.* 153 (1967) 1523.
- [112] C. E. Jones and V. L. Teplitz, *Phys. Rev.* 159 (1967) 1271;
J. B. Bronzan and C. E. Jones, *Phys. Rev.* 160 (1967) 1494.
- [113] J. H. Schwarz, *Phys. Rev.* 162 (1967) 1671.
- [114] R. Hwa, *Phys. Rev.* 162 (1967) 1706.
- [115] P. V. Landshoff and J. C. Polkinghorne, *Phys. Rev.* 181 (1969) 1989.
- [116] R. L. Kelly, G. L. Kane and F. Henyey, *Phys. Rev. Letters* 24 (1970) 1511;
G. L. Kane, F. Henyey, D. R. Richards, M. Ross and G. Williamson, *Phys. Rev. Letters* 25 (1970) 1519. Many references to earlier work are given in ref. [104].
- [117] M. Ross, F. S. Henyey and G. L. Kane, *Nucl. Phys.* B23 (1970) 269.
- [118] P. J. O'Donovan, *Phys. Rev.* 185 (1969) 1902.
- [119] R. J. Rivers, *Nuovo Cimento* 63A (1969) 697.
- [120] J. Finkelstein and M. Jacob, *Nuovo Cimento* 56A (1968) 681.
- [121] L. Durand and Y. T. Chiu, *Phys. Rev.* 139 (1965) B646.
- [122] R. Torgerson, *Phys. Rev.* 143 (1966) 1194;
See also G. Thiotopoulos and S. B. Trieman, *Phys. Rev.* 192 (1970) 805.
- [123] R. Oehme, *Phys. Rev. Letters* 10 (1969) 450; *Phys. Rev. D2* (1970) 801.
- [124] P. Kaus and F. Zachariasen, *Phys. Rev. D1* (1970) 2962;
J. S. Ball, G. Marchesini and F. Zachariasen, *Phys. Letters* 32B (1970) 583.
- [125] V. N. Gribov and A. A. Migdal, *Sov. J. of Nucl. Phys.* 8 (1969) 583, 703.
- [126] R. C. Arnold and M. L. Blackmon, *Phys. Rev.* 176 (1968) 2082.
- [127] M. L. Blackmon and G. R. Goldstein, *Phys. Rev.* 179 (1969) 1480.
- [128] M. L. Blackmon, *Phys. Rev.* 178 (1969) 2385;
M. L. Blackmon, G. Kramer and K. Schilling, *Phys. Rev.* 183 (1969) 1452;
M. L. Blackmon and G. R. Goldstein, *Phys. Rev. D1* (1970) 2675, 2707.
- [129] P. Finkler, *Phys. Rev. D1* (1970) 1172.
- [130] E. J. Squires, preprint, *Generalized unitarity and fixed J-plane poles* (1970), unpublished.

- [131] R. Carlitz and M. Kislinger, *Phys. Rev. Letters* 24 (1970) 186.
- [132] F. Halzen, A. Kumar, A. D. Martin and C. Michael, *Phys. Letters* 32B (1970) 111.
- [133] R. Dolen, D. Horn and C. Schmid, *Phys. Rev.* 166 (1968) 1768.
- [134] A. Donnachie in T. W. Priest and L. L. J. Vick (Eds.), *Particle interactions at high energies* (Oliver and Boyd, London, 1967).
- [135] J. M. Blatt and V. F. Weiskopf, *Theoretical nuclear physics* (Wiley, New York, 1952);
H. A. Weidenmüller, *Phys. Letters* 24B (1967) 441.
- [136] A. Donnachie and R. G. Kirsopp, *Nucl. Phys.* B10 (1969) 433.
- [137] Y. C. Liu and S. Okubo, *Phys. Rev. Letters* 19 (1967) 190;
C. Ferro-Fontan et al., *Nuovo Cimento* 58A (1968) 534.
- [138] R. J. N. Phillips, *Lectures on Regge phenomenology* (1970), unpublished.
- [139] R. Amblard et al., Submitted to Lund Conference (1969);
V. Barger and R. J. N. Phillips, *Phys. Rev.* 187 (1969) 2210.
- [140] C. Schmid, *Phys. Rev. Letters* 20 (1968) 689.
- [141] C. B. Chiu and A. Kotanski, *Nucl. Phys.* B7 (1968) 615; B8 (1968) 553.
- [142] P. D. B. Collins, R. C. Johnson and E. J. Squires, *Phys. Letters* 27B (1968) 23.
- [143] P. D. B. Collins, R. C. Johnson and G. G. Ross, *Phys. Rev.* 176 (1968) 1952.
- [144] See also the lectures of M. Jacob, *Duality in strong interaction*, CERN Th. 1010 (1969), unpublished and;
H. Harari, *Duality and hadron dynamics* (1969) unpublished.
- [145] P. G. O. Freund, *Phys. Rev. Letters* 20 (1968) 235.
- [146] H. Harari, *Phys. Rev. Letters* 20 (1968) 1395.
- [147] C. F. Chiu and J. Finkelstein, *Phys. Letters* 27B (1968) 510.
- [148] C. Schmid, *Nuovo Cimento Letters* 1 (1969) 165;
V. Barger and C. Michael, *Phys. Rev.* 186 (1969) 1592.
- [149] H. Harari, *Phys. Rev. Letters* 22 (1969) 562.
- [150] J. L. Rosner, *Phys. Rev. Letters* 22 (1969) 689.
- [151] J. L. Rosner, *Phys. Rev. Letters* 21 (1968) 950.
- [152] R. K. Logan and D. P. Roy, *Nuovo Cimento Letters* 3 (1970) 517.
- [153] H. Harari and Y. Zarmi, *Phys. Rev.* 187 (1969) 2230.
- [154] R. C. Johnson, *Phys. Rev.* 183 (1969) 1406.
- [155] G. Veneziano, *Nuovo Cimento* 57A (1968) 190.
- [156] D. Silvers and J. Yellin, Review of recent work on narrow resonance models, UCRL-19418 (unpublished).
- [157] C. J. Goebel, unpublished report, see Harari ref. [144].
- [158] F. Wagner, *Nuovo Cimento* 63A (1969) 393.
- [159] C. Lovelace, *Phys. Letters* 28B (1968) 264.
- [160] C. Schmid, *Phys. Letters* 28B (1968) 348.
- [161] V. A. Alessandrini, P. G. O. Freund, R. Oehme and E. J. Squires, *Phys. Letters* 27B (1968) 456.
- [162] P. D. B. Collins, G. G. Ross and E. J. Squires, *Nucl. Phys.* B10 (1969) 475.
- [163] G. A. Ringland and R. J. N. Phillips, *Nucl. Phys.* B13 (1969) 274.
- [164] C. Lovelace, CERN preprint Th. 1041 (1969) unpublished;
S. Humble, *Nuovo Cimento Letters* 2 (1969) 541;
D. Atkinson et al., *Phys. Letters* 29B (1969) 423;
K. Huang, *Phys. Rev. Letters* 23 (1969) 903;
N. F. Bali, D. D. Coon and J. W. Dash, *Phys. Rev. Letters* 23 (1969) 900;
M. Suzuki, *Phys. Rev. Letters* 23 (1969) 205;
G. Cohen-Tannoudji et al., *Phys. Rev. Letters* 26 (1971) 112.
- [165] G. Altarelli and H. R. Rubinstein, *Phys. Rev.* 178 (1969) 2165.
- [166] S. Mandelstam, *Phys. Rev.* 184 (1969) 1625.
- [167] V. A. Alessandrini and D. Amati, *Phys. Letters* 29B (1969) 193.
- [168] K. Igi, *Phys. Letters* 28B (1968) 330;
M. Virasoro, *Phys. Rev.* 184 (1969) 1621;
Y. Hara, *Phys. Rev.* 182 (1969) 1906;
K. Igi and F. Storrow, *Nuovo Cimento* 62A (1969) 972;
I. Inami, *Nuovo Cimento* 63A (1969) 987;
K. Fretzi and K. Igi, *Nuovo Cimento* 63A (1969) 609.
- [169] E. L. Berger and G. C. Fox, *Phys. Rev.* 188 (1969) 2120.

- [170] M. A. Virasoro, *Phys. Rev. Letters* 22 (1969) 37;
 Chan Hong-Mo, *Phys. Letters* 28B (1969) 425;
 Chan Hong-Mo and T. S. Tsun, *Phys. Letters* 28B (1969) 485;
 J. L. Hopkinson and E. Plahte, *Phys. Letters* 28B (1969) 489;
 Z. Koba and H. B. Nielsen, *Nucl. Phys. B10* (1969) 633.
- [171] K. Bardakci and H. Ruegg, *Phys. Letters* 28B (1968) 342.
- [172] C. Lovelace, Veneziano theory, CERN Th. 1123 (1970) unpublished.
- [173] Chan Hong-Mo, Multi-particle phenomenology, CERN Th. 1089 (1969) unpublished.
- [174] S. Mandelstam, ref. [166] and *Phys. Rev. D1* (1970) 1720, 1734, 1745;
 K. Bardakci and M. E. Halpern, *Phys. Rev.* 183 (1969) 1456;
 K. Kikkawa, B. Sakita and M. A. Virasoro, *Phys. Rev.* 184 (1969) 1701.
- [175] V. Alessandrini, D. Amati, M. Le Bellac and D. Olive, Dual multi-particle theory, CERN Th. 1160 (1970) unpublished.
- [176] D. J. Gross, *Nucl. Phys. B13* (1969) 467;
 S. Fubini, D. Gordon and G. Veneziano, *Phys. Letters* 29B (1969) 679.
- [177] M. Ahmad, Fayyazuddin and Riazuddin, *Phys. Rev. Letters* 23 (1969) 504;
 I. Bender and H. J. Rothe, *Nuovo Cimento Letters* 2 (1969) 477;
 F. Drago, *Nuovo Cimento Letters* 2 (1969) 712.
- [178] G. C. Fox, Skeletons in the Regge cupboard, Talk at 1969 Stony Brook Conference, unpublished.
- [179] E. J. Squires, Regge pole phenomenology, Lectures at Heidelberg Summer School (1970), unpublished.
- [180] R. J. N. Phillips, ref. [138].
- [181] L. Durand, Review of Reggeism, Coulter conference on high energy physics (1969), unpublished.
- [182] R. Logan, *Phys. Rev. Letters* 14 (1965) 414.
- [183] R. J. N. Phillips and W. Rarita, *Phys. Rev.* 139B (1965) 1336.
- [184] G. Höhler et al., *Phys. Letters* 20 (1966) 79.
- [185] F. Arbad and C. B. Chiu, *Phys. Rev.* 147 (1966) 1045.
- [186] R. J. N. Phillips, *Nuovo Cimento* 45 (1966) 245.
- [187] B. Desai, D. Gregorich and Ramachandran, *Phys. Rev. Letters* 18 (1967) 565.
- [188] S. Minami et al., *Nuovo Cimento Letters* 3 (1970) 124.
- [189] V. Barger and R. J. N. Phillips, *Phys. Rev.* 187 (1969) 2210.
- [190] J. P. De Brion and A. Darem, *Nucl. Phys. B16* (1970) 111.
- [191] A. Ahmadzadeh and J. C. Jackson, *Phys. Rev.* 187 (1969) 2078.
- [192] S. Y. Chiu, B. R. Desai and D. P. Roy, *Phys. Rev.* 187 (1969) 1896.
- [193] R. C. Johnson and E. J. Squires, *Phys. Letters* 32B (1970) 365.
- [194] L. Sertorio and M. Toller, *Phys. Rev. Letters* 19 (1967) 1146.
- [195] A. Ahmadzadeh and W. B. Kaufman, *Phys. Rev.* 188 (1969) 2438.
- [196] F. Arbab, N. F. Bali and J. W. Dash, *Phys. Rev.* 158 (1967) 1515.
- [197] C. Michael, *Nucl. Phys. B8* (1968) 431.
- [198] J. N. J. White, *Nucl. Phys. B13* (1969) 139.
- [199] B. J. Hartley, R. W. Moore and K. M. J. Moriarty, *Phys. Rev.* 187 (1969) 1921.
- [200] F. Henyey et al., *Phys. Rev.* 182 (1969) 1579.
- [201] R. Aviv and D. Hora, *Phys. Rev.* 186 (1969) 1510.
- [202] R. J. N. Phillips and W. Rarita, *Phys. Rev. Letters* 15 (1965) 807.
- [203] K. W. Lai and J. Louie, *Nucl. Phys. B19* (1970) 205.
- [204] P. R. Auvil, F. Halzen, C. Michael and J. Weyers, *Phys. Letters* 31B (1970) 303.
- [205] R. D. Mathews, *Nucl. Phys. B11* (1969) 339.
- [206] G. C. Fox and L. Sertorio, *Phys. Rev.* 176 (1968) 1739.
- [207] J. P. Ader, M. Capdeville and Ph. Salin, *Nucl. Phys. B3* (1967) 407.
- [208] J. Froyland, *Nucl. Phys. B11* (1969) 204.
- [209] G. L. Kane, F. Henyey, D. R. Richards, M. Ross and G. Williamson, ref. [116].
- [210] M. Colocci, *Nuovo Cimento Letters* 4 (1970) 53.
- [211] B. Gorezyca and M. Hayashi, *Acta Physica Polonica* 36 (1969) 47.
- [212] H. Harari, Photoproduction mechanisms, in: Proc. 4th Int. Symp. on electron and photon interactions, Daresbury, 1969.
- [213] P. A. Collins et al., *Nucl. Phys. B20* (1970) 381.
- [214] R. Diebold, *Phys. Rev. Letters* 22 (1969) 204.
- [215] R. J. N. Phillips, *Nucl. Phys. B2* (1967) 394.

- [216] R. C. E. Devenish, Nucl. Phys. B14 (1969) 639.
- [217] F. Arbab and H. W. Dash, Phys. Rev. 163 (1967) 1603.
- [218] C. D. Froggatt, Nucl. Phys. B6 (1968) 421.
- [219] Z. Ming Ma et al., Phys. Rev. Letters 24 (1970) 1031.
- [220] M. L. Blackmon and G. R. Goldstein, Phys. Rev. D1 (1970) 2675.
- [221] J. L. Jackson and C. Quigg, Nucl. Phys. B22 (1970) 301.
- [222] I. Bender, Dorsch and H. J. Rothe, Nuovo Cimento 62 (1969) 1026.
- [223] P. D. B. Collins and F. D. Gault, University of Durham preprint (1970), unpublished.
- [224] R. Diebold, High-energy photoproduction, SLAC preprint SLAC-PUB-673 (1969), unpublished.
- [225] E. Gotsman, Phys. Rev. 186 (1969) 1543.
- [226] J. P. Ader and M. Capdeville, Nucl. Phys. B17 (1970) 127.
- [227] A. Dar, Dips and spikes in $d\sigma/dt$ for high energy exchange reactions, unpublished (1970).
- [228] J. Froyland, Nucl. Phys. B12 (1969) 410.
- [229] F. J. Hadjiioannou and P. N. Pouloupoulos, Nuovo Cimento Letters 3 (1970) 384.
- [230] V. Barger and D. Cline, Phys. Rev. Letters 21 (1968) 392.
- [231] E. A. Pascos, Phys. Rev. Letters 21 (1968) 1855.
- [232] K. Igi, S. Matsuda, Y. Oyanagi and H. Sato, Phys. Rev. Letters 21 (1968) 580.
- [233] V. Barger and P. Weiler, Phys. Letters 30B (1969) 105.
- [234] V. Barger and C. Michael, Phys. Rev. Letters 22 (1969) 1330.
- [235] R. L. Kelly et al., ref. [116].
- [236] E. L. Berger and G. Fox, Argonne preprint ANL/HEP 7019 (1970), unpublished.
- [237] F. Drago et al., Phys. Letters 31B (1970) 647.
- [238] A. D. Martin and C. Michael, Phys. Letters 32B (1970) 294.
- [239] See e.g., A. D. Martin, in: G. Höhler (Ed.) Springer tracts in modern physics, Vol. 55 (Springer, Berlin, 1970).
- [240] V. Barger, Phys. Rev. 179 (1969) 1371.
- [241] V. Barger, D. Cline and J. Matos, Phys. Letters 29B (1969) 121.
- [242] G. V. Dass, C. Michael and R. J. N. Phillips, Nucl. Phys. B9 (1969) 549.
- [243] W. Rarita, R. J. Riddell, C. B. Chiu and R. J. N. Phillips, Phys. Rev. 163 (1968) 1611.
- [244] A. P. Contogouris and J. Tran Thanh Van, Phys. Rev. Letters 19 (1967) 1352.
- [245] M. Ciftan and G. Patsakos, Phys. Rev. D1 (1970) 215.
- [246] S. Fenster and K. C. Wali, Phys. Rev. D1 (1970) 1401.
- [247] G. C. Joshi and A. Fagnamenta, Phys. Rev. D1 (1970) 3117.
- [248] B. K. Pal, Phys. Rev. D1 (1970) 1405.
- [249] C. B. Chiu and J. Finkelstein, Nuovo Cimento 57A (1968) 649; 59A (1969) 92.
- [250] R. C. Arnold and M. L. Blackmon, Phys. Rev. 176 (1968) 2082.
- [251] M. L. Blackmon and G. R. Goldstein, Phys. Rev. 179 (1969) 1480.
- [252] S. C. Frautschi and B. Margolis, Nuovo Cimento 56A (1968) 1155.
- [253] I. Y. Pomeranchuk, JETP (Sov. Phys.) 7 (1958) 499.
- [254] L. R. Ignoli and G. Violini, Phys. Letters 31B (1970) 533.
- [255] V. Barger and R. J. N. Phillips, Phys. Rev. Letters 24 (1970) 291.
- [256] R. J. Eden, Phys. Rev. D2 (1970) 529.
- [257] A. Martin, CERN report Th. 1075 (1969), unpublished.
- [258] V. Barger and R. J. N. Phillips, Phys. Letters 31B (1970) 643.
- [259] J. Finkelstein, Phys. Rev. Letters 24 (1970) 172.
- [260] R. Arnowitz and P. Rotelli, Nuovo Cimento Letters 4 (1970) 179.
- [261] G. G. Beznogihl et al., Phys. Letters 30B (1969) 274.
- [262] G. Höhler, F. Steiner and R. Strauss, Z. Physik 233 (1970) 430.
P. Achuthan, H. G. Schlaile and F. Steiner, Nucl. Phys. B24 (1970) 398.
- [263] K. S. Kolberg and B. Margolis, Phys. Letters 31B (1970) 50.
- [264] Y. Hara, Phys. Letters 23 (1966) 696.
- [265] A. H. Mueller and T. L. Trueman, Phys. Rev. 160 (1967) 1296, 1306.
- [266] H. R. Rubinstein, G. Veneziano and M. A. Virasoro, Phys. Rev. 167 (1968) 1441.
- [267] M. Damashek and F. J. Gilman, Phys. Rev. D1 (1970) 1319.
- [268] I. Van Hove, in: Garnjost (Ed.), Proc. 13th Int. Conf. on high energy physics, University of California Press, 1967).
- [269] V. Barger and D. Cline, Phys. Rev. Letters 24 (1970) 1313.
- [270] T. J. Weare, Nuovo Cimento Letters 4 (1970) 251.

- [271] L. Di Lella, in: G. von Dardel (Ed.), Proc. Lund Int. Conf. on elementary particles, 1969.
- [272] D. R. O. Morrison, in ref. [271].
- [273] C. Michael, Phys. Letters 29B (1969) 230.
- [274] P. G. O. Freund, Phys. Rev. Letters 21 (1968) 1375.
- [275] M. B. Bari and M. S. K. Razmi, Phys. Rev. D2 (1970) 2054.
- [276] E. J. Squires, ref. [179] has given a vigorous defence of this viewpoint.
- [277] See, e.g.: P. D. B. Collins and R. C. Johnson, Phys. Rev. 177 (1969) 2472; 182 (1969) 1755; 185 (1969) 2020.
- [278] P. D. B. Collins, R. C. Johnson and E. J. Squires, Phys. Letters 26B (1968) 223.
- [279] E. J. Squires and P. J. S. Watson, Ann. Phys. 41 (1967) 409.
- [280] V. Barger and C. Michael, Phys. Rev. 186 (1969) 1592.
- [281] M. Spiro and A. Derem, Nuovo Cimento Letters 4 (1970) 533.
- [282] R. J. N. Phillips and W. Rarita, Phys. Rev. 140 (1965) B200.
- [283] M. L. Blackmon and K. C. Wali, Phys. Rev. D2 (1970) 258.
- [284] B. Carreras and A. Donnachie, Nucl. Phys. B16 (1970) 35.
- [285] J. Bothe and J. R. Fulco, Phys. Rev. 182 (1970) 1837.
- [286] C. Meyers and Ph. Salin, Nucl. Phys. B19 (1970) 237.
- [287] D. Cline, J. Matos and D. D. Reeder, Phys. Rev. Letters 23 (1969) 1318.
- [288] G. V. Dass and C. Michael, Phys. Rev. 175 (1968) 1774.
- [289] D. Griffiths and R. J. Jabbur, Nucl. Phys. B11 (1969) 7.
- [290] G. Gidal et al., Phys. Rev. Letters 23 (1969) 994.
- [291] M. Krammer and U. Maor, Nucl. Phys. B13 (1969) 651.
- [292] K. Kajantie and P. V. Rusikanen, Nucl. Phys. B13 (1969) 437.
- [293] M. Le Bellac and G. Plaut, Nuovo Cimento Letters 1 (1969) 721.
- [294] C. B. Chiu and S. Matsuda, Phys. Letters 31B (1970) 455.
- [295] B. Dii and M. Le Bellac, Nuovo Cimento 53A (1968) 158.
- [296] A. P. Contogouris, J. P. Lebrun and G. von Bochman, Nucl. Phys. B13 (1969) 246.
- [297] R. A. Miller, Phys. Rev. D2 (1970) 598.
- [298] J. Tran Thanh Van, Nuovo Cimento Letters 3 (1970) 678.
- [299] A. P. Contogouris and J. P. Lebrun, Nuovo Cimento 64A (1969) 627.
- [300] G. Benfatto, F. Niccio and G. C. Rossi, Nuovo Cimento 64A (1969) 1033.
- [301] A. Dar, T. L. Watt and V. F. Weisskopf, Phys. Letters 30B (1969) 264.
- [302] R. P. Bajpai and A. Donnachie, Phys. Letters 30B (1969) 344.
- [303] A. Capella and J. Tran Thanh Van, Nuovo Cimento Letters 1 (1969) 321.
- [304] C. Meyers et al., Nucl. Phys. B23 (1970) 99.
- [305] A. Krzywicki and J. Tran Thanh Van, Phys. Letters 30B (1969) 185.
- [306] D. Birnbaum et al., Phys. Letters 31B (1970) 484.
- [307] D. J. Millman and R. Henzi, Nucl. Phys. B19 (1970) 637.
- [308] M. Markytan and P. Schmid, Nuovo Cimento Letters 3 (1970) 51.
- [309] L. M. Nath and D. J. George, Nuovo Cimento Letters 1 (1969) 111.
- [310] B. Harper et al., Phys. Rev. 168 (1968) 1773.
- [311] J. Geike and K. H. Mutter, Phys. Rev. 184 (1969) 1551.
- [312] A. B. Kaidakov and B. M. Karnakov, Phys. Letters 29B (1969) 372.
- [313] N. Kwak and L. Nicholas, Phys. Rev. 187 (1969) 2088.
- [314] D. G. Fincham et al., Nucl. Phys. B13 (1969) 161.
- [315] P. A. Collins et al., Phys. Rev. D1 (1970) 2619.
- [316] P. Genshi, Nuovo Cimento Letters 2 (1969) 381.
- [317] G. Benfatto et al., Nuovo Cimento Letters 1 (1969) 537.
- [318] M. L. Blackmon et al., Nucl. Phys. B12 (1969) 495.
- [319] J. Froyland and D. Gordon, Phys. Rev. 177 (1969) 2500.
- [320] R. F. Amann, Phys. Rev. D2 (1970) 561.
- [321] Y. Noiret et al., Phys. Letters 26B (1968) 454.
- [322] R. P. Bajpai and A. Donnachie, Nucl. Phys. B17 (1970) 453.
- [323] J. V. Beaupre and E. A. Pascos, Phys. Rev. D1 (1970) 2040.
- [324] F. L. Anderson et al., Phys. Rev. Letters 23 (1969) 721.
- [325] B. Carreras and A. Donnachie, Nucl. Phys. B19 (1970) 349.
- [326] G. S. Abrams and U. Maor, Phys. Rev. Letters 25 (1970) 621.
- [327] S. Minami, Nuovo Cimento Letters 4 (1970) 48.
- [328] P. R. Auvil, F. Halzen and B. Margolis, Phys. Letters 32B (1970) 709.

- [329] R. Wit, *Nuovo Cimento* 69A (1970) 312.
- [330] W. Rarita, *Phys. Rev. D1* (1970) 3185.
- [331] W. J. Meggs and A. M. Gleeson, *Nucl. Phys. B19* (1970) 323.
- [332] B. Kayser, *Phys. Rev. D1* (1970) 306.
- [333] R. K. Roychoudhury, R. Perrin and B. H. Bransden, *Nucl. Phys. B16* (1970) 461.
- [334] S. Y. Chiu and B. R. Desai, *Phys. Rev.* 188 (1969) 2215.
- [335] L. Chadua, *Phys. Rev.* 186 (1969) 1463.
- [336] R. E. Mickens and S. R. Deans, *Nuovo Cimento Letters* 2 (1969) 495.
- [337] E. Ferrari and G. Violini, *Nuovo Cimento Letters* 4 (1970) 483.
- [338] C. Daum, C. Michael and C. Schmid, *Phys. Letters* 31B (1970) 222.
- [339] T. Inami, *Nuovo Cimento* 63A (1969) 937.
- [340] M. Lusignoli et al., *Nuovo Cimento Letters* 2 (1969) 419.
- [341] V. Barger and D. Cline, *Nuovo Cimento Letters* 2 (1969) 307.
- [342] C. Lovelace, *Nucl. Phys. B12* (1969) 233.
- [343] F. J. Gilman, H. Harrari and Y. Zarmi, *Phys. Rev. Letters* 21 (1968) 373.
- [344] R. G. Roberts, *Nuovo Cimento* 69A (1970) 321.
- [345] S. Sohlo and E. Byckling, *Nuovo Cimento Letters* 3 (1970) 608.
- [346] M. Greco, *Phys. Letters* 31B (1970) 216.
- [347] M. Jacon and J. Weyers, *Nuovo Cimento* 66A (1970) 401.
- [348] J. M. Kaplan and D. Schiff, *Nuovo Cimento Letters* 3 (1970) 19.
- [349] A. Capella et al., *Nuovo Cimento* 63 (1969) 141.
- [350] V. Barger, C. Michael and R. J. N. Phillips, *Phys. Rev.* 185 (1969) 1852.
- [351] W. P. Hesse et al., *Phys. Rev. Letters* 25 (1970) 613.
- [352] T. P. Cheng and W.-K. Tung, *Phys. Rev. Letters* 24 (1970) 851.
- [353] C. A. Dominguez, C. Ferro-Fontan and R. Suaya, *Phys. Letters* 31B (1970) 365.
- [354] G. Venturi, *Phys. Rev.* 187 (1969) 2147.
- [355] E. Gotsman, P. D. Mannheim and U. Maor, *Phys. Rev.* 186 (1969) 1703.
- [356] J. Daboul, *Nucl. Phys. B7* (1968) 651.
- [357] D. D. Reeder and K. V. L. Sarma, *Phys. Rev.* 172 (1968) 1368.
- [358] C. Michael, *Nucl. Phys. B13* (1969) 644.
- [359] E. L. Berger and G. C. Fox, *Phys. Rev. Letters* 25 (1970) 1783.
- [360] A. Firestone et al., *Phys. Rev. Letters* 25 (1970) 958.
- [361] T. Roth and G. H. Renninger, *Phys. Rev. D2* (1970) 1293.